

Derivation of Routing Parameters from Cross-section Survey

Final Report

**Professor D W KNIGHT
(University of Birmingham)**

**Report SR 568
March 2000**



Address and Registered Office: HR Wallingford Ltd. Howbery Park, Wallingford, OXON OX10 8BA
Tel: +44 (0) 1491 835381 Fax: +44 (0) 1491 832233

Registered in England No. 2562099. HR Wallingford is a wholly owned subsidiary of HR Wallingford Group Ltd.

Contract

This report describes work funded by the Ministry of Agriculture, Fisheries and Food under Commission FD0101 with HR Wallingford. Publication implies no endorsement by the Ministry of Agriculture, Fisheries and Food of the report's conclusions or recommendations.

The work was carried out by Dr X N Tang at the University of Birmingham under the supervision of Professor D W Knight of the University and Dr P G Samuels of HR Wallingford. The Ministry's Nominated Project Officer was Mr J R Goudie. HR's Nominated Project Officer was Dr S W Huntington.

Prepared by Paul G Samuels
(name)
Specialist in Soil Systems
(Title)

Approved by David Lamberton
(name)
Director
(Title)

Date 29/9/03

© Ministry of Agriculture, Fisheries and Food, Copyright 2000

Forward

Derivation of Routing Parameters from Cross-section Survey, Final Report

This report is a verbatim transcript of the end-of-project report to MAFF that was prepared at the University of Birmingham in consultation with Dr P G Samuels of HR Wallingford. The research is described in greater detail in the PhD thesis prepared by Dr X N Tang at the University of Birmingham on this topic, which was also issued as report TR 94 (September 1999) from HR Wallingford.



**THE UNIVERSITY
OF BIRMINGHAM**

SCHOOL OF CIVIL ENGINEERING

**DERIVATION OF ROUTING PARAMETERS
FROM CROSS SECTION SURVEY**

**Final report on
MAFF sponsored research
at the University of Birmingham
for HR Wallingford**

October 1999

Edgbaston, Birmingham, B15 2TT United Kingdom.

DERIVATION OF ROUTING PARAMETERS FROM CROSS SECTION SURVEY

MAFF sponsored research at the University of Birmingham, School of Civil Engineering,
undertaken for HR Wallingford

TABLE OF CONTENTS

	Page No.
<i>Notation</i>	
1. Introduction	1
1.1 Background to the research	1
1.2 Aims of the research	1
2. Theoretical background	1
2.1 Equations for open channel flow	1
2.2 The Muskingum-Cunge method	4
2.3 Overbank flow	5
3. Numerical experiments	6
3.1 Inbank flow	6
3.2 Overbank flow	7
3.3 Elimination of the dip and oscillation phenomena	10
3.4 Volume conservation	10
4. Analytical work	10
4.1 The governing equations	10
4.2 The diffusion wave equation of Price	11
4.3 Accurate diffusion wave modelling by Cappelaere	12
5. The wave speed-discharge relationship derived from geometry	13
5.1 Simple channels	13
5.2 Compound channels	15
5.2.1 Introduction	15
5.2.2 Fixed boundary methods	15
5.2.3 Vertical moving boundary methods	17
6. Application of new $c \sim Q$ predictive method to natural rivers	18
6.1 River Wye, Erwood to Belmont	18
6.2 River Avon, Evesham to Tewkesbury	19
7. Guidance on how to determine the $c \sim Q$ relationship for natural rivers	19
7.1 Applicability of the VPMC method	19
7.2 Schematisation of river survey	21
7.3 Derivation of $c \sim Q$ relationship from cross section survey	23
8. Conclusions	24
Acknowledgements	26
References	27
Tables 1 & 2	30
Figs 1-28	
Appendices 1 - 4	

NOTATION

The following symbols are used in this report :

- a = integer, used in (20);
- a_o = attenuation parameter, defined in (24);
- A = cross-sectional area of flow;
- b = half bottom width of main channel; integer used in (20);
- B = breadth or width of channel;
- B_f = floodplain width;
- B_f' = modified floodplain width (48);
- B_k = flooded width on floodplain at bankfull stage (inbank flow);
- B_o = initial flooded width at bankfull stage (geometric boundary);
- B_1 = initial flooded width at bankfull stage (storage boundary);
- B_s = width of channel at water surface;
- B1 to B4 = width parameters in RIBAMAN method;
- c = kinematic wave speed;
- c' = corrected kinematic wave speed for longitudinal pressure gradient;
- c_o = kinematic wave speed used in (23);
- cor = correction factor to account for longitudinal pressure gradient;
- C = empirical resistance coefficient;
- C_2 = second standard coefficient in Muskingum method;
- COH = coherence, defined in (18);
- C_r = Courant number ($= c\Delta t/\Delta x$);
- D = diffusion coefficient;
- D' = corrected diffusion coefficient for longitudinal pressure gradient;
- D1 to D4 = depth parameters in RIBAMAN method;
- f = Darcy-Weisbach resistance coefficient;
- g = gravitational acceleration;
- h = depth;
- H = flow depth in main channel;
- H_c = bankfull depth;
- H_f = height of geometric floodplain boundary above bankfull level (See Fig. 17);
- H_{fl} = height of upper floodplain storage boundary above bankfull level (See Fig. 17);
- H_s = inbank depth not affected by floodplain;
- I = inflow;
- k & k' = pressure correction coefficients; constant;
- K = routing parameter in Muskingum-Cunge method, defined in (11);
- $K(h)$ = conveyance coefficient ($= AR^{2/3}/n$), used in (25);
- L = length of routing channel;
- m = empirical coefficient (for Manning's formula, $m = 2/3$, Chezy's, $m = 1/2$);
- n = Manning's roughness coefficient;
- n_c = Manning's roughness coefficient for main channel;
- n_f = Manning's roughness coefficient for floodplain;
- N1 to N3 = real number (≥ 1) for prescribing floodplain boundary;
- O = outflow;
- p = exponent for section shape, Eq. (39);
- P = wetted perimeter of cross-section;
- q^* = lateral inflow;
- Q = discharge (unsteady);
- Q_{bf} = bankfull discharge;

- Q_n = discharge at normal depth (steady);
 \overline{Q}_p = mean peak discharge
 Q_s = main channel discharge not affected by floodplain (corresponding to H_s);
 $\langle Q \rangle$ = reference discharge used in VPMC method;
 r = shape constant parameter, used in (42);
 R = hydraulic radius ($= A/P$);
 S = storage;
 S_o = channel bed slope;
 S_f = channel friction slope;
 $s_c ; s_f$ = side slope of main channel ($1 : s_c$) and floodplain ($1 : s_f$) [vertical : horizontal];
 t = time;
 T = flood duration;
 T_p = time of peak discharge in (17);
 V = cross section mean velocity of flow ($= Q/A$);
 V_c = mean velocity of flow in main channel;
 V_f = mean velocity of flow in floodplain;
 V_o = mean velocity of flow at normal depth;
 VS = side slope of valley floodplain ($VS : 1$, vertical : horizontal);
 x = distance along channel;
 z = side slope of main channel ($1 : z$, vertical : horizontal);

Greek symbols

- α = routing parameter in Muskingum-Cunge method;
 β = momentum correction coefficient; curvature parameter in (17);
 ε = routing parameter in Muskingum-Cunge method, defined in (12); and in (22);
 γ = Fr^2 in (22);
 η = $hQ/(2S_oA) = hV_o/(2S_o)$ in (20);
 μ = adjustment factor to account for dropping higher derivatives in (34);
 ϕ = shape coefficient in (20);
 Φ = constant of proportionality in (39) with dimensions of $[L]^{2-n}$;
 Δx = distance interval;
 Δt = time interval;

Subscripts

- bf = bankfull;
 c = conveyance; main channel;
 f, fl = floodplain;
 i = i ' th sub component of a larger sum;
 n = normal depth value;
 s = storage;
 $base$ = base flow or base wave speed;
 $p, peak$ = peak flow or peak wave speed;

Acronyms

- COH = vertical division method for $H \sim Q$ calculation;
 $CPMC$ = constant parameter Muskingum-Cunge method;

CQOB-4 = c ~ Q curve produced by fixed boundary, variant 4;
CQVMB-2 = c ~ Q curve produced by vertical moving boundary, variant 2;
CQVMB-3 = c ~ Q curve produced by vertical moving boundary, variant 3;
DD = diagonal division method for H ~ Q calculation;
FB = fixed boundary method;
FSR = Flood studies report, 1975;
ISIS = river modelling software (from HR Wallingford & Halcrow);
MVPMC3 = variable parameter Muskingum-Cunge method (3 point, moving vertical);
NERC = Natural Environment Research Council;
PGTA = postgraduate teaching assistant;
QA = quality assurance;
RIBAMAN = River basin management (software);
VD = vertical division method for H ~ Q calculation;
VMB = vertical moving boundary method;
VPMC = variable parameter Muskingum-Cunge method;
VPMC4-1 = variable parameter Muskingum-Cunge method (4 point, variant 1);
VPMC4-4 = variable parameter Muskingum-Cunge method (4 point, variant 4);
VPMC4-H = variable parameter Muskingum-Cunge method (4 point, with $\partial h/\partial x$ correction);

DERIVATION OF ROUTING PARAMETERS FROM CROSS SECTION SURVEY

Final report, October 1999

MAFF sponsored research at the University of Birmingham, School of Civil Engineering, undertaken for HR Wallingford

1. Introduction

1.1 Background to the research

This report summarises a research programme into the derivation of routing parameters from cross section survey, undertaken in the School of Civil Engineering at the University of Birmingham for HR Wallingford. The contract between HR Wallingford and the University of Birmingham was signed in January 1996, and followed discussions between Dr P G Samuels (HR) and Professor D W Knight (UB) throughout 1995. The contract ran for three years, from December 1995 to December 1998. Over this three year period, MAFF contributed £24,000 and the School of Civil Engineering contributed £22,440 towards this research programme.

Mr Xiaonan Tang was appointed by the University as a postgraduate teaching assistant (PGTA) in December 1995, and worked under the direct supervision of Professor Knight, in addition to receiving external supervision from Dr Samuels through regular meetings. Quarterly reports were submitted to HR Wallingford & MAFF throughout the contract period and were used as a means of assessing progress and highlighting key issues requiring further work. A number of Working Documents were also produced, 29 in all, summarising results and ideas as the research developed. At the conclusion of the three year period, Mr Tang submitted a PhD thesis, which was examined in May 1999. The degree was conferred on Dr Tang in June 1999. This final report now highlights some of the key issues arising from this research programme. In the interests of brevity, only 28 Figures are included. Further details may be found in Tang (1999) and in the 3 journal papers by Tang, Knight & Samuels (1999a & b, 2000), reproduced in Appendices 1-3. The titles of the various Working Documents are listed in Appendix 4.

1.2 Aims of the research

The aims of the research were as follows :

- 1) to develop a simple method for estimating routing parameters from cross section survey
- 2) to test the method against flood propagation data from UK rivers

As a preliminary exercise, it was necessary to examine the basis of flood routing procedures for inbank and overbank flow, and to develop an efficient scheme for the VPMC method of flood routing.

2. Theoretical background

2.1 Equations for open channel flow

For unsteady one-dimensional flow in an open channel, the principles of mass and momentum conservation lead to the well known St Venant equations (Cunge, Holly & Verwey, 1980)

$$\frac{\partial A}{\partial t} + \frac{\partial Q}{\partial x} = q^* \quad (1)$$

$$\frac{\partial Q}{\partial t} + \frac{\partial}{\partial x} \left(\beta \frac{Q^2}{A} \right) + gA \left(\frac{\partial h}{\partial x} + S_f - S_o \right) = 0 \quad (2)$$

where Q = discharge, A = cross-sectional area of flow, t = time, x = distance along channel, q^* = lateral inflow/outflow per unit length, S_f = friction slope, S_o = bed slope, and β = momentum correction coefficient. For the case of a uniform bed slope channel and with $\beta = 1.0$, the momentum equation may be expressed in terms of the section mean velocity, $V (= Q/A)$, and the depth of flow, h , to give the friction slope, S_f , as

$$S_f = S_o - \frac{\partial h}{\partial x} - \frac{V}{g} \frac{\partial V}{\partial x} - \frac{1}{g} \frac{\partial V}{\partial t} \quad (3)$$

steady uniform flow \rightarrow |
 steady non-uniform flow \rightarrow |
 unsteady non-uniform flow \rightarrow |

Various categories of flow may therefore be attributed to the various terms in (3), as indicated above. For steady uniform flow, with $S_f = S_o$, and denoting Q_n as the discharge at the normal depth, $h = h_n$, then combining (3) with a resistance law, such as that given by Manning's equation, $Q_n = K S_o^{1/2}$, yields the relationship between the unsteady discharge, Q , and steady discharge, Q_n as

$$Q = Q_n \left[1 - \frac{1}{S_o} \frac{\partial h}{\partial x} - \frac{V}{g S_o} \frac{\partial V}{\partial x} - \frac{1}{g S_o} \frac{\partial V}{\partial t} \right]^{1/2} \quad (4)$$

kinematic wave \rightarrow |
 diffusion wave \rightarrow |
 full dynamic wave \rightarrow |

where the terms are again grouped to indicate different types of flood routing model. The diffusion model then results from combining (1) & (4) to give the convection-diffusion equation in the standard form (no lateral inflow case) as

$$\frac{\partial Q}{\partial t} + c \frac{\partial Q}{\partial x} = D \frac{\partial^2 Q}{\partial x^2} \quad (5)$$

in which c = kinematic wave speed, and D = diffusion coefficient, given respectively by

$$c = \frac{1}{B} \frac{dQ}{dh} \quad (6)$$

$$D = \frac{Q}{(2BS_o)} \quad (7)$$

where B = surface width. It follows from (5) that the discharge in a channel during a flood event has the characteristics of a wave that translates and attenuates. It should be noted that in the

context of river engineering, both c and D in (5) are functions of the discharge Q , making the solution of the equation difficult.

The reduction of the one dimensional (1-D) St Venant equations to the convection-diffusion equation implies that the relationship between the stage and the discharge is no longer uniquely defined from simple steady flow formulae, such as the Manning equation assuming $S_f = S_o$, but is of a more complex looped nature (Henderson, 1966; Knight, 1989). The gradient of the stage discharge curve is related to the kinematic wave speed by (6), and thereby indicates that during a flood c will vary with Q , as dQ/dh and B change with time. For a simple rectangular channel the wave speed is related to the cross section mean velocity, V , by

$$c = V \left[\frac{5}{3} - \frac{4h}{3(B+2h)} \right] \quad (8)$$

indicating that in the limit of a very wide channel $c = 5/3$ x velocity. More complex analytical relationships between c & V (or c & Q) may be established for other 'simple' channel shapes, such as those shown in Fig. 1, and these are discussed further in Section 5.1. By definition, the flow in these simple channels is regarded as being 'inbank', since all the flow is contained within the main channel section. For 'overbank' flow, the shape of the cross section becomes more complicated, as shown by some typical examples of what are known as 'compound' channels in Figs 2 & 3. For these cross sectional shapes, the corresponding relationship between c & V (or c & Q) is then even more difficult to determine analytically. Analysis and discussion of the $c \sim Q$ relationships for these shapes are reserved until Section 5.2.

The routing of a flood down a one-dimensional channel may be accomplished by solving either (1) & (2) or (5). One relatively simple and effective solution procedure to the latter equation is the Variable Parameter Muskingum-Cunge (VPMC) method, which allows for the variation of the travel time constant, K , and the distance weighting parameter, ϵ , in the basic routing equations used in the original Muskingum method (Bedient & Huber, 1988):

$$I - O = \frac{dS}{dt} \quad (9)$$

$$S = K[\epsilon I + (1 - \epsilon)O] \quad (10)$$

where I = inflow, O = outflow and S = storage. Cunge (1969) showed that K and ϵ may be related to the wave speed, c , and the attenuation parameter, α , by

$$K = \frac{\Delta x}{c} \quad (11)$$

$$\epsilon = \frac{1}{2} - \frac{D}{c\Delta x} = \frac{1}{2} - \frac{\alpha \bar{Q}_p}{Lc\Delta x} \quad (12)$$

where \bar{Q}_p = mean peak discharge and L = length of routing reach. The diffusion coefficient, D , is linked to α by

$$D = \frac{\alpha \bar{Q}_p}{L} \quad (13)$$

Provided c and α are known for all Q , then the values of K and ε may be determined for all Q and a flood hydrograph may be routed explicitly through a system of river channels. Typical wave speed and attenuation parameters are shown in Fig. 4, and some actual data are shown in Fig. 5, taken from the River Wye [Flood Studies Report (NERC, 1975)].

Natural rivers do not exhibit a simple relationship between c and h (or Q), as expressed by (8), since the cross section of the channel is usually more complex, as already indicated by Fig. 3. Moreover in natural rivers with significant floodplains, there are usually high irregularities in both cross-sectional shape and longitudinal form. The relationship between c and Q is therefore more like that indicated in Fig. 4, in which the wave speed typically increases to a maximum value at around $2/3$ of bankfull flow, Q_{bf} , then drops steeply to a minimum value at a low floodplain depth, and thereafter gradually increases with discharge as the floodplain becomes more inundated. It therefore follows that the flood wave speed in a natural river has a close relationship with the geometry of the cross section. A typical $c \sim Q$ relationship is then generally that of two power functions, one for the main channel flow and another for the floodplain flow, linked by an S-type transition curve, as illustrated in Fig. 5. This link between the $c \sim Q$ curve and the cross section geometry has been utilised in commercial software for some time (e.g. RIBAMAN & ISIS software, produced by Halcrow & HR Wallingford), but the fundamentals of the linkage are still not properly understood. One of the main aims of this research was therefore to understand this link better in order to develop a simple method for estimating routing parameters from cross section survey.

In order to represent overbank flow more closely, it was necessary to modify (6) so that it accounted for floodplain storage. This storage arises from the fact that when overbank flow occurs, only some of the cross section may actually be used for conveyance, the remainder of the cross section having regions where typically no flow occurs and water is essentially just being stored. Discriminating between the two may readily be achieved by writing (6) as

$$c = \left(\frac{1}{B} \right)_s \left(\frac{dQ}{dh} \right)_c \quad (14)$$

where the subscripts s & c refer to storage and conveyance respectively. The cross section of any river channel must therefore be partitioned according to some set of rules or procedure, following schematisation of the geometry.

2.2 The Muskingum-Cunge method

Since the Muskingum method of flood routing was introduced by McCarthy (unpublished paper, 1938), it has been extensively studied and used in river engineering practice. The method was improved by Cunge (1969), who linked the routing parameters to channel properties and flow characteristics, based on an approximation error obtained by a Taylor series expansion of the grid specification and the diffusion analogy. Since Cunge's work, the Muskingum-Cunge method has been extensively studied [e.g. Natural Environment Research Council (1975), Ponce and Yevjevich (1978), Ponce and Theurer (1982), Price (1985), Ponce and Changanti (1994), Ponce et al. (1996)]. It is based on (6) & (7) and the convection-diffusion equation, equation (5).

The Variable Parameter Muskingum-Cunge (VPMC) method is one in which the routing parameters are recalculated for each computational cell as a function of local flow values, whereas

in the Constant Parameter Muskingum-Cunge (CPMC) method, they are evaluated using only a single 'representative' flow value and are kept constant throughout the whole computation in time. One of the main difficulties in applying the VPMC method is in selecting an appropriate 'reference' discharge that is truly representative of the local flow in each computational cell. This has been shown to have a definite bearing upon accuracy [e.g. Ponce and Yevjevich (1978), Koussis (1983), Ponce and Chaganti (1994)], particularly with respect to the systematic non-conservation of volume.

The VPMC method remains one of the better approximate methods for flood routing and is still frequently used (Weinmann & Laurenson, 1979; Ponce & Chaganti, 1994). It is available within the ISIS and RIBAMAN software as the preferred option for flood analysis at a catchment scale. See RIBAMAN (1994) and ISIS (1995). It is particularly appropriate for rapid assessment of flow behaviour in ungauged or partially gauged natural rivers. Its main advantage over full 1-D hydrodynamic modelling based on the St Venant equations is that it does not require detailed channel geometry or roughness values. Instead two simple flood routing parameters, the wave speed, c , and the attenuation, α , are used and include the effects of uncertainty in roughness coefficient and irregularities in width, depth and bed slope of the channel reach. The two parameters also account for the storage effects of the floodplains.

2.3 Overbank flow

As a river changes from inbank to overbank flow, not only does the cross section shape of the channel change significantly, but also the streamwise pathways for flow may also alter considerably, as for example when the original main river channel is of a meandering nature contained within a valley of a more uniform shape and planform. There is therefore in nature a continuum of hydraulic processes that occur within a river as the discharge increases, with additional processes coming into action above the bankfull level. There is therefore inevitably a significant increase in the complexity of the flow behaviour once overbank flow starts. Whereas inbank flows may be treated as if they were predominately 1-D flows in the streamwise direction, despite known 3-D mechanisms being present in all flows, overbank flows must be treated differently as certain 3-D processes begin to be especially important, particularly the main channel/floodplain interaction. It is this interaction amongst others that makes the analysis of floodplain flows inherently difficult.

Some issues that need special consideration when overbank flow occurs are :

- use of hydraulic radius, R , in calculations (abrupt change at bankfull stage)
- interaction between main river and floodplain flows (lateral shear)
- proportion of flow on floodplain (between sub areas)
- flood routing parameters (wave speed and attenuation)
- storage effects of the floodplain (not all section conveys water)
- heterogeneous roughness (roughness differences between river and floodplains)
- unusual variation of resistance parameters (local, zonal & global)
- significant variation of resistance parameters (with depth & flow regime)
- critical flow (definition, control points)
- hydraulic structures (afflux, by-passing, etc.)
- distribution of boundary shear stresses (affects sediment, mixing & erosion)
- sediment transport (rate, equilibrium shape, deposition, etc.)
- valley and channel slopes for meandering channels (sinuosity)

General reviews of overbank flow processes are readily available, such as those by Anderson et al. (1996), Knight & Shiono (1996) and Knight (1999). Some of the particular issues listed above are dealt with elsewhere by Archer (1993), Ashworth et al. (1996), Atabay & Knight (1999), Cao & Knight (1996), Knight & Demetriou (1983), Knight, Shiono & Pirt (1989), Knight, Yuen & Alhamid (1994), Lambert & Myers (1998), Myers et al. (1999), Knight & Samuels (1999), Shiono & Knight (1990), Shiono & Knight (1991), Shiono et al. (1999) and Yuen & Knight (1990).

By way of illustration of one of these issues, Figs 6 & 7 show the cross sectional shape and the variation of Manning's n resistance coefficient with depth for the River Severn at Montford, taken from Knight, Shiono & Pirt (1989). These results are based on field measurements of the lateral distribution of depth-averaged velocity, water surface slope and geometry over a wide range of flows, from which the discharges in the sub-areas of the main channel (mc) and its two floodplains (fp) could be calculated. These values, together with values of the water surface slope, allowed the variation with depth of the section mean Manning's n , also known as the global (composite) value, and the sub-area or zonal (n_{mc} & n_{fp}) Manning's n resistance coefficients to be calculated. The section mean (composite) value of n is shown to apparently decrease as the discharge increases and the flow begins to go overbank. This is despite the obvious additional roughness being present at the margins of the channel and on the floodplain. This effect is entirely fictitious, and is due to the use of the hydraulic radius, R , which changes abruptly at this bankfull stage. Once overbank flow is established, the effective roughness of the main channel (n_{mc}) appears to increase rapidly, due to the retarding effect of the mixing processes (lateral momentum transfer) at the main channel/floodplain interface. Conversely the effective roughness of the floodplains (n_{fp}) appears to become very small ($n \sim 0.010$), despite its actual value being around 0.040. Fig. 7 thus highlights the care that needs to be taken when dealing with overbank flow and simulating it through 1-D or 2-D models.

The many other topics that some of these issues raise will not be pursued further in this report, but should not be forgotten when dealing with floods in natural rivers. As the flood discharge varies throughout the hydrograph, temporal and spatial changes in channel resistance may also occur from flow/sediment interaction leading to changes in bed form, or from flow/vegetation interaction leading to flattening of pliable material.

3. Numerical experiments

3.1 Inbank flow

In order to clarify the individual features and differences between the various numerical schemes for the VPMC method, a series of numerical tests was undertaken to examine certain technical issues in the Constant Parameter Muskingum-Cunge method (CPMC), the Variable Parameter Muskingum-Cunge method (VPMC), and Price's Diffusion Model (PRDM). The various schemes were compared using a wide range of inbank flows, based on recently published scenarios by Ponce et al. (1978, 1994), Perumal (1994) and in the Flood Studies Report (NERC, 1975). All the numerical experiments [See Table 3-1 in Tang (1999)] were restricted to the condition of a rectangular channel with constant slope and roughness. Standard input hydrographs were used, and outflow hydrographs produced by routing down a 100 km length of prismatic channel. In all some 22 different prismatic channels were tested. One typical set of results is shown in Fig. 8, for the channels used in the original FSR studies (1975), indicating how the attenuation varies for different bed slopes. Fig. 8 also shows the necessity for undertaking numerical tests in channels with small bed gradients, as may be seen by the results for $S_0 = 0.0001$ where the attenuation is

significant. The peak outflow, the time to peak and the volume loss were three indicators that were used to compare results. Different resolutions in time and space were also used to produce different dimensionless values of $\Delta x/L$ (reach/total channel length) and Cr (Courant Number, $Cr = c\Delta t/\Delta x$).

The variable parameters (K & ε) are normally evaluated using a 'reference' discharge, based on the flow at local computational points. In current practice this is usually taken to be some arbitrary average value of some of the grid points for each computational cell. See Fig. 9. For example the commonly used 3 point schemes would use grid points $\{j, n\}$, $\{j, n+1\}$ and $\{j+1, n\}$, omitting the 4th point which is forward in both space and time $\{j+1, n+1\}$. Studies were made of three 3 point schemes and three 4 point schemes for comparative purposes. As might be expected, the 4 point schemes generally gave better results than the 3 point schemes. However, the inclusion of the 4th point in defining the 'reference' discharge is problematic, since it is initially unknown, and therefore leads to an implicit type of solution with another level of iteration. Of all the 4 point schemes tested, the scheme labelled VPMC4-H, described next, was regarded as the best.

The important feature of volume conservation in the VPMC method was also examined for these 6 numerical schemes. The volume loss between outflow and inflow hydrographs was found to be significant ($> 10\%$ for shallow slopes) for some standard 3 point schemes of solution. This was improved ($< 8.0\%$ for $S_o = 0.0001$) using a 4 point scheme (VPMC4-1), and improved even further ($< 0.5\%$ for $S_o = 0.0001$) using a 4 point scheme (VPMC4-H) with the longitudinal pressure term taken into account by the method outlined by Cappelaere (1997). Further details of these tests are given in Tang, Knight & Samuels (1999a), and reproduced in Appendix 1. Empirical formulae were formulated, based on these numerical tests, as a guide for determining the volume loss when the VPMC method is applied. See Fig. 10. Analytical proofs that the CPMC method conserves volume but VPMC does not, were formulated and are given in the Appendices to Tang et al. (1999a).

A study was also made of the 'leading edge dip' in the outflow, where the initial few values of the routed outflow hydrograph can drop below the initial steady base flow, Q_{base} , and can even produce negative discharges. Also there is the undesirable occurrence of negative weighting parameter, ε , which typically should lie between 0 and 0.5. Upper and lower limits to the time step, Δt , and the lower limit for Δx were established as :

$$\Delta t \geq \frac{\Delta x}{c_{base}} \left(1 - \frac{Q_{base}}{BS_o c_{base} \Delta x} \right); \quad \Delta t \leq \frac{\Delta x}{c_{peak}}; \quad \Delta x \geq \frac{Q_{peak}}{BS_o c_{peak}} \quad (15)$$

(lower limit, C_2 positive) (upper limit, $Cr \leq 1$) (lower limit, ε positive)

where C_2 refers to the 2nd standard coefficient in the Muskingum method and the subscripts *base* and *peak* distinguish between prescribed values. Many published data do not comply strictly with these conditions and therefore make their test results or benchmarking suspect.

3.2 Overbank flow

Having established what appeared to be a sound computational scheme for the VPMC method (VPMC4-H), further numerical tests were undertaken on compound channels, representing the more severe test case of overbank flow. In order not to pre-empt the result, tests were also conducted with 2 of the more promising schemes for inbank flow tested earlier, a modified 3 point

scheme and the standard 4 point scheme used by most other workers (MVPMC3 & VPMC4-4 respectively).

Numerical tests were undertaken based on the 'hypothetical' river channel used by Ackers (1992 & 1993), since this channel has been used by the author for other purposes and its features are well documented. The channel shape is shown schematically in Fig. 2, and represents a small river with a trapezoidal section, 15 m wide at the base, 1.5 m deep, side slopes of 1:1, flanked by two symmetric floodplains, each 20 m wide, leading to embankments on each side also with 1:1 side slopes. Standard input hydrographs (symmetric and asymmetric) were used. For example, for a typical value of $Q_p = 107 \text{ m}^3\text{s}^{-1}$ ($Q_p/Q_{bf} = 2$, where $Q_{bf} = 53.44 \text{ m}^3\text{s}^{-1}$, for a channel with $S_o = 0.003$, $n_c = 0.030$) these were :

Symmetric inflow hydrograph

$$\begin{aligned} Q(t) &= 43.5 [1 - \cos(\pi t / 15)] + 20 & t < 30 \text{ hours} \\ Q(t) &= 20 & t \geq 30 \end{aligned} \quad (16)$$

Asymmetric inflow hydrograph

$$Q(t) = 20 + 87 \left[t / T_p \exp(1 - t / T_p) \right]^\beta \quad (17)$$

where $\beta = 6$ (curvature parameter), $T_p = 15$ hours (inflow peak time)

Outflow hydrographs were obtained after routing down a 20 km length of prismatic channel. The majority of tests involved 8 different prismatic channels.

The peak outflow, the time to peak and the volume loss were again used as the three indicators to compare results. A wide ranging series of numerical tests was undertaken, in which different methods were adopted for computing the stage-discharge relationship for overbank flow, different roughnesses were adopted for the floodplain relative to the main channel ($n_f/n_c = 1$ to 5, with $n_c = 0.030$), the bed slopes were varied (generally only 2 values were used, 0.003 & 0.0003) and the ratio of input peak ($Q_p = 310$ & $210 \text{ m}^3\text{s}^{-1}$) to bankfull flow ($Q_{bf} = 30$ & $10 \text{ m}^3\text{s}^{-1}$) was varied (generally $Q_p/Q_{bf} = 1.1$ to 10) in order to examine the effect of low to high inundation levels. The different bed slopes gave values of $Q_{bf} = 53.4$ & $16.9 \text{ m}^3\text{s}^{-1}$ respectively. See Table 4-1 in Tang (1999) for full details. The number of numerical tests was therefore considerable, covering a wide range of parameters that might be expected in practice. Figs 11 to 13 illustrate just a small selection of some of these tests.

Fig. 11 shows a comparative set of results for these overbank flow tests with $S_o = 0.003$, $n_f/n_c = 2$, $Q_p/Q_{bf} = 1.25, 2.0$ & 3.0 , and a symmetric inflow hydrograph appropriate for each Q_p/Q_{bf} value. The effect of the floodplain is to delay the rise of the outflow hydrograph, as some water goes into storage on the floodplain, creating the characteristic 'shoulder' on each rising limb. On the falling limb of each outflow hydrograph it is apparent that there is a steep reduction in discharge as the flow reverts back to inbank flow from being overbank flow. This sudden reduction is seen to cause oscillations in the numerical output, referred to as 'trailing edge oscillations'. Fig. 12 shows a comparative set of results for different bed slopes, with $n_f/n_c = 2$, $Q_p = 107 \text{ m}^3\text{s}^{-1}$, $Q_p/Q_{bf} = 2, 2.83, 3.88$ & 6.33 and an asymmetric inflow hydrograph. As the channel bed slope decreases from 0.003 to 0.0003, it is clear that the attenuation increases and the trailing edge oscillations diminish, eventually disappearing at mild slopes. Fig. 13 shows the effect

of floodplain roughness for one bed slope, $S_o = 0.003$. These issues are examined in more detail later in Section 3.3.

Of the many 1-D methods that could be used for determining the overbank $H \vee Q$ relationship within the wave speed calculation method, the vertical division method (VD), the diagonal division method (DD), the area method (Area) and the coherence method (COH) of Ackers were used. In each of these methods the cross sectional area of the channel is divided into a number of different sub-areas, the discharges calculated for each sub-area, and then summed to give the total discharge for a given stage. How the channel is conceptually divided into sub-areas is the key to a successful stage-discharge predictor. The VD method involves dividing the channel by vertical division lines, usually at the interface between the main channel and its floodplain, as shown by the line AB in Fig. 3. Alternatively, in the DD method, the dividing line is drawn diagonally, as shown by line CD in Fig. 3. In the area method, the interaction is accounted for by subtracting from the main channel cross sectional area, an area ΔA for each floodplain, as shown in Fig. 2. In the COH method, the channel is divided into any number of sub-areas and wetted perimeter elements, each associated with its own roughness. The 'coherence' is then defined as the ratio of the basic conveyance calculated by treating the channel as a single unit, with perimeter weighting of the friction factor, to that calculated by summing the basic conveyances of the separate zones. The 'coherence' of a channel may be expressed by

$$COH = \frac{\sum_{i=1}^{i=n} A_i \sqrt{\left[\frac{\sum_{i=1}^{i=n} A_i / \sum_{i=1}^{i=n} (f_i P_i)}{\sum_{i=1}^{i=n} [A_i \sqrt{(A_i / (f_i P_i))}]}\right]}}{\sum_{i=1}^{i=n} [A_i \sqrt{(A_i / (f_i P_i))}]}} \quad (18)$$

For further details on all these 1-D stage-discharge prediction methods, see Ackers (1993), Knight (1996 & 1999) and Tang (1999).

The overbank routing results indicated that the floodplain has a great effect upon the routed time to peak, the attenuation of the peak discharge and the shape of the outflow hydrographs. The timing and attenuation of the outflow peak generally increases with increasing roughness of floodplain, particularly for mild slope channels. Like inbank flows, the VPMC method still suffers some volume loss of outflow for overbank flow (e.g. < 1% for $S_o > 0.001$, but up to 9% for $S_o = 0.0001$). Fig. 14 shows the empirically fitted equations through the numerical results on volume loss, plotted in a similar way to Fig. 10 for inbank flow. It is interesting to note that the volume of routed outflow becomes a gain, not a loss, when the bed slope is small, provided $Q_{base} > Q_{bf}$ (e.g. up to 6% when $S_o = 0.0003$ with $n_f/n_c = 5$). Generally the loss or gain values of routed outflow increase with increasing roughness of floodplains (e.g. about 5% when n_f/n_c varies from 1 to 5 for $S_o = 0.0003$).

In addition to the well known leading edge 'dip', the phenomenon of 'trailing edge oscillations', illustrated in Figs 11 & 13, and referred to earlier was explored during the course of undertaking these numerical experiments on routing floods in steep channels. The trailing edge oscillations had been encountered in earlier MAFF sponsored research at HR Wallingford (see Morris, 1994). Some examples are also shown in Figs 5-7 & 11 of Tang, Knight & Samuels (1999b), reproduced in Appendix 2. These oscillations are a consequence of the variation in the convective wave speed between the floodplain and main channel flows in a compound channel and have not, to the Author's knowledge, been reported in the open literature before.

3.3 Elimination of the dip and oscillation phenomena

The conditions which produce both the well known 'leading edge dip' and the newly discovered oscillations in the recession limb of the hydrograph were investigated both analytically and numerically by Tang (1999). Both the 'dip' and 'oscillations' may be eliminated by applying the following condition to the selection of space and time steps :

$$\begin{aligned} [c\Delta t - Q/(BS_o c)]_{max} &\leq \Delta x \leq [c\Delta t + Q/(BS_o c)]_{min} & (19) \\ \text{(oscillations)} & & \text{(dip)} \end{aligned}$$

These conditions strictly apply only to the range of cases studied, and need to be extended to cover a wider range of conditions that might be encountered in practice.

3.4 Volume conservation

Although the volume losses cited earlier in Sections 3.1 & 3.2 may appear to be relatively small, it should be remembered that volume errors are important in a number of respects. Firstly, from a quality assurance (QA) point of view, there is an increasing requirement that models be tested against benchmark values, with an obvious test that the model should conserve volume. Second, in the simulation of a long hydrologic time series, it simply is not possible to use the St Venant method for flood routing in all the rivers in a river basin network, and therefore simpler methods such as the VPMC method need to be employed. Although there may be little change in peak flood flows, despite volume gains or losses, systematic volume errors will be critical for water resource assessments. Third, volume conservation is important from a flood forecasting perspective, because public safety is an issue and flow forecasting software is now classified as 'safety critical' software with consequent QA implications.

4. Analytical work

4.1 The governing equations

The generalised continuity and momentum equations were analysed in order to appreciate the approximations that are customarily made in reducing them to the well known St Venant equations, (1) & (2), widely used in river engineering. At the same time the generalised diffusion wave equation was derived from linearising the momentum equation by considering perturbations from a reference condition to give

$$\frac{\partial Q}{\partial t} + c \frac{\partial Q}{\partial x} = \eta \left\{ [(1+\phi)k - k'] - \left[\left(2b \frac{c}{V_o} - 1 \right) \beta - a \left(\frac{c}{V_o} \right)^2 \right] Fr^2 \right\} \frac{\partial^2 Q}{\partial x^2} \quad (20)$$

in which $\eta = hQ/(2S_o A) = hV_o/(2S_o)$, $\phi = A/(h\partial A/\partial h) = A/(Bh)$, a shape coefficient for the channel cross section ($\phi = 1$ for a rectangular section), k & k' are a pressure correction terms, β = momentum correction coefficient, a & b = integers equal to either 0 or 1, so if a or b is equal to zero (unity), the local or convective term is excluded (included) from (in) the equation, and Fr = Froude number ($Fr^2 = [BQ^2/(gA^3)]_o = [V^2/(gh)]_o$). The group of terms on the RHS of (20) thus indicates the basis of the diffusion coefficient, D , employed in (5). Writing $c/V_o = m_1$, then (20) may be regarded as a generalised wave equation that leads to 4 types of model :

- | | |
|------------------------------|----------------|
| 1) non-inertial model | (a = 0, b = 0) |
| 2) local inertial model | (a = 1, b = 0) |
| 3) convective inertial model | (a = 0, b = 1) |
| 4) full inertial model | (a = 1, b = 1) |

A comparative analysis shows that for $1 < \beta < 1.5$, which is likely to be true for most natural rivers, the non-inertial model is the best approximation to the full inertial model. The non inertial model thus offers a good approximation with high reliability for flood routing in practical applications.

For those cases in which the pressure distribution is approximately hydrostatic, i.e. the flow is not highly curved and only gradually varying, then $k = k' = 1$ and (20) becomes

$$\varepsilon = \frac{1}{2} - \frac{D}{c\Delta x} = \frac{1}{2} \left[1 - (1 - \beta Fr^2) \left(\frac{Q}{BS_o c \Delta x} \right)_o \right] \quad (21)$$

Equation (21) again indicates the nature of the diffusion coefficient, D.

Some attention was also paid to the basic convective-diffusion equation (5), in which c & D both generally vary with Q. By assuming that c & D are both constant, (5) was transformed into a pure diffusion equation and then solved mathematically. This new analytical solution by Tang (1999) to (5) with constant coefficients now needs to be developed further for practical use.

4.2 The diffusion wave equation of Price

Price (1973 & 1985) exploited the fact that the inertial terms, i.e. the first and second terms in (2), are generally much smaller than the remaining terms. The 1D momentum equation may therefore be written in the form

$$\varepsilon \gamma \left[\frac{1}{gA} \frac{\partial Q}{\partial t} + \frac{1}{gA} \frac{\partial}{\partial x} \left(\beta \frac{Q^2}{A} \right) \right] + \varepsilon \frac{\partial h}{\partial x} + S_f - S_o = 0 \quad (22)$$

in which the inertial terms are of order $\varepsilon \gamma$ and the pressure term is of order ε , where ε is a characteristic ratio of the water surface slope (relative to the bed) to the bed slope (i.e. $\varepsilon = (\partial h / \partial x) / S_o$ and $\gamma = Fr^2$). For most flood events $\varepsilon \gamma \ll \varepsilon \ll 1$. It should be noted that the symbol ε used here is not the routing parameter, but that used by Tang (1999) to be consistent with his notation. By making various approximations (22) may be combined with (1) to give the basic flood routing equation used by Price, valid for any typical Froude number, in the form

$$\frac{\partial Q}{\partial t} + c_o \frac{\partial Q}{\partial x} + \varepsilon c_o \frac{\partial}{\partial t} \left(\frac{a_o}{c_o^2} \frac{\partial Q}{\partial x} \right) = c_o q^* - \varepsilon \gamma c_o \frac{\partial}{\partial t} \left(\frac{Q_o q}{2gAS_o} \right) + o(e^2) \quad (23)$$

in which the kinematic wave speed is $c_o (= dQ/dA)$, and the attenuation parameter, a_o is given by

$$a_o = \frac{Q_o}{2BS_o} \left[1 + \frac{\gamma B}{gA} \left(\frac{2Qc_o}{A} - \frac{Q^2}{A^2} \right) \right] \quad (24)$$

Equations (23) & (24) are thus a more general forms of (5) & (7). Equation (23) forms the basis of the PRDM, referred to in Section 3.1. More recent work by Sivapalan et al. (1997) has improved on Price's method and produced the most generalised form of the non-linear diffusion wave equation, which shows that the wave speed-discharge relation should exhibit hysteresis.

4.3 Accurate diffusion wave modelling by Cappelaere

By neglecting the inertial terms, i.e. the last two terms, in (3), and using $S_f = Q^2/K^2(h)$, where $K(h) = \text{conveyance} (= AR^{2/3}/n)$, and (h) indicates a function of depth, then

$$\frac{Q^2}{K^2(h)} = S_o - \frac{\partial h}{\partial x} \quad (25)$$

where $Q = \text{unsteady discharge}$, now a function of h and $\partial h/\partial x$ only. The discharge, Q , may be written in terms of the steady discharge, $Q_n(h)$, as has already been done in (4), which now simplifies to

$$Q = Q_n(h) \cdot cor \quad (26)$$

where
$$Q_n(h) = K(h) S_o^{1/2} \quad (27)$$

and
$$cor = \left[1 - \frac{1}{S_o} \frac{\partial h}{\partial x} \right]^{1/2} \quad (28)$$

The factor, *cor*, is therefore introduced as a dimensionless 'correction' factor, which accounts for the effect of the longitudinal pressure gradient, $\partial h/\partial x$ (i.e. $cor = 1$ for $\partial h/\partial x = 0$). Differentiating (1) and (25) with respect to x and t respectively, assuming $\partial A/\partial t = B(h)\partial h/\partial t$, and combining to eliminate $\partial h/\partial t$, gives a convective-diffusion equation similar to (5), except that it has modified coefficients, c' and D' , as

$$\frac{\partial Q}{\partial t} + c' \frac{\partial Q}{\partial x} = D' \frac{\partial^2 Q}{\partial x^2} \quad (29)$$

where

$$c' = \frac{Q}{BK} \frac{dK}{dh} + \frac{K^2}{2B^2Q} \left[\left(\frac{\partial B}{\partial x} \right)_h + \left(\frac{\partial B}{\partial h} \right) \frac{\partial h}{\partial x} \right] \quad (30)$$

$$D' = K^2/(2BQ) \quad (31)$$

This is why in (4), the description of 'diffusion wave' is used when this approximation is made neglecting the two inertial terms. Because Q is a function of h and $\partial h/\partial x$, it follows that c' and D' are as well. The variable h may be eliminated from these expressions by making further approximations. Cappelaere (1997) showed that the modified wave speed and diffusion coefficients, c' and D' , which include the effects of $\partial h/\partial x$, can be approximately expressed in terms of the original coefficients, c and D , by using the same correction term, *cor*. Ignoring $\partial B/\partial x$, it may be shown that

$$c' = \frac{c}{2} \left[\text{cor} \cdot \left(1 + \frac{Q_n}{D} \frac{dD}{dQ_n} \right) + \frac{1}{\text{cor}} \left(1 - \frac{Q_n}{D} \frac{dD}{dQ_n} \right) \right] \quad (32)$$

and $D' = D \cdot \text{cor}$ (33)

The correction coefficient, *cor*, is still *h*-dependent, but it can be evaluated from *Q* and $\partial Q/\partial x$ by differentiating (25) with respect to *x* and combining it with (1), in order to eliminate $\partial Q/\partial x$. This then gives

$$\text{cor} \approx \sqrt{1 - \mu \frac{2D}{c\langle Q \rangle} \frac{\partial Q}{\partial x}} \quad (34)$$

where μ is an adjustment factor to take account of the above treatment, and $\langle Q \rangle$ is the 'reference' discharge. The numerical value of μ will depend on the size and shape of the channel, as well as the shape of the routed hydrograph. The numerical tests described in Section 3 indicated that $\mu = 0.4$ gave the best results with regard to volume conservation for inbank flows using rectangular channels, and $\mu = 0.2$ for overbank flows using trapezoidal compound channels. These μ values are specific to the cross section geometries tested, and are not recommended as being generic values for all inbank and overbank flows. Further work is needed on this topic.

For a rectangular channel, (32) reduces to that given by Cappelaere

$$c' = c \cdot \text{cor} \quad (35)$$

Equations (32) & (33) with (34) provide expressions for wave speed and diffusion coefficients (*c*' & *D*'), with only *Q* and $\partial Q/\partial x$ as variable and the prescribed functions $c(Q_n)$ and $D(Q_n)$ as parameters. Together with (26) & (29) they constitute a fully determined PDE (partial differential equation) system. There are 5 equations for 5 unknowns, *Q*, Q_n , *cor*, *c*' & *D*'. Cappelaere solved these equations using an operator-splitting numerical approach, dealing with the convective and diffusive terms separately.

5. The wave speed-discharge relationship derived from geometry

5.1 Simple channels

The generalised form of (8) was derived for the common channel shapes shown in Fig. 1 as follows. For a kinematic wave, with $S_o = S_f$, a general resistance law may be written as

$$Q = CAR^m \sqrt{S_o} \quad (36)$$

in which *C* = empirical coefficient, *R* = *A/P*, $m = 2/3$ (Manning) or $1/2$ (Chezy). Assuming S_f to be constant with depth, then from (6) the relation between wave speed, *c*, and section mean velocity, *V* ($= Q/A$), is

$$c = V \left[(m+1) - \frac{mR}{B} \frac{dP}{dh} \right] \quad (37)$$

For a trapezoidal channel [Fig. 1(a)], having a bottom width of $2b$ and a side slope of $1 : z$ (vertical : horizontal) the general relationship between *c* and discharge, *Q*, is

$$c = \frac{Q}{A} \left[(m+1) - \frac{2mh(2b+zh)\sqrt{1+z^2}}{(2b+2h\sqrt{1+z^2})(2b+2zh)} \right] \quad (38)$$

This can obviously be readily transformed into the corresponding equations for a rectangular channel ($z = 0$) [Fig. 1(b)] or a triangular channel ($b = 0$) [Fig. 1(c)].

For the so-called exponential channel, whose area is A , the general shape of the cross section may be expressed as

$$A = \Phi h^p \quad (39)$$

where Φ is a constant of proportionality with dimensions of $[L]^{2-p}$ and p is an exponent. Thus when $p = 1, 2$ the cross-sectional shapes are rectangular and triangular respectively. When $p = 3/2$, it is parabolic [Fig. 1(d)], and when it is $5/2$, it is cusp shaped [Fig. 1(e)].

For a parabolic channel, the general shape of the cross section can be expressed as

$$h = \frac{1}{k} B^2 \quad (40)$$

in which k is a constant ($=2.25\Phi^2$) which determines the shape of the section. Applying (37) gives the $c \sim Q$ relationship for a parabolic channel as

$$c = \frac{Q}{A} \left[(m+1) - \frac{8mh(k+16h)}{12(k+16h)h + 3k\sqrt{(k+16h)h} \ln \left[\frac{4\sqrt{h} + \sqrt{(k+16h)}}{\sqrt{k}} \right]} \right] \quad (41)$$

For a cusp-shaped channel, the general shape of the cross section can be expressed as

$$rh^3 = B^2 \quad (42)$$

in which r is the shape constant parameter ($= 6.25\Phi^2$). This then yields the $c \sim Q$ relationship for a cusp shaped channel as

$$c = \frac{Q}{A} \left[(m+1) - \frac{27mrh(16+9rh)}{5[(16+9rh)^2 - 64\sqrt{16+9rh}]} \right] \quad (43)$$

It can be seen from (38), (41) & (43) that the wave speed, c , is related to the mean cross-section velocity, V , and that $V < c < (m+1)V$. It is also evident that for inbank flows in all the channel shapes examined, the $c \sim Q$ relationship is a single power functional curve, which implies that the kinematic wave speed increases as the discharge increases or the stage rises.

5.2 Compound channels

5.2.1 Introduction

The $c \sim Q$ relationship for overbank flow is much more complex than for inbank flow due to two factors. Firstly, the cross sectional shape often changes abruptly at the bankfull stage, as shown by the typical natural river cross section in Fig. 6, or by the schematic ones in Figs 15 - 18. This makes the use of the hydraulic radius problematic, due to its discontinuous nature as the flow goes overbank. Secondly, once the flow exceeds bankfull, the stage-discharge relationship is complicated by the lateral transfer of momentum between the main river channel and the floodplains, and some of the other influences noted in Section 2.3. This makes the calculation of the stage-discharge relationship, which is required in differential form in (6), also problematic. The combined effect of both these factors makes the $c \sim Q$ relationship no longer a single power functional curve, as was the case for inbank flow, but a two part function, joined by a S-shaped transition, as shown in Fig. 5.

The impact of both these factors on the $c \sim Q$ relationship was studied by examining firstly the influence of the geometry of the cross section and then secondly the influence of the various computational stage discharge prediction methods. The RIBAMAN software code formed the basis of the first study, since the method of schematising the cross section geometry lent itself to easy adaptation. Furthermore, it included a methodology for handling some of the issues outlined earlier. In particular, its method of partitioning the cross section for floodplain storage, as described in Section 2.1, was based on (14) and involved relatively straightforward fixed boundaries. Being the simplest method, this was studied first.

5.2.2 Fixed boundary methods

A simple but somewhat arbitrary technique is adopted within the RIBAMAN software, which redefines a new flow boundary for calculating the conveyance of the channel, shown schematically in Fig. 15(a). Part of the cross-section is designated for storage, labelled as 'storage only', with the remaining part being designated for conveyance, labelled as 'active flow'. Fig. 16 shows the various parameters required when using this method. In the RIBAMAN method, a new upper boundary (straight line) is redefined for the conveyance part of the calculation, $(dQ/dH)_c$, whereas the lower boundary (linear schematisation of actual floodplain geometry) is retained for the calculation of the top water surface breadth, B_s . To undertake these calculations there are 9 geometric parameters which are required to be selected : B1 - B4, D1 - D4 and the valley side slope, VS, defined as follows :

- B1 = bed width of main channel
- B2 = top width of main channel
- B3 = total floodplain width, from left bank to right bank
- B4 = average flooded width at bankfull stage
- D1 = depth of main channel
- D2 = depth above bankfull for full floodplain inundation
- D3 = depth above bankfull for full width flow
- D4 = depth below bankfull at which isolated flooding begins
- VS = valley side slope (*N.B.* not like z , is VS : 1, vertical : horizontal)

The parameters D4 and B4 represent the depth and width respectively at which water on the floodplain changes from isolated patches of storage to a continuous downstream conveyance of flow. Because of the fixed geometric and conveyance boundaries, and the fact that in the

RIBAMAN method the overbank conveyance is calculated by the simple divided channel method (VD), this approach is referred to as the fixed boundary (FB) method.

The Ackers 'hypothetical river channel was adapted for a series of tests, with different values selected for D2, D3, D4, B3 and B4, but constant values for others, i.e. B1 = 15m, B2 = 18m, D1 = 1.5m, VS = 1, S_o = 0.003, n_c = 0.030 and n_f = 0.060. In some cases symmetric or asymmetric floodplains were also tested, as indicated by the general schematic compound channel shown in Fig. 17. In general it was found that the c ~ Q relationships could be altered at will, and that some parameters affected different parts of the c ~ Q curves more than others, as would be expected. For example, it was found that D2 had a significant effect on the transition curve when the water goes just overbank, and that D4 & B4 influenced the point at which the transition curve started. See for example the set of results in Fig. 19, in which D4 is varied (D4 = 0, 0.15, 0.3 & 0.4 m), D2 = 0.1 m, and D3 = 0.3 m. Increasing the parameter B3 had the effect of shifting the position of the whole overbank component of the c ~ Q curve, as shown by Fig. 20, in which B3 was varied (B3 = 25, 32, 38, 48, & 58 m), D2 = 0.1 m, and D3 = D4 = 0.3 m. Conversely, as B3 is reduced, the c ~ Q relationship tends towards a single curve, like that for inbank flow, as the channel cross section tends towards a more 'simple' shape.

Despite being able to be produce reasonable c ~ Q curves, it was difficult to determine how best to actually select the parameters B1 - B4 & D1 - D4, particularly as no guidance is given in the RIBAMAN manual. Furthermore, Figs 19 & 20 show that there were still sharp changes around the maximum and minimum values of the c ~ Q relationships, which are not like the smooth transitional curves that are observed in natural rivers, as already seen in Fig. 5. It was therefore concluded that the RIBAMAN method, although useful, is not entirely appropriate for producing smooth c ~ Q relationships. For these reasons it was decided to develop the cross section via a series of curved functions, rather than by a series of straight lines.

A modified RIBAMAN method, code named CQOB-4, was therefore developed in which curved boundaries were used, shown schematically in Fig. 15(b). Fig. 18 shows the application of this approach to a compound cross section, in which curved boundaries are used not only to define the actual geometric boundary (lower boundary), but also used to define the flow conveyance calculation boundary (upper boundary). Various curved functions were assumed and the resulting c ~ Q curves examined. Continuous and non-continuous tangent or power function curves were tried and were found generally to give better results for the c ~ Q relationship than those from the straight line model. The schematic cross section and functions used in this new method are illustrated in Fig. 18 and defined as follows :

(i) *Inbank part*

[Main channel geometric boundary]

$$x' = [B_k + (H_c - H_s)s_c] \left(\frac{H - H_s}{H_c - H_s} \right)^{N1} \quad (45)$$

(ii) *Overbank part*

[Floodplain geometric boundary]

$$x = [B_f - B_0 + H_f s_f] \left(\frac{H - H_c}{H_f} \right)^{1/N2} \quad (46)$$

(iii) *Overbank part*

[Upper boundary for conveyance calculations]

$$x = [B_f - B_1 + H_{\beta} s_f] \left(\frac{H - H_c}{H_{\beta}} \right)^{1/N_3} \quad (47)$$

where N_1 , N_2 & N_3 are any real numbers (≥ 1), and the remaining symbols are defined as :

- B_f = floodplain width
- B_k = flooded floodplain width at bankfull stage (for main channel)
- B_0 = initial flooded width at bankfull stage (for geometric boundary)
- B_1 = the initial flooded width at bankfull stage (for conveyance boundary)
- H = total water depth in main channel
- H_c = bankfull depth
- H_{β} = affected floodplain depth
- H_s = main channel depth, corresponding to the affected inbank discharge, Q_s
- s_c, s_f = side slopes of main channel and floodplain respectively
(1 : s_c & 1 : s_f , vertical : horizontal)

When $N_1 = N_2 = N_3 = 1$ this method becomes equivalent to the original RIBAMAN method. Although these curved boundaries considerably improve the RIBAMAN method, there were still some unsatisfactory features around the minimum point on the $c \sim Q$ curve. It was felt therefore that further improvement might be made by allowing the storage/conveyance proportion to vary directly as the stage rises, simulating how real rivers probably behave. Accordingly a vertical moving boundary (VMB) approach was developed.

5.2.3 Vertical moving boundary methods

In the previous method using fixed boundaries, the floodplain storage effect is accounted for by modifying the conveyance of the channel. As has been shown in Section 5.2.2, this is a rationally acceptable approach, but has its limitations. An alternative approach is to use vertical moving boundaries (VMB) for evaluating the channel conveyance, in order to account for the floodplain storage effect, shown schematically in Fig. 15(c). Conceptually, this vertical flow boundary is imagined to move from the junction between the main channel and the floodplain towards the outer edge of the floodplain, as the depth on the floodplain increases. Several modes of movement were examined, the most promising ones being given the code names of CQVMB-2 and CQVMB-3.

In the CQVMB-2 model, the conveyance of the channel was calculated by a moving vertical boundary, defined by B_f' , as shown in Fig. 18, given by the following expression :

$$B_f' V_c = B_f V_f$$

or $B_f' = B_f V_f / V_c \quad (48)$

where V_c & V_f are the main channel and floodplain velocities respectively, computed by any of the conventional calculation methods for overbank flow (VD, DD, Area, COH, etc.). The actual floodplain width is assumed to be equal to B_f , but applying (48) gives a new floodplain width, B_f' , which is then used to re-calculate $(dQ/dH)_c$ and $(1/B)_s$ to give the wave speed for that particular depth or discharge. In such a way the resulting B_f' increases from zero towards B_f as the flow

depth on the floodplain increases. This model does not require any parameters to be chosen and relies solely on the geometry and hydraulic features of the routing reach or river.

In the CQVMB-3 method, the vertical boundary for the conveyance calculation moves across the floodplain, and where it intersects the storage curve, given by (47), it defines a 'storage' zone to the right of the vertical line as also shown in Fig. 18. The amount of storage thus varies with depth and with the parameters involved in (46) & (47). However, the storage width term, $(1/B)_s$, is obtained from the actual floodplain boundary, defined by (46). As can be seen from (46) & (47), four parameters (H_f , N_2 , N_3 & H_{fl}) determine the upper flow boundary and the lower geometric floodplain boundary.

A comparison was made by Tang (1999) between the $c \sim Q$ curves produced by all the different fixed boundary (FB) and vertical moving boundary (VMB) models tested. Of interest here is a direct comparison between the CQOB-4 and CQVMB-3 models, since different floodplain storage volumes (V_s) are involved, arising from different storage boundaries being employed in the two models for evaluating the term $(dQ/dH)_c$ in (14). Some comparative tests were therefore undertaken using the parameters shown in Table 1, and the resulting $c \sim Q$ curves are shown in Fig. 21 and the differences in dead floodplain storage in Fig. 22.

The results indicate that using the same parameters both models produce similar $c \sim Q$ curves, but the wave speeds produced by CQVMB-3 (runs C1 - C4) are larger than those by CQOB-4 (Runs D1 - D4) for the same discharge, especially around bankfull stages. The $V_s \sim Q$ curves produced by CQVMB-3 have a maximum at a certain stage of overbank flow, whereas the curves by CQOB-4 do not, with V_s gradually increasing to a limiting value at high flow or stage. Generally V_s by CQVMB-3 is less than that by CQOB-4 for the same discharge, which explains why the wave speed by the former model is larger than that by the latter model. On this basis, it would appear that the CQVMB-3 model is somewhat better than the CQOB-4 model.

6. Application of new $c \sim Q$ predictive method to natural rivers

6.1 River Wye, Erwood to Belmont

The 69.8 km long Erwood-Belmont reach on the River Wye is ideal for studying flood routing because the reach has a large floodplain, no important tributaries, and the mean annual lateral inflow ($\sim 14 \text{ m}^3\text{s}^{-1}$) is small enough to be neglected in comparison with the mean annual flood discharge ($560 \text{ m}^3\text{s}^{-1}$) at Belmont. The total area of the floodplain along the reach is 28.57 km^2 , and the average bed slope of the river reach is 0.88×10^{-3} (Price, 1975). For the purposes of analysis, an average cross-section of the main river channel was obtained from a schematisation based on surveyed cross sections (taken in 1969), in which all the cross sections were simply positioned together based on its individual centre line, as shown in Fig. 23. Although this method of schematisation is known to be not necessarily the best, it was deliberately chosen to test the robustness of the $c \sim Q$ prediction method, based on very approximate geometric data. The following dimensions for the main channel were obtained from Fig. 23, using a trapezoidal approximation :

bed width	42.0 m
main channel depth	4.32 m
side slopes	1 : 1.04 (left side, vertical : horizontal)
	1 : 2.47 (right side, vertical : horizontal)

The average width of the floodplain was estimated to be 410 m, obtained by dividing the whole floodplain area (28.57 km²) by the total reach length (69.8 km). In the present study a symmetric compound channel, with a Manning's coefficient of 0.035 and 0.060 for the main channel and the floodplain respectively, was used to predict the $c \sim Q$ relationship. Based on the average geometry given above, and the assumed hydraulic roughness properties of the channel, the calculated reach mean bankfull discharge was estimated to be 425 m³s⁻¹, sufficiently close to the value of ~ 440 m³s⁻¹ used elsewhere by Knight in FSR teaching material.

Fig. 24 gives the comparison between the real data established by Price (1975) and the predicted $c \sim Q$ relationships using both CQVMB-2 & CQVMB-3 and the parameters shown in Table 1. This result shows that Runs A5 & C4 are in good agreement with the field data. This demonstrates that both models are capable of predicting the $c \sim Q$ relationship well, based on simple estimates of the geometry of the cross section and hydraulic characteristics of the river reach alone.

6.2 River Avon, Evesham to Tewkesbury

The second test reach was the Evesham-Pershore reach of the River Avon. The reach length was 18.2 km, and its average bed slope 0.41×10^{-3} . In a similar way to the previous case study, an average cross section of the main channel was also obtained through a trapezium schematisation based on the surveyed cross-sections, taken from the cross-section data file of an ISIS study for the River Avon by HR Wallingford. The following dimensions for the main channel were obtained from Fig. 25, using a trapezoidal approximation :

bed width	16.4 m
main channel depth	5.00 m
side slopes	1 : 1.97 (left side, vertical : horizontal)
	1 : 2.30 (right side, vertical : horizontal)

As detailed data about the area of the floodplain within the reach was not available, an average width was taken as 600 m, after another study at HR Wallingford using the FLOUT software package. The Manning roughness coefficients for the main channel and the floodplains were taken as 0.034 and 0.060 respectively. The calculated reach average bankfull discharge was estimated to be 182 m³s⁻¹.

Fig. 26 shows the field data (taken from Flucomp Manual, EX999, HR Wallingford) and the predicted $c \sim Q$ curves by both the CQVMB-2 and CQVMB-3 models using the parameters shown in Table 2. It can be seen that Runs A4 & C4 agree well with the field data, except for one anomalous inbank flow at around 50 m³s⁻¹. This point was affected by the many navigation structures along the river which reduce the effective hydraulic gradient for ordinary flows. Fig 26 again confirms that both models are appropriate under some conditions to predict $c \sim Q$ relationships based on the geometry and hydraulic characteristics of the river reach alone.

7. Guidance on how to determine the $c \sim Q$ relationship for natural rivers

7.1 Applicability of the VPMC method

As noted in Section 2, the diffusion wave model, which is the basis of the Muskingum-Cunge method is based on a simplified form of the St Venant equations (1) & (2). In other words the VPMC method ignores the inertial terms in the momentum equation, since they are often very small compared with the bed slope for floods in natural rivers. The criterion for using the VPMC

method therefore needs to be established first, prior to applying it. Although a complete theory for the analysis of the shallow water waves in channels with arbitrary cross-section does not exist, a condition for a division of the shallow water wave band has been analysed and developed by Lighthill & Whitham (1955), Ponce & Simons (1977), Ponce & Yevjevich (1978), Ponce, Li & Simons (1978), Ponce et al. (1996), Menendez & Norscini (1982) and Moussa & Bocquillon (1996), using the method of linear stability analysis. In practical terms the most useful criteria for the application of kinematic and diffusion models are those by Ponce, Li & Simons (1978).

Using linear perturbation analysis on a sinusoidal flood wave along a prismatic wide rectangular channel, Ponce, Li & Simons (1978) obtained the following criteria for an accuracy of at least 95% in the wave amplitude after one propagation period :

(i) *Application of the kinematic wave model*

$$TS_o(V_o/h_o) \geq 171 \quad (49)$$

in which T = wave period, S_o = bed slope and V_o & h_o = normal velocity and depth for the mean flow event [(i.e. $Q_o = (Q_{base} + Q_{peak})/2$]. In order to illustrate (49), values of $S_o = 0.001$, $h_o = 5$ m and $V_o = 1.0 \text{ ms}^{-1}$ are used in the following Table to indicate the limiting flood period, T , above which the kinematic wave model is valid (i.e. $T \geq 171h_o/(S_oV_o)$). Other figures can be readily constructed by simple multiplication/division.

h_o (m)	=	10	5	1
V_o (ms^{-1})	=	1	1	1
S_o	=	10^{-4}	10^{-3}	10^{-2}

\therefore greater than T (days/hrs)	=	197.9 days	9.9 days	4.75 hrs
--	---	------------	----------	----------

The figures show that the kinematic model is only suitable for long duration flood waves in large rivers with mild bed gradients, or for short duration floods in shallow channels with steep bed slopes (e.g. urban environment). Under these conditions it is likely that there will be little attenuation and the flood wave movement can be estimated by simple convection. However, for most practical purposes, it is unlikely that the criterion will be met and diffusion wave or full dynamic wave simulations will be required.

(ii) *Application of the diffusion wave model*

$$TS_o(g/h_o)^{1/2} \geq 31 \quad (50)$$

Strictly the number on the right hand side of (50) depends on the Froude number of the flow. Ponce gives a value of 45 for ($0.01 < Fr < 1.0$), but may be as low as 16 for the bandwidth of ($0.1 < Fr < 0.4$), but recommends the use of 31 for practical purposes. Applying (50) gives

h_o (m)	=	10	5	1
S_o	=	10^{-4}	10^{-3}	10^{-2}

\therefore greater than T (days/hrs)	=	3.62 days	6.15 hrs	0.27 hrs
--	---	-----------	----------	----------

These figures indicate that the diffusion wave model is much more applicable than the kinematic model, and that the restrictions on T are much less onerous. The diffusion model, including the VPMC method is therefore suited for a wider range of flood conditions. This is confirmed by Samuels (1989) who showed that (50) may be expressed in terms of a typical backwater length, L , where $L = 0.7h_0/S_0$, as

$$T \geq \approx 45 \frac{L}{V_0} Fr \quad (51)$$

For typical UK conditions, with $V_0 = 1.5\text{m/s}$, $L = 5\text{ km}$ and $Fr = 0.3$, this gives $T > 12$ hours, which lies within the range shown by the Table. The corresponding condition for the kinematic wave model is

$$T \geq \approx 250 \frac{L}{V_0} \quad (52)$$

Ponce's criterion (50) was checked by Abidin (1999), applied to the FSR (1975) rectangular channel data, solving the full St Venant equations (1) & (2), using the ISIS software. The FSR - 1975 channels were rectangular with a width of 50 m, Manning roughness of 0.035 and were 100 km in length. Fig. 27 shows the errors in amplitude using the VPMC method, in comparison with the St Venant solutions. The bed slope corresponding to Ponce Number criterion ($PN = 31$) was 0.000173 (for $T = 45$ hrs). From Fig. 27 it may be seen that the bed slope corresponding to a 5% difference in outflow peak between by St Venant and VPMC4-H is calculated to be 0.000177, confirming that $PN = 31$ is a suitable criterion for the applicability of the diffusion wave model. It should be also noted from Fig. 27 that the errors become very large once the criterion is broken. For example the errors could be up to 18% (28% for VPMC4-4) when they are used for a channel with a bed slope of 10^{-4} . This is one reason why within the RIBAMAN software there is a default minimum bed slope of 0.001, below which the VPMC method is not recommended. It is clear that this restriction should be replaced by the more appropriate technical condition, specified by (50). Errors in wave speed, as opposed to wave amplitude, will give slightly different limiting Ponce numbers. See Abidin (1999) for full details of these tests.

(iii) Application of the full dynamic wave equation model

Further studies of the VPMC method and its accuracy in compound channels have been undertaken by Abidin (1999), who examined overbank flow in many different channel configurations. Full St Venant solutions were again compared with the VPMC method within RIBAMAN and a particular study made of the influence of floodplain width and roughness. Ponce's criterion was again found to be satisfactory for all those cases studied, as a means of delineating the conditions under which the VPMC method is applicable.

7.2 Schematisation of river survey

The schematisation of the river cross section, including its floodplain, is an important element in constructing a mathematical simulation model of any 1-D flow, as well as in any flood routing procedure. It should not be treated just as a question of digitising numerous survey data, but rather as an art of blending the geometry and hydraulic features together in parallel. General rules for cross section location and the data requirements of 1-D models are given in Samuels (1990 & 1995) and Defalque et al. (1993). Detailed information on calibration criteria for 1-D models is given by Morris (1994) and Anastasiadou-Partheniou & Samuels (1998), boundary roughness

effects in routing models by Kawecki (1973) and the influence of lateral flow over a floodplain by Walton & Price (1975). Without an appreciation of these effects, any 1-D model is liable to be less accurate and useful than it might otherwise be, given the approximations already inherent in the 1-D approach. Quality assurance criteria should also not be neglected, as indicated by Seed, Samuels & Ramsbottom (1993).

There are a number of methods for schematising river cross-sections, as outlined by Seed (1997), but these are mainly related to low flow and sediment transport issues. For the purposes of flood routing, it is suggested that the main river channel be schematised by overlaying cross-section data at bankfull level, using the water surface as a common datum, and making lateral adjustments until all the main flow areas are roughly aligned. A simple schematic 5 point representation may then be made for most main river channel geometries, dividing the cross section into 4 linear elements as shown by the central region of Fig. 28. In many cases a 4 point representation may be sufficient, approximating the river cross-section as a simple trapezoidal channel. Indeed this method was used earlier for the Severn, Wye & Avon river reaches, shown in Figs 6, 23 & 25, and proved to be quite adequate. The aim should be to take a 'broad brush' approach, commensurate with the general features, and bearing in mind that the VPMC method only requires gross hydraulic features and is quite tolerant of this level of approximation. Likewise the floodplains should be treated by adding only 2 additional points per floodplain, as also indicated in Fig. 28. It is quite appropriate to divide floodplain areas by reach lengths to get an estimate of floodplain dimensions, as done for the River Wye. The simplest general overall shape of the cross-section should therefore be composed of 9 points, giving 8 sub-areas. Obviously where there are significant changes in floodplain or channel width, the compositing of several sections together will not be possible, and individual reaches may have to be specified. However, the aim should be to minimise the amount of data being used, bearing in mind the purpose to which they are put. This is in contrast to the amount of cross-section data normally required for river modelling, as for example collected through Section 105 surveys and used routinely within ISIS for producing flood risk maps.

Having obtained a schematic 'representative' cross-section for the reach, or collection of river reaches, the gross geometry then needs to be developed further for use in either of the following methods :

- (i) RIBAMAN method, by selection of the appropriate parameters, D1-D4, B1-B4
- (ii) new method, by selection of N1 to N3, and using equations (45) to (47)

The new method is the preferred method, in which curved boundaries are adopted, as illustrated in Fig. 18. Guidance about the choice of the various parameters required in (45) to (47) is as follows :

- 1) N1 should be around (2 to 4);
- 2) B_k should be around $(0.1 \text{ to } 0.5)B_f$, and affects the size of the initial isolated parts of flooding;
- 3) H_s corresponds to Q_s , which is typically $(0.3 \text{ to } 0.7) Q_{bf}$, depending on the floodplain interaction. Alternatively, for typical UK rivers, make $(H_c - H_s) \approx 0.1 \text{ m to } 0.5 \text{ m}$, depending on the bank top irregularities.
- 4) N2 should be around (1 to 4) and affects the slope of the transition part of the $c \sim Q$ curve
- 5) H_{fl} is approximately $(0.2 \text{ to } 0.8)H$, and affects the overbank part of the $c \sim Q$ curve
- 6) N3 should be around (2 to 4), and affects the lower part of the $c \sim Q$ curve

- 7) H_f is approximately $(0 \text{ to } 0.8)H$, and affects the transition part of the $c \sim Q$ curve
- 8) $B_1 \leq B_k \leq B_0$
- 8) B_k = average flooded floodplain width at bankfull stage

If however the RIBAMAN method is adopted, then the following guidance is given about the choice of the various parameters D1-D4 & B1-B4, shown in Fig. 16 :

Some of the parameters (B_1, B_2, B_3, D_1 & D_2) are based directly on the schematised cross-section and are identical to the geometric values. The simplified shape shown in Fig. 16 should be adopted for the net effect of left hand and right hand sided floodplains, provided the parameters D_2, D_3, D_4 & B_4 are compatible. The parameter B_3 is intended to be an estimate of the entire channel width, including left and right side floodplains, and Fig. 16 should not be construed as just representing an asymmetric channel. Where there are significant differences between each side, then individual left and right values are required, as specified in Fig. 17. As far as possible the schematic in Fig. 16 should be adopted. The parameter D_4 is likely to be $\sim (1/10)D_1$ and as Fig. 19 has shown, affects the beginning of the influence of the floodplain. B_4 affects the inundation width at bankfull, and should be chosen to represent regions of edge storage, such as small embayments or tributary inlets, as well as topographic features of the main channel. It is suggested that $B_4 \approx 0.1$ to 0.3 of the floodplain width ($B_3 - B_2$). D_3 is an important parameter, especially in relation to D_2 , as it affects the amount of floodplain storage (shaded area in Fig. 16). Its value should be chosen carefully, bearing in mind the amount of floodplain vegetation and likely dead zones on the floodplain caused by variability in floodplain geometry. Both these factors will tend to increase the value of D_3 .

7.3 Derivation of $c \sim Q$ relationship from cross section survey

Having obtained a schematic cross-section for the reach, or collection of river reaches, using linear or curved functions, the geometry may then be used directly in one of the following 4 methods :

- (i) RIBAMAN method, with fixed boundaries D1-D4 & B1-B4
- (ii) new method (CQOB-4), with fixed boundaries and (45) to (47)
- (iii) vertical moving boundary method No. 1 (CQVMB-2), and (48)
- (iv) vertical moving boundary method No. 2 (CQVMB-3), and (45) to (47)

Of these 4 methods, the last one, (iv), is the preferred method, since it gives the smoothest $c \sim Q$ relationship. This preferred method uses a vertical moving boundary, together with curved floodplain and conveyance boundaries, as specified in the previous section, 7.2. The other methods, (i) - (iii), are listed for completeness, as being alternative methods that are useful and give reasonable results, albeit with some limitations. Some of the irregularities can be smoothed out in ISIS by choosing spline interpolation through a reduced number of data points.

The vertical moving boundary method (No. 2, coded CQVMB-3) has been described in detail in Section 5.2.3. In this method the moving boundary alters both the storage and conveyance width as the depth of flow increases on the floodplain. The method will generate smooth $c \sim Q$ curves, as indicated by the examples shown in Fig. 21.

8. Conclusions

(i) Governing equations

1. A generalised diffusion wave equation, (20), with the inertial terms included, has been derived. This may be reduced to 4 sub-models, with the non-inertial model giving the best approximation to the full inertial model for natural rivers.

2. The VPMC method, which is based upon the diffusion wave model, (5), is shown to be restricted by the condition $PN \geq 31$, where $PN = \text{Ponce number} = TS_0(g/h_0)^{1/2}$.

3. The effects of the longitudinal pressure gradient term, $\partial h/\partial x$, on wave speed and attenuation may be included in the VPMC method by the technique suggested by Cappelaere. The correction factor *cor*, defined in (28), may be used to modify both the wave speed and diffusion coefficient, c & D , defined in (6) & (7), for use in the more general form (29), by using (33) & (34).

4. Cappelaere's technique has been developed further by the introduction of a factor μ in (34), which defines *cor*. Optimum results for volume conservation, for those cases tested, were obtained with $\mu = 0.4$ (inbank flow) and $\mu = 0.2$ (overbank flow). However, these μ values should be treated with caution until further testing is carried out for a wider range of channel shapes.

5. A new analytical solution has been given to (5) by Tang (1999), for constant coefficients, c & D .

(ii) Numerical experiments

6. A wide range of inbank and overbank flows have been routed down sufficiently long channels with prismatic sections to provide benchmark solutions for the VPMC method.

7. A proof that the VPMC method does not conserve volume is presented. Volume losses (up to 8%) occur in most standard VPMC schemes. The loss may be considerably reduced by choosing an alternative routing scheme, such as the VPMC4-H scheme.

8. It has been shown that 4 point averaging is superior to 3 point averaging for evaluating mean values of the non-linear terms. The VPMC4-H scheme, with routing parameters c and D modified to account for the effect of the longitudinal hydrostatic pressure gradient term, has been shown to give the best results.

9. Two empirical formulae have been presented for the amount of volume loss when the VPMC4-H method is used. Figs 10 and 14 show that volume loss is small for both inbank flow ($< 0.5\%$) and overbank flow ($< 1\%$) when $S_0 \geq 0.0001$.

10. The leading edge dip can be eliminated by selection of appropriate selection of space and time steps according to (15). Elimination of the dip implies that the coefficient C_2 in the Muskingum-Cunge method remains positive, and that the weighting coefficient, ε , is positive.

11. Some unrealistic oscillations were found to occur in the recession stage of the outflow when the channel bed slope is steep, as shown by Figs 11 & 13. They may be eliminated by applying (19).

(iii) Link between $c \sim Q$ relationship and cross-section geometry

12. For inbank flow, the wave speed, c , is related to the mean cross-section velocity, V , as indicated by (38), (41) & (43). For all the simple channel shapes shown in Fig. 1, the $c \sim Q$ relationship is a single power functional curve, which implies that the kinematic wave speed increases as the discharge increases or the stage rises.

13. For overbank flow, the $c \sim Q$ relationship is more complex and no longer a single monotonic curve. The wave speed typically increases to a maximum value at around 2/3 of bankfull flow, then drops steeply to a minimum value at a low floodplain depth, and thereafter gradually increases with discharge as the floodplain becomes more inundated. A typical $c \sim Q$ relationship is then generally that of two power functions, one for the main channel flow and another for the floodplain flow, linked by an S-type transition curve, as shown in Figs 4 & 5.

14. In overbank flow the floodplain storage may be accounted for by distinguishing between that part of the cross-section which is used for conveyance, and that part in which no flow occurs and is essentially just a dead zone. Discriminating between the two is readily achieved by writing (6) as (14). It therefore follows that the cross section of any river channel must be partitioned according to some set of rules or procedure, following schematisation of the geometry.

(iv) Practical application to flood routing

15. A method of schematising river survey for input into a VPMC model is described in detail in Section 7.2. A schematic cross-section may be developed either by the RIBAMAN method, using linear elements as shown in Fig. 16, or by the new method, using curved boundaries as shown in Fig. 18 and through equations (45) to (47). The curved boundary option gives a smoother $c \sim Q$ relationship and is therefore the preferred method.

16. A 'broad brush' approach should be taken in defining the 'representative' geometry of the river cross-section(s), commensurate with the general features of the routing reach(es). The simplest general cross-sectional shape is that shown in Fig. 28, with 8 linear elements. It is quite appropriate to divide floodplain areas by reach lengths to get an estimate of floodplain widths. It should be borne in mind that the VPMC method only requires gross hydraulic features and is quite tolerant of this level of approximation. In many instances, the main river channel may be approximated by a trapezoidal section, as adopted herein for the Severn, Wye & Avon river reaches, shown in Figs 6, 23 & 25.

17. Four methods have been given in Section 7.3 to account for floodplain storage. The preferred method is one based on a vertical moving boundary, using the curved boundary option in the new method, described in detail in Section 5.2.3. Guidance about the selection of parameters $N1$ to $N3$ and related parameters in (45) & (47), required in the CQVMB-3 model, is given in Section 7.2.

18. Cross section survey data from reaches of the River Wye and River Avon have been used to predict the $c \sim Q$ relationship over a wide range of inbank and overbank flows. Figs 24 & 26 show that the results compare favourably with measured wave speed data, thus indicating that the $c \sim Q$ relationship may be derived from cross-section survey.

19. The methodology for predicting the $c \sim Q$ relationship greatly reduces the reliance upon field data, which are usually difficult to collect over a sufficiently wide range of discharges to build up

a picture of the entire $c \sim Q$ curve. The proposed method has particular relevance to ungauged rivers and where flood estimates are required at a catchment scale.

20. The new method for predicting wave speed is restricted to cases where there is little lateral inflow and no hydraulic structures within the routing reach. Where these are important, it is suggested that routing using the St Venant equation is undertaken.

21. The 2 objectives set out in Section 1.2 for this research have been met.

(v) Recommendations for further research

1. Testing of the new method against a wider selection of routed floods in natural rivers for which there are good $c \sim Q$ data.
2. A study of the effect of different stage-discharge calculation methods for overbank flow on flood routing behaviour.
3. A study of the adjustment factor, μ , including the development of an automated algorithm for finding μ for flows in channels of any shape.
4. Investigation of the various parameters required in (45) to (47) to schematise a cross-section, and how they may be applied to natural river data.
5. Inclusion of the effect of lateral inflow on wave speed and attenuation for benchmarked cases through the additional coefficient C_4 in the Muskingum-Cunge method.

Acknowledgements

The Author is grateful to MAFF for co-sponsoring this research programme over a three year period from commission FD0101 at HR Wallingford. He is especially indebted to Dr Xiaonan Tang for his sustained effort and computational work in bringing this research to a successful conclusion. He is also grateful to Dr Paul G Samuels, of HR Wallingford, for his many helpful comments during the course of this research work. Finally he wishes to thank the School of Civil Engineering at the University of Birmingham for awarding Dr Tang a Postgraduate Teaching Assistant post for the duration of this programme, thus enabling him to undertake the work.

Publication of this report does not necessarily imply endorsement by MAFF of the conclusions and recommendations.

References

- Abidin, M.R.Z., 1999, "Hydrological and hydraulic sensitivity analyses for flood modelling with limited data", PhD thesis, The University of Birmingham.
- Ackers, P., 1992, "Hydraulic design of two stage channels", *Proc. Instn Civ. Engrs Wat., Marit. & Energy*, 96, Dec., Paper No. 9988, pp 247-257.
- Ackers, P., 1993, "Flow formulae for straight two-stage channels", *Journal of Hydraulic Research*, IAHR, Vol. 31, No. 4, pp 509-531.
- Ackers, P., 1993, "Stage-discharge functions for two-stage channels: the impact of new research", *Journal of the Institution of Water and Environmental Management*, Vol. 7, No. 1, February, pp 52-61.
- Anastasiadou-Partheniou, L. and Samuels, P.G., 1998, "Automatic calibration of computational river models", *Proc. Instn Civ. Engrs Wat., Marit. & Energy*, 130, Issue 3, Sept., Paper No. 11665, pp 154-162.
- Anderson, M.G., Walling D.E.S., & Bates, P.D., 1996, *Floodplain Processes*, J. Wiley. pp 1-658.
- Archer, N., 1993, "Discharge estimate for Britain's greatest flood : River Tyne, 17th November 1771" *BHS 4th National Hydrology Symposium*, Cardiff, pp 4.1- 4.6.
- Ashworth, P.J., Bennett, S.J., Best, J.L. and McLelland, S.J., 1996, "Coherent flow structures in open channels", J Wiley, pp 1-733.
- Atabay, S. and Knight, D.W., 1999, "Stage discharge and resistance relationships for laboratory alluvial channels with overbank flow", In *River Sedimentation* [Eds A W Jayawardena, J H W Lee & Z Y Wang], *Proc. Seventh International Symposium on River Sedimentation, Hong Kong, December 1998*, pp 223-229.
- Bedient, P.B. and Huber, W.C., 1988, "Hydrology and floodplain analysis", Addison-Wesley, Reading, Massachusetts.
- Cao, S. and Knight, D.W., 1996, "Regime theory of alluvial channels based upon the concepts of stream power and probability", *Proc. Instn. of Civil Engineers, Water, Maritime and Energy Division*, London, Vol. 118, Sept., Paper No. 11029, pp 160-167.
- Cappelaere, B., 1997, "Accurate diffusive wave routing", *Journal of Hydraulic Engineering*, ASCE, Vol. 123, No. 3, March, pp 174-181.
- Cunge, J.A., 1969, "On the subject of a flood propagation computation method (Muskingum method)", *Journal of Hydraulic Research*, IAHR, Vol. 7, No. 2, pp 205-230.
- Cunge, J.A., Holly, F.M., and Verwey, A., 1980, "Practical aspects of computational river hydraulics", Pitman, London.
- Defalque, A., Wark, J.B., and Walmsley, N., 1993, "Data density in 1-D river models", *HR Wallingford*, Internal Report, SR 353, March pp 1-20.
- Henderson, F.M., 1966, "Open channel flow", Macmillan, New York.
- ISIS, 1995, "ISIS Flow - User Manual, Version 1.3", Beta release, Halcrow/HR Wallingford, UK.
- Kawecki, M.W., 1973, "Boundary roughness for natural rivers", *HR Wallingford*, Report, INT 120, October, pp 1-28.
- Knight, D.W., and Demetriou, J.D., 1983, "Flood plain and main channel flow interaction", *Journal of Hydraulic Engineering*, ASCE, Vol. 109, No. 8, August, pp 1073-1092.
- Knight, D.W., Shiono, K., and Pirt, J., 1989, "Prediction of depth mean velocity and discharge in natural rivers with overbank flow", *Proc. Int. Conf. on Hydraulic and Environmental Modelling of Coastal, Estuarine and River Waters*, (Ed. R. A. Falconer et al.), University of Bradford, Gower Technical Press, Paper 38, pp 419-428.
- Knight, D.W., 1989, "Hydraulics of flood channels", in *Floods : Hydrological, sedimentological and geomorphological implications* (Ed K Beven), Chapter 6, J. Wiley, pp 83-105.
- Knight, D.W. and Shiono, K., 1990, "Turbulence measurements in a shear layer region of a compound channel", *Journal of Hydraulic Research*, IAHR, Vol. 28, No. 2, 1990, pp 175-196, (Discussion in *IAHR Journal*, 1991, Vol. 29, No. 2, pp 259-276).
- Knight, D.W., Yuen, K.W.H. and Alhamid, A.A.I., 1994, "Boundary shear stress distributions in open channel flow", in *Physical Mechanisms of Mixing and Transport in the Environment*, (Ed. K. Beven, P. Chatwin & J. Millbank), J. Wiley,
- Knight, D.W., and Abril, B., 1996, "Refined calibration of a depth averaged model for turbulent flow in a compound channel", *Proc. Instn of Civil Engineers, Water, Maritime and Energy*, (submitted for publication), pp 1-14.
- Knight, D.W., 1996, "Issues and directions in river mechanics - closure of sessions 2, 3 and 5", In *Issues and directions in hydraulics*, [Ed T Nakato & R Ettema], An Iowa Hydraulics Colloquium in honour of Professor John F Kennedy, Iowa Institute of Hydraulic Research, Iowa, USA, Balkema, pp 435- 462.
- Knight, D.W. and Shiono, K., 1996, "River channel and floodplain hydraulics", in *Floodplain Processes*, (Eds Anderson, Walling & Bates), Chapter 5, J Wiley, pp 139-181.
- Knight, D.W., 1999, "Flow mechanisms and sediment transport in compound channels", *Proc. 1st Sino-US Workshop on Sediment Transport and Disasters*, 15-17 March, Special Issue of *International Journal of Sediment Research*, [Eds Z. Y. Wang, T. W. Soong & B.C. Yen], Vol. 14, No. 2, Beijing, China, pp 217-236.
- Knight, D.W., and Samuels, P.G., 1999, "Localised modelling of bridges, sluices and hydraulic structures under flood flow conditions", MAFF Conference of River and Coastal Engineers, Keele University, July, pp 1-10.
- Koussis, A.D., 1983, "Unified theory for flood and pollution routing", *Journal of Hydraulics Division*, ASCE, Vol. 109, No. 12, December, pp 1652-1664.
- Lambert, M.F. and Myers, W.R.C., 1998, "Estimating the discharge capacity in straight compound channels", *Proc. Instn. of Civil Engineers, Water, Maritime and Energy Division*, London, Vol. 130, June, pp 84-94.

- Lighthill, M.J. and Whitham, G.A., 1955, "On kinematic waves : 1. Flood movement in long rivers", *Proc. Roy. Soc., London*, Series A, Vol. 229, pp 281-316.
- Menendez, A.N. and Norscini, R., 1982, "Spectrum of shallow water waves : an analysis", *Journal of Hydraulics Division*, ASCE, Vol. 108, No. 18, January, pp 75-93.
- Morris, M.W., 1994, "Calibration criteria for 1D river models", *HR Wallingford*, Internal Report, SR 391, May, pp 1-31
- Moussa, R. and Bocquillon, C., 1996, "Criteria for the choice of flood routing methods in natural channels", *Journal of Hydrology*, Vol. 186, pp 1-30.
- Myers, W. R. C., Cassells J., Knight, D.W. & Brown, F.A., 1999, "Resistance coefficients for inbank and overbank flows", *Proc. Instn. of Civil Engineers, Water, Maritime and Energy Division*, London, Vol. 138, June, pp 105-115.
- NERC, 1975, "Flood Studies Report", Vols 1-5, Natural Environmental Research Council, NERC, Swindon, UK..
- Perumal, M., 1994, "Hydrodynamic derivation of a variable parameter Muskingum method. II Verification", *Hydrological Sciences Journal*, Oxford, UK, Vol. 39(5), pp 443-458.
- Ponce, V.M. and Simons, D.B., 1977, "Shallow wave propagation in open channel flow", *Journal of Hydraulics Division*, ASCE, Vol. 103, No. 12, December, pp 1461-1476.
- Ponce, V.M. and Yevjevich, V., 1978, "Muskingum-Cunge methods with variable parameters", *Journal of Hydraulics Division*, ASCE, Vol. 104, No. 12, December, pp 1663-1667.
- Ponce, V.M., Li, R.M. and Simons, D.B., 1978, "Applicability of kinematic and diffusion models", *Journal of Hydraulics Division*, ASCE, Vol. 104, No. HY3, March, pp 353-360.
- Ponce, V.M. and Theurer, F.D., 1982, "Accuracy criteria in diffusion routing", *Journal of Hydraulics Division*, ASCE, Vol. 108, No. HY6, June, pp 747-757.
- Ponce, V.M. and Chaganti, P.V., 1994, "Muskingum-Cunge method revised", *Journal of Hydrology*, Vol. 163, pp 433-439.
- Ponce, V.M., Lohani, A.K. and Scheyging, C., 1996, "Analytical verification of Muskingum-Cunge routing", *Journal of Hydrology*, Vol. 174, pp 235-241.
- Price, R. K., 1978, "A river catchment flood model", *Proc. Instn. of Civil Engineers*, London, Vol. 65, Paper 8141, September, pp 655-668.
- Price, R. K., 1973, "Flood routing methods for British rivers", *Proc. Instn. of Civil Engineers*, London, Vol. 55, Paper 7674, December, pp 913-930.
- Price, R. K., 1985, "Flood routing ", in *Developments in Hydraulic Engineering -3* (Ed. P Novak), Elsevier, pp 129-173.
- RIBAMAN, 1994, "River Basin Management Software User Manual", Version 1.22A, July, HR Wallingford.
- Samuels, P.G., 1989, "Backwater length in rivers", *Proc. Instn. Civ. Engrs*, Part 2, Vol. 87, December, pp 571-582.
- Samuels, P.G., 1990, "Cross-section location in 1D models", *Proc. Int. Conf. on River Flood Hydraulics*, (Ed. W.R. White), Wallingford, September, J. Wiley & Sons, Paper K1, pp 339-348.
- Samuels, P.G., 1995, "Uncertainty in flood level prediction", *HYDRA 2000*, Proc. 26th IAHR Congress, London, (Ed. A Irvine), Vol. 1, Paper 1D12, pp 567-572.
- Seed, D.J., Samuels, P.G., and Ramsbottom, D.M., 1993, "Quality assurance in computational river modelling", *HR Wallingford*, Report, SR 374, October, pp 1-29.
- Seed, D.J., 1997, "Lateral variations of sediment transport in rivers", *HR Wallingford*, Report, SR 454, March, pp 1-25.
- Shiono K. & Knight, D.W., 1990, "Mathematical models of flow in two or multi stage straight channels", *Proc. Int. Conf. on River Flood Hydraulics*, (Ed. W.R. White), J. Wiley & Sons, Wallingford, September, Paper G1, pp 229-238.
- Shiono, K. and Knight, D.W., 1991, "Turbulent open channel flows with variable depth across the channel", *Journal of Fluid Mechanics*, Vol. 222, pp 617-646 (and Vol. 231, October, p 693).
- Shiono, K., Muto, Y., Knight, D.W., and Hyde, A.F.L., 1999, "Energy losses due to secondary flow and turbulence in meandering channels with overbank flow", *Journal of Hydraulic Research*, IAHR, (in press).
- Sivapalan, M., Bates, B.C. and Larsen, J.E., 1997, "A generalised, non-linear, diffusion wave equation : theoretical development and application", *Journal of Hydrology*, Vol. 192, pp 1-16.
- Tang X., 1999, "Derivation of the wave speed-discharge relationship from cross section survey for use in approximate flood routing methods", PhD thesis, The University of Birmingham.
- Tang, X., Knight, D.W. and Samuels, P.G., 1999a, "Volume conservation in variable parameter Muskingum-Cunge method", *Journal of Hydraulic Engineering*, ASCE, Vol. 125, No. 6, pp 610-620.
- Tang, X., Knight, D.W. and Samuels, P.G., 1999b, "Variable parameter Muskingum-Cunge method for flood routing in a compound channel", *Journal of Hydraulic Research*, IAHR, Vol. 37, No. 5, pp 1-24.
- Tang, X., Knight, D.W. and Samuels, P.G., 2000, "Wave speed-discharge relationship from cross section survey", *Journal of Water & Maritime Engineering*, Proc. Instn. Civil Engrs, joint ICE/IAHR, (submitted for publication).
- Walton, R. and Price, R.K., 1975, "Influence of lateral flow over a flood plain on flood waves", *HR Wallingford*, Internal Report, INT 140, March, pp 1-25.
- Weinmann and Laurenson, 1979, "Approximate flood routing methods : a review", *Journal of Hydraulics Division*, ASCE, Vol. 105, No. HY12, December, pp1521-1536.
- Weinmann and Laurenson, 1981, "Closure to "Approximate flood routing methods : a review", *Journal of Hydraulics Division*, ASCE, Vol. 107, No. HY9, September, pp 1112-1114.
- Wong, T.H.F. and Laurenson, E.M., 1983, "Wave speed-discharge relations in natural rivers", *Water Resources Research*, Vol. 19, No. 3, March, pp 701-706.
- Wong, T.H.F. and Laurenson, E.M., 1984, "A model of flood wave speed-discharge characteristics of rivers", *Water Resources Research*, Vol. 20, No. 12, December, pp 1883-1890.

Yuen, K.W.H. and Knight, D.W., 1990, "Critical flow in a two stage channel", *Proc. Int. Conf. on River Flood Hydraulics*, (Ed. W.R. White), Wallingford, September, J. Wiley & Sons, Paper G4, pp 267-276.

CQVMB-3	CQOB-4	B_0/B_f	H_f/H	N2	H_{ff}/H	N3
C1	D1	1/5	1/4	1	1/3	1
C2	D2	"	"	4	"	2
C3	D3	"	1/3	1	"	1
C4	D4	"	1/5	1	1/5	1
Notes		$Q_s/Q_{bf} = 1/2, N1 = 3$ & $B_k = B_0$				

Table 1. Values of parameters used in comparing two models, CQVMB-3 & CQOB-4, for predicting the $c \sim Q$ relationship with $B_1 = 0$

Run	B_k/B_f	Q_s/Q_{bf}	N1	B_0/B_f	H_f/H	N2	H_{ff}/H	N3
Erwood - Belmont								
A5	1/5	0.3	2	1/5	0.65	3.5	-	-
C4	"	"	"	"	1/6	1.5	4/5	2.5
Evesham - Pershore								
A4	2/9	0.3	2	1/4	3/4	1.5	-	-
C4	"	"	"	"	1/4	"	1/3	2

Table 2. Values of parameters used in predicting $c \sim Q$ relationships for the Wye and Avon Rivers

LIST OF FIGURES

- Fig. 1 Typical shapes of channel cross-sections with inbank flow
- Fig. 2 A typical schematised compound channel with overbank flow, showing the area method for calculating the discharge
- Fig. 3 A typical natural compound channel with overbank flow, showing the sub-division methods for calculating the discharge
- Fig. 4 Typical kinematic wave speed-discharge and attenuation-discharge curves
- Fig. 5 Example of wave speed-discharge curve for River Wye, Erwood to Belmont reach (after NERC, 1975)
- Fig. 6 Cross section of River Severn at Montford bridge (after Knight et al., 1989)
- Fig. 7 Variation of Manning's n with depth for overbank flow at Montford bridge, River Severn (after Knight et al., 1989)
- Fig. 8 Outflow hydrographs by VPMC4-4 for flow in a 50m wide rectangular channel at different bed slopes [from Tang, Knight & Samuels (1999a)]
- Fig. 9 Computational grid cell
- Fig. 10 Volume loss for inbank flows using VPMC4-4 and VPMC4-H schemes
- Fig. 11 Routed hydrographs for overbank flow, with variable peak to bankfull flow ($Q_p/Q_{bf} = 1.25, 2.0 \text{ \& } 3.0$)
- Fig. 12 Routed hydrographs for overbank flow, with variable bed slope ($S_o = 0.003, 0.0015, 0.0008 \text{ \& } 0.0003$)
- Fig. 13 Routed hydrographs for overbank flow, with variable floodplain roughness ($n_f = 0.090, 0.120 \text{ \& } 0.150$, with $n_c = 0.030$)
- Fig. 14 Volume loss for overbank flows using VPMC4-4 and VPMC4-H schemes
- Fig. 15 Schematic representation of storage for overbank flow
- (a) the RIBAMAN method with linear boundaries
 - (b) the modified RIBAMAN method with curved boundaries
 - (c) The moving boundary method
- Fig. 16 Schematic compound cross section used in RIBAMAN
- Fig. 17 General schematic compound cross section (RIBAMAN style)
- Fig. 18 Schematic compound cross section as used in CQOB-4, CQVMB-2 & CQVMB-3
- Fig. 19 Comparison of $c \sim Q$ curves for variable D4 by RIBAMAN method (with $D2 = 0.1 \text{ m}$, $D3 = 0.3 \text{ m}$ and $D4 = 0, 0.15, 0.3 \text{ \& } 0.4 \text{ m}$)

- Fig. 20 Comparison of $c \sim Q$ curves for variable B_3 by RIBAMAN method (with $D_2 = 0.1$ m, $D_3 = D_4 = 0.3$ m and $B_3 = 25, 32, 38, 48$ & 58 m)
- Fig. 21 Comparison of $c \sim Q$ curves by CQVMB-3 (Runs C1-C4) and CQOB-4 (Runs D1-D4)
- Fig. 22 Comparison of dead storage volumes of floodplain by CQVMB-3 (Runs C1-C4) and CQOB-4 (Runs D1-D4)
- Fig. 23 Cross sections of River Wye, Erwood to Belmont reach
- Fig. 24 Comparison of predicted and actual $c \sim Q$ relationships for River Wye, Erwood to Belmont reach
- Fig. 25 Cross sections of River Avon, Evesham to Pershore reach
- Fig. 26 Comparison of predicted and actual $c \sim Q$ relationships for River Avon, Evesham to Pershore reach
- Fig. 27 Relationship between amplitude error (St Venant - VPMC) and bed slope applying Ponce's criterion (FSR channel, $Q = 500$ m³s⁻¹)
- Fig. 28 General schematic cross-section composed of 8 linear elements

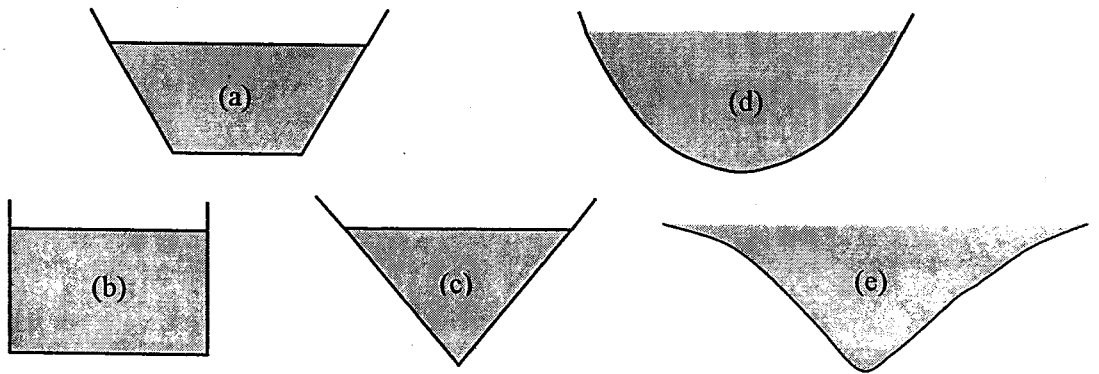


Fig.1 Typical simple cross-sectional shapes with inbank flow

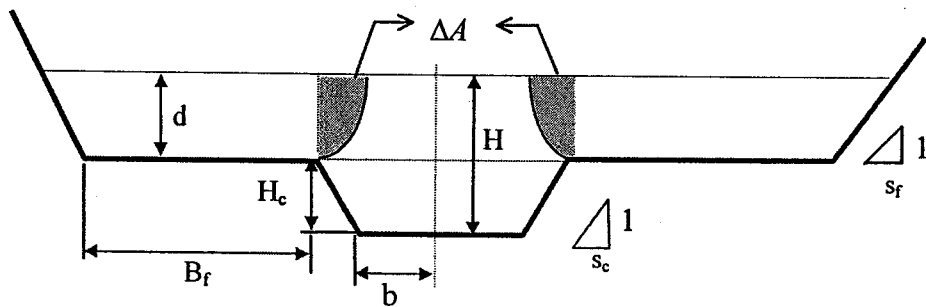


Fig.2 A typical schematized compound channel with overbank flow, showing the area method for calculating the discharge

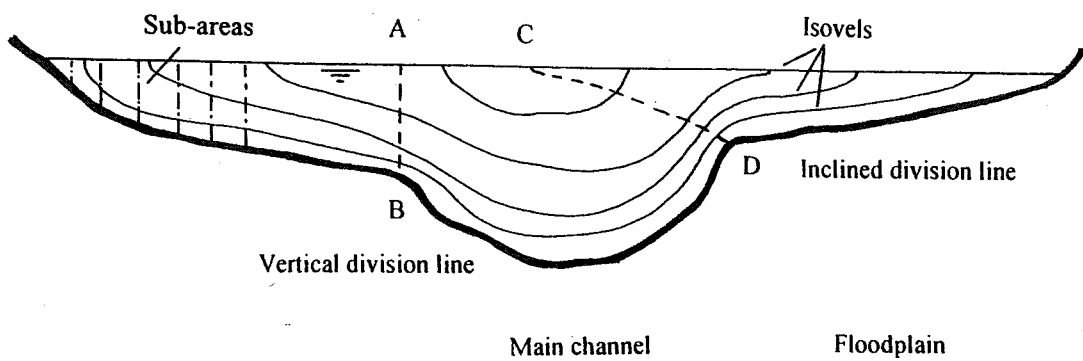


Fig.3 A typical natural compound channel with overbank flow, showing the sub-division methods for calculating the discharge

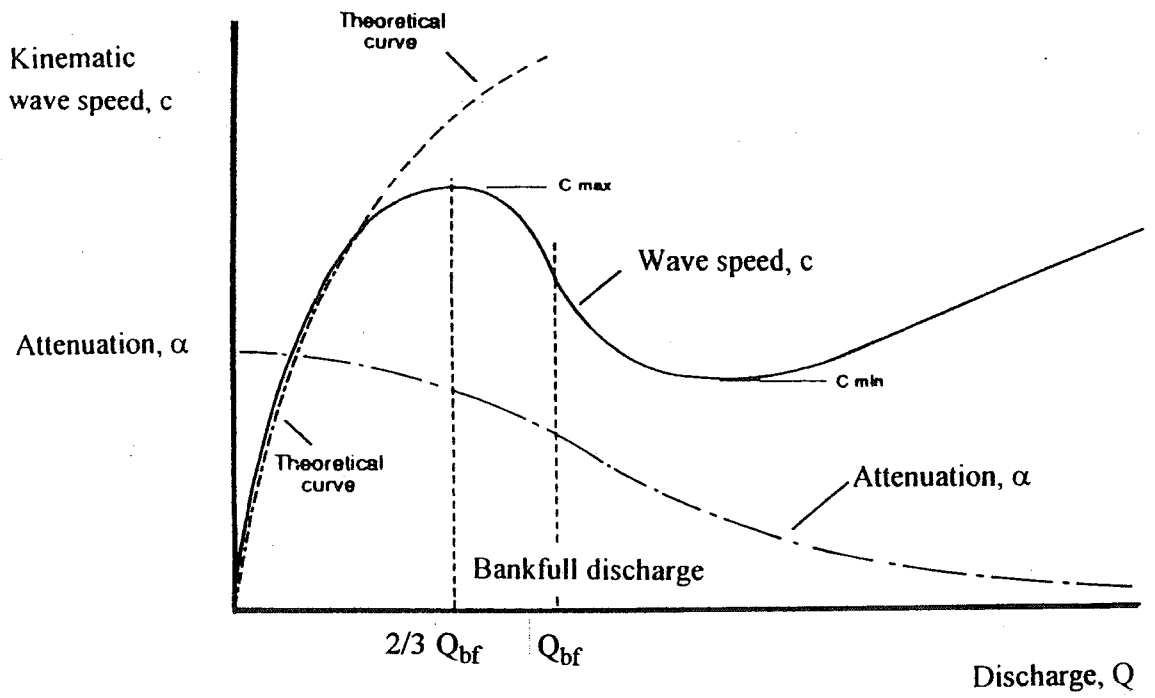


Fig. 4 Typical kinematic wave speed-discharge and attenuation-discharge curves

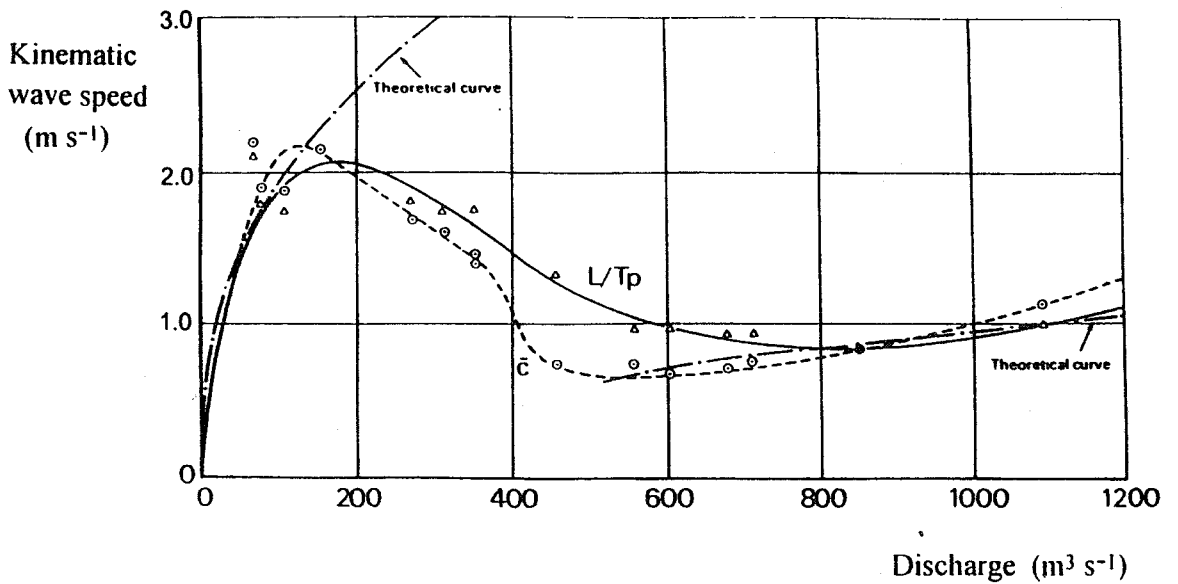


Fig. 5 Example of wave speed-discharge curve for River Wye, Erwood to Belmont reach (after NERC, 1975)

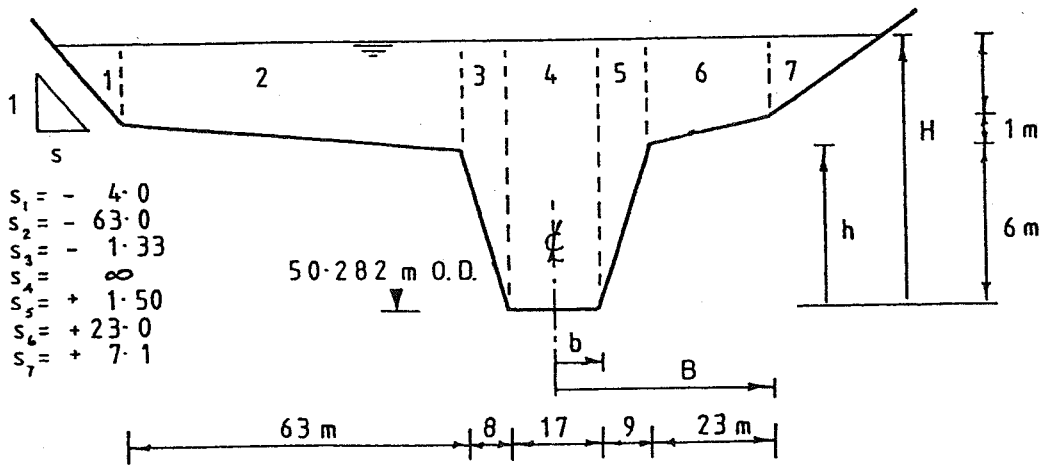


Fig. 6 Cross section of River Sever at Montford bridge (after Knight et al., 1989)

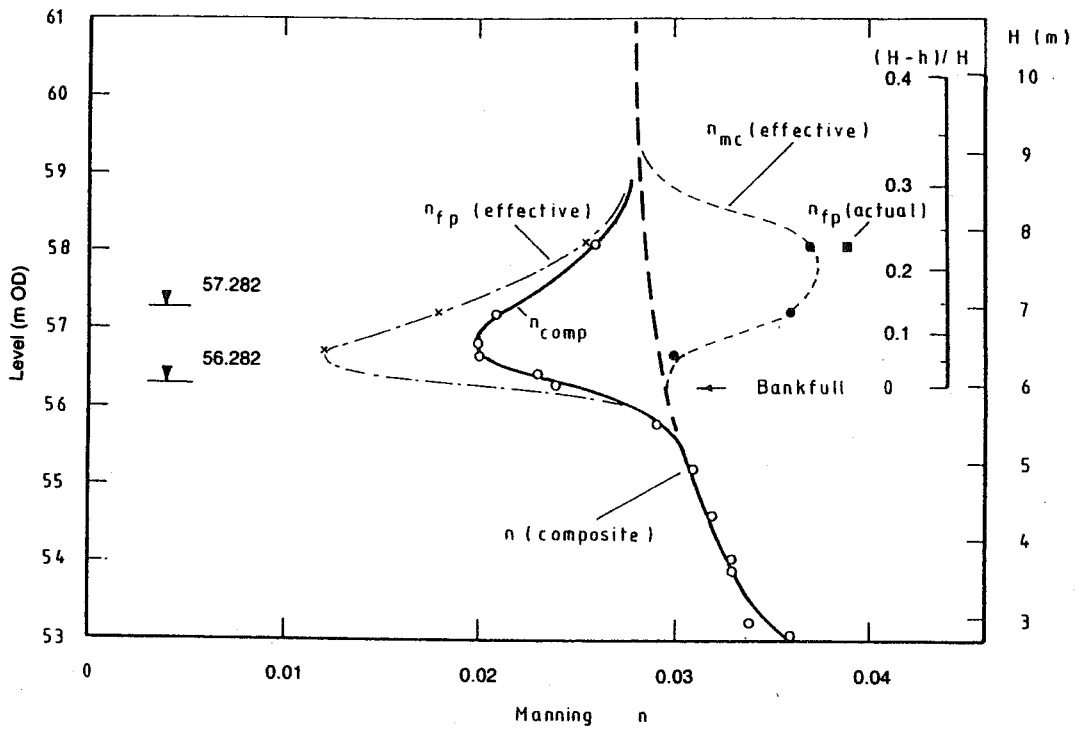


Fig. 7 Variation of Manning's n with depth for overbank flow at Montford bridge, River Sever (after Knight et al., 1989)

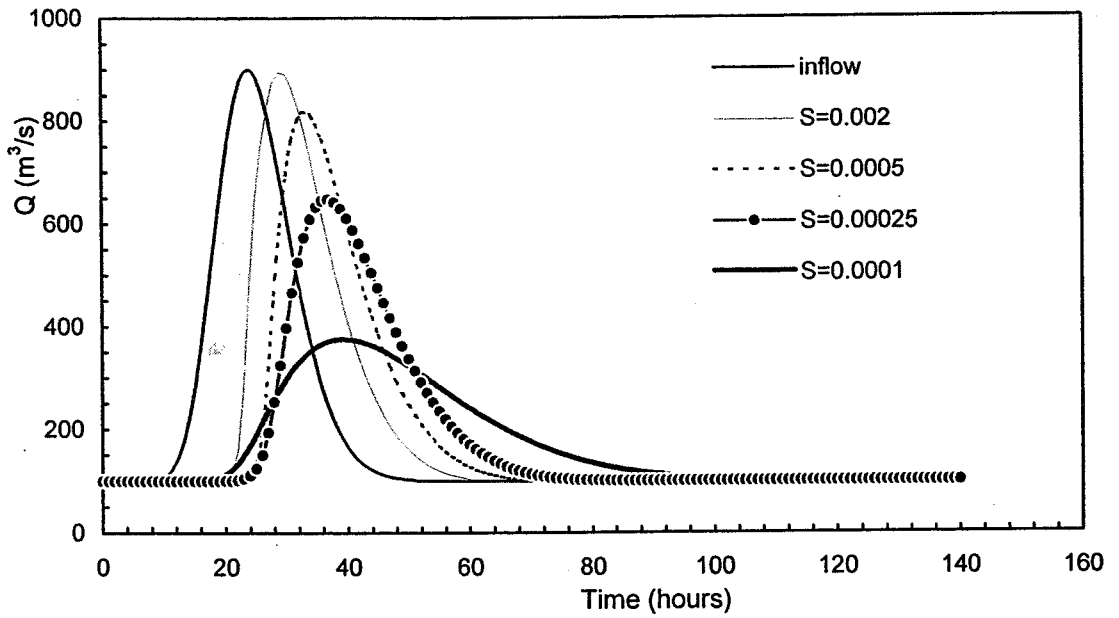


Fig.8 Hydrographs of outflows by VPMC4-4 for flow in a 50m wide rectangular channel at different bed slopes (from Tang, Knight & Samuels, 1999a)

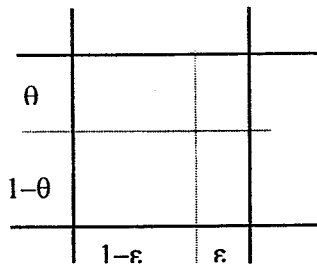


Fig.9 Computational grid cell

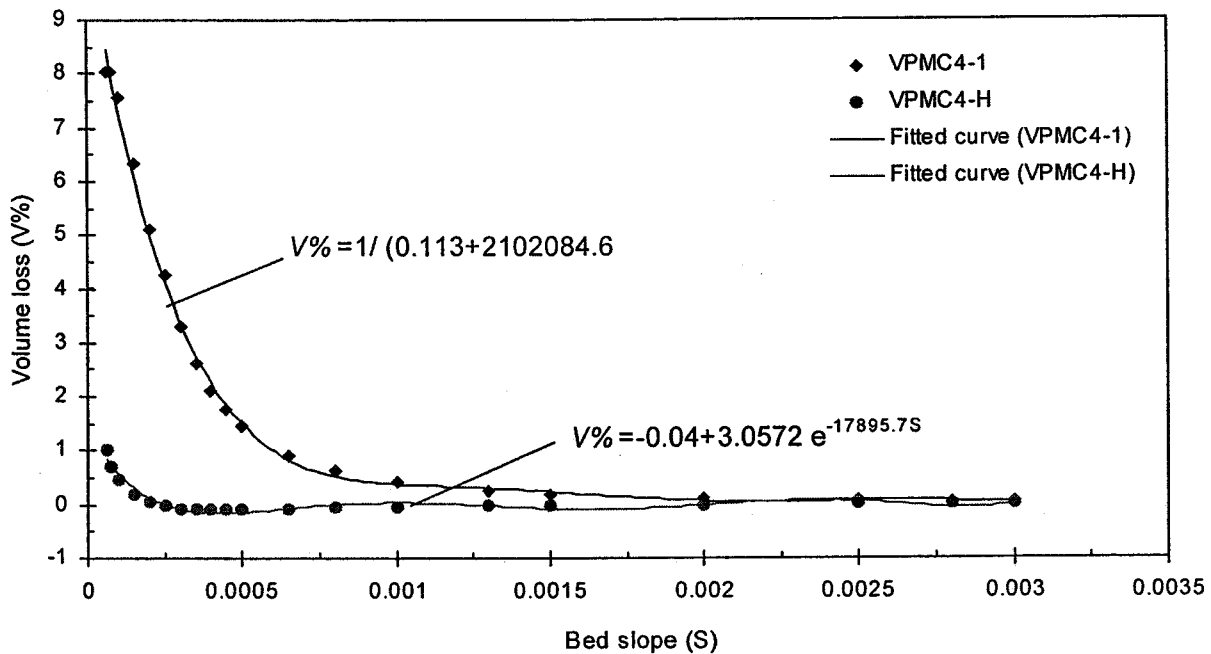


Fig.10 Volume loss for inbank flows using VPMC4-4 & VPMC4-H

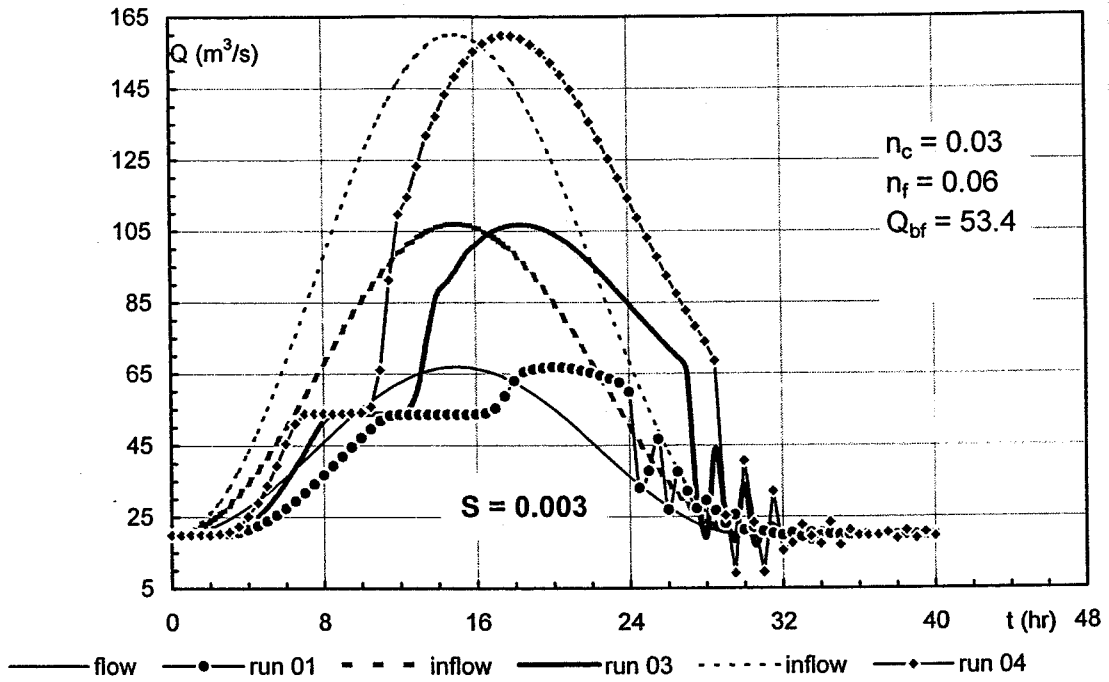


Fig.11 Routed hydrographs for overbank flow, with variable peak to bankfull flow ($Q_p/Q_{bf}=1.25, 2, 3$)

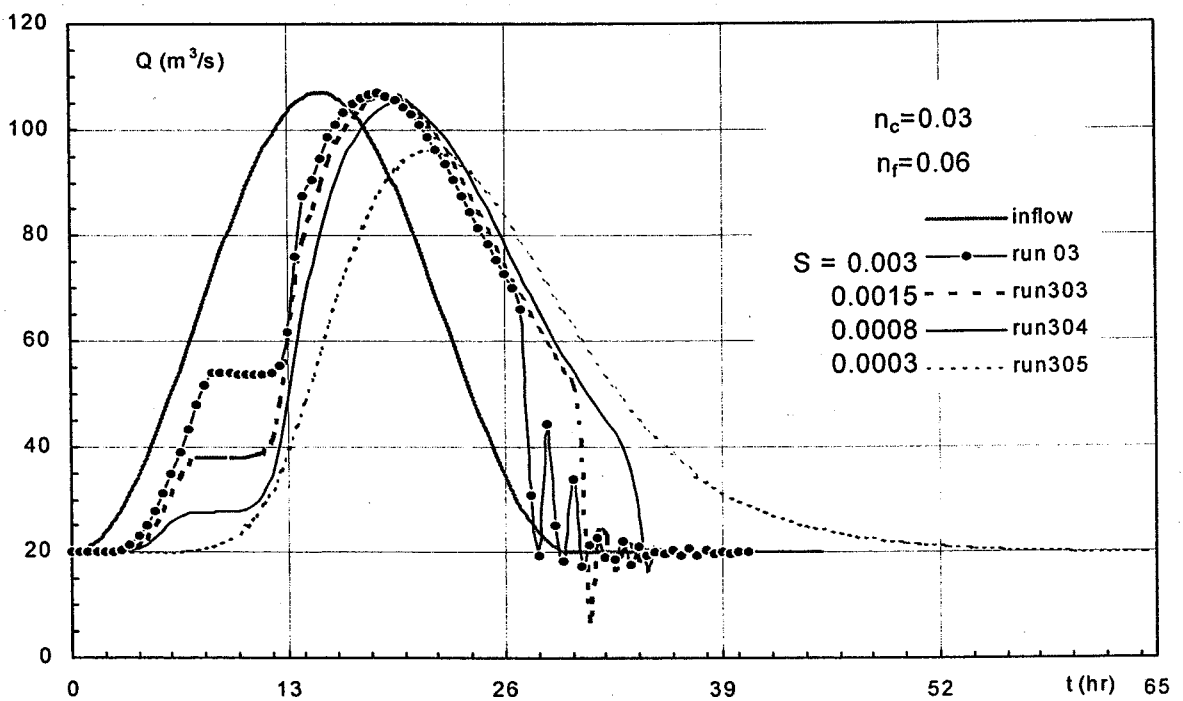


Fig.12 Routed hydrographs for overbank flow, with variable bed slopes ($S_0 = 0.003, 0.0015, 0.0008$ & 0.0003 for $Q_p = 107 m^3/s$ and $n_f = 0.06$)

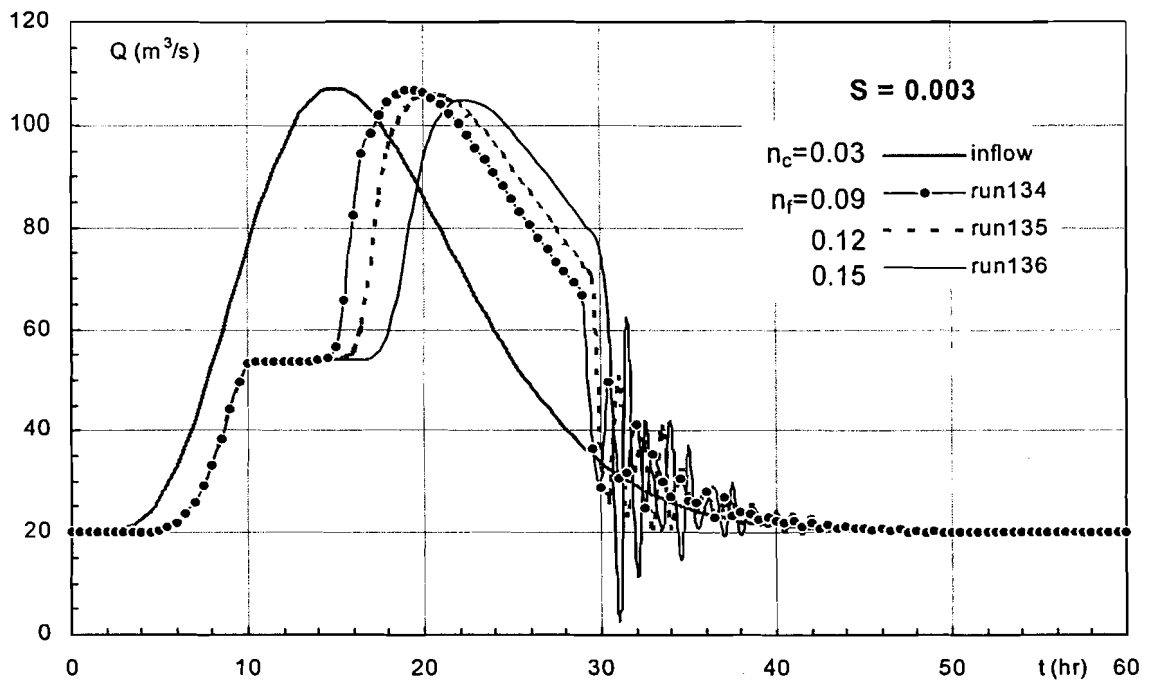


Fig.13 Routed hydrographs for overbank flow, with variable floodplain roughness with ($n_f = 0.090, 0.120$ & 0.150 with $n_c = 0.03$ for $S_0 = 0.003$)

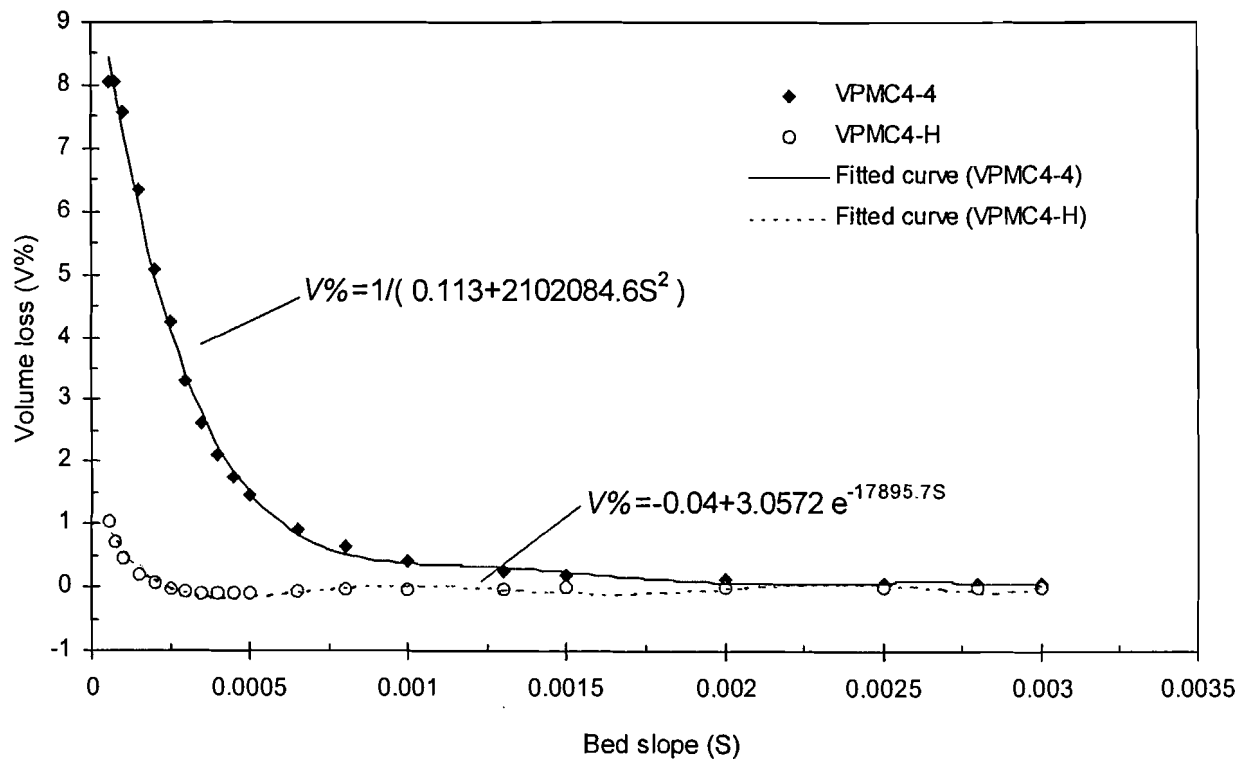


Fig.14 Volume loss for overbank flows using VPMC4-4 & VPMC4-H schemes

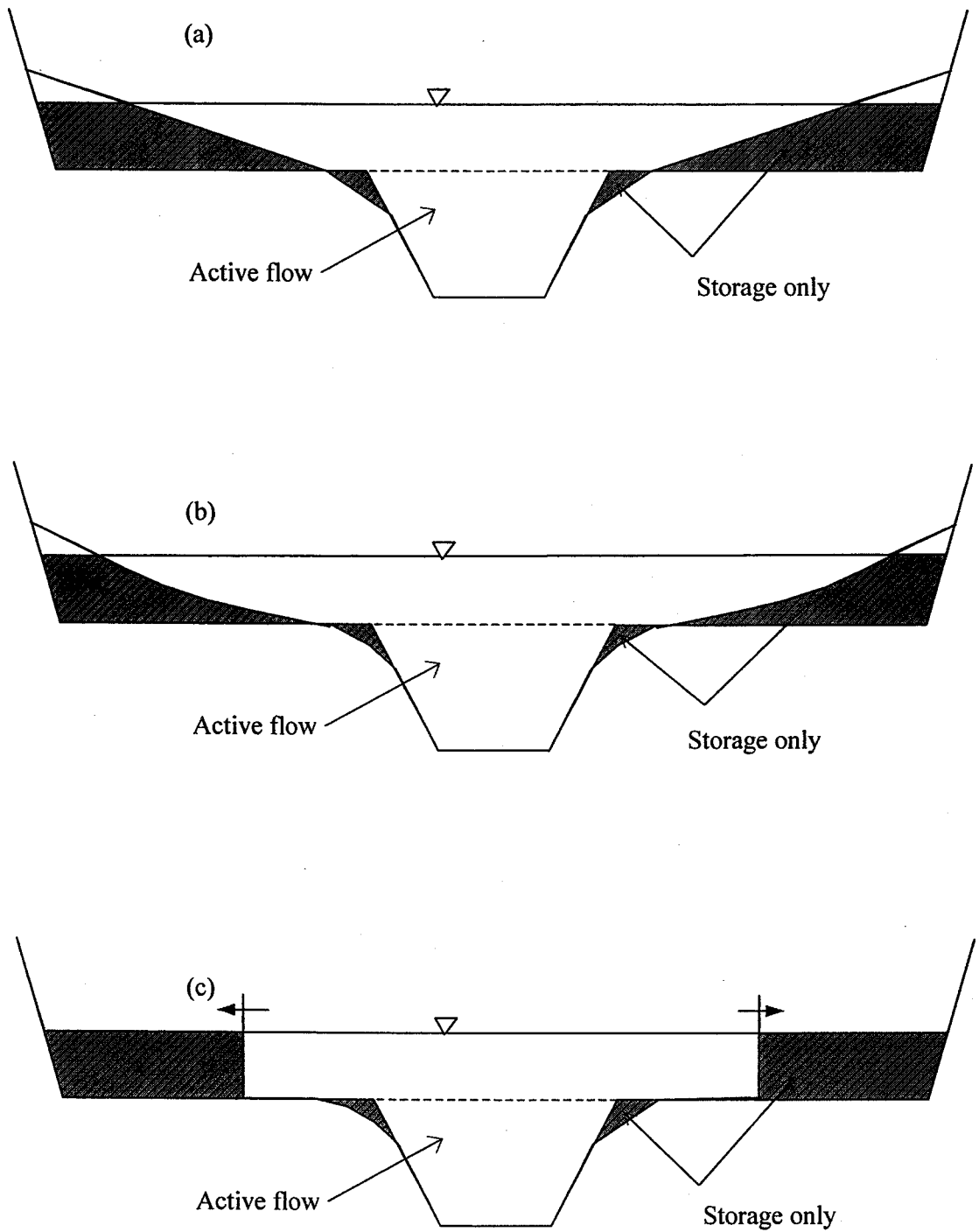


Fig.15 Schematic representation of storage for overbank flow

- (a) the RIBAMAN method with linear boundaries
- (b) the modified RIBAMAN method with curved boundaries
- (c) the moving boundary method

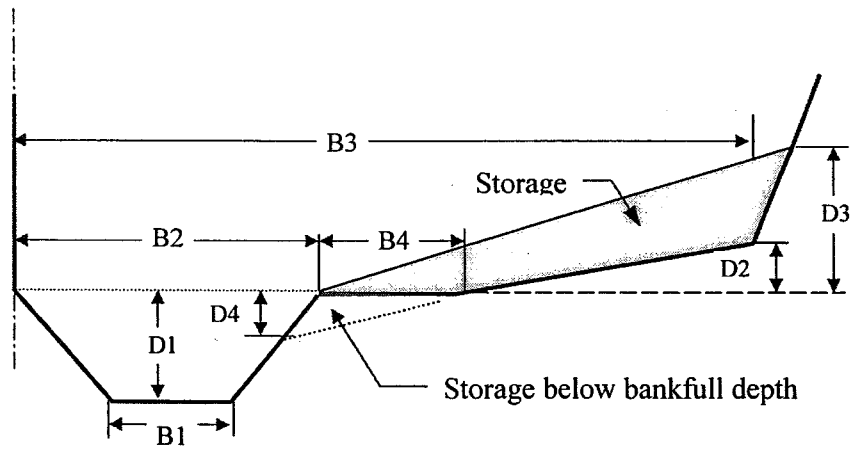


Fig. 16 Schematic compound cross-section used in RIBAMAN

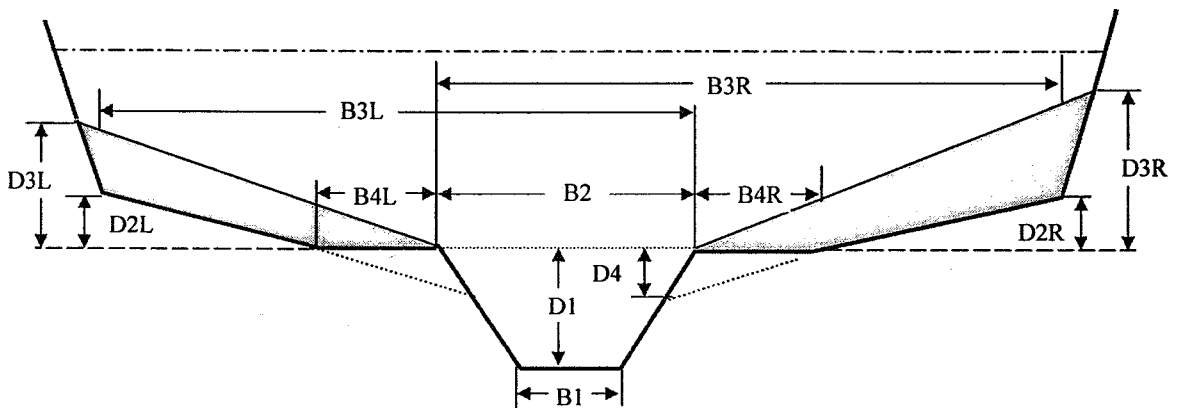


Fig.17 General schematic compound cross-section (RIBAMAN style)

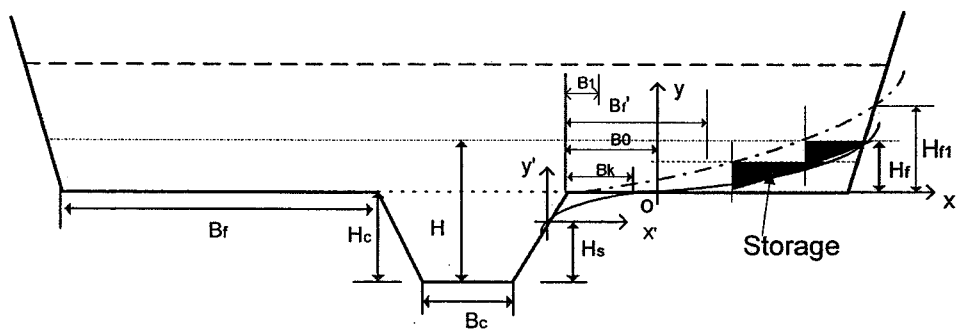


Fig.18 Schematic compound cross-section (CQOB-4, CQVMB-2/3)

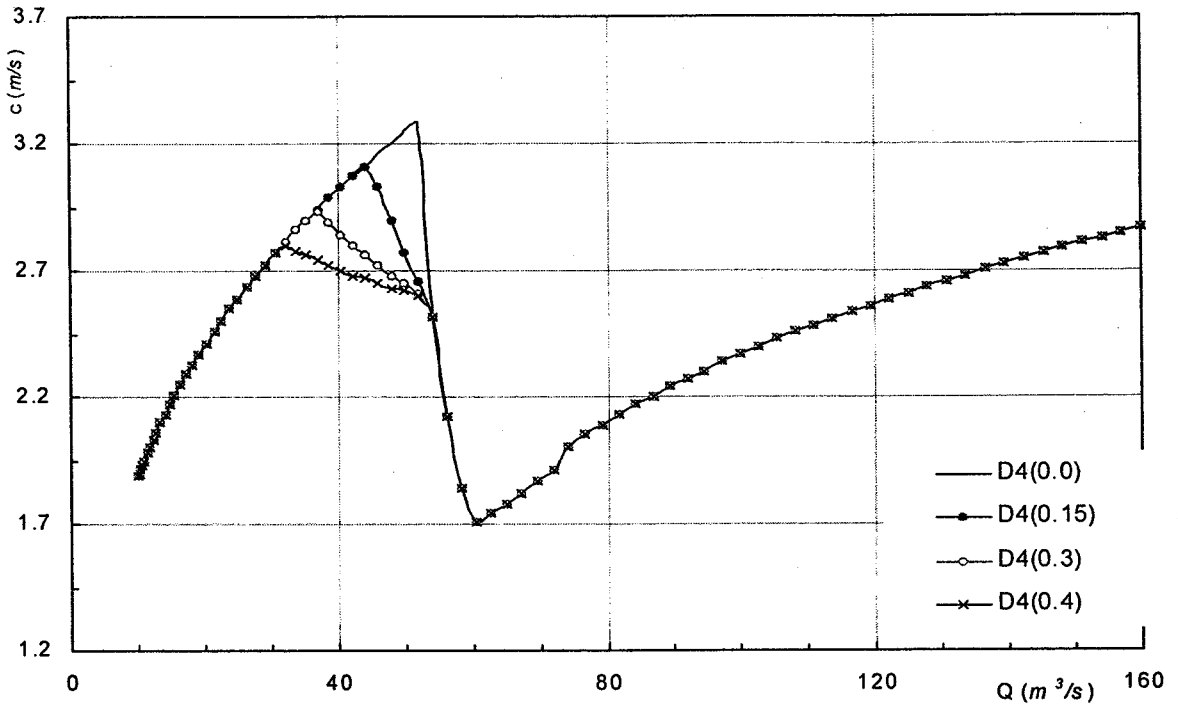


Fig.19 Comparison of $c\sim Q$ curves for variable $D4$ by RIBAMAN method (with $D2 = 0.1m$, $D3 = 0.3m$ and $D4=0, 0.15, 0.3$ & $0.4m$)

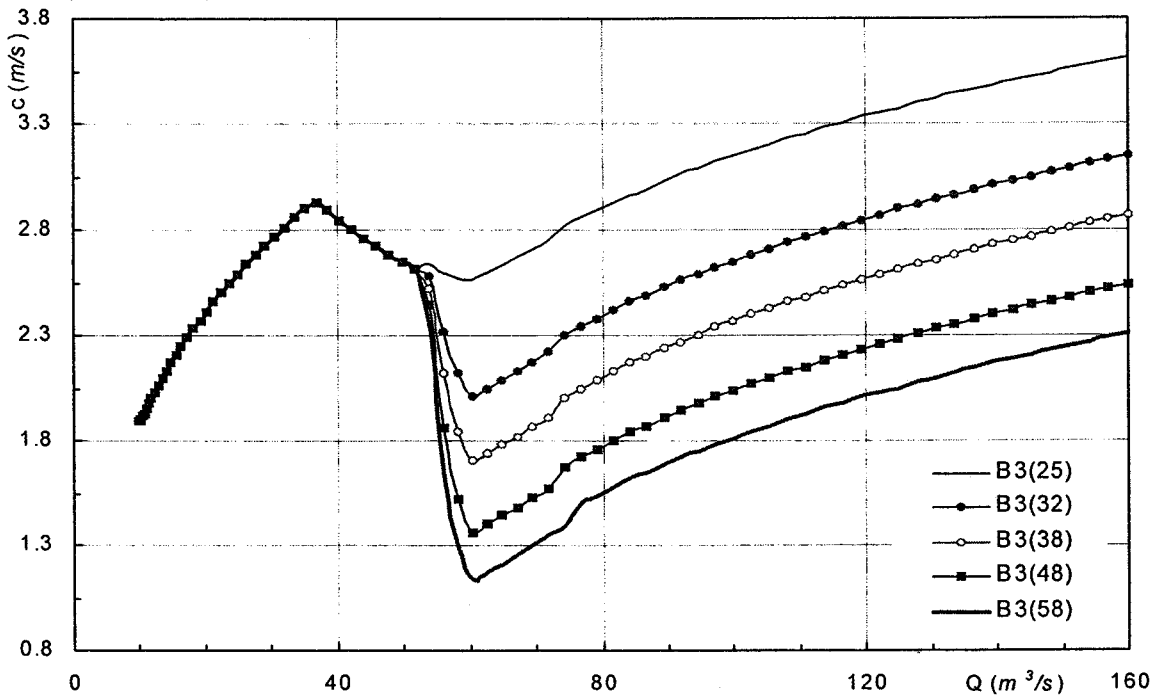


Fig.20 Comparison of $c\sim Q$ curves for variable $B3$ by RIBAMAN method (with $D2 = 0.1m$, $D3 = D4 = 0.3m$ and $B3 = 25, 32, 38, 48$ & $48m$)

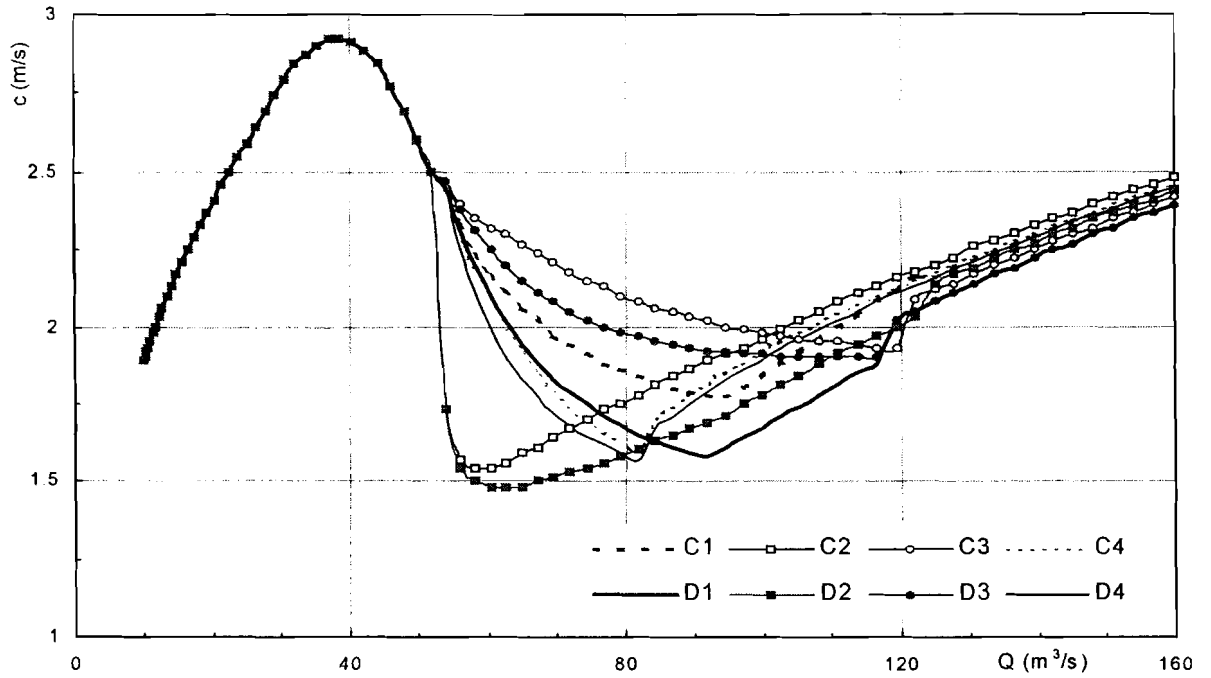


Fig.21 Comparison of $c \sim Q$ curves by CQVMB-3 (Runs C1-C4) and CQOB-4 (Runs D1-D4)

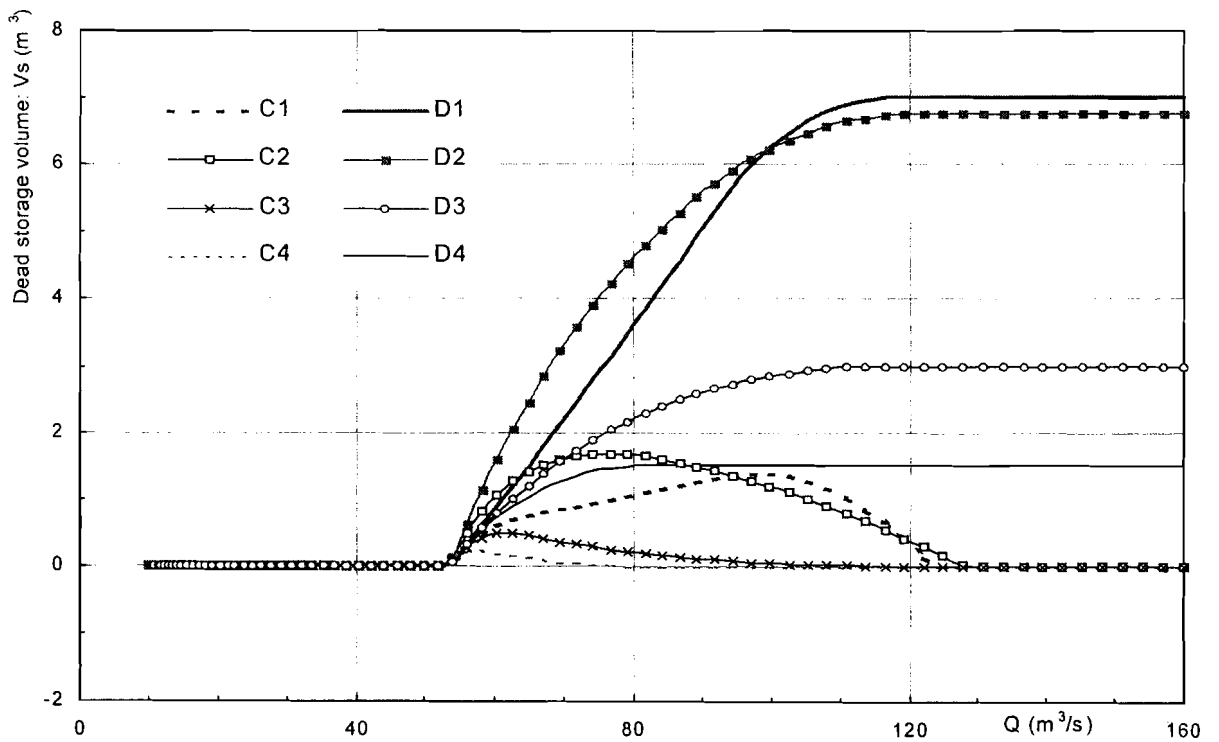


Fig.22 Comparison of dead storage volumes of floodplain by CQVMB-3 (Runs C1-C4) and CQOB-4 (Runs D1-D4)

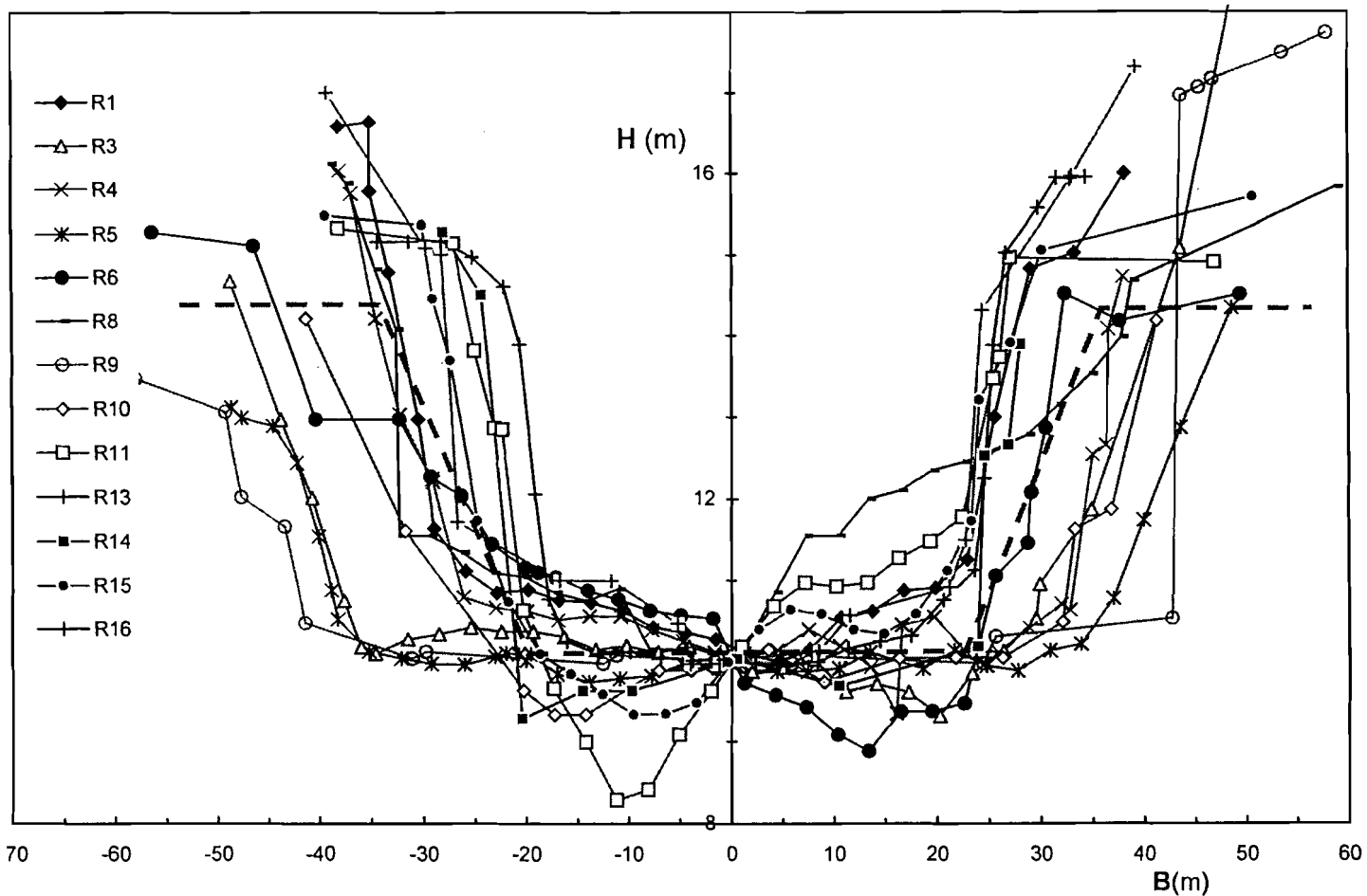


Fig.23 Cross-sections of River Wye, Erwood to Belmont reach

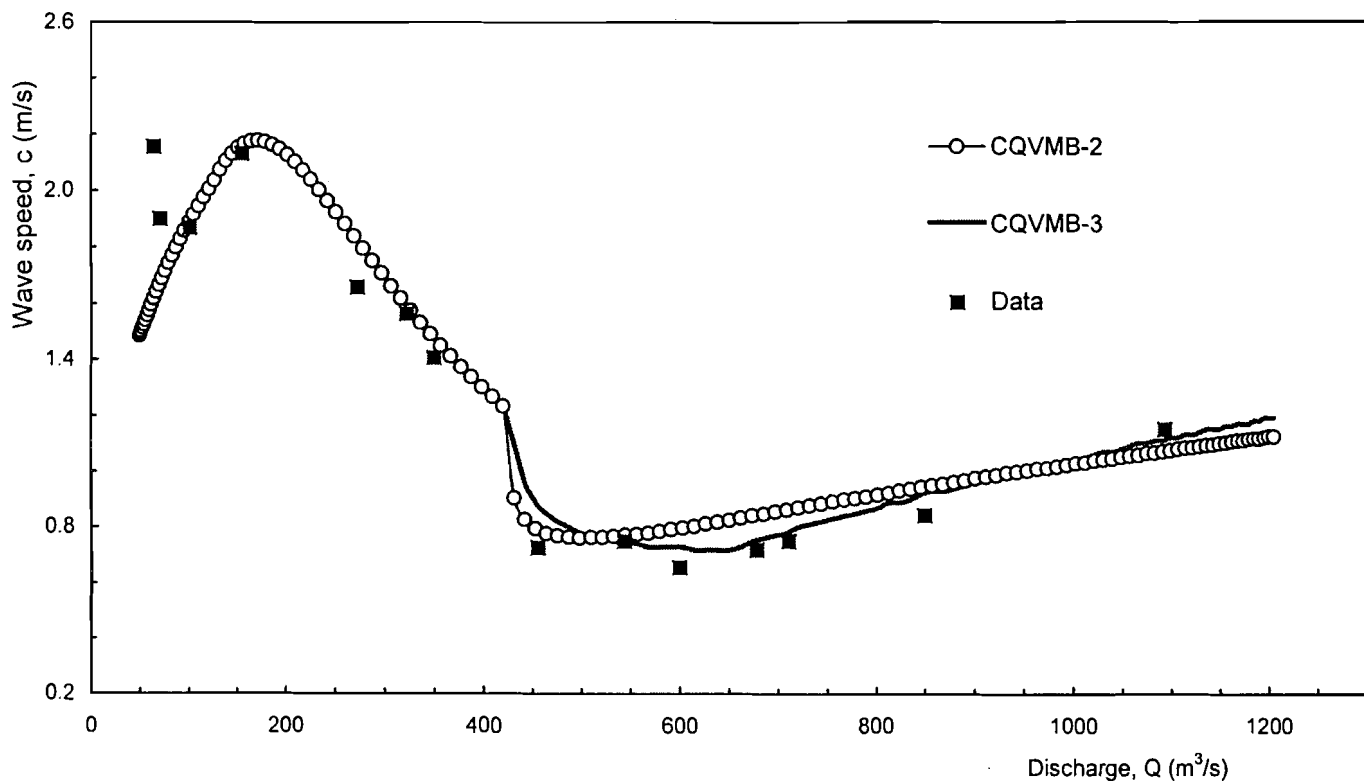


Fig.24 Comparison of predicted and actual $c \sim Q$ relationships for River Wye, Erwood-Belmont reach

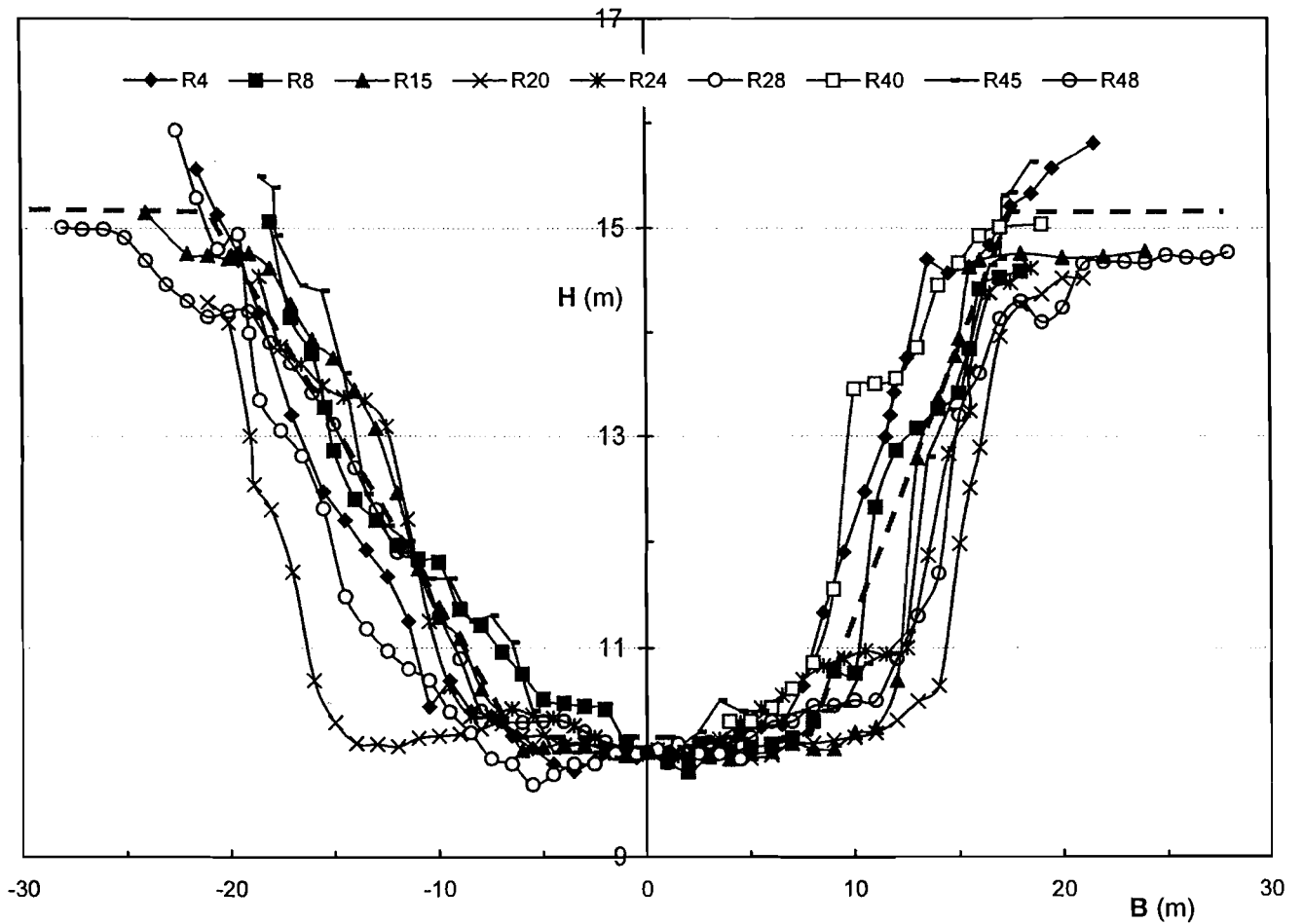


Fig.25 Cross sections of River Avon, Evesham-Pershore reach

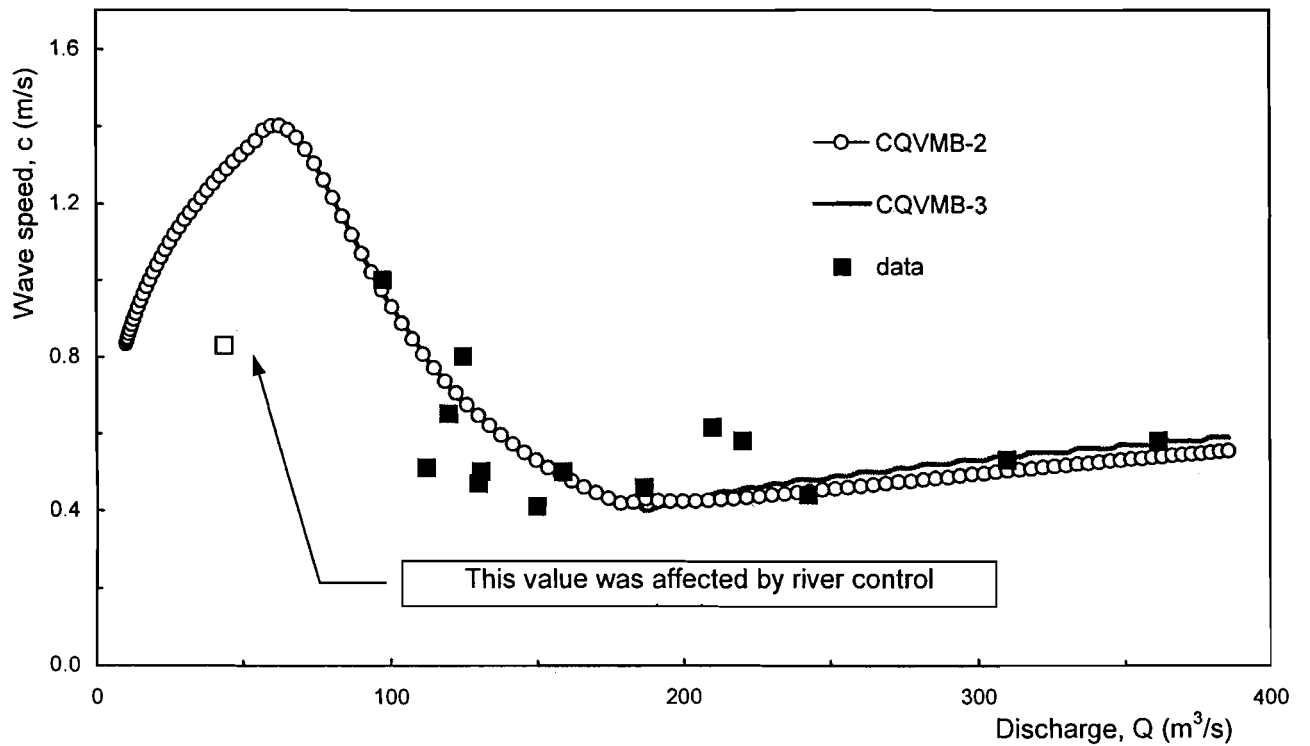


Fig.26 Comparison of predicted and actual $c \sim Q$ relationships for Rive Avon, Evesham to Pershore reach

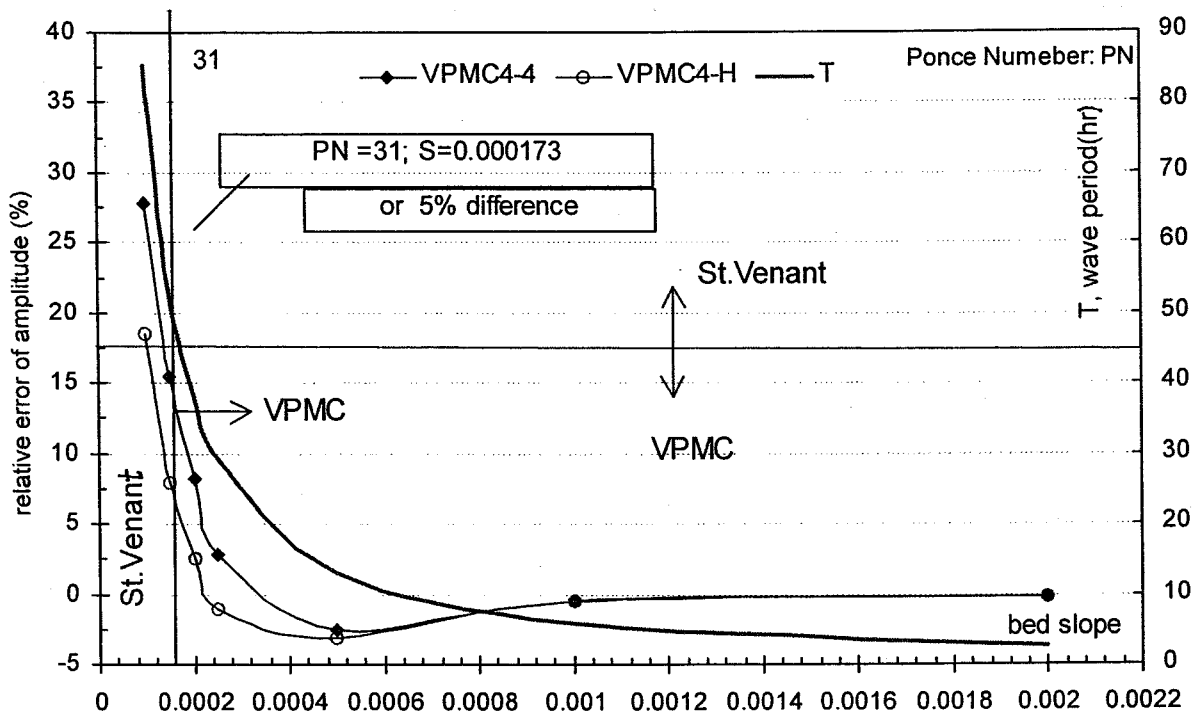


Fig.27 Relationship between amplitude error (St. Venant - VPMC) and bed slope applying Ponce's criterion (FSR channel, $Q=500 \text{ m}^3/\text{s}$)

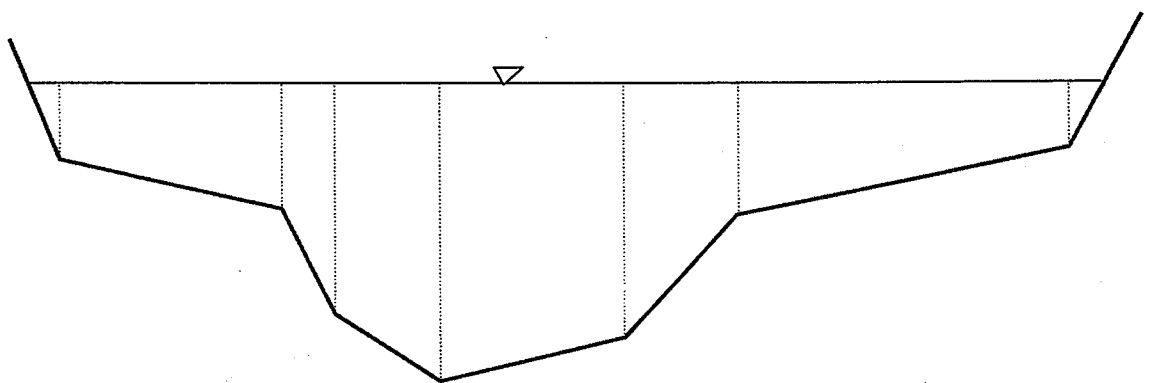


Fig.28 General schematic cross-section composed of 8 linear elements

APPENDIX 1

Tang, X., Knight, D.W. and Samuels, P.G., 1999a, "Volume conservation in variable parameter Muskingum-Cunge method", *Journal of Hydraulic Engineering*, ASCE, Vol. 125, No. 6, pp 610-620.

APPENDIX 2

Tang, X., Knight, D.W. and Samuels, P.G., 1999b, "Variable parameter Muskingum-Cunge method for flood routing in a compound channel", *Journal of Hydraulic Research*, IAHR, Vol. 37, No. 5, pp 1-24.

APPENDIX 3

Tang, X., Knight, D.W. and Samuels, P.G., 2000, "Wave speed-discharge relationship from cross section survey", *Journal of Water & Maritime Engineering*, Proc. Instn. Civil Engrs, joint ICE/IAHR, (submitted for publication).

APPENDIX 4

List of Working Documents produced during the course of this research.

APPENDIX 1

Tang, X., Knight, D.W. and Samuels, P.G., 1999a, "Volume conservation in variable parameter Muskingum-Cunge method", *Journal of Hydraulic Engineering*, ASCE, Vol. 125, No. 6, pp 610-620.

VOLUME CONSERVATION IN VARIABLE PARAMETER MUSKINGUM-CUNGE METHOD

By Xiao-Nan Tang,¹ Donald W. Knight,² Member, ASCE,
and Paul G. Samuels,³ Member, ASCE

ABSTRACT: The simple Variable Parameter Muskingum-Cunge (VPMC) method is still frequently used for flood routing. However, difficulties arise in the selection of an appropriate "reference" discharge for evaluating the routing parameters and in the small volume loss that can occur. Several commonly used schemes for the VPMC method are compared through a series of numerical experiments that cover different channel bed slopes and different space/time steps. The tests show that 4-point schemes are better than 3-point schemes, that a certain amount of volume loss (up to 8%) still occurs in all schemes, and that an empirical relationship exists between the volume loss and channel bed slope (S). A new scheme for the VPMC method is presented, with the routing parameters (c and D) being modified to take into account the longitudinal hydrostatic pressure gradient term. This scheme improves the routed hydrographs, not only with regard to the sensitivity of the outflow peak for given space and time steps, but also with regard to volume loss, typically less than 0.5% even for a channel with $S = 0.0001$.

INTRODUCTION

Volume conservation is an important issue for river simulation modellers for a number of reasons. First, from a quality assurance (QA) point of view, there is an increasing requirement that models be tested against benchmark values, with an obvious test being that the model should conserve volume. Second, in the simulation of a long-time hydrologic series, typically several years of flood events at a catchment scale, it simply is not possible to use the Saint-Venant method for flood routing in all the rivers in a river basin network, and therefore simpler methods such as the Variable Parameter Muskingum-Cunge (VPMC) method need to be employed. Despite volume gains or losses there may be little change in peak flood flows. However, systematic volume errors will be critical for water resource assessments. Third, volume conservation is important from a flood forecasting perspective, because public safety is an issue and flow forecasting software is now classified as "safety critical" software, with consequent QA implications.

Since the Muskingum method of flood routing was introduced by G. T. McCarthy (unpublished paper, 1938), it has been extensively studied and used in river engineering practice. The method was improved by Cunge (1969), who linked the routing parameters to channel properties and flow characteristics, based on the approximation error obtained by a Taylor series expansion of the grid specification and the diffusion analogy. Since Cunge's work in 1969, the well-known Muskingum-Cunge method has been extensively studied [National Environment Research Council (NERC) 1975; Ponce and Yevjevich 1978; Ponce and Theurer 1982; Price 1985; Ponce and Chaganti 1994; Ponce et al. 1996], including both the constant-parameter and the variable-parameter versions. The VPMC method has been studied a great deal in recent years because of its nonlinear nature and simplicity. In the VPMC method, the routing parameters are recalculated for

each computational cell as a function of local flow values, whereas in the Constant Parameter Muskingum-Cunge (CPMC) method, they are evaluated using only a single "representative" flow value and are kept constant throughout the whole computation in time. The main difficulty in applying the VPMC method is selecting an appropriate "reference" discharge that is truly representative of the local flow in each computational cell. This has been shown to have a definite bearing upon accuracy (Ponce and Yevjevich 1978; Koussis 1983; Ponce and Chaganti 1994), particularly with respect to the systematic nonconservation of volume, which although small is perceptible.

This paper examines in detail the features of some commonly used schemes for the VPMC method, along with two new schemes, through a series of numerical tests with different channel bed slopes and with different resolutions of space step (Δx) and time step (Δt). The tests show that the four-point schemes are better than the three-point schemes and that of the four-point schemes, the best is the one termed VPMC4-1 in this paper. This scheme is then modified to account for the effect of the longitudinal hydrostatic pressure gradient term ($\partial h/\partial x$) on the routing parameters (c and D), following the suggestion of Cappelaere (1997). In comparison with the conventional VPMC schemes, this modified scheme has desirable features, particularly volume conservation, for a large range of channel bed slopes. Based on the numerical tests, an empirical relationship between percent volume loss and bed slope is obtained, which serves as a guide for the practical application of the VPMC4-1 method.

MUSKINGUM-CUNGE METHOD

In most natural rivers, the inertial or the acceleration terms [i.e., terms containing the derivative of discharge (Q) with respect to distance (x) or time (t)] in the momentum equation are negligible in comparison with the bed slope (Henderson 1966; Price 1985). In the absence of any lateral flows, the continuity and the momentum equations, which constitute the Saint-Venant equations for gradually varied, unsteady open-channel flow in a prismatic section, reduce to (Weinmann and Laurenson 1979)

$$\frac{\partial Q}{\partial t} + c \frac{\partial Q}{\partial x} = D \frac{\partial^2 Q}{\partial x^2} \quad (1)$$

where $c = dQ/dA = (1/B)dQ/dH =$ kinematic wave speed; and $D = Q/(2BS) =$ diffusion coefficient, in which $B =$ top width of flow and $S =$ channel bed slope.

¹Res. Fellow, School of Civ. Engrg., Univ. of Birmingham, Edgbaston, Birmingham, B15 2TT, U.K.

²Prof. of Water Engrg., School of Civ. Engrg., Univ. of Birmingham, Edgbaston, Birmingham, B15 2TT, U.K.

³Specialist in Fluvial Sys., Water Mgmt. Group, HR Wallingford, Howbery Park, Wallingford, Oxon, OX10 8BA, U.K.

Note. Discussion open until November 1, 1999. To extend the closing date one month, a written request must be filed with the ASCE Manager of Journals. The manuscript for this paper was submitted for review and possible publication on December 1, 1997. This paper is part of the *Journal of Hydraulic Engineering*, Vol. 125, No. 6, June, 1999. ©ASCE, ISSN 0733-9429/99/0006-0610-0620/\$8.00 + \$.50 per page. Paper No. 17136.

If both inertial and pressure forces are neglected, the Saint-Venant equations reduce to the well-known kinematic wave equation (Lighthill and Whitham 1955):

$$\frac{\partial Q}{\partial t} + c \frac{\partial Q}{\partial x} = 0 \quad (2)$$

Cunge (1969) demonstrated that the conventional Muskingum equations are analogous to a convection-diffusion equation, (1). He obtained the following difference equation (3), by differencing and approximating (2) with standard finite difference replacements for $\partial/\partial t$ and $\partial/\partial x$ from the box scheme, using a spatial weighting factor (ϵ) and a temporal weighting factor (θ), which was assumed to be 0.5, and matching the numerical diffusion with the physical diffusion D .

$$Q_{j+1}^{n+1} = C_1 Q_j^n + C_2 Q_j^{n+1} + C_3 Q_{j+1}^n \quad (3)$$

where j = spatial index; n = temporal index; and

$$C_1 = (K\epsilon + 0.5\Delta t)/[K(1 - \epsilon) + 0.5\Delta t] \quad (4)$$

$$C_2 = (-K\epsilon + 0.5\Delta t)/[K(1 - \epsilon) + 0.5\Delta t] \quad (5)$$

$$C_3 = [K(1 - \epsilon) - 0.5\Delta t]/[K(1 - \epsilon) + 0.5\Delta t] \quad (6)$$

and the routing parameters K and ϵ are given by

$$K = \frac{\Delta x}{c} \quad (7)$$

$$\epsilon = \frac{1}{2} \left(1 - \frac{Q}{BSc\Delta x} \right) \quad (8)$$

where Δt = time step; and Δx = space step.

EVALUATION OF ROUTING PARAMETERS (K , ϵ)

The variable parameters (K , ϵ) are normally evaluated using a "reference discharge" based on the flow at local computational grid points. In current practice this is often taken to be some arbitrary average value of some grid points for each computational cell. By using such an approach, the following schemes for evaluating K and ϵ are considered.

Three-point schemes are based on the flow values of the known grid points: (j, n) , $(j, n + 1)$, and $(j + 1, n)$. For convenience they are denoted as points 1, 2, and 3, respectively, as shown in Fig. 1. The scheme-labeling convention is similar to that used by Ponce and Chaganti (1994):

- Scheme (a). VPMC3:

$$\langle Q \rangle = \left(\sum Q_i \right) / 3, \langle c \rangle = \left(\sum c_i \right) / 3 \\ = \left[\sum f(Q_i) \right] / 3; \quad i = 1, 2, 3$$

- Scheme (b). MVPMC3:

$$\langle Q \rangle = \left(\sum Q_i \right) / 3, \langle c \rangle = f(\langle Q \rangle)$$

- Scheme (c). VPMC3-1:

$$\langle c \rangle = \left(\sum c_i \right) / 3 = \left[\sum f(Q_i) \right] / 3 \text{ for } K; \\ \left\langle \frac{Q}{c} \right\rangle = \left[\sum (Q_i/c_i) \right] / 3 \text{ for } \epsilon$$

Four-point schemes are based on the values of all four grid points: (j, n) , $(j, n + 1)$, $(j + 1, n)$, and $(j + 1, n + 1)$. Again,

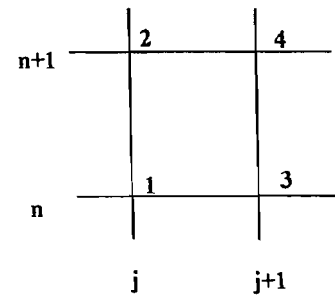


FIG. 1. Computational Grid Cell

they are denoted as points 1, 2, 3, and 4, respectively, as shown in Fig. 1.

- Scheme (d). VPMC4:

$$\langle Q \rangle = \left(\sum Q_i \right) / 4, \langle c \rangle = \left(\sum c_i \right) / 4 \\ = \left[\sum f(Q_i) \right] / 4; \quad i = 1, 2, 3, 4$$

- Scheme (e). MVPMC4:

$$\langle Q \rangle = \left(\sum Q_i \right) / 4, \langle c \rangle = f(\langle Q \rangle)$$

- Scheme (f). VPMC4-1:

$$\langle c \rangle = \left(\sum c_i \right) / 4 = \left[\sum f(Q_i) \right] / 4 \text{ for } K; \\ \left\langle \frac{Q}{c} \right\rangle = \left[\sum (Q_i/c_i) \right] / 4 \text{ for } \epsilon$$

For all schemes, values within brackets (i.e., $\langle c \rangle$ and $\langle Q/c \rangle$) are the reference values for evaluating K and ϵ in (7) and (8), and $c = f(Q)$ denotes that c is a function of discharge (Q).

In fact, Schemes (a), (b), (d), and (e) are those investigated by Ponce and Chaganti (1994). The 3-point schemes are explicit and linear in Q_4 , while the 4-point schemes are explicit but require some iteration to calculate $\langle Q \rangle$ and $\langle c \rangle$ because of the unknown Q_4 being involved in the averages.

CONCEPT OF VOLUME CONSERVATION

In order to investigate the volume-conservation properties of the VPMC method for flood routing, which should be important for practical computations, it is necessary to state what volume conservation is and how to calculate it from the inflow and outflow hydrographs. Based on the water-storage balance equation, the storage volume within a reach can mathematically be expressed by the difference between the inflow, I , and the outflow, Q , as

$$\frac{dV}{dt} = I - Q \quad (9)$$

where V = storage volume within the routed reach. By integration over time, from 0 (initial) to T (final), (9) becomes

$$V_T - V_0 = \int_0^T I dt - \int_0^T Q dt \quad (10)$$

where $V_T - V_0 = \Delta V$, which is actually the change in storage for the whole reach over the period of time from 0 to T . In the initial steady-flow stage, assuming a prismatic channel reach of length (L) and a cross-sectional area (A), the stored

water volume, V can be calculated as $V = AL$. If T is taken to be long enough so that Q_T (final value of outflow) is equal to Q_0 (initial value of outflow) and Q_T is equal to I_0 (initial value of inflow), then assuming a unique relationship between water level and discharge in the interior of the model reach, $V_T = V_0$. Thus, when $\int_0^T I dt - \int_0^T Q dt = 0$, volume is being conserved; otherwise, volume is not conserved for the particular routing method under review.

In the present study, the volume-conservation feature of a routed outflow hydrograph is evaluated by an index, Vol%, which is defined by

$$\text{Vol}\% = \frac{\int_0^T Q dt}{\int_0^T I dt} \times 100 \quad (11)$$

in which $\int_0^T I dt$ and $\int_0^T Q dt$ are computed by numerical integration using Simpson's rule, e.g.

$$\int_0^T Q dt = \frac{\Delta t}{3} \left[Q(0) + 4 \sum_{i=1}^{M-1} Q(i\Delta t) + 2 \sum_{i=2}^{M-2} Q(i\Delta t) + Q(M\Delta t) \right] \quad (12)$$

where $T = M\Delta t$. The value of T used varied with channel slope and typically was between 90 and 140 h.

As indicated by many researchers (e.g., Ponce and Yevjevich 1978; Koussis 1980; Ponce and Chaganti 1994), the CPMC method conserves volume exactly for the outflow hydrograph, but the VPMC method does not. This can be demonstrated analytically, as shown in Appendixes I and II, respectively. It should be noted that in Appendix I for compatibility with the finite-difference CPMC equations to be ensured, the trapezoidal rule is used.

COMPARISON OF SCHEMES FOR VPMC METHOD

Test Condition

To clarify the individual features and differences between the various schemes for the VPMC method described previously, a series of tests were carried out using different channel bed slopes and different resolutions in space and time. The channels adopted were the same as those analyzed in the Flood Studies Report (FSR) (NERC 1975), which were rectangular channels with a width of 50 m, a Manning's coefficient n of 0.035, and a total channel length L of 100 km, but with different bed slopes S ranging from 0.002 to 0.0001.

A synthetic inflow hydrograph (NERC 1975) was defined as

$$Q(t) = Q_{\text{base}} + (Q_{\text{peak}} - Q_{\text{base}}) \left[\frac{t}{T_p} \exp \left(1 - \frac{t}{T_p} \right) \right]^{\beta} \quad (13)$$

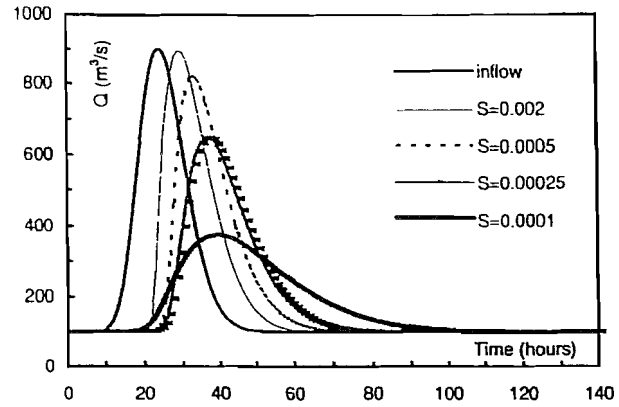


FIG. 2. Hydrographs of Outflows by VPMC4-1 for Different Bed Slopes

where $\beta = 16$ (curvature parameter); $Q_{\text{peak}} = 900 \text{ m}^3/\text{s}$; $Q_{\text{base}} = 100 \text{ m}^3/\text{s}$; and $T_p = 24 \text{ h}$. In the tabular data that follows, T_p = time to peak of inflow and t_p = time to peak of outflow.

For all the VPMC schemes tested, the routing parameter c (wave speed) was calculated based on Manning's formula. Some outflow hydrographs using VPMC4-1 for the FSR channels with different bed slopes are shown in Fig. 2. The attenuation clearly increases as the bed slope decreases, as would be expected from (8), because ϵ , accounting for the attenuation, decreases as S decreases, which is why channels with a small bed slope are such a severe test for volume conservation.

Effect of $\Delta x/L$ and $\Delta t/T_p$ on Results

The routed results by all VPMC schemes and the CPMC method, for $S = 0.002, 0.001, 0.0005, 0.00025,$ and 0.0001 , were compared. Table 1 illustrates the times to peak, t_p ; peak outflows, Q_{po} ; and volume index, Vol%, defined by (11) for one representative slope of $S = 0.00025$ and each computational scheme. In each case $\Delta t = 1 \text{ h}$, but Δx is variable, i.e., $\Delta x/L$ is variable. The CPMC method applied here is the same as in the FSR (NERC 1975). The impact of different space steps on outflow peak values for all bed slopes is illustrated in Fig. 3. The values of $\Delta x/L$ and $\Delta t/T_p$ were chosen for convenience, as the physical length of the flood wave is typically much greater than the length of the routing reach.

In order to compare the effect of different values of $\Delta t/T_p$ on the routed results, five resolutions of Δt (0.25, 0.5, 1, 1.5, and 2 h) were selected for the bed slope cases, one for a steep channel of $S = 0.001$, the other for a mild channel of $S = 0.00025$, keeping Δx constant (at 4,000 and 6,250 m, respectively). The results are shown in Fig. 4, and one representative set, again for $S = 0.00025$, is shown in Table 2.

From these tests, the following conclusions can be drawn:

1. All the schemes for the VPMC method give exactly the same time to peak, or t_p . Moreover t_p is not affected by the selection of $\Delta x/L$ (see Table 1), but it is slightly af-

TABLE 1. Comparison of Routed Results for $S = 0.00025$ with Different $\Delta x/L$

Model (1)	NO DIP PRESENT											
	$\Delta x/L = 1/80; Cr = 6.15$			$\Delta x/L = 1/40; Cr = 3.08$			$\Delta x/L = 1/16; Cr = 1.23$			$\Delta x/L = 1/8; Cr = 0.62$		
	t_p (2)	Q_{po} (3)	Vol% (4)	t_p (5)	Q_{po} (6)	Vol% (7)	t_p (8)	Q_{po} (9)	Vol% (10)	t_p (11)	Q_{po} (12)	Vol% (13)
CPMC	36	681.94	100.0	36	682.00	100.0	36	682.40	100.0	36	683.79	100.0
VPMC3	37	645.31	95.47	37	645.84	95.58	37	647.40	95.90	37	650.17	96.39
MVPMC3	37	645.60	95.51	37	646.16	95.62	37	647.94	95.96	37	651.13	96.53
VPMC3-1	37	645.29	95.46	37	645.76	95.56	37	647.26	95.87	37	650.05	96.34
VPMC4	37	647.73	95.98	37	647.83	95.98	37	647.96	95.96	37	648.78	95.91
MVPMC4	37	647.93	96.01	37	648.06	96.02	37	648.32	96.01	37	649.67	96.03
VPMC4-1	37	647.69	95.97	37	647.70	95.96	37	647.98	95.94	37	648.62	95.85

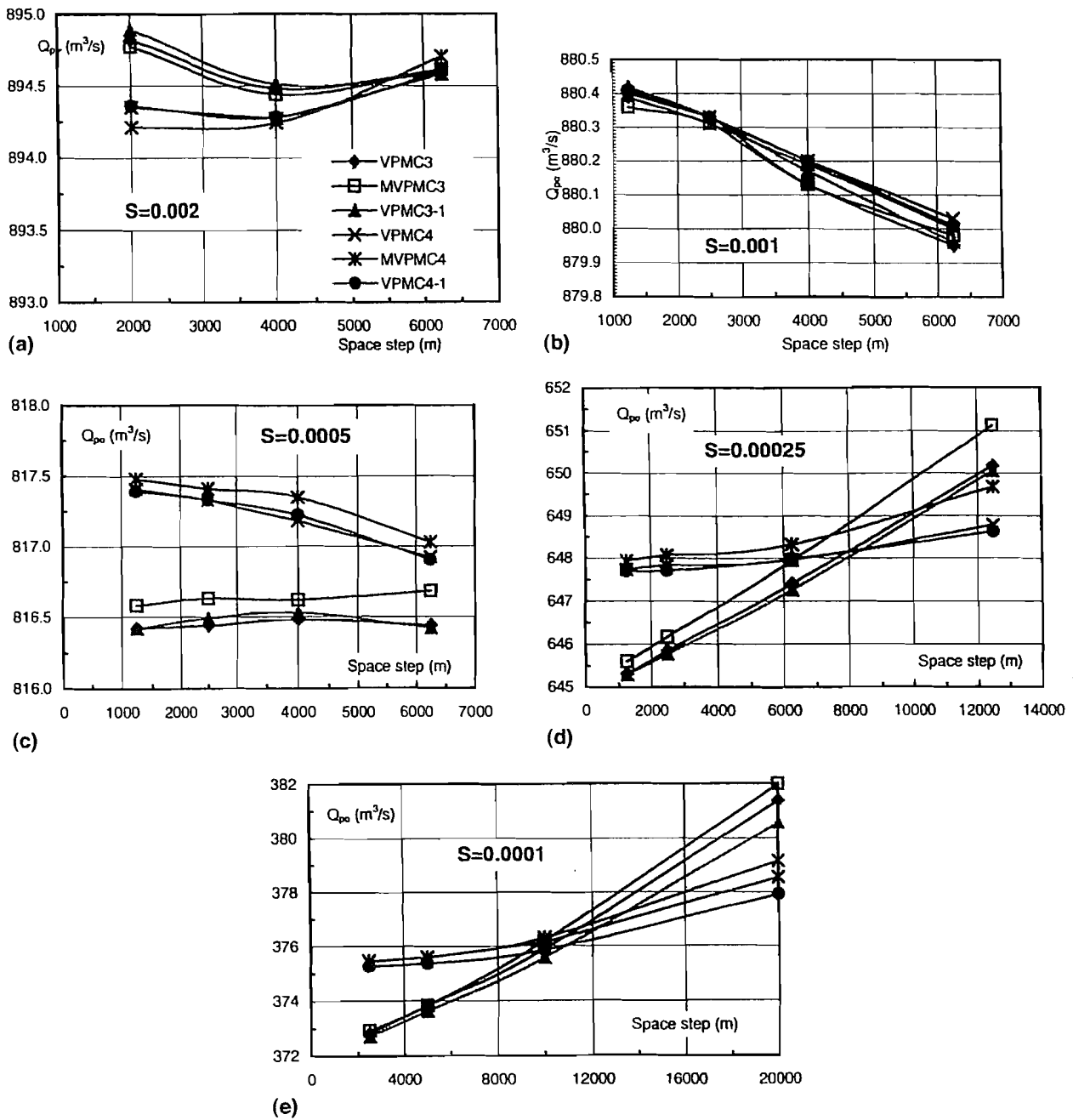


FIG. 3. Comparison of Schemes of VPMC Method for Different Space Steps

- ected by different $\Delta t/T_p$ values, by about one time step (see Table 2).
- The CPMC method always conserves volume, whatever the bed slope and resolution of Δx and Δt . In contrast, the VPMC method suffers a certain amount of volume loss, which depends on the bed slope. This volume loss is cumulative in space and can be assessed only by routing through a long enough reach. This study shows that the volume loss is very small ($<0.5\%$) for steep channels ($S \geq 0.001$), just about tolerable ($<4.5\%$) for mild slope channels ($0.00025 \leq S < 0.001$), but unacceptable (up to 8%) for very mild slope channels ($S = 0.0001$).
 - In terms of volume loss, $MVPMC3 \leq VPMC3$ and $MVPMC4 \leq VPMC4$ for all cases, although the differences between the pairs of methods are quite small ($<0.15\%$). The differences decrease but the volume losses increase as the bed slope decreases. Volume losses for VPMC3 and VPMC3-1 are approximately equal, and volume losses for VPMC4 and VPMC4-1 are approxi-

- mately equal for most cases, except for the case of the very mild slope channel ($S = 0.0001$).
- The volume loss for all the 4-point schemes is less than that for all the three-point schemes. The difference diminishes (from 0.6%) as $\Delta x/L$ values decrease for all channels, and this difference gradually disappears when $\Delta x/L \geq 1/10$, at which point there is a tendency for the "dip" phenomenon to be induced.
- The effect of different $\Delta x/L$ values on the routed peak discharge, Q_{po} , is quite small for steep channels ($S \geq 0.002$) but increases as the bed slope decreases. All the three-point schemes are significantly affected by different space steps Δx . However, the four-point schemes are relatively uninfluenced by different space steps, especially when the $\Delta x/L < 1/10$ (see Fig. 3). Among the four-point schemes, both VPMC4-1 and VPMC4 exhibit less variation for Q_{po} .
- The effect of different $\Delta t/T_p$ values demonstrates that all the schemes appear to be slightly affected in steep chan-

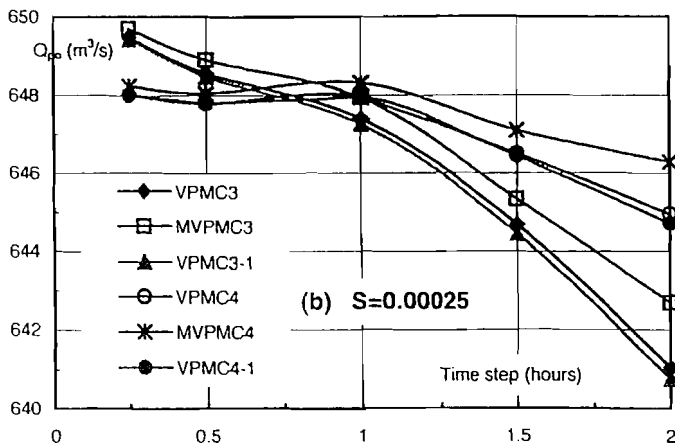
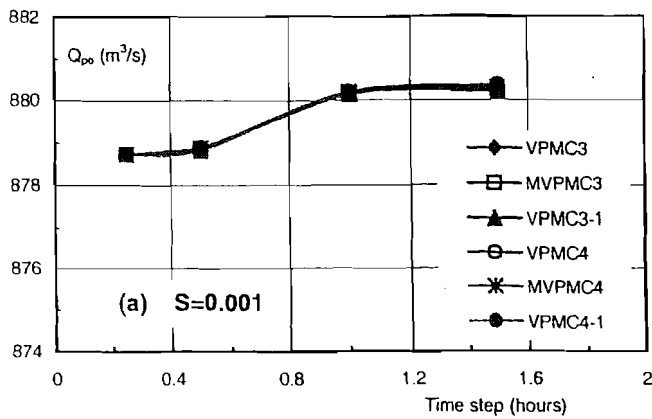


FIG. 4. Comparison of Schemes of VPMC Method for Different Time Steps

nels. For milder channels, all the 3-point schemes are affected by the different Δt values, whereas the four-point schemes are relatively uninfluenced, except when $\Delta t/T_p$ is large [larger than $1/12$ in this case, as shown in Table 2 and Fig. 4(b)]. From the point of view of Q_{po} sensitivity to Δx and Δt , VPMC4-1 and VPMC4 both show good features.

7. Tables 1 and 2 and Fig. 3 (for $S = 0.00025$) and Fig. 4(b) show the effect of grid refinement and Courant number ($Cr = c\Delta t/\Delta x$). For mild slope channels the four-point schemes converge, whereas the three-point schemes do not. Table 2 shows that the peak flow converges when $Cr \leq 1$. The Courant numbers in Tables 1 and 2 have been determined using the crest wave speed, given by $c = L/(t_p - T_p)$.

In summary from the point view of Q_{po} sensitivity and less volume loss, the four-point schemes are better than the three-

point schemes, and VPMC4-1 is the best scheme overall for the VPMC method.

Effect of "Dip" and Negative ϵ on Results

As is well known, under certain conditions, the Muskingum-Cunge method for flood routing will produce some unrealistic phenomena. The obvious one is the leading-edge "dip" in the outflow, where the initial few values of the routed outflow hydrograph can drop below the initial steady flow value and can even produce negative discharges. Also there is the undesirable occurrence of negative weighting parameter (ϵ). Normally in practice ϵ is taken to be within the limits $0 \leq \epsilon \leq 0.5$ (Miller and Cunge 1975; Weinmann and Laurenson 1979). It will be shown later that this dip phenomenon is a peculiarity of the numerical scheme and that it is inherent in the analytical formulation of the method. Both undesirable phenomena can be eliminated under certain conditions, which are discussed by others (Tang et al. 1999). See also Morton and Mayers (1994). The occurrence of dip phenomena can affect the results in the following ways:

- Generally small $\Delta x/L$ values give no leading-edge dip. However, when larger values (obtained when there were fewer segments in the reach) were used, a dip occurred. The dip occurs for both steep channels ($S = 0.002$ with $\Delta x/L \geq 1/5$) and very mild slope channels ($S = 0.0001$ with $\Delta x/L \geq 1/2$).
- When it occurs, the dip will significantly affect the routed peak discharge up to 10% for VPMC3), normally increasing the value of the outflow peak for the same $\Delta t/T_p$. This might be expected since the dip, which is present in the initial stage, in fact artificially stores the water in the reach and subsequently releases it gradually, thereby causing a slight increase in the peak discharge.
- Once the dip occurs, although Q_{po} increases, the volume losses are slightly affected. For the four-point schemes, the losses are generally less than 1%, whereas for the three-point schemes, they are somewhat larger at 3%, especially for mild slope channels, as pointed out previously.

To understand the effect of negative ϵ , and of controlling negative ϵ and the leading-edge dip on the routed results, some results are compared in Table 3 for one selected scheme, the VPMC4-1, applied to channels with bed slopes of $S = 0.002$ and $S = 0.00025$. The rule for controlling negative ϵ was taken as the following: if $\epsilon < 0$, then let $\epsilon = 0$. The rule for controlling the dip was taken as the following: if Q_i (outflow discharge) $< Q_{base}$, then $Q_i = Q_{base}$.

Table 3 shows the following:

1. The effect of controlling the leading-edge dip is insignificant on the timing and magnitude of the peak dis-

TABLE 2. Comparison of Routed Results for $S = 0.00025$ with Different $\Delta t/T_p$

Model (1)	NO DIP PRESENT ($\Delta x = 6,250$ m)														
	$\Delta t/T_p = 1/96$; $Cr = 0.31$			$\Delta t/T_p = 1/48$; $Cr = 0.64$			$\Delta t/T_p = 1/24$; $Cr = 1.23$			$\Delta t/T_p = 1/16$; $Cr = 1.78$			$\Delta t/T_p = 1/12$; $Cr = 2.67$		
	t_p (2)	Q_{po} (3)	Vol% (4)	t_p (5)	Q_{po} (6)	Vol% (7)	t_p (8)	Q_{po} (9)	Vol% (10)	t_p (11)	Q_{po} (12)	Vol% (13)	t_p (14)	Q_{po} (15)	Vol% (16)
CPMC	35.5	683.55	100.0	35.5	683.44	100.0	36	682.40	100.0	36	681.84	100.0	36	680.99	100.0
VPMC3	36.75	649.48	96.14	36.5	648.58	95.99	37	647.40	95.90	37.5	644.69	96.08	36	641.05	95.64
MVPMC3	36.75	649.70	96.17	36.5	648.92	96.03	37	647.94	95.96	37.5	645.34	95.95	36	642.69	95.79
VPMC3-1	36.75	649.44	96.12	36.5	648.49	95.97	37	647.26	95.87	37.5	644.45	95.78	38	640.76	95.57
VPMC4	36.75	648.02	95.74	37	647.79	95.75	37	647.96	95.96	37.5	646.51	96.18	36	644.95	96.24
MVPMC4	36.75	648.24	95.77	36.5	648.06	95.78	37	648.32	96.01	37.5	647.10	96.26	36	646.29	96.37
VPMC4-1	36.75	648.01	95.73	37	647.79	95.74	37	647.98	95.94	37.5	646.43	96.14	36	644.71	96.19

TABLE 3. Routed Results with Dip Control and Truncation of Negative ϵ , Using VPMC4-1

Bed slope (1)	Δx (m) (2)	Δt (h) (3)	Dip (control) (4)	$-\epsilon$ (truncation) (5)	t_p (6)	Q_{po} (7)	Vol% (8)
0.002	10,000	0.5	No	—	29.5	894.28	99.86
0.002	10,000	0.5	Yes	—	29.5	894.28	99.89
0.002	1,000	0.5	—	No	29.5	894.65	99.90
0.002	1,000	0.5	—	Yes	29.5	896.72	99.99
0.00025	25,000	1.0	No	—	37	650.26	95.38
0.00025	25,000	1.0	Yes	—	36	653.69	96.78
0.00025	6,250	1.0	—	No	37	647.98	95.94
0.00025	6,250	1.0	—	Yes	36	817.90	101.69

charge (<0.5%) but, as would be expected, it increases the volume of outflow by a small amount. This implies that the dip does not need to be controlled. A dip normally indicates insufficient and spatial grid resolution.

- Truncation of the negative value of ϵ has a significant effect on the magnitude of the peak discharge (up to a 26% difference), particularly for small bed slope channels. Where truncation is used, the peak discharge is increased. This is to be expected since the numerical dissipation is approximately proportional to $(\epsilon - 1/2)$, arising from $D = (1/2 - \epsilon)c\Delta x$. In fact, limiting ϵ to positive values causes inequality between physical and numerical diffusion, which does not comply with the principle behind the VPMC method.

Figs. 5(a and b) illustrate the individual effects of dip control and truncation of negative ϵ values and show the following:

- The occurrence of a negative value of ϵ does not have a perceptible effect on the shape of the hydrograph, but truncating the negative ϵ does.

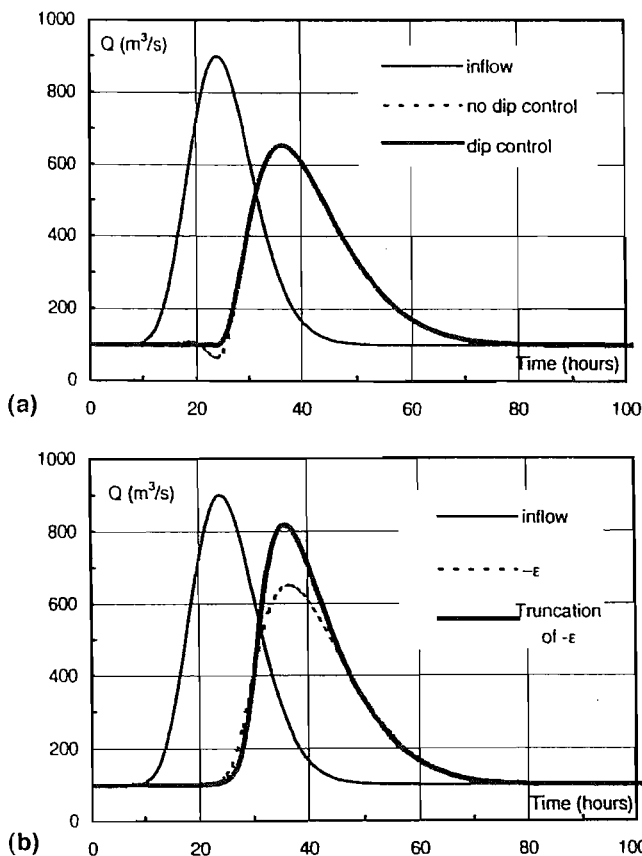


FIG. 5. (a) Effect of "Dip" Control on Outflow Hydrograph by VPMC4-1 ($S = 0.00025$); (b) Effect of Truncation of $-\epsilon$ Value on Hydrograph ($S = 0.00025$)

- The occurrence of a leading-edge dip does not have a noticeable effect on the subsequent shape of the hydrograph, except in the region of the leading-edge dip.

As pointed out by other researchers (Strupczewski and Kundzewicz 1980), the realistic range of ϵ is from $-\infty$ to 0.5, which can also be seen from (8). Therefore, truncating a negative ϵ value is not recommended.

MODIFIED SCHEME FOR VPMC TO IMPROVE VOLUME CONSERVATION

As noted earlier, the VPMC method is actually a diffusion analogy method, in which the routing parameters K and ϵ are linked to the wave speed c and the diffusion parameter D . Both c and D , which are calculated based on uniform flow because of the complexity of unsteady flow, are usually assumed to be a function of a "reference" discharge only. Although the VPMC method is derived from the convection-diffusion equation (1), the parameters c and D are evaluated without reference to the effect of the longitudinal hydrostatic pressure gradient term $\partial h/\partial x$, which becomes increasingly important as the slope of the channel decreases. Recently, Cappelaere (1997) pointed out that the reason for volume loss in the standard variable-parameter diffusion flood routing model seems to be that it does not include the effect of such a pressure term ($\partial h/\partial x$) when calculating c and D .

Cappelaere (1997) showed that the effect of the pressure term on c and D can be approximately expressed in terms of a correction term, cor , as follows:

$$Q = Q_n \cdot cor \quad (14)$$

where Q = unsteady discharge; Q_n = steady discharge at normal depth; and

$$cor \approx \sqrt{1 - \frac{2D}{cQ} \frac{\partial Q}{\partial x}} \quad (15)$$

in which c and D are the values based on the local reference discharge only, and do not include the effect of the longitudinal hydrostatic pressure term ($\partial h/\partial x$); cor is the correction coefficient applied to c and D (rectangular channels only) to give

$$c' = c \cdot cor \quad (16)$$

$$D' = D/cor \quad (17)$$

where c' and D' are the corresponding parameters including the effect of the pressure term.

A diffusive wave equation for the variable h can be derived in a similar form to (1)

$$\frac{\partial h}{\partial t} + c' \frac{\partial h}{\partial x} = D' \frac{\partial^2 h}{\partial x^2} \quad (18)$$

It then follows that the correction term, cor , is in fact given by

$$cor = \sqrt{1 - \frac{1}{S} \frac{\partial h}{\partial x}} \quad (19)$$

Combining (18) and (19) with the continuity equation gives

$$cor = \sqrt{1 - \frac{2D}{cQ} \left(\frac{\partial Q}{\partial x} + BD' \frac{\partial^2 h}{\partial x^2} \right)} \quad (20)$$

In the new modified scheme, since

$$Q = cor \langle Q \rangle \quad (21)$$

where $\langle Q \rangle$ is taken as the "reference" discharge adopted by the VPMC scheme, and

$$\frac{\partial Q}{\partial x} = (Q_{j+1}^{n+1} + Q_{j+1}^n - Q_j^{n+1} - Q_j^n) / 2\Delta x \quad (22)$$

then for the sake of consistency with (15), cor is expressed by the following modified form:

$$cor = \sqrt{1 - \mu \frac{2D}{c\langle Q \rangle} \frac{\partial Q}{\partial x}} \quad (23)$$

where μ = adjustment factor that takes into account the effect of the $\partial^2 h / \partial x^2$ term. The numerical value of μ will depend on the size and shape of the channel as well as on the shape of the routed hydrograph. Further numerical tests were undertaken for various μ values using NERC (1975), channels with different widths, as shown in Table 4, in which VPMC4-H is denoted as the corresponding VPMC4 scheme with the above modification included. Table 4 shows the following:

1. The value of μ is closely related to both bed slope and channel width B . For steep channels ($S = 0.003$), the routed results (both Q_{po} and Vol%) are little affected by μ values, but for mild channels ($S \leq 0.0008$), they are significantly affected. This is because the correction factor cor is greatly affected by small bed slopes. In comparing (20) and (23), it is clear that μ is a function of both B and $\partial^2 h / \partial x^2$, the latter making quite an important contribution to cor as the bed slope increases.
2. Again from (20), it is seen that μ is also dependent on B , implying that the μ should increase as the width B decreases. This is demonstrated in the test results, shown in Table 4, where the best results for the whole range of bed slopes tested are obtained with $\mu \approx 0.65$ for $B = 25$ m, $\mu \approx 0.4$ for $B = 50$ m, and $\mu \approx 0.3$ for $B = 100$ m.

In the following examples on rectangular channels ($B = 50$ m), the value of μ was taken to be equal to 0.4, which was deemed to be suitable over a wide range of bed slopes.

Results

For simplicity, only the MVPMC3 and VPMC4 schemes have been used in the comparison, because these two schemes

TABLE 5. Summary of Channel Data of Perumal (1998)

Channel type (1)	Bed slope (2)	Manning's n (3)
I	0.0002	0.04
II	0.0002	0.02
III	0.002	0.04

are commonly used (Garbrecht and Brunner 1991; Perumal and Ranga Raju 1998). Moreover, these two schemes were chosen to compare with the corresponding VPMC4 scheme with the above modification, known herein as the VPMC4-H scheme. Tests were undertaken on the FSR channels (NERC 1975) and rectangular channels (Perumal and Ranga Raju 1998) with a total length of 40 km and a width of 50 m. Results are summarized in Table 5. The input hydrograph used by Perumal and Ranga Raju (1998) was

$$Q(t) = Q_{base} + (Q_{peak} - Q_{base}) \left(\frac{t}{T_p} \right)^{1(\gamma-1)} \exp \left[\frac{1 - t/T_p}{\gamma - 1} \right] \quad (24)$$

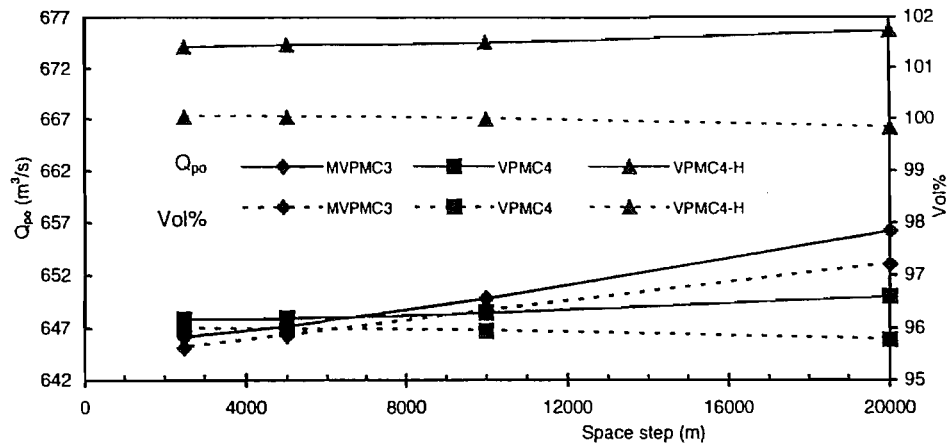
where γ = curvature parameter (1.15); $Q_{base} = 100$ m³/s; $Q_{peak} = 1,000$ m³/s; and $T_p = 10$ h.

The results for two typical channels, with bed slopes of 0.00025 and 0.0002 and n values of 0.035 and 0.040, respectively, are shown in Fig. 6. The results clearly show that the VPMC4-H scheme improves the routed results. Not only is there little variation in Q_{po} for different $\Delta x/L$ or $\Delta t/T_p$ if no "dip" exists, but also there is improved volume conservation, with a volume loss of less than 0.4% even for a very mild slope channel with $S = 0.0001$. To show how the shape of the outflow hydrograph is modified by VPMC4-H, the routed outflow hydrographs by CPMC, VPMC3, VPMC4-1, and VPMC4-H for a typical bed slope [e.g., $S = 0.00025$ of NERC (1975)] are compared in Fig. 7. The CPMC method does not have the nonlinear trend, which steepens the rising limb. On the other hand, all the VPMC methods show steeping of the rising limb, followed by a corresponding flattening of the receding limb. In this case, VPMC4-H shows the improved nonlinearity of the outflow hydrograph, i.e., a steeper rate of rise and a more gradual recession. The new VPMC method, with routing parameters c and D modified to account for the effect of the longitudinal hydrostatic pressure gradient term, appears therefore to route floods more realistically.

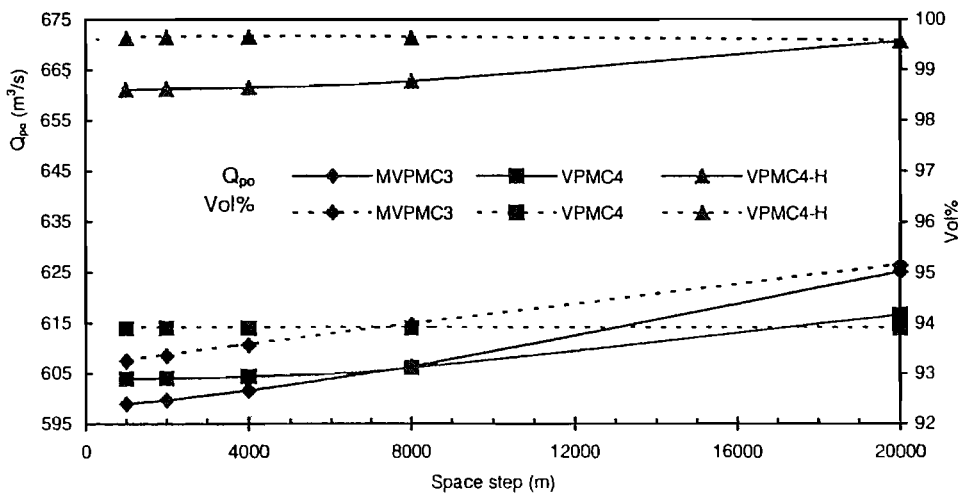
TABLE 4. Tests with Different μ Values by VPMC4-H

Width, B (m) (1)	Bed slope	$S = 0.003$		$S = 0.0008$		$S = 0.00025$		$S = 0.0001$	
	μ value (2)	Q_{po} (3)	Vol% (4)	Q_{po} (5)	Vol% (6)	Q_{po} (7)	Vol% (8)	Q_{po} (9)	Vol% (10)
25	1.0	895.01	100.07	837.58	100.95	603.27	105.94	NA	NA
25	0.65	894.90	100.02	836.02	100.17	580.04	100.25	397.80	100.35
25	0.6	894.92	100.01	835.82	100.05	576.11	99.52	391.14	98.60
25	0.5	894.95	99.99	835.32	99.83	567.86	98.07	377.61	95.77
25	0.4	894.94	99.98	834.77	99.59	559.69	96.65	364.01	93.79
25	[VPMC4]	894.94	99.92	832.43	98.64	520.73	91.13	318.84	85.72
50	1.0	897.58	100.06	867.73	100.95	702.04	106.03	NA	NA
50	0.8	897.61	100.04	867.38	100.65	693.65	104.01	NA	NA
50	0.6	897.60	100.02	867.02	100.35	684.85	102.01	445.37	104.95
50	0.5	897.60	100.01	866.84	100.20	679.76	101.02	434.58	101.92
50	0.4	897.55	99.99	866.61	100.04	674.02	100.02	423.48	99.49
50	0.3	897.56	99.98	866.43	99.88	668.07	99.02	411.90	97.29
50	[VPMC4]	897.57	99.95	865.88	99.41	647.91	95.97	375.59	91.63
100	1.0	896.98	100.07	875.09	101.12	730.73	106.48	NA	NA
100	0.8	897.23	100.05	875.05	100.82	724.15	104.71	NA	NA
100	0.6	897.36	100.02	874.99	100.50	716.65	102.91	477.78	106.96
100	0.5	897.48	100.01	874.96	100.34	712.35	102.00	467.66	104.48
100	0.4	897.59	99.99	874.94	100.17	707.56	101.09	457.03	102.22
100	0.3	897.64	99.98	874.90	100.00	702.14	100.16	445.77	100.12
100	[VPMC4]	897.94	99.94	874.80	98.50	684.89	97.30	410.49	94.42

Note: $\Delta x = 5,000$ m; $\Delta t = 1$ h. NA = no result available (solution is not convergent).



a) $S = 0.00025, n=0.035$



b) $S = 0.0002, n=0.04$

FIG. 6. Comparison of MVPMC3, VPMC4, and VPMC4-H for Different Space Steps: (a) NERC (1975), $S = 0.00025$; (b) Perumal (1988), Type I

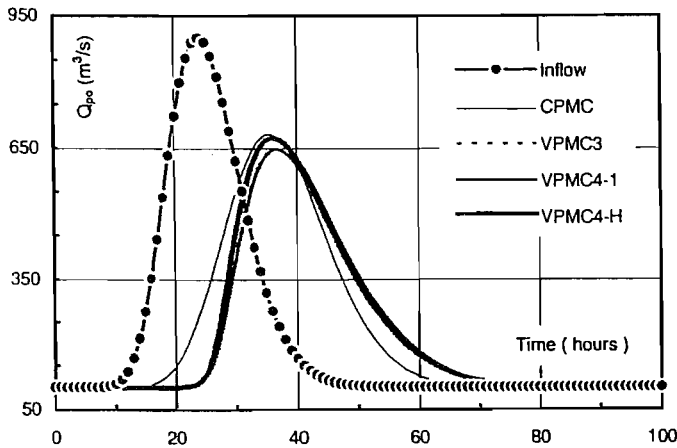


FIG. 7. Comparison of Outflow Hydrographs by CPMC, VPMC3, VPMC4-1, and VPMC4-H ($S = 0.00025$)

To illustrate the relationship between volume lost percentage and bed slope, a series of tests for selected VPMC4-1 and VPMC4-H were undertaken on NERC (1975) channels with $\Delta t = 1$ h and $\Delta x = 5,000$ m.

Using VPMC4-1 method, the following empirical formula was obtained:

$$V\% = 1/(0.113 + 2,102,084.6S^2) \quad (25)$$

$$S \in [0.00006, 0.003] \text{ with } R^2 = 0.9989$$

Using the VPMC4-H method, the following empirical formula was obtained:

$$V\% = -0.0403 + 3.0572e^{-17.895.7S} \quad (26)$$

$$S \in [0.00006, 0.003] \text{ with } R^2 = 0.9829$$

where S = channel bed slope; and $V\%$ = volume loss percentage, which is calculated as follows:

$$V\% = \frac{\text{Volume (inflow)} - \text{Volume (outflow)}}{\text{Volume (inflow)}} \times 100 \quad (27)$$

Both (25) and (26) are illustrated in Fig. 8 for the range of bed slopes tested. Fig. 8 shows that the volume losses by both VPMC4-1 and VPMC4-H are small ($<0.5\%$) in a steep channel ($S \geq 0.001$), but they will increase quickly around $S = 0.0005$ and $S = 0.0001$, respectively, and their differences increase with decreasing bed slope. This implies that VPMC4-

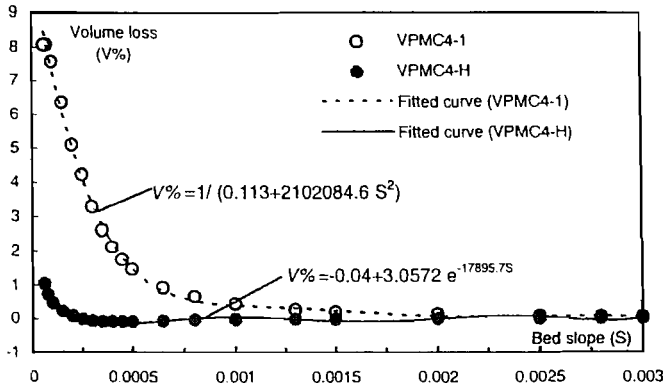


FIG. 8. Volume Loss Percentage (V%) versus Bed Slopes for VPMC4-1 and VPMC4-H

H can be applied to a wider range of bed slopes than VPMC4-1. It should be noted that the volume loss percentage does depend on the time of integration, but in these tests the integration time was kept fixed.

CONCLUSIONS

The following conclusions may be drawn from this study:

1. All the schemes for the VPMC method give the same time to peak, or t_p . Moreover, t_p is not affected by the selection of $\Delta x/L$, but it is slightly affected by different $\Delta t/T_p$ values.
2. The attenuation of peak flow increases as the bed slope decreases, which is the main factor contributing to the diffusion of the flow wave, as can be seen from $D = Q/2BS$.
3. The CPMC method always conserves volume, whatever the bed slope and resolution of Δx and Δt , the VPMC method suffers a certain amount of volume loss, which depends on the bed slope. The volume loss appears to be small for steep channels but is much larger for very mild channels, which implies that much care is required when the VPMC method is employed in the very mild slope channels.
4. In terms of volume loss, $MVPMC3 \leq VPMC3$ and $MVPMC4 \leq VPMC4$ for all cases, although the differences are quite small (<0.15%). The differences decrease but the volume losses increase as the bed slope decreases. Volume losses for VPMC3 and VPMC3-1 are approximately equal, as are volume losses for VPMC4 and VPMC4-1 for most cases, except for the very mild channel case ($S = 0.0001$). The volume losses for all the four-point schemes are less than those for all the 3-point schemes, unless $\Delta x/L$ is too large ($\geq 1/10$), which will then induce the "dip" phenomenon.
5. The effect of different $\Delta x/L$ values on the routed peak discharge, Q_{po} , is quite small for steep channels ($S \geq 0.002$) but increases for milder slope channels as the bed slopes decrease. All the 3-point schemes are significantly affected by different space steps Δx . However, the 4-point schemes are relatively uninfluenced by different space steps. Among the 4-point schemes, both the VPMC4-1 and VPMC4 schemes exhibit less variation for Q_{po} than the other schemes.
6. From the point view of sensitivity of Q_{po} to different Δx and Δt , the four-point schemes are better than the three-point schemes, and the former have relatively less volume loss. Moreover, VPMC4-1 is the best scheme overall for the VPMC method.
7. A series of tests show that the VPMC4-H scheme (VPMC4 with routing parameters c and D modified to

account for the effect of the longitudinal hydrostatic pressure gradient term) gives desirable results, with this scheme not only having less sensitivity for Q_{po} for different Δx or Δt but also having improved volume conservation (better than 0.5% in very mild slope channels, e.g., $S = 0.0001$).

8. Two empirical formulas, (25) and (26) for VPMC4-1 and VPMC4-H, respectively, based on these numerical test cases, may act as a guide for determining the volume loss when the VPMC method is applied.
9. The leading-edge dip has a negligible effect on the timing and magnitude of the outflow peak, but the dip increases the volume of outflow by a small amount.
10. The truncation of negative ϵ values has a significant effect on the routed peak discharge (up to a 26% difference) and the shape of the outflow hydrograph, but a negative ϵ value seems to have little effect on the routed results. Hence the restriction that ϵ is positive should not be made in practical applications of flood routing methods.

APPENDIX I. DEMONSTRATION OF VOLUME CONSERVATION FOR CPMC METHOD

Below are two approaches that prove the CPMC method always conserves the volume of routed outflow.

Approach One: Analytical Form of Muskingum Equations

According to the conventional Muskingum equations

$$\frac{dV}{dt} = I - Q \quad (28)$$

$$V = K[\epsilon I + (1 - \epsilon)Q] \quad (29)$$

where I = inflow; Q = outflow; V = storage volume in a considered reach; and K and ϵ are parameters in the Muskingum method, which are linked to wave speed and attenuation, as shown by (7) and (8).

Combining (28) and (29) gives the following equation:

$$K\epsilon \frac{dI}{dt} + K(1 - \epsilon) \frac{dQ}{dt} = I - Q \quad (30)$$

For the Muskingum method, both K and ϵ are constant. Integrating (30) over the time period from 0 to T ($T = M\Delta t$) yields

$$\int_0^T \left(K\epsilon \frac{dI}{dt} \right) dt + \int_0^T \left[K(1 - \epsilon) \frac{dQ}{dt} \right] dt = \int_0^T I dt - \int_0^T Q dt \quad (31a)$$

where

$$\int_0^T I dt \text{ is the volume of inflow, denoted as } V_i \quad (31b)$$

and

$$\int_0^T Q dt \text{ is the volume of outflow, denoted as } V_o \quad (31c)$$

Because both K and ϵ are constant for the Muskingum method, (31) can be written as

$$V_i - V_o = K\epsilon[I_T - I_0] + K(1 - \epsilon)[Q_T - Q_0] \quad (32)$$

If the time period of the integral is selected large enough to keep $I_T = I_0$ and $Q_T = Q_0$, then (32) becomes $V_i - V_o = 0$, or $V_i = V_o$.

Therefore, the volume of the routed outflow is always equal

to that of the inflow. Thus the analytic Muskingum method always conserves volume of the routed hydrograph.

Approach Two: CPMC Discrete Form of Muskingum Method

The difference scheme of the Muskingum-Cunge method is as follows:

$$Q_{j+1}^{n+1} = C_1 Q_j^n + C_2 Q_j^{n+1} + C_3 Q_{j+1}^n \quad (33)$$

and

$$C_1 + C_2 + C_3 = 1 \quad (34)$$

For the CPMC method, the parameters K and ϵ are evaluated by a single representative discharge during the whole routing process and consequently are constant. Thus the coefficients C_1 , C_2 , and C_3 in (33) are also constant.

In order to calculate the volume of inflow or outflow, the corresponding hydrographs need to be integrated over a selected time period. In practice, this can be achieved by numerical integration, using such methods as the trapezoidal rule (35) or Simpson's formula (12). To ensure compatibility with the finite-difference CPMC equations, the trapezoidal rule is used:

$$VOL = \Delta t \left[\frac{Q^0 + Q^M}{2} + \sum_{n=1}^{M-1} Q^n \right] \quad (35)$$

where VOL = total volume of inflow or outflow hydrograph; Δt = fixed time step; and the whole time period for volume calculation is T , which is subdivided into M sections, each having Δt (i.e., $T = M\Delta t$).

Eq. (33) can be summed over all time steps to give

$$\sum_{n=0}^{M-1} Q_{j+1}^{n+1} = \sum_{n=0}^{M-1} C_1 Q_j^n + \sum_{n=0}^{M-1} C_2 Q_j^{n+1} + \sum_{n=0}^{M-1} C_3 Q_{j+1}^n \quad (36)$$

We observe that

$$\sum_{n=0}^{M-1} Q_{j+1}^{n+1} = \sum_{n=0}^{M-1} Q_{j+1}^n + (Q_{j+1}^M - Q_{j+1}^0) \quad (37a)$$

and

$$\sum_{n=0}^{M-1} Q_j^{n+1} = \sum_{n=0}^{M-1} Q_j^n + (Q_j^M - Q_j^0) \quad (37b)$$

Inserting (37a) and (37b) into (36) gives

$$\begin{aligned} \sum_{n=0}^{M-1} Q_{j+1}^n + (Q_{j+1}^M - Q_{j+1}^0) &= C_1 \sum_{n=0}^{M-1} Q_j^n \\ &+ C_2 \left[\sum_{n=0}^{M-1} Q_j^n + (Q_j^M + Q_j^0) \right] + C_3 \sum_{n=0}^{M-1} Q_{j+1}^n \end{aligned} \quad (38)$$

Rearranging (38) produces

$$\begin{aligned} (1 - C_3) \sum_{n=0}^{M-1} Q_{j+1}^n &= (C_1 + C_2) \sum_{n=0}^{M-1} Q_j^n + C_2(Q_j^M - Q_j^0) \\ &- (Q_{j+1}^M - Q_{j+1}^0) \end{aligned} \quad (39)$$

According to $C_1 + C_2 + C_3 = 1$ (i.e., $1 - C_3 = C_1 + C_2$), (39) can be rearranged into

$$\sum_{n=0}^{M-1} [Q_{j+1}^n - Q_j^n] = \frac{1}{C_1 + C_2} [C_2(Q_j^M - Q_j^0) - (Q_{j+1}^M - Q_{j+1}^0)] \quad (40)$$

If the subscripts j and $j + 1$ denote inflow and outflow, respectively, then from (35) it follows that for inflow

$$(VOL)_{in} = \Delta t \left[\frac{Q_j^0 + Q_j^M}{2} + \sum_{n=1}^{M-1} Q_j^n \right] \quad (41)$$

and for outflow,

$$(VOL)_{out} = \Delta t \left[\frac{Q_{j+1}^0 + Q_{j+1}^M}{2} + \sum_{n=1}^{M-1} Q_{j+1}^n \right] \quad (42)$$

Subtracting (41) from (42) gives

$$\begin{aligned} (VOL)_{out} - (VOL)_{in} &= \Delta t \left[\frac{1}{2} (Q_{j+1}^0 - Q_j^0 + Q_{j+1}^M - Q_j^M) + \sum_{n=1}^{M-1} [Q_{j+1}^n - Q_j^n] \right] \end{aligned} \quad (43)$$

Rearranging (43) gives

$$\begin{aligned} (VOL)_{out} - (VOL)_{in} &= \Delta t \left[\frac{1}{2} (Q_j^0 - Q_{j+1}^0 + Q_{j+1}^M - Q_j^M) + \sum_{n=0}^{M-1} [Q_{j+1}^n - Q_j^n] \right] \end{aligned} \quad (44)$$

Substituting (40) into (44) and rearranging yields

$$\begin{aligned} (VOL)_{out} - (VOL)_{in} &= \frac{\Delta t}{2(C_1 + C_2)} [(C_2 - C_1)(Q_j^M - Q_j^0) + (C_1 + C_2 - 2)(Q_{j+1}^M - Q_{j+1}^0)] \end{aligned} \quad (45)$$

So if the time period T is selected to be large enough to satisfy the conditions that $Q_j^M = Q_j^0$; $Q_{j+1}^M = Q_{j+1}^0$, then, (45) becomes

$$(VOL)_{out} - (VOL)_{in} = 0 \quad (46)$$

Therefore, (46) also demonstrates that the volume of the routed outflow is always the same as that of the inflow using the CPMC method. Hence the discrete CPMC method always conserves volume exactly if the initial and final states of the simulation coincide.

APPENDIX II. DEMONSTRATION OF VOLUME NONCONSERVATION FOR VPMC METHOD

From (31) for the Muskingum method

$$\int_0^T \left(K\epsilon \frac{dI}{dt} \right) dt + \int_0^T \left[K(1 - \epsilon) \frac{dQ}{dt} \right] dt = \int_0^T I dt - \int_0^T Q dt \quad (47)$$

Using the same notation as that in (31a) and (31b), (47) can be written as

$$V_i - V_o = \int_0^T \left(K\epsilon \frac{dI}{dt} \right) dt + \int_0^T \left[K(1 - \epsilon) \frac{dQ}{dt} \right] dt \quad (48)$$

(I) (II)

Similarly, if the total integral time (T) is divided into M subparts, with each having the same time step of Δt (i.e., $T = M\Delta t$), then Term (I) in (48) can be written as

$$\sum_{i=1}^M (K\epsilon)_i (\Delta I)_i = (K\epsilon)_M I_M - (K\epsilon)_1 I_0 + \sum_{i=1}^{M-1} [(K\epsilon)_i - (K\epsilon)_{i+1}] I_i \quad (49)$$

Similarly, Term (II) in (48) can be written as

$$\begin{aligned} \sum_{i=1}^M [K(1 - \epsilon)]_i (\Delta Q)_i &= [K(1 - \epsilon)]_M Q_M - [K(1 - \epsilon)]_1 Q_0 \\ &+ \sum_{i=1}^{M-1} \{ [K(1 - \epsilon)]_i - [K(1 - \epsilon)]_{i+1} \} Q_i \end{aligned} \quad (50)$$

- Δx = space step.
- Δt = time step; and
- θ = temporal weighting coefficient;
- μ = adjustment factor, Eq. (23);
- γ = curvature parameter of inflow hydrograph, Eq. (24);
- factient, Eq. (8);
- ϵ = Muskingum routing parameter, spatial weighting coefficient, Eq. (13);
- β = curvature parameter of inflow hydrograph, Eq. (13);
- x = longitudinal coordinate;
- $\text{Vol}\%$ = volume loss/gain percentage of outflow, Eq. (27);
- $V\%$ = final storage volume;
- V_t = volume of outflow, Eq. (31c);
- V_i = volume of inflow, Eq. (31b);
- V_0 = initial storage volume;
- V = storage volume;
- t_p = time to peak of outflow;
- t = time variable;
- T_p = time to peak of inflow;
- T = whole time period (= $M\Delta t$);
- S = channel bed slope;
- Q_r = routed outflow;
- Q_{po} = peak flow of routed outflow;
- Q_{peak} = inflow peak flow, Eqs. (13) and (24);
- Q_{base} = inflow base flow, Eqs. (13) and (24);
- Q_n = steady discharge at normal depth;
- Q = reference discharge;
- Q = discharge;
- n = temporal index, time superscript;
- L = total routed channel length;
- K = Muskingum routing parameter, Eq. (7);
- j = spatial index, space subscript;
- i = index of corner points at computational cell;
- l = inflow discharge hydrograph;
- h = water flow depth;
- D' = corrected diffusion coefficient;
- D = diffusion coefficient [$= Q/(2B\Delta x)$];
- Cr = Courant number ($Cr = c\Delta t/\Delta x$);
- nal hydrostatic pressure gradient, Eq. (14);
- cor = correction coefficient to account for effect of longitudinal
- (c) = reference kinematic wave speed;
- c' = corrected kinematic wave speed;
- c = kinematic wave speed;
- C_2 = routing coefficient of Muskingum equation;
- C_1 = routing coefficient of Muskingum equation;
- B = channel width at water surface;
- A = wetted cross-sectional area of flow;

The following symbols are used in this paper:

APPENDIX IV. NOTATION

ing methods: A review." *J. Hydr. Div., ASCE*, 105(12), 1521-1536.

Weinmann, P. E., and Laursen, E. M. (1979). "Approximate flood routing methods." *J. Hydr. Div., ASCE*, 105(12), 1521-1536.

Muskingum-Cunge method for flood routing in a compound channel." *J. Hydr. Res., Delft, The Netherlands*, in press.

Tang, X., Knight, D. W., and Samuels, P. G. (1999). "Variable parameter routing method for flood routing in a compound channel." *visited*. *J. Hydr.*, 48, 327-342.

Strupczewski, W., and Kundzewicz, Z. (1980). "Muskingum method revisited." *J. Hydr.*, 48, 327-342.

neering, No. 3, P. Novak, ed., Elsevier, 129-173.

Price, R. K. (1985). "Flood routing." *Developments in Hydraulic Engineering*, with variable parameters." *J. Hydr. Div., ASCE*, 104(12), 1663-1667.

Ponce, V. M., and Yevjevich, V. (1978). "Muskingum-Cunge methods routing." *J. Hydr. Div., ASCE*, 108(6), 747-757.

Ponce, V. M., and Theurer, F. D. (1982). "Accuracy criteria in diffusion routing." *J. Hydr. Div., ASCE*, 108(6), 747-757.

Ponce, V. M., Lohani, A. K., and Scheyhing, C. (1996). "Analytical verification of Muskingum-Cunge routing." *J. Hydr.*, 174, 235-241.

revised." *J. Hydr.*, 163, 439-443.

Ponce, V. M., and Chaganti, P. V. (1994). "Muskingum-Cunge method

hydrograph routing method: II Evaluation." *J. Hydrologic Engng.*, ASCE, 3(2), 115-121.

Pernual, M., and Ranga Raju, K. G. (1998). "Variable-parameter stage-Flood Routing Studies, Vol. 3, NERC, London.

Natural Environment Research Council. (1975). "Flood studies report." *University Press, Cambridge.*

differential equations: An introduction, 1st Ed., The Cambridge University Press, Cambridge.

Morton, K. W., and Mayers, D. F. (1994). *Numerical solution of partial flows.* "Unsteady flow in open channels," K. Mahmood and V. Yevjevich, eds., Water Resources Publications, Fort Collins, Colo.

Miller, W. A., and Cunge, J. A. (1975). "Simplified equations of unsteady flow movement in long rivers." *Proc. Roy. Soc., London, Series A*, 229, 281-316.

Lighthill, M. J., and Whitham, G. A. (1955). "On kinematic waves: I. Flood movement in long rivers." *Proc. Roy. Soc., London, Series A*, 117(5), 629-642.

Kousis, A. D. (1983). "Accuracy criteria in diffusion routing: A discussion." *J. Hydr. Div., ASCE*, 109(5), 803-806.

Kousis, A. D. (1980). "Comparison of Muskingum method difference schemes." *J. Hydr. Div., ASCE*, 106(5), 925-929.

Macmillan, New York.

Henderson, F. M. (1966). *Open channel flow*, "Chapter 9: Flood routing." for compound sections." *J. Hydr. Engng., ASCE*, 117(5), 629-642.

Gabrecht, G., and Brunner, G. (1991). "Hydrologic channel-flow routing (Muskingum method)." *J. Hydr. Res.*, 7(2), 205-230.

Cunge, J. A. (1969). "On the subject of a flood propagation method (Muskingum method)." *J. Hydr. Res.*, 7(2), 205-230.

Engng., ASCE, 123(3), 174-181.

Cappelaere, B. (1997). "Accurate diffusive wave routing." *J. Hydr. Engng.*, ASCE, 123(3), 174-181.

APPENDIX III. REFERENCES

This paper describes work funded by the Ministry of Agriculture, Fisheries and Food (MAFF) under their Commission FD01 (River Flood Prediction) at HR Wallingford. Publication implies no endorsement by the MAFF of the paper's conclusions or recommendations. The work was undertaken for HR Wallingford in the School of Civil Engineering at the University of Birmingham.

ACKNOWLEDGMENTS

the outflow. normally exhibits a nonconservation form for the volume of method is used. This demonstrates that the VPMC method is generally not equal to that of the inflow when the VPMC Therefore, (54) shows that the volume of the routed outflow

$$V_i \neq V_o \quad (54)$$

that is

$$V_i - V_o \neq 0 \quad (53)$$

Therefore (52) shows that in general $K_n \neq K_{i+1}$, and $[K(1 - \epsilon)]_i \neq [K(1 - \epsilon)]_{i+1}$. In the VPMC method, both K and ϵ are variable. Generally

$$\sum_{i=1}^{M-1} \{ [K(1 - \epsilon)]_i - [K(1 - \epsilon)]_{i+1} \} Q_i \quad (52)$$

When T (which equals $M\Delta t$) is large enough to have $I_M - I_0$ and $Q_M = Q_0 = I_0$, (51) becomes

$$\sum_{i=1}^{M-1} \{ [K(1 - \epsilon)]_i - [K(1 - \epsilon)]_{i+1} \} Q_i \quad (51)$$

inserting (49) and (50) into (48) gives

$$V_i - V_o = (K\epsilon)_M I_M - (K\epsilon)_0 I_0 + [K(1 - \epsilon)]_M Q_M - [K(1 - \epsilon)]_0 Q_0 + \sum_{i=1}^{M-1} \{ [K(1 - \epsilon)]_i - [K(1 - \epsilon)]_{i+1} \} I_i$$

APPENDIX 2

Tang, X., Knight, D.W. and Samuels, P.G., 1999b, "Variable parameter Muskingum-Cunge method for flood routing in a compound channel", *Journal of Hydraulic Research*, IAHR, Vol. 37, No. 5, pp 1-24.

Variable parameter Muskingum-Cunge method for flood routing in a compound channel

Méthode Muskingum-Cunge à paramètres variables pour la propagation des crues en chenaux à lits composés

XIAONAN TANG and DONALD W KNIGHT, *School of Civil Engineering, The University of Birmingham, Edgbaston, Birmingham, B15 2TT, UK*

PAUL G SAMUELS, *HR Wallingford, Wallingford, Oxon, OX10 8BA, UK*

ABSTRACT

This paper investigates the properties of the Variable Parameter Muskingum-Cunge method (VPMC) for flood routing, using several hypothetical flood hydrographs in a prismatic compound channel with significant floodplains. Two variants of the VPMC method (MVP3, VPMC4-1) are tested and these tests show that VPMC4-1 is relatively better. However, both schemes still suffer, to different degree, a loss of outflow volume which depends on bed slope and roughness of the floodplains. Furthermore, a well-known initial leading edge 'dip' occurs under certain conditions, and a less well-known phenomenon, referred to as trailing edge 'oscillations', is found to occur on the recession stage of the outflow hydrograph in steep channels. These oscillations become more serious as the roughness of the floodplains increases, but gradually disappear with decreasing bed slope. These oscillations are a consequence of the variation in the convective wave speed in a compound channel and have, to the Authors' knowledge, not been reported before in the literature on flood routing. A condition for selecting appropriate space and time steps in order to eliminate both 'dip' and 'oscillations' is obtained. A scheme with the routing parameters (c and D) modified to take account for the effect of the longitudinal hydrostatic pressure term is compared with an earlier VPMC method and shown to exhibit an improvement in terms of volume loss. Two empirical relationships to estimate the percentage of volume loss for a given bed slope are presented. Finally, different approaches for predicting the c - Q relationship in the VPMC method are shown to have some effect on the outflow hydrographs, particularly for compound channels with mild bed slopes.

RESUME

L'article examine les propriétés de la méthode Muskingum-Cunge à paramètres variables (Variable Parameter Muskingum-Cunge method: VPMC) pour la propagation des crues, en utilisant plusieurs hydrogrammes hypothétiques de crue, dans des chenaux composés prismatiques présentant un lit majeur significatif. Deux variantes de la méthode VPMC (MVP3, VPMC4-1) ont été testées et ces tests montrent que la méthode VPMC4-1 est relativement meilleure. Cependant, les deux schémas sont affectés, à des degrés divers, d'une perte de volume de débit sortant, qui dépend de la pente longitudinale et de la rugosité des plaines d'inondation. En plus, sous certaines conditions, le front de l'onde présente une sorte de dépression bien connue. Moins connues sont les espèces d'oscillations suivant l'onde et qui se produisent lors de la décrue de l'hydrogramme dans les chenaux à forte pente de fond. Ces oscillations deviennent significatives quand la rugosité des plaines d'inondation augmente, et disparaissent progressivement pour des pentes de fond plus faibles. Ces oscillations sont la conséquence de la variation de la célérité de l'onde de convection dans un chenal composé, et n'ont, à la connaissance des auteurs, pas été reportées auparavant dans la littérature de la propagation des crues. Une condition a été développée, pour choisir les pas de temps et d'espace appropriés pour éliminer tant la dépression que les oscillations. Un schéma avec modification des paramètres de propagation (c et D) pour tenir compte des effets des termes de pression hydrostatique longitudinale, permet de réduire la perte de volume, par comparaison avec une méthode VPMC antérieure. Deux relations empiriques sont présentées pour estimer le pourcentage de volume perdu pour une pente de fond donnée. Finalement, on montre que différentes approches utilisées pour prédire la relation c - Q dans la méthode VPMC ont quelque effet sur l'hydrogramme du débit à l'aval, particulièrement dans le cas de chenaux composés à faible pente de fond.

Revision received September, 1998. Open for discussion till April 30, 2000.

Introduction

The Muskingum-Cunge method with Variable Parameters (i.e. VPMC) for flood routing has received much attention in recent research literature (e.g. Ponce & Yevjevich, 1978; Koussis, 1978, 1980, 1983; Weinmann & Laurenson, 1979; Ponce & Theurer, 1982; Younkin & Merkel, 1988a, 1988b; Garbrecht & Brunner, 1991; Perumal, 1992; Ponce & Chaganti, 1994; Ponce et al. 1996). However the majority of these researchers have focused on certain features of this method, such as accuracy criteria, volume conservation, and the commonly known leading edge 'dip', for example, and have mainly concentrated on inbank flows in channels of simple cross sectional shape. As is well known, the VPMC method exhibits a number of distinct advantages, such as:

- It produces consistent results with varying grid resolutions (Ponce & Theurer, 1982; Jones, 1983);
- It is comparable to the diffusion wave routing (Cunge, 1969; Miller & Cunge, 1975);
- It is a nonlinear method and simulates the wave steepening (Ponce & Chaganti, 1994).

However, the VPMC method still suffers some deficiencies, most notably a small but perceptible volume loss (Ponce & Chaganti, 1994) and the initial leading edge 'dip' (Tang et al., 1999), and these issues still appear to dominate the discussion in the literature.

Very few studies have been undertaken on these features of the VPMC method when applied to overbank flows in channels with a compound cross section, which is surprising, given their significance in practical applications of flood routing. One of the reasons for this is that the characteristics of flow in compound channels are complicated and still relatively poorly understood (Knight & Shiono, 1996). In this study, a series of numerical experiments are carried out to explore the general features of the VPMC method, applied to flood routing in compound channels. Tests show that a significant deformation (flattening) of the rising limb of the outflow hydrograph occurs, which demonstrates the important effect of floodplain storage on the hydrograph propagation. In a similar manner to inbank flows, the VPMC method still produces a small but perceptible volume loss in the outflow hydrograph, depending on the channel bed slope and roughness of the floodplain. A new non physical phenomenon, that of trailing edge oscillations in the recession stage of the outflow, was found to be produced by the VPMC method when applied in steep compound channels ($S \geq 0.003$). These oscillations disappear with decreasing channel bed slope. A variant of the VPMC method is also discussed in which the routing parameters, c & D (wave speed and diffusion coefficient), are modified to account for the effect of the longitudinal hydrostatic pressure term. This method was developed by the authors (Tang et al., 1999) for inbank flows and shows good volume conservation. This variant shows a significant improvement on volume conservation compared to the more commonly used VPMC schemes in compound channels. Finally both 'dip' and oscillation phenomena are discussed, and the conditions for eliminating such unrealistic phenomena are given, thus enhancing the practical application of the VPMC method.

Routing schemes

The Muskingum-Cunge routing scheme has been well documented in previous work by Cunge (1969), Ponce & Yevjevich (1978), Koussis (1980, 1983), Miller & Cunge (1975) and Weinmann & Laurenson (1979). This method is actually a kinematic wave routing method, in which the kinematic wave equation is transformed into an equivalent diffusive wave equation by matching the physical diffusion to the numerical diffusion resulting from the imperfectly centered finite differ-

ence scheme (Smith, 1980). Thus the Muskingum-Cunge method accounts for both the convection and diffusion of the flood wave. The routing parameters can be linked to physical channel properties and flow characteristics (Cunge, 1969), and when these parameters are recalculated and updated as a function of local flow values for each computational cell, the routing parameters are variables in time (Price, 1985).

As is well-known, flood wave movement can be described by the equations for 1-D unsteady open-channel flow, known as the St. Venant equations, in terms of discharge Q as variable, shown as:

$$\frac{\partial A}{\partial t} + \frac{\partial Q}{\partial x} = 0 \quad (\text{continuity equation}) \quad (1)$$

$$\frac{\partial Q}{\partial t} + \frac{\partial}{\partial x} \left(\beta \frac{Q^2}{A} \right) + gA \frac{\partial h}{\partial x} + gA(S_f - S) = 0 \quad (\text{momentum equation}) \quad (2)$$

where x is longitudinal distance in the downstream direction, t is time, A is wetted cross-sectional area, B is water surface width, h is the depth of flow, S is bed slope of the channel, β is momentum correction coefficient (≈ 1), and S_f is friction slope (slope of energy line).

In most natural rivers, the inertial or the acceleration terms (i.e. terms containing the derivative of discharge (Q) with respect to x or t) in the momentum equation are so small to be negligible in comparison with the bed slope term (Henderson, 1966; Price, 1985). The above two equations then reduce to a convective-diffusion equation (Weinmann & Laurenson, 1979):

$$\frac{\partial Q}{\partial t} + c \frac{\partial Q}{\partial x} = D \frac{\partial^2 Q}{\partial x^2} \quad (3)$$

where $c = dQ/dA = (1/B)dQ/dh$ – kinematic wave speed;
 $D = Q/(2BS)$ – diffusion coefficient.

If both inertial and pressure forces are neglected, the St. Venant equations reduce to the well-known kinematic wave equation (Lighthill & Whitham, 1955):

$$\frac{\partial Q}{\partial t} + c \frac{\partial Q}{\partial x} = 0 \quad (4)$$

The difference scheme of the Muskingum-Cunge method can be obtained by applying the four point box scheme to (4) with a spatial weighting factor (ϵ) and a temporal weighting factor (θ), where θ is assumed to be 1/2, and matching the numerical diffusion with the physical diffusion produced by D (Miller & Cunge, 1975; Weinmann & Laurenson, 1979). Thus at any grid box (see Fig. 1):

$$Q_{j+1}^{n+1} = C_1 Q_j^n + C_2 Q_j^{n+1} + C_3 Q_{j+1}^n \quad (5)$$

with

$$C_1 = (K\varepsilon + 0.5\Delta t)/[K(1 - \varepsilon) + 0.5\Delta t] \quad (6)$$

$$C_2 = (-K\varepsilon + 0.5\Delta t)/[K(1 - \varepsilon) + 0.5\Delta t] \quad (7)$$

$$C_3 = [K(1 - \varepsilon) - 0.5\Delta t]/[K(1 - \varepsilon) + 0.5\Delta t] \quad (8)$$

in which j is a spatial index, n is a temporal index (see Fig. 1); Q is the total discharge; and Δt is the time step in the finite difference cell. The routing parameters K & ε are given in terms of flow, channel and grid specifications:

$$K = \frac{\Delta x}{c_r} \quad (9)$$

$$\varepsilon = \frac{1}{2} \left(1 - \frac{Q_r}{BSc_r\Delta x} \right) \quad (10)$$

where Δx is the space step of the finite difference cell; c_r is a representative flood wave celerity; Q_r is a representative discharge.

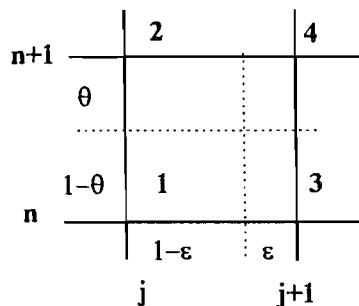


Fig. 1. Computational grid cell.

The variation of routing parameters can be implemented in the calculation by evaluating the coefficients (K , ε) for every computational cell as a function of updated values of discharge and wave celerity, which at a grid point (j , n) is defined as:

$$c = \left. \frac{dQ}{dA} \right|_{j,n} \quad (11)$$

where A is the flow area. The relation between discharge and wave celerity can be obtained by using Manning's uniform flow equation. Based on an averaging technique of local flow values at each computational grid point (see Fig. 1), two schemes are used in the present study to evaluate the parameters (K , ε), referred to as MVPMC3 and VPMC4-1:

$$\text{MVPMC3: } Q_r = (\Sigma Q_i)/3, c_r = f(Q_r); i = 1, 2, 3$$

This scheme was proposed by Ponce & Chaganti (1994). The subscript (r) denotes the responding representative values to evaluate K & ϵ in equations (9) & (10) for every computational cell, and $c = f(Q)$ denotes that c is a function of discharge (Q).

$$\text{VPMC4-1: } c_r = (\Sigma c_i)/4 = [\Sigma f(Q_i)]/4 \quad \text{for } K; \quad i = 1, 2, 3, 4$$

$$\left(\frac{Q}{c}\right)_r = [\Sigma(Q_i/c_i)]/4 \quad \text{for } \epsilon$$

This scheme has been proposed by the Authors (Tang et al, 1999) and requires iteration to calculate Q_r and c_r since they involve the unknown Q_4 .

Estimation of wave speed – discharge relationships for flows in compound channels

In order to determine the routing parameters (K , ϵ), the relationship between c and Q , which is defined by equation (11) or the stage-discharge curve, is required. Overbank flow in a compound channel is complex, typically three dimensional and significantly different from inbank flow. One obvious feature of overbank flow is the bank of vertical interface vortices which exist between the main channel and the adjacent floodplain(s) due to the difference in velocities. This interface significantly affects the velocity distribution, and consequently the distribution of discharge between the main channel and the floodplain. Therefore a proper understanding of this momentum transfer between the main channel and its floodplain will improve the accuracy of the discharge calculation, and will also be of benefit to flood routing, sediment transport, and other phenomena.

Unfortunately the discharge calculation for compound channels is based mainly on refined one-dimensional methods of analysis. Two-dimensional approaches are receiving increasing attention (Abril & Knight, 1999; Knight & Shiono 1996; Knight & Abril, 1996), and some effort is also being put into three-dimensional analysis (Shiono & Lin 1992; Younis 1996). However, both of these are more complex and inconvenient to use in practice. The basic idea of 1-D approaches is to subdivide the channel into a number of discrete sub-channels, usually the main channel and the adjacent floodplains, to calculate the discharge for each part, with or without consideration of the interaction effect, and to sum them, possibly with some adjustment, to give the total channel conveyance. Typical 1-D methods which are currently used are as follows:

1 Vertical division method (VD)

There are several Vertical Division methods which are based on altering the wetted perimeter of the sub-area to account for the effects of interaction. It is assumed that the flows in the main channel and its adjoining floodplains are independent. Typically the vertical division line between the main channel and its floodplains is included in the wetted perimeter for the discharge calculation of the main channel flow, but is excluded in the wetted perimeter for the discharge calculation of the floodplain flow. This is intended to have the effect of retarding the flow in the main channel and enhancing it in the floodplain. However simply altering the wetted perimeter by the vertical line does not completely reflect the interaction effect because this interaction effect is not a simple function as the floodplain water depth increases (Knight & Demetriou, 1983; Knight & Shiono, 1990). It is found that this approach generally overpredicts flow rate (Wormleaton & Merrett, 1990) and

conceptually it is flawed since it implies an imbalance of shear forces at the interface. However, improvements may be made to this method, as recently shown by Lambert & Myers (1998).

2 Diagonal division method (DD)

In this method it is assumed that there is a zero-shear stress line, which commences from the main channel/floodplain junction and is inclined towards the centre of the main-channel water surface, separating the main channel from its floodplains. The total discharge is then obtained through summing up the discharges in each of the three individual zones. The idea of drawing a division line having zero shear stress is logically acceptable, but the main difficulty is in finding the position of this division line for all shapes of channel and flow depths, due to the three-dimensional nature of the velocity fields. Experimental results demonstrate that the shear stresses on the diagonal division line are negligible, except for small relative floodplain flow depths (Wormleaton et al. 1982; Knight & Hamed, 1984), which are commonly experienced when a river just goes overbank.

3 Area method

In this method, a zero shear stress is assumed to act on an interface between the main channel and its floodplains, with an arbitrary position (see Fig. 2). The flow areas for each part of the channel are then adjusted, as given by (Stephenson & Kolovopoulos, 1990):

$$A_{cc} = A_c - 2(\Delta A) \quad (12)$$

$$A_{ff} = A_f + 2(\Delta A) \quad (13)$$

where A_{cc} , A_{ff} = modified area of main channel and floodplain respectively, and the correction area (ΔA) can be obtained from the equilibrium of forces acting on the floodplain, where a vertical interface divides the main channel from the floodplain, given by:

$$\Sigma F_f - \tau_v d = \rho g A_f S \quad (14)$$

in which ΣF_f = shear force on the wetted perimeter of the floodplain per unit streamwise length, τ_v = apparent shear stress on the vertical interface, and d = flow depth over floodplain.

If the arbitrary interface with zero stress is used, then it follows that,

$$\Sigma F_f = \rho g (A_f + \Delta A) S \quad (15)$$

Combining (14) & (15), and rearranging gives,

$$\Delta A = [\tau_v / (\rho g S)] d \quad (16a)$$

or

$$\Delta A = \tau_v d \quad (16b)$$

where τ_r = the relative apparent shear stress on the vertical division interface, $\tau_v / (\rho g S)$, and τ_v is given herein by the Prinos-Townsend empirical equation (Prinos & Townsend, 1984):

$$\tau_v = 0.874(\Delta V)^{0.92}(d/H)^{-1.129}(W_f/W_c)^{-0.514} \quad (17)$$

where H = total flow depth of channel; W_c, W_f = main channel width and floodplain width at bank-full stage respectively; ΔV = difference between velocity in main channel and floodplain. Equation (17) is based on experimental results for varied cross sections and rough floodplains including the data of Wormleaton et al (1982) and Knight & Demetriou (1983). It should be noted that this method is only valid within the range of empirical results employed and is not generally applicable.

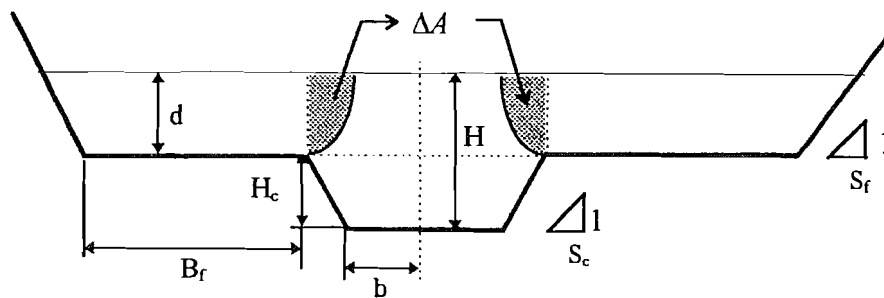


Fig. 2. The trapezoidal compound cross-section.

4 "Coherence" method (COH)

This one-dimensional approach is based on the 'coherence' concept proposed by Ackers (1992, 1993). A number of experiments on compound channels in the large scale UK Flood Channel Facility (FCF) at HR Wallingford (see Knight & Sellin, 1987; Knight & Shiono, 1990), have shown that there are four distinct regions of flow behaviour for compound channels, and that these depend on the depth of floodplain flow (Ackers, 1993). The actual discharge may be computed by adjustment to the basic discharge calculation: $Q_{basic} = Q_c + Q_f$ to allow for the effect of momentum exchange between the main river channel and its floodplains in each region of flow. Depending on the region of flow, this can be achieved via either a discharge deficit, DISDEF, or a discharge adjustment factor, DISADF, as follows:

$$Q = Q_{basic} - \text{DISDEF} \quad (18)$$

$$Q = \text{DISADF} \times Q_{basic} \quad (19)$$

Ackers defined the basic conveyance of any channel in a modified form as

$$K_D = Q / \sqrt{8gS} = A \sqrt{A / (fP)} \quad (20)$$

where f = friction coefficient and P = wetted perimeter.

He then linked the discharge adjustment factors for each region to the channel “coherence” (COH), which is defined as the ratio of the basic conveyance (calculated by treating the channel as a single unit) to that computed by summing the basic conveyances of the separate zones, as defined by:

$$COH = \frac{\sum_{i=1}^{i=n} A_i \sqrt{\sum_{i=1}^{i=n} A_i / \sum_{i=1}^{i=n} (f_i P_i)}}{\sum_{i=1}^{i=n} [A_i \sqrt{A_i / (f_i P_i)}}] \quad (21)$$

where n = number of separate lateral zones into which the channel is divided.

This method is more reasonable than the previous methods given, as the discharge is directly modified by the discharge adjustment factors, which are linked to the coherence of the channel. The method has also been widely used in practice (Wark, James & Ackers, 1994).

Application of VPMC method to compound channels

Conditions considered

The VPMC method was applied to hypothetical floods passing through trapezoidal compound channels with no lateral inflows to the routing reach. Two types of inflow hydrographs were used for all the test runs, which were as follows:

Symmetric inflow hydrograph:

$$Q(t) = 0.5(Q_{peak} - Q_{base})[1 - \cos(\pi t/T_p)] + Q_{base} \quad 0 < t < 2T_p \quad (22)$$

$$Q(t) = Q_{base} \quad t \geq 2T_p, t < 0 \quad (23)$$

Asymmetric inflow hydrograph:

$$Q(t) = Q_{base} + (Q_{peak} - Q_{base})[(t/T_p) \exp(1 - t/T_p)]^\beta \quad (24)$$

where $\beta = 6$ (curvature parameter), $T_p = 15$ hours (time to peak flow), Q_{base} = baseflow discharge of inflow (10 m³/s), and Q_{peak} = peak discharge of inflow (Q_{pi}), which varies from 59 m³/s to 214 m³/s in this study. (See NERC, 1975)

The trapezoidal channels employed for all the runs were based on the hypothetical benchmark compound channels introduced by Ackers (1992, 1993). Each channel was 20 km in length and had the following dimensions for the cross-section (See Fig. 2):

bed width $2b = 15$ m; (N.B. b = semi-width of bed of main channel)

bankfull depth $H_c = 1.5$ m ;

two flood plains with each width $B_f = 20$ m;

main channel and flood plain channel side slopes ($S_c = S_f = 1$)

Manning's coefficient for the main channel was $n_c = 0.03$, whereas for the floodplain it varied from $n_f = 0.03$ to 0.12. The routing channel bed slope varied from $S = 0.003$ to 0.0001. In the discussion below, in the relationship between c and Q for evaluating K , ϵ was obtained by the 'COH' method unless some other methods are mentioned. A typical $c \sim Q$ relationship for a trapezoidal compound channel is shown in Fig. 3, based on Eq. (11).

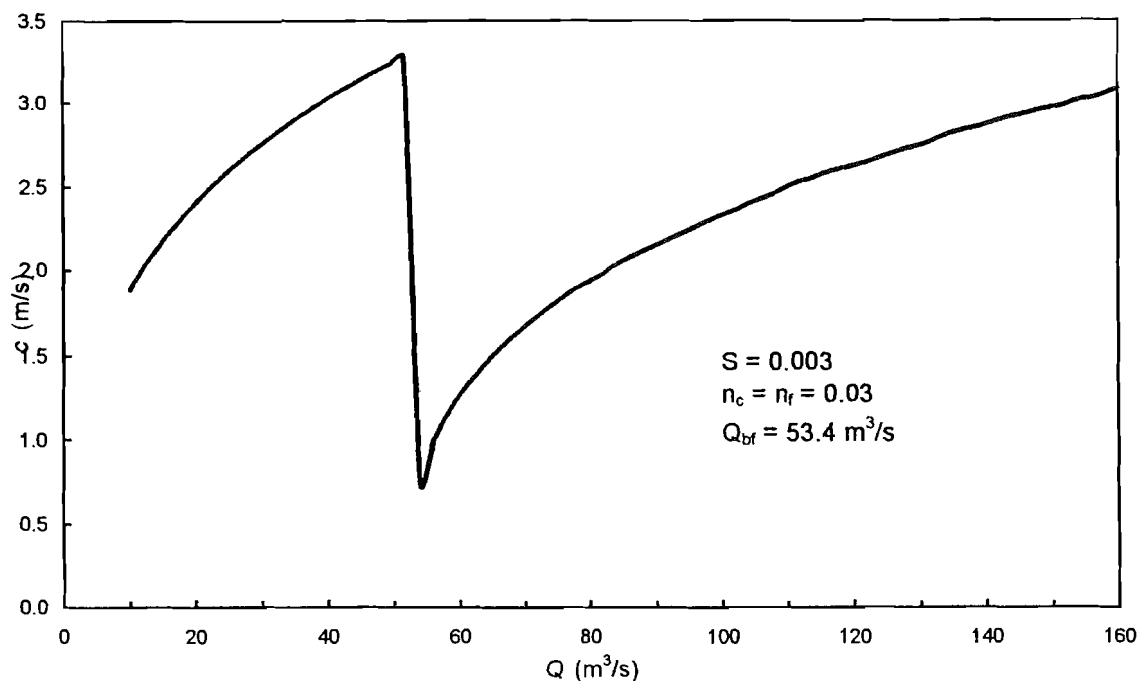


Fig. 3. A $c \sim Q$ relationship in a trapezoidal compound channel.

Comparison of results by MVPMC3 and VPMC4-1 schemes

Comparisons of the two schemes of MVPMC3 and VPMC4-1 were carried out for different resolutions of Δx and Δt with symmetric inflow and asymmetric inflow hydrographs ($Q_{peak} = 100 \text{ m}^3/\text{s}$) in the compound channel and with $S = 0.0003$ and $n_f = 0.06$. The results are compared in Table 1. It should be noted that in all the following Tables the volume conservation feature of a routed outflow hydrograph is evaluated by an index, Vol %, which is defined by:

$$\text{Vol}\% = \frac{\int_0^T Q dt}{\int_0^T I dt} \times 100 \quad (25)$$

where

$$\int_0^T I dt, \int_0^T Q dt$$

denote the volumes of inflow and outflow respectively, within the whole time period of T , and are computed by numerical integration using Simpson's rule.

Table 1. Results by MVPMC3 and VPMC4-1 in a compound channel.

S = 0.0003		Symmetric inflow						Asymmetric inflow					
(n _r = 0.06)		MVPMC3			VPMC4-1			MVPMC3			VPMC4-1		
Δt	Δx	t _p	Q _{po}	Vol%	t _p	Q _{po}	Vol%	t _p	Q _{po}	Vol%	t _p	Q _{po}	Vol%
0.5hr	500 m	22	88.13	97.38	22	88.18	97.46	22.5	85.48	98.82	22.5	85.55	99.04
	1000	22	88.17	96.52	22	88.18	96.50	22.5	85.51	98.58	22.5	85.54	98.63
	2000	22	88.23	97.31	22	88.17	96.53	22.5	85.65	99.15	22.5	85.55	98.72
	4000	22	88.39	99.45	22	88.19	96.52	22.5	85.87	100.24	22.5	85.58	98.74
(dip)	10000	21.5	89.10	102.93	21.5	88.61	97.50	22	86.42	101.74	22	85.90	99.36
0.25	1000	21.75	88.22	97.15	21.75	88.19	97.11	22.5	85.60	98.98	22.5	85.53	98.87
0.5		22	88.17	96.52	22	88.18	96.50	22.5	85.51	98.58	22.5	85.54	98.63
1.0		22	88.10	97.40	22	88.19	97.40	23	85.35	98.65	23	85.50	98.88
1.5		22.5	87.76	97.80	22.5	87.90	97.65	22.5	85.40	98.88	22.5	85.64	99.24

The principal effects are as follows:

- The time to peak of outflow is affected very little by different Δx and Δt values, with changes within one time step or so for both MVPMC3 and VPMC4-1;
- With increasing Δx , an initial leading edge 'dip' forms in the outflow hydrograph, as shown in Fig. 4. This is accompanied by some increase of outflow peak values, which is not surprising since the initial "dip", in fact, artificially stores the water in the reach and subsequently releases it gradually, thereby causing an increase in peak discharge. This effect is most pronounced for the MVPMC3 method;

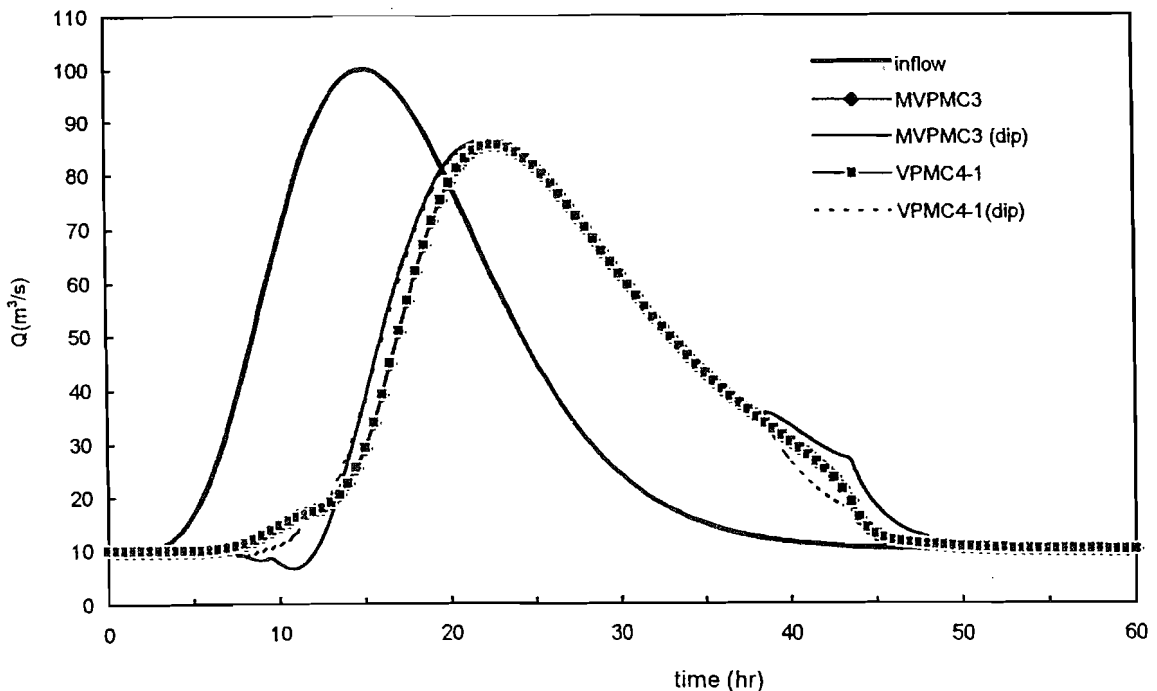


Fig. 4. Comparison of outflow hydrographs by MVPMC3 & VPMC4-1 (S = 0.0003).

- The effect of different Δx on routed peak discharge, Q_{po} , is negligible when no 'dip' exists, particularly for the VPMC4-1 method. However it does affect the volume of outflow, more so for MVPMC3 than VPMC4-1;
- Similarly the effect of different Δt values on routed Q_{po} is generally small, in particular for the VPMC4-1 method. However once again it does affect the volume of outflow, more so for MVPMC3 than VPMC4-1;
- In general, the volume loss by both VPMC schemes is less for the asymmetric inflow hydrograph than that for the symmetric inflow hydrograph. VPMC4-1 is somewhat better than MVPMC3 considering its sensitivity to different Δx and Δt .

Bed slope effect on routed results

The two types of inflow hydrographs (symmetric and asymmetric) with $Q_{peak} = 100 \text{ m}^3/\text{s}$ were routed by VPMC4-1 in the compound channel with $n_f = 0.06$ for four different bed slopes ($S = 0.003, 0.0001, 0.0005 \text{ \& } 0.0003$). Key parameters from the results are given in Table 2, and Fig. 5 gives the outflow hydrographs using asymmetric inflows for the four different bed slopes.

Table 2. Effect of bed slopes upon results by VPMC4-1.

$\Delta x=1000m, \Delta t=0.5 \text{ hr}$	Symmetric inflow			Asymmetric inflow		
Bed slope	t_p	Q_{po}	Vol%	t_p	Q_{po}	Vol%
0.003	18.5	99.76	98.95	18.5	99.70	99.14
0.001	19.5	98.68	98.37	19.5	98.37	99.05
0.0005	20.5	95.22	98.45	21.0	93.96	99.53
0.0003	22.0	88.19	97.40	22.5	85.54	98.63

Notes: $\Delta x = 1000 \text{ m}, \Delta t = 0.5 \text{ hr}$.

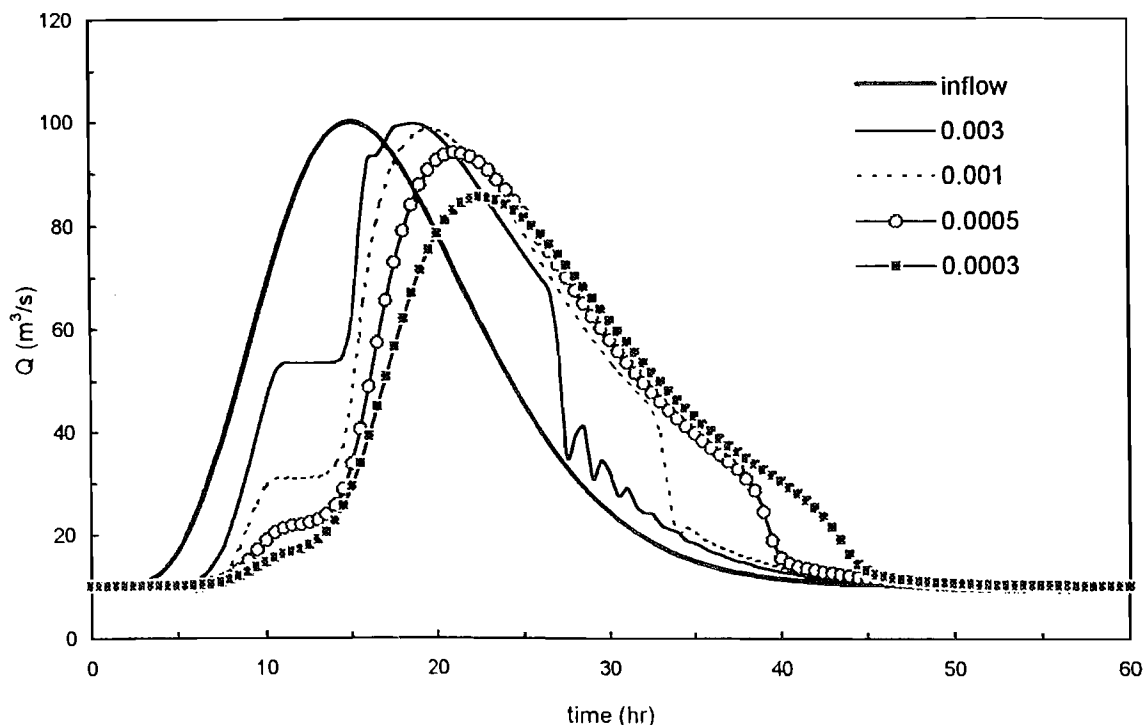


Fig. 5. Outflow hydrographs by VPMC4-1 for different bed slopes.

The following conclusions can be drawn:

- 1) As the channel bed slope becomes milder, the time to peak and the attenuation of the peak flow increase (See Table 2 & Fig. 5);
- 2) The time to peak and peak flow values of the outflow are similar for both inflow hydrographs, but the volume loss is less for asymmetric inflow than that for symmetric inflow. This implies that the volume conservation feature in the VPMC method is affected by the value of dQ/dt in the falling limb of the inflow hydrographs;
- 3) Unlike inbank flow, unrealistic oscillations occur during the recession of the outflow in steep channels (e.g. $S \geq 0.003$). The oscillations gradually become smaller with decreasing bed slope and eventually disappear.

Effect of different ratios of inflow peak to bankfull flow and different n_f on oscillations

To explore the characteristics of these oscillations, simulations were undertaken using the VPMC4-1 method in a steep compound channel, 20km in length, with $n_f = 0.06$ and $S = 0.003$, routing an asymmetric inflow hydrograph with varying peak discharges ($Q_{pi} / Q_{bf} = 1.25, 1.5, 2$ and 4, where Q_{pi} = peak inflow and Q_{bf} = the bankfull discharge). The effect of different floodplain roughness ($n_f / n_c = 1.5, 2, 3, 4$) on the routed outflows was also investigated, using the asymmetric inflow with $Q_{peak} = 100m^3/s$. Both sets of results are summarised in Table 3. The corresponding outflow hydrographs are illustrated in Figs 6 & 7 respectively.

Table 3. Results of different inflow peak discharge and roughness of floodplain.

S = 0.003, $Q_{bf} = 53.4 m^3/s$					S = 0.003, $Q_{peak} = 100 m^3/s$				
Q_{pi} / Q_{bf}	Q_{pi}	t_p	Q_{po} / Q_{pi}	Vol(%)	n_r / n_c	n_r	t_p	Q_{po}	Vol(%)
1.25	67	19.5	0.996	98.97	1.5	0.045	18.0	99.90	99.50
1.5	80	19.0	0.999	99.08	2.0	0.06	18.5	99.76	98.95
2	107	18.5	0.998	99.20	3.0	0.09	19.5	99.49	98.39
4	214	17.5	0.998	99.53	4.0	0.12	20.5	98.93	97.65

Notes: $\Delta x = 1000 m$, $\Delta t = 0.5 hr$.

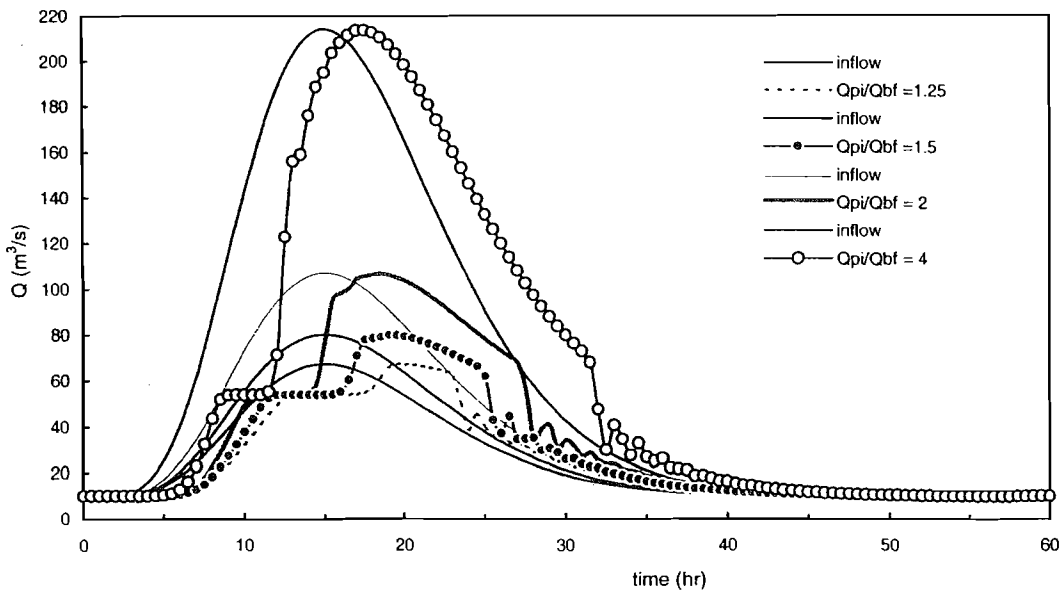


Fig. 6. Effect of different ratios of inflow peak to bankfull discharge on results for $S = 0.003$.

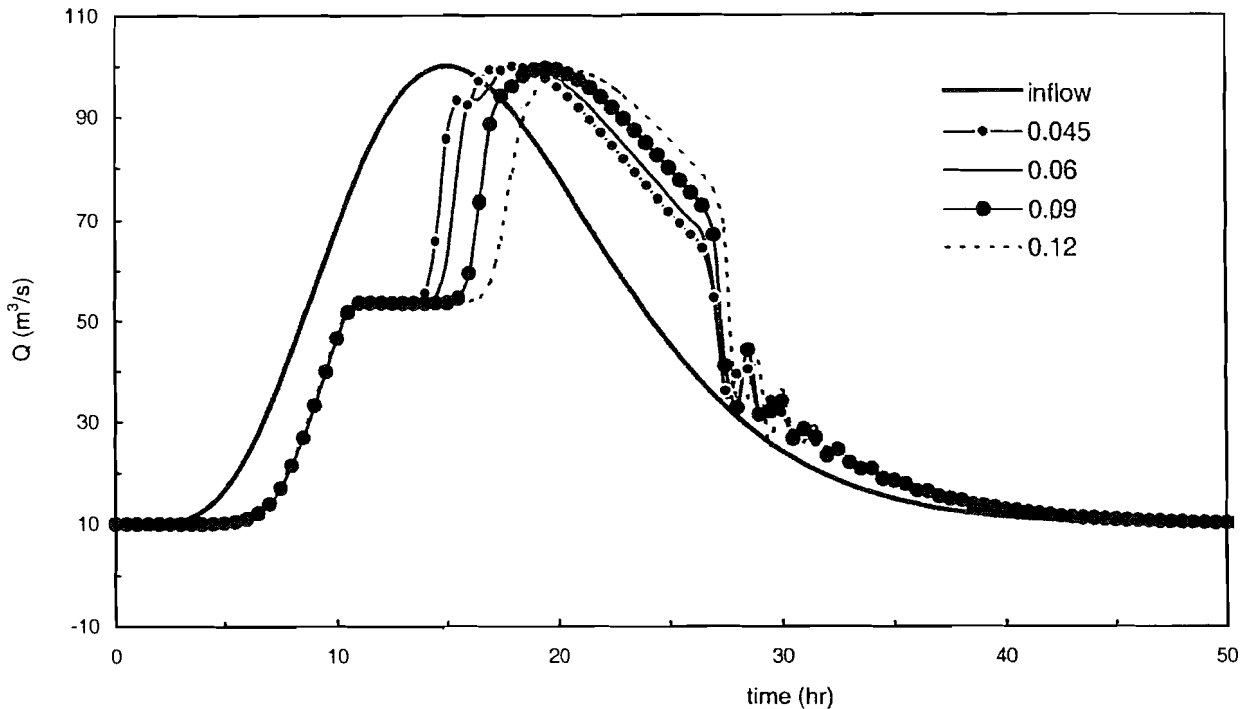


Fig. 7. Effect of different roughness of floodplain on the outflow hydrographs ($S = 0.003$).

From these tests, the following conclusions are obtained:

- 1) The routed time to peak becomes smaller with increasing ratio of inflow peak discharge to bankfull discharge (Q_{pi}/Q_{bf}). This implies that the role of storage on the floodplain for small Q_{pi}/Q_{bf} greatly delays the propagation of peak flow. The time to peak of the outflow increases as the roughness of the floodplain (n_f) increases, indicating that the rougher floodplains significantly delay the flood wave, as would be expected;
- 2) The ratio of outflow peak to inflow peak (Q_{po}/Q_{pi}) is almost the same for different inflow peak to bankfull discharge ratios (Q_{pi}/Q_{bf}) in these test cases. This might suggest that flood wave diffusion is independent of the Q_{pi}/Q_{bf} ratio;
- 3) The attenuation of the inflow peak generally increases with increasing floodplain roughness. This implies that rough floodplains make a significant contribution to flood wave diffusion;
- 4) The volume values of the outflow hydrographs indicate that generally volume is not being conserved, although the volume loss is small. The volume loss increases with increasing floodplain roughness, and decreases slightly with increasing Q_{pi}/Q_{bf} ;
- 5) Fig. 6 shows that there is a significant shoulder in the rising limb of the outflow hydrograph, which occurs around bankfull flow, but the duration of each shoulder becomes shorter as the ratio Q_{pi}/Q_{bf} increases. The oscillations in the recession stage occur later and become progressively more serious with increasing Q_{pi}/Q_{bf} ratios;
- 6) Fig. 7 shows that the roughness of the floodplain (n_f) has a significant influence on the outflow hydrographs. The shoulder in the rising limb lasts longer, and the oscillations on the recession become more serious, with increasing floodplain roughness.

VPMC for flood routing using different prediction methods for $c \sim Q$ curves

In the VPMC method, the evaluation of the routing parameters (K, ϵ) requires the wave speed or $c \sim Q$ curves. These implicitly involve one of the approaches to determining the conveyance capac-

ity of compound channels, such as the VD, DD, Area and 'COH' 1-D methods described previously. In order to understand the impact of these methods on the VPMC method for flood routing, an asymmetric inflow hydrograph ($Q_{peak} = 100 \text{ m}^3/\text{s}$) was routed by VPMC4-1 down the trapezoidal compound channel with $n_c = 0.03$ and $n_f = 0.06$ for two bed slopes: $S = 0.003$ and 0.0003 . These routed results are given in Table 4, which shows that:

Table 4. Comparison of results using VD, DD, Area & COH methods.

$\Delta x=1000\text{m}, \Delta t=0.5\text{hr}$	S = 0.003			S = 0.0003			
	Methods	t_p	Q_{po}	Vol%	t_p	Q_{po}	Vol%
	VD	18.0	99.93	99.77	22.0	88.35	98.86
	DD	18.5	99.87	99.33	22.0	87.57	99.16
	Area	18.0	99.88	99.88	21.0	90.87	99.23
	COH	18.5	99.70	99.10	22.5	85.54	98.62

Notes: $\Delta x = 1000 \text{ m}$, $\Delta t = 0.5 \text{ hr}$.

- The routed time to peak is affected somewhat by the method for the $c \sim Q$ prediction which is employed, particularly for the milder slope channels;
- The outflow peak values are more affected by the choice of method for a mild slope channel ($S = 0.0003$), than a steep slope channel ($S = 0.003$). Similar behaviour was found for the volume difference between the outflow hydrographs. The COH method is seen to produce a slightly larger volume loss than that by the other methods, although the differences are small. It should be noted that the different bed slopes imply different Q_{pi}/Q_{bf} ratios;
- The differences in the outflow hydrographs for $S = 0.0003$ are illustrated in Fig. 8, which shows the trends highlighted in Table 4. The hydrographs produced by the V-D and DD methods give almost the same result. The area method gives the maximum rate of rise on the rising limb, whereas the COH method gives the lowest.

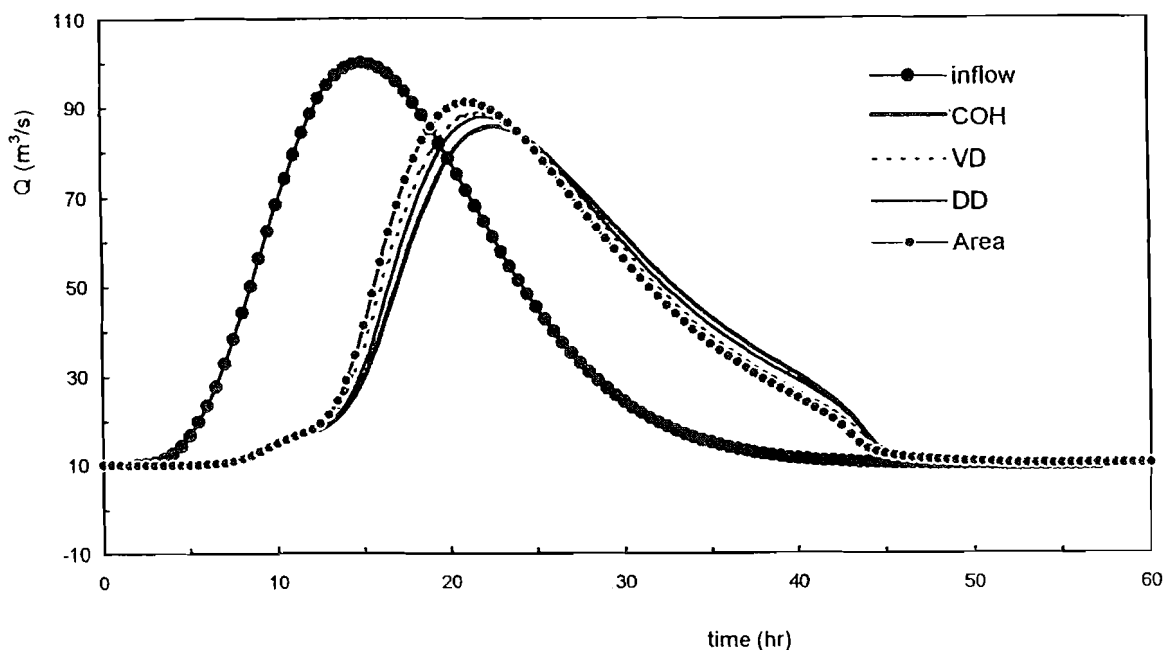


Fig. 8. Comparison on outflow hydrographs using different $c \sim Q$ prediction methods for $S = 0.0003$.

A modified VPMC scheme to improve the volume conservation

Introduction to a modified scheme for VPMC

In the VPMC method, the routing parameters (K & ϵ) are evaluated from the wave speed c and the diffusion parameter D , both of which are based on uniform flow relationships due to the complexity of unsteady flow. Usually c & D are a function of a reference discharge only. Unfortunately for these fixed methods for c & D , the VPMC method always suffers some volume loss of outflow for both simple and compound channels. Most recently, Cappelaere (1997) pointed out that the reason for volume loss in the standard variable parameter diffusion flood routing model arises from not including the effect of the longitudinal hydrostatic pressure term ($\partial h/\partial x$) in the calculations for c & D . If c & D are to be evaluated to take account of the effect of this "pressure" term, then c & D need to be modified as follows (Cappelaere, 1997):

$$c' = c \cdot cor \quad (26)$$

$$D' = D/cor \quad (27)$$

where the correction term, cor , can be expressed approximately (Tang et al, 1999) by:

$$cor = \sqrt{1 - \mu \frac{2D}{cQ_r} \frac{\partial Q}{\partial x}} \quad (28)$$

in which c & D are the values based on the uniform flow formulae and so do not include the effect of the pressure term ($\partial h/\partial x$), c' & D' are the corresponding parameters including the effect of the pressure term, μ is a free parameter, and

$$\frac{\partial Q}{\partial x} \approx (Q_{j+1}^{n+1} + Q_{j+1}^n - Q_j^{n+1} - Q_j^n)/2\Delta x$$

In this study, several μ values were tested and it was found that $\mu = 0.2$ gave the best results for producing good conservation in volume of outflow. Therefore 0.2 was used for the μ value in all the runs reported below.

Results

For simplicity of comparison, only the VPMC4-1 scheme is compared with the VPMC4 scheme with the above modification (herein it is called VPMC4-H). The tests used a symmetric inflow hydrograph ($Q_{peak} = 200 \text{ m}^3/\text{s}$, $Q_{base} = 5 \text{ m}^3/\text{s}$), routed along the previously used trapezoidal compound channel with a floodplain roughness, $n_f = 0.06$ and bed slopes $S = 0.003$ to 0.0001 . Table 5 summarises the routed results. The corresponding percentage volume loss is shown plotted against the bed slope in Fig. 9.

Table 5 shows that:

- 1) The VPMC4-1 scheme always suffers, to varying degrees, a volume loss, depending on the channel features. Generally the volume loss is small (about 0.3 %) for steep channels (e.g. $S = 0.003$), but quite large (up to 9.3%) for mild slope channels ($S = 0.0001$);

- 2) In contrast, the VPMC4-H scheme, with routed parameters c & D modified to account for the effect of the longitudinal hydrostatic pressure term ($\partial h/\partial x$), exhibits relatively good volume conservation characteristics for overbank flow. Usually the volume loss is less than 1% for $S > 0.0001$, but for $S = 0.0001$, there is a net gain, of up to 5%.
- 3) Based on these test results, the following empirical formula for estimating the degree of volume loss by the VPMC4-1 & VPMC4-H methods are suggested:

Table 5. The routed results by VPMC4-1 & VPMC4-H for different bed slopes.

Bed slope S	VPMC4-1				VPMC4-H			
	t_p	Q_{po}	Vol(%)	V%	t_p	Q_{po}	Vol(%)	V%
0.003	17.5	199.70	99.36	0.64	17.5	199.70	99.63	0.37
0.00028	17.5	199.62	99.57	0.43	17.5	199.62	99.80	0.20
0.0025	17.5	199.58	99.64	0.36	17.5	199.58	99.75	0.25
0.002	17.5	199.26	99.69	0.31	17.5	199.26	99.76	0.24
0.00175	18.0	199.02	99.65	0.35	18.0	199.03	99.80	0.20
0.0015	18.0	198.96	99.48	0.52	18.0	198.96	99.83	0.17
0.0012	18.0	198.39	99.19	0.81	18.0	198.39	99.32	0.68
0.001	18.5	197.74	98.30	1.70	18.5	197.74	98.61	1.39
0.0008	18.5	196.63	97.97	2.03	18.5	196.65	98.44	1.56
0.00065	19.0	194.96	98.24	1.76	19.0	194.99	98.93	1.07
0.0005	19.0	191.64	97.73	2.27	19.0	191.81	99.12	0.88
0.00045	19.5	189.84	97.37	2.63	19.5	190.06	98.91	1.09
0.0004	19.5	187.25	97.33	2.67	19.5	187.69	99.30	0.70
0.00035	20.0	183.53	97.17	2.83	20.0	184.19	99.31	0.69
0.0003	20.0	178.11	96.61	3.39	20.0	179.41	99.11	0.89
0.00025	20.5	170.01	95.65	4.35	20.5	172.15	99.69	0.31
0.0002	21.0	157.59	94.34	5.66	20.5	161.56	99.96	0.04
0.00015	21.0	139.42	92.75	7.25	21.0	145.86	100.79	-0.79
0.0001	19.5	116.85	90.77	9.23	19.5	125.69	104.71	-4.71

Notes: $\Delta x = 2000$ m, $\Delta t = 0.5$ hr

– Using VPMC4-1 method:

$$V\% = -0.3813 + 0.006251S^{-0.8} \quad (29)$$

$$S \in [0.00001, 0.003] \text{ with } R\text{-squared value } R^2 = 0.985.$$

and

– Using VPMC4-H method:

$$V\% = -2.1848 + 0.1516S^{-0.5} - 0.00174/S \quad (30)$$

$$S \in [0.00001, 0.003] \text{ with } R\text{-squared value } R^2 = 0.939.$$

in which S = channel bed slope, and $V\%$ = volume loss percentage, which is calculated by:

$$V\% = \frac{\text{Volume(inflow)} - \text{Volume(outflow)}}{\text{Volume(inflow)}} \times 100 \quad (31)$$

These equations are illustrated in Fig. 9, together with the tabulated data. It should be emphasized that these equations should not be used outside the range of slopes for which they were derived.

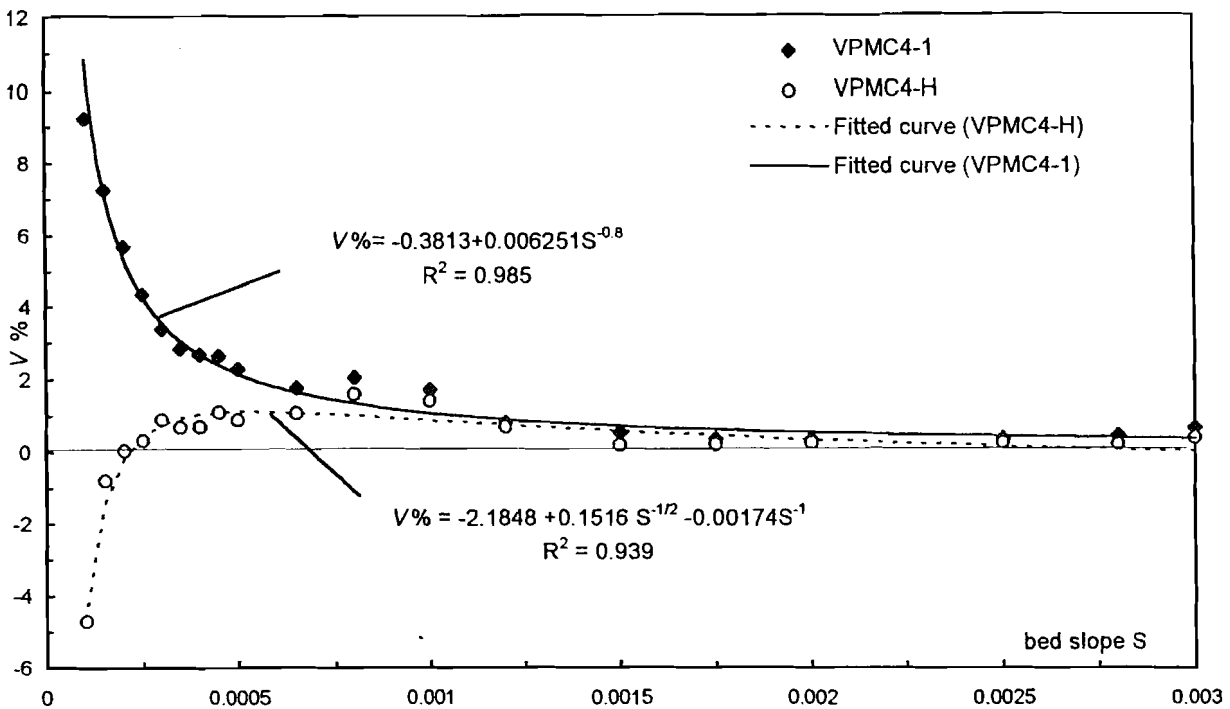


Fig. 9. Volume loss percentage ($V\%$) vs bed slopes by the VPMC method in a compound channel.

Fig. 10 illustrates the difference between the outflow hydrographs produced by the VPMC4-1 & VPMC4-H methods in a typical compound channel with $n_f = 0.06$ and $S = 0.0002$. It is seen that the VPMC4-H hydrograph rises faster and recedes slower than the VPMC4-1 one.

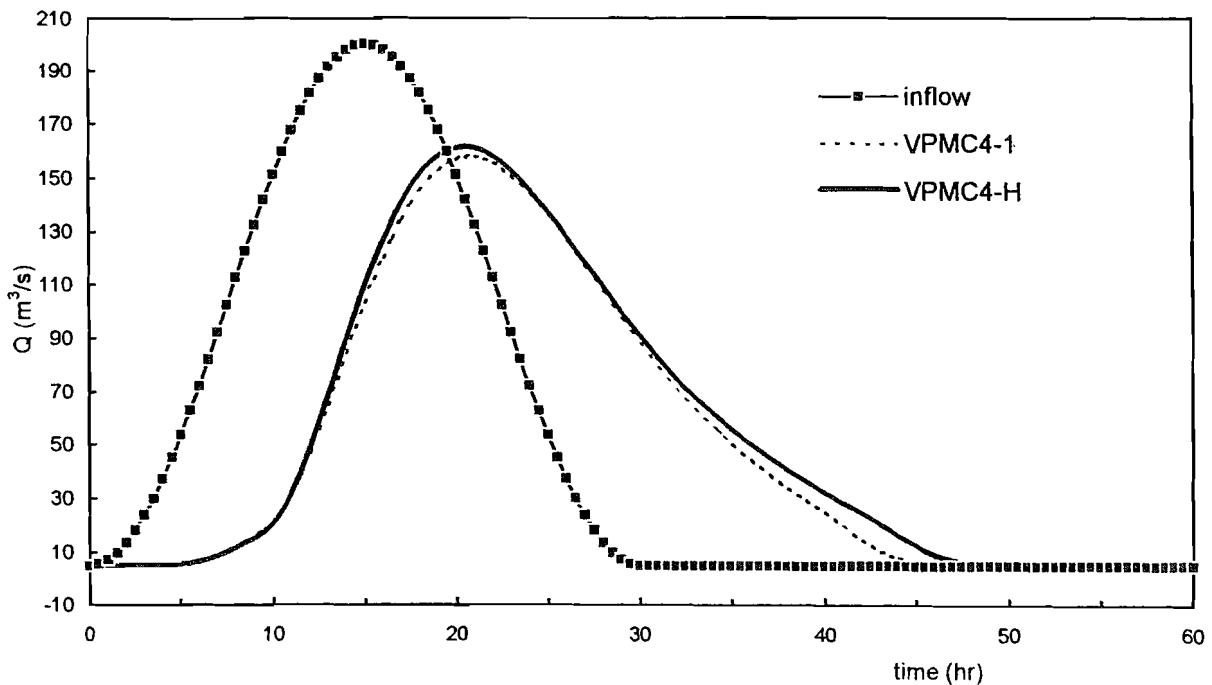


Fig. 10. Outflow hydrographs by VPMC4-1 & VPMC4-H in a typical compound channel ($S = 0.0002$).

Discussion on elimination of 'dip' and 'oscillation' phenomena

Introduction

It is the experience of most users that, under certain conditions, the Muskingum-Cunge method will produce some physically unrealistic phenomena. Most notably they are the reduced flow or negative flow in the initial stage of the outflow hydrograph, commonly called the initial leading edge 'dip', which occurs for both inbank and overbank flows, and the oscillations in the recession stage of the outflow hydrograph which occurs for overbank flows in steep compound channels. The initial 'dip' was explicitly highlighted by Nash (1959), and later discussed by Gill (1979, 1992), Ponce & Theurer (1982), Koussis (1983) and Hjelmfelt (1985), who suggested remedial measures to eliminate it. A standard mathematical treatment of the box scheme is given by Morton & Mayers (1994, pp. 109–111).

It should be pointed out that such a 'dip' or 'oscillation' phenomenon results from the difference form used in the Muskingum method. From the difference equation usually used in the numerical solution, the coefficients in equation (5) should satisfy the maximum principle in order to get a stable solution (Morton & Mayers, 1994), who state that mathematically any variable, say discharge $Q(x, t)$, is bounded above and below by the extremes attained by the initial data and the values on the boundary up to time t . This implies that all the coefficients in equation (5) have to be positive, otherwise the computed results would be perturbed. We see from (5) that

$$Q_{j+1}^{n+1}$$

is given as a weighted mean of three values on the previous time level, but from equations (6) to (8), due to:

$$K(1 - \varepsilon) + 0.5\Delta t = 0.5K[1 + Q/(BSc\Delta x)] + 0.5\Delta t > 0 \quad (32)$$

two of the weighting coefficients (C_2 & C_3) may be negative, and only C_1 is strictly positive. It is therefore possible for the solution of (5) to have a 'dip' or oscillations with internal maxima and minima under certain conditions. For example, for convenience in the analysis and without loss of generality, if the discharge variable is reduced by subtracting the initial steady flow, Q_0 , i.e. the base flow, from the inflow and outflow discharges, then (5) becomes,

$$\bar{Q}_{j+1}^{n+1} = C_1\bar{Q}_j^n + C_2\bar{Q}_j^{n+1} + C_3\bar{Q}_{j+1}^n \quad (33)$$

in which the overbar, "–", denotes the value of the reduced discharge variables.

It is then seen that by applying the scheme (33) to the first time interval, and given that

$$\bar{Q}_{j+1}^0 = \bar{Q}_j^0 = 0,$$

it follows that:

$$\bar{Q}_{j+1}^1 = C_2\bar{Q}_j^1 \quad (34)$$

Therefore when $C_2 < 0$, (34) shows that

$$\bar{Q}_{j+1}^1 < 0,$$

thus implying that a reduced outflow, negative flow, or “dip” occurs at the initial stage. As found through a number of numerical tests by Ponce & Theurer (1982), as well as those conducted by the authors, the ‘dip’ is closely related to the values of the coefficient C_2 , i.e. where a ‘dip’ occurs, the value of C_2 is negative.

In the current tests on the VPMC method applied to compound channels, it was also found that the oscillation phenomenon is related to the value of the coefficient C_3 , i.e. when oscillations occur, the value of C_3 is also negative. In order therefore to eliminate these unrealistic phenomena the following conditions are suggested:

- If $C_2 \geq 0$, no initial leading edge ‘dip’ occurs;
- If $C_3 \geq 0$, no oscillations appear.

Based on equations (7) & (8), the above conditions are expressed respectively as:

$$\Delta x \leq c\Delta t + Q/(BSc) \tag{35}$$

$$\Delta x \geq c\Delta t - Q/(BSc) \tag{36}$$

Thus to avoid the occurrence of both ‘dip’ and oscillations in the VPMC method, Δx must satisfy the following condition:

$$\begin{matrix} [c\Delta t - Q/(BSc)]_{max} \leq \Delta x \leq [c\Delta t + Q/(BSc)]_{min} \\ \text{(oscillations)} & & \text{(dip)} \end{matrix} \tag{37}$$

Example

Two symmetric inflow hydrographs ($Q_{peak} = 107$ & 214 m^3/s and $Q_{base} = 20$ m^3/s) are routed by MVPMC3 in a trapezoidal compound channel with a floodplain roughness $n_f = 0.06$ and a bed slope $S = 0.003$. If the condition (37) is applied in this case, it becomes:

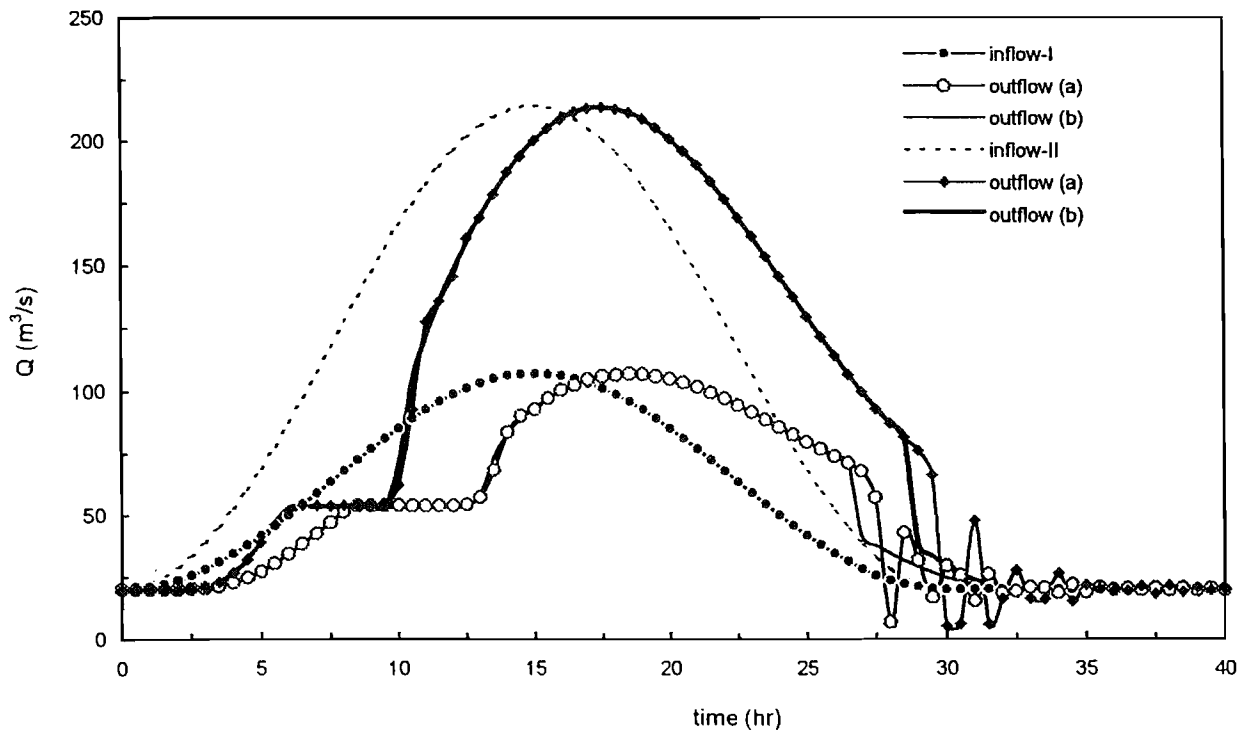
$$\begin{matrix} 3.28\Delta t - 293.8 \leq \Delta x \leq 0.57\Delta t + 542.2 \\ \text{(oscillations)} & & \text{(dip)} \end{matrix} \tag{38}$$

Thus there are several sets of Δx and Δt which will satisfy the above condition (38). For example, if $\Delta t = 300$ seconds, then $\Delta x = 700m$ can satisfy this condition. For comparison purposes, a set with $\Delta t = 1800$ seconds and $\Delta x = 1000m$, which satisfies the dip condition but not the oscillation condition in (38), was also undertaken. The results are compared in Table 6, which shows that the time to peak and peak amplitude of the outflow are almost the same when condition (38) is employed. Fig. 11 shows that indeed the oscillations were eliminated in the outflow hydrographs when condition (38) was adopted. However this condition has some effect on the volume values of outflow,

and the Table shows that some volume loss still occurs. This implies that the volume loss is one of the main limitations of the VPMC method, and that some unrealistic phenomena, such as the initial 'dip' and oscillation of the outflow hydrograph, can be eliminated through the selection of Δx and Δt which satisfy the condition (37).

Table 6. Results using the condition (37).

$S = 0.003$ ($L = 21 \text{ km}$)	$\Delta x = 1000 \text{ m}, \Delta t = 1800 \text{ s}$ (a)			$\Delta x = 700 \text{ m}, \Delta t = 300 \text{ s}$ (b)		
	t_p	Q_{po}	Vol%	t_p	Q_{po}	Vol%
I: $Q_{\text{peak}} = 107$	18.5	106.83	99.72	18.5	106.80	98.60
II: 214	17.5	213.72	99.07	17.5	213.69	99.08



Fi. 11. Outflow hydrographs by MVPMC3 using the condition (37) in a compound channel ($S = 0.003$).

Conclusions

The main conclusions are as follows:

1. The numerical tests show that both MVPMC3 and VPMC4-1 suffer some volume loss in the outflow hydrographs. A leading edge 'dip' may occur at large Δx values, and this significantly increases the outflow peak values, and consequently the volume of outflow, mostly notably for MVPMC3 method;
2. The routed peak discharge is not affected very much by different Δx or Δt values when there is no 'dip', particularly for the VPMC4-1 method. The selection of Δx and Δt affects the volume of outflow by MVPMC3 significantly, but less so by VPMC4-1. In this sense, VPMC4-1 is better than MVPMC3;
3. Although the time to peak and peak values of the outflow are similar for both inflow hydrograph shapes, the volume loss is less for asymmetric than for symmetric shaped inflow

hydrographs. This implies that the volume conservation feature of the VPMC method is affected by the value of dQ/dt in the falling limb of the inflow hydrographs;

4. Unlike inbank flow, non-physical oscillations occur on the recession stage of the outflow hydrograph for steep compound channels (e.g. $S \geq 0.003$). They become smaller with decreasing bed slope and eventually disappear;
5. The time to peak increases with decreasing ratio of inflow peak discharge to bankfull discharge (Q_{pi}/Q_{bf}), or with increasing roughness of the floodplain (n_f). The latter indicates that rough floodplains significantly delay the travel of the flood wave, as would be expected;
6. The ratio of outflow peak to inflow peak (Q_{po}/Q_{pi}) is almost the same for different inflow peak to bankfull discharge ratios (Q_{pi}/Q_{bf}). This suggests that flood wave diffusion is nearly independent of the Q_{pi}/Q_{bf} ratio;
7. The attenuation of the inflow peak generally increases with milder bed slope and with increasing roughness of the floodplain, which implies that both bed slopes and rougher floodplains make a significant contribution to flood wave diffusion;
8. In a steep compound channel, there is a significant shoulder in the rising limb of the outflow hydrograph, which occurs around bankfull flow. The duration of this shoulder increases with decreasing ratios of Q_{pi}/Q_{bf} or with increasing roughness of the floodplains. The oscillations in the recession stage become more serious with increasing ratios of Q_{pi}/Q_{bf} or floodplain roughness;
9. Different prediction methods for the $c \sim Q$ curves for VPMC have some influence on the routed results. The effect is very small for steep channels ($S \geq 0.003$), but significant for milder slope channels, most notably on the peak value of the outflow. The VD and DD methods produce almost the same values of outflow peak, lying in between the biggest, produced by the Area method, and the smallest, by the COH method.
10. The newly-introduced VPMC4-H scheme, with routed parameters c & D modified to account for the effect of the longitudinal hydrostatic pressure term ($\partial h/\partial x$), possesses relatively good volume conservation characteristics for overbank flow, its volume loss being typically less than 1% for $S < 0.0001$. By comparison, the conventional VPMC4-1 scheme may suffer quite a large volume loss, e.g. up to 9.3% for $S = 0.0001$, although the volume loss is small for steep channels (about 0.3 %). Based on the results of these numerical tests in compound channels, two empirical formula (29) & (30) are presented for estimating the percentage of volume loss in the outflow hydrographs for the VPMC4-1 and VPMC4-H methods respectively;
11. Finally, equation (37) has been presented for eliminating both the initial leading 'dip' and the oscillations in the recession stage of the outflow hydrograph in compound channel flow. The time to peak and peak amplitude of the outflow are almost the same when condition (37) is employed, but some volume loss of outflow still occurs. This implies that the volume loss is still one of the limitations of the VPMC method, although some unrealistic phenomena, such as the initial 'dip' and oscillation of outflow hydrograph, may be present. These can be eliminated through the proper selection of Δx and Δt satisfying the conditions stipulated by equation (37).

Acknowledgements

This paper describes work funded by the Ministry of Agriculture, Fisheries and Food (MAFF) under their Commission FD01 (River Flood Protection) at HR Wallingford. Publication implies no endorsement by the Ministry of Agriculture, Fisheries and Food of the paper's conclusions or recommendations. The work was undertaken for HR Wallingford in the School of Civil Engineering at the University of Birmingham.

References

- ABRIL, J.C. and KNIGHT, D.W., (1999). "Accurate stage-discharge prediction in compound channels using a finite element method for depth-averaged turbulent flow", Proceedings of the Institution of Civil Engineers, Water Maritime and Energy, (submitted for publication).
- ACKERS, P. (1992). "Hydraulic design of two stage channels", Proceedings of the Institution of Civil Engineers, Water Maritime and Energy, Vol. 96, No. 9988, pp. 247–257.
- ACKERS, P. (1993). "Stage-discharge functions for two-stage channels: the impact of new research", Journal of the Institution of Water and Environmental Management, Vol. 7, No. 1, pp. 52–61
- CAPPELLAERE, B. (1997). "Accurate diffusive wave routing", Journal of Hydraulic Engineering, Vol. 123, No. 3, pp. 174–181.
- CUNGE, J.A. (1969). "On the subject of a flood propagation method (Muskingum method)", Journal of Hydraulic Research, ASCE, Vol. 7, No. 2, pp. 205–230.
- GARBRECHT, J., and BRUNNER, G. (1991). "Hydrologic channel-flow routing for compound sections", Journal of Hydraulic Engineering, ASCE, Vol. 117, No. 5, pp. 629–641.
- GILL, M.A. (1979). "Translatory characteristics of the Muskingum method of flood routing", Journal of Hydrology, Vol. 40, pp. 17–29.
- GILL, M. A. (1992). "Numerical solution of Muskingum equation", Journal of Hydraulic Engineering, ASCE, Vol. 118, No 5, pp. 804–809.
- HENDERSON, F.M. (1966). "Open channel flow" , Chapter 9 – Flood routing, The Macmillan Co., New York.
- HJELMFELT, A.T. (1985). "Negative Outflows from Muskingum Flood Routing", Journal of Hydraulic Engineering, ASCE, Vol. 111, No. 6, pp. 1010–1014.
- JONES, S.B. (1983). "Accuracy criteria in diffusion routing: a discussion", Journal of Hydraulic Engineering, ASCE, Vol. 109, No. 5, pp. 801–803.
- KNIGHT, D.W., and DEMETRIOU, J. D. (1983). "Flood plain and main channel flow interaction", Journal of the Hydraulic Division, ASCE, Vol. 109, No. 8, pp. 1073–1092.
- KNIGHT, D.W., and HAMED, M.E. (1984). "Boundary shear in symmetric compound channels", Journal of the Hydraulic Engineering, ASCE, Vol. 110, No. 10, pp. 1412–1430.
- KNIGHT, D.W. and SELLIN, R.H.J., (1987). "The SERC Flood Channel Facility", Journal of the Institution of Water and Environmental Management, Vol. 1, No. 2, October, pp. 198–204.
- KNIGHT, D.W., and SHIONO, K. (1990). "Turbulence measurements in a shear layer region of a compound channel", Journal of Hydraulic Research, IAHR, Vol. 28, No. 2, pp. 175–196 (Discussion in IAHR Journal, 1991, Vol. 29, No. 2, pp. 259–276).
- KNIGHT, D.W., and SHIONO, K. (1996). "River channel and floodplain hydraulics", Chapter 5, in Floodplain Processes, edited by Anderson, Walling and Bates, J. Wiley, pp. 139–181.
- KNIGHT, D.W. and ABRIL, J.C., (1996). "Refined calibration of a depth-averaged model for turbulent flow in a compound channel", Proceedings of the Institution of Civil Engineers, Water Maritime and Energy, Vol. 118, Sept., pp. 151–159.
- KOUSSIS, A.D. (1978). "Theoretical estimations of flood routing parameters", Journal of Hydraulics Division, ASCE, Vol. 104, No. 1, pp. 109–115.
- KOUSSIS, A.D. (1980). "Comparison of Muskingum method difference schemes", Journal of Hydraulics Division, ASCE, Vol. 106, No. 5, pp. 925–929.
- KOUSSIS, A.D. (1983). "Accuracy criteria in diffusion routing: a discussion", Journal of Hydraulic Engineering, ASCE, Vol. 109, No. 5, pp. 803–806.
- LAMBERT, M.F. and MYERS, W.R. (1998). " Estimating the discharge capacity in straight compound channels ", Proceedings of the Institution of Civil Engineers, Water Maritime and Energy, Vol. 130, June, Paper No. 11530, pp. 84–94.
- LIGHTHILL, M.J. and WHITHAM, G.A. (1955). "On kinematic waves: I. Flood movement in long rivers", Proc. Roy. Soc., London, Series A, Vol. 229, pp. 281–316.
- MILLER, W.A., and CUNGE, J.A. (1975). "Simplified equations of unsteady flow", Unsteady flow in open channels, by K Mahamood and V Yevjevixh, Water Resources Publication, Ft. Collins, Colo.
- MORTON, K.W., and MAYERS, D.F. (1994). "Numerical solution of partial differential equations: An introduction", The Cambridge University Press, 1st Version, Cambridge, UK.
- NASH, J.E. (1959). "A note on the Muskingum method of flood routing", Journal of Geophysics Research, Vol. 64, No. 8, pp. 1053–1056.
- Natural Environment Research Council, (1975). "Flood Studies Report", Volume 3, Flood Routing Studies, NERC, London, UK.
- PERUMAL, M. (1992). "Multilinear Muskingum flood routing method", Journal of Hydrology, Vol. 133, No. 3–4, pp. 259–272.

- PONCE, V.M., and YEVJEVICH, V. (1978). "Muskingum-Cunge methods with variable parameters", Journal of the Hydraulics Division, ASCE, Vol. 104, No. HY12, pp. 1663-1667.
- PONCE, V.M and THEURER, F.D. (1982). "Accuracy criteria in diffusion routing", Journal of the Hydraulics Division, ASCE, Vol. 108, No. HY6, pp. 747-757.
- PONCE, V.M., and CHAGANTI, P.V. (1994). "Muskingum-Cunge method revised", Journal of Hydrology, Vol. 163., pp. 433-439.
- PONCE, V.M., LOHANI, A.K., and SCHEYGING, C. (1996). "Analytical verification of Muskingum-Cunge routing", Journal of Hydrology, Vol. 174, pp. 235-241.
- PRICE, R.K. (1985). "Flood routing", In Developments in Hydraulic Engineering, No. 3, [Ed. P. Novak], Elsevier, pp. 129-173.
- PRINOS, P., and TOWNSEND, R. (1984). "Comparison of methods for prediction discharge in compound open channels", Advance in Water Resources, Vol. 7, No. 12, pp. 180-187.
- SHIONO, K., and LIN, B. (1992). "Three dimensional numerical model for two stage open channel flows", Hydrocomp '92, 25-29 May, Budapest, Hungary, pp. 123-130.
- SMITH, A. A. (1980). "Generalized approach to kinematics flood routing", Journal of Hydrology, Vol. 45, No. 1-2, pp. 71-89.
- STEPHENSON, D. and KOLOVOPOULOS, P., (1990). "Effects of momentum transfer in compound channels", Journal of the Hydraulics Engineering, ASCE, Vol. 116, No. 12, December, pp. 1512-1522.
- TANG, X, KNIGHT, D.W. and SAMUELS, P.G., (1999). "Volume conservation characteristics of the variable parameter Muskingum-Cunge method for flood routing", Journal of Hydraulic Engineering, ASCE Vol. 125, No. 6, June, pp. 610-620.
- WARK, J.B., JAMES, C.S. and ACKERS, P., (1994). "Design of straight and meandering compound channels", National Rivers Authority R & D Report No. 13, pp. 1-86.
- WEINMANN, P.E., and LAURENSEN, E.M. (1979). "Approximate flood routing methods: a review", Journal of Hydraulics Division, ASCE, Vol. 105, No. 12, pp. 1521-1536.
- WORMLEATON, P.R., and MERRETT, D. J. (1990). "Improved method of calculation for steady uniform flow in prismatic main channel / flood plain sections", Journal of Hydraulic Research, Vol. 28, No. 2, pp. 157-174.
- WORMLEATON, P.R., ALLEN, J., and HADJIPANOS, P. (1982). "Discharge assessment in compound channel flow", Journal of Hydraulic Division, ASCE, Vol. 108, No. 10, pp. 975-993.
- YOUNIS, B. A. (1996). "Progress in turbulence modelling for open channel flows", Chapter 11, in Floodplain Processes, edited by Anderson, Walling and Bates, J. Wiley, pp. 299-332.
- YOUNKIN, L.M., and MERKEL, W.H. (1988a). "Range of application for reach routing with the variable parameter diffusion model", 24th Annual Conference, American Water Resources Association, Milwaukee, Wis., pp. - .
- YOUNKIN, L.M., and MERKEL, W.H. (1988b). " Evaluation of diffusion models for flood routing", Proceeding of National Conference on Hydraulic Engineering, ASCE, Colorado, Spring, Colo., pp. 674-680.

Notations

The following symbols are used in this paper:

- A wetted cross-sectional area of flow;
- A_c flow area of main channel;
- A_{cc} modified flow area of main channel;
- A_f flow area of floodplain;
- A_{ff} modified flow area of floodplain;
- b half bed width of main channel; (as used by Ackers and Knight & Demetriou)
- B_f floodplain width
- c kinematic wave speed;
- c' corrected kinematic wave speed;
- C_1 routing coefficient of Muskingum equation;
- C_2 routing coefficient of Muskingum equation;
- C_3 routing coefficient of Muskingum equation;
- cor correction coefficient to account for effect of the pressure gradient;

c_r	reference wave speed;
D	diffusion coefficient;
d	flow depth on floodplain
D'	corrected diffusion coefficient;
h	flow depth;
H	total flow depth of compound channel;
H_c	bankfull depth;
i	index of corner points at a computational cell;
j	space subscript;
K	Muskingum routing parameter;
K_D	Conveyance, defined by equation (20)
L	total routed channel length;
n	time subscript;
n_c	main channel roughness;
n_f	floodplain roughness;
Q	discharge;
Q_{base}	inflow baseflow;
Q_{bf}	bankfull discharge;
Q_c	discharge of main channel floodplain;
Q_f	discharge of floodplain;
Q_{peak}	Q_{pi} , inflow peak flow;
Q_{po}	peak flow of routed outflow;
Q_r	representative discharge;
S	channel bed slope;
S_c	main channel side slope;
S_f	floodplain side slope;
t	time variable;
T	whole time period;
T_p	time to peak of inflow;
t_p	time to peak of outflow;
V	flow velocity
$V\%$	volume loss/gain percentage of outflow;
$Vol\%$	volume percentage of outflow to inflow;
W_c	width of main channel;
W_f	floodplain width at bankfull stage;
x	longitudinal coordinate;
μ	adjustment factor;
β	momentum correction coefficient; curvature parameter of inflow hydrograph;
ε	Muskingum routing parameter;
θ	temporal weighting coefficient;
τ_r	relative apparent shear stress;
ΔA	Area correction;
Δt	time step; and
Δx	space step.

APPENDIX 3

Tang, X., Knight, D.W. and Samuels, P.G., 2000, "Wave speed-discharge relationship from cross section survey", *Journal of Water & Maritime Engineering*, Proc. Instn. Civil Engrs, joint ICE/IAHR, (submitted for publication).

WAVE SPEED-DISCHARGE RELATIONSHIP FROM CROSS-SECTION SURVEY

By XiaoNan Tang ¹, Donald W Knight ² and Paul G Samuels ³

- 1- Research Fellow, School of Civil Engineering, The University of Birmingham, Edgbaston, Birmingham, B15 2TT, UK
- 2- Professor of Water Engineering, School of Civil Engineering, The University of Birmingham, Edgbaston, Birmingham, B15 2TT, UK
- 3- Specialist in Fluvial Systems, Water Management Department, HR Wallingford, Howbery Park, Wallingford, Oxon, OX10 8BA, UK

ABSTRACT

This paper tackles a practical problem in flood routing, the estimation of the speed of propagation of the flood wave. It is well known that this propagation speed varies with the discharge in quite a complex manner for natural rivers. The principal innovative step in this paper is the identification of a relatively simple conceptual model of river geometry to obtain two methods for generating realistic wave speeds from standard river cross section survey. These are verified against data from two rivers in the UK, showing good agreement with wave speeds deduced from long term flow records. This work is expected to be of particular value in building forecasting models of ungauged or partially gauged river systems, as it removes the need for long concurrent records to estimate wave speeds.

Keywords: Floods, Rivers, Routing, Wave speed, Compound channel

Notation

- A = cross-sectional area of flow;
- B = channel width at water surface;
- b = half bottom width of main channel;
- B_f = floodplain width;
- B_f' = modified floodplain width, Eq. (15);
- B_k = flooded width on floodplain at bankfull stage (inbank flow);
- B_0 = initial flooded width at bankfull stage (geometric boundary);

- B_1 = initial flooded width at bankfull stage (storage boundary);
 C = empirical resistance coefficient, Eq. (3);
 c = kinematic wave speed for uniform flow;
 d = flow depth over floodplain;
 g = gravitational acceleration;
 h = flow water depth;
 H = total flow depth in compound channel;
 H_c = main channel depth;
 H_f = height of geometric floodplain boundary above bankfull level;
 H_{f1} = height of upper floodplain storage boundary above bankfull level (see Fig.12);
 H_s = inbank depth not affected by floodplain (corresponding to Q_s);
 k = constant for parabolic section shape, Eq. (7)
 m = empirical exponent [for Manning's formula $m = 2/3$, Chezy's $m = 1/2$]
 n = Manning's roughness coefficient
 $N1 \sim N3$ = real number (≥ 1) for describing floodplain boundary;
 p = exponent for section shape, Eq. (6);
 P = wetted perimeter of the cross-section
 Q = discharge;
 Q_{bf} = bankfull discharge;
 Q_n = the discharge of steady uniform flow or normal flow
 Q_s = inbank discharge not affected by floodplain (corresponding to H_s);
 r = constant for cross section shape, Eq. (9);
 R = hydraulic radius;
 S_0 = channel bed slope;
 s_c, s_f = side slope of main channel (1:z) and floodplain respectively;
 S_f = friction slope (slope of energy line);
 t = time;
 V = mean velocity of cross section;
 V_c = mean velocity of main channel;
 V_f = mean velocity of floodplain;
 V_s = dead volume of floodplain storage;
 x = distance along channel;
 x', y', y = lateral & vertical distances, (see Fig. 12 & Eqs 12-14) ;
 z = side slope (1 : z, vertical : horizontal);
 Φ = constant of proportionality, Eq. (6).

1. INTRODUCTION

One of most important parameters in flood routing is the wave speed, at which the flood wave travels along the river reach downstream. Strictly speaking, this wave speed is the speed with which the flood wave crest or peak moves downstream. This speed can be obtained readily from recorded hydrographs at either end of a reach, or it may be given by the rating curve at a particular cross section¹ using

$$c = \frac{dQ}{dA} = \frac{1}{B} \frac{dQ}{dH} \quad (1)$$

in which c = speed of the flood wave movement;
 Q = flow discharge;
 A = area of cross-section of the channel;
 H = water depth and
 B = water surface width.

A general form of the looped rating curve can be expressed² as

$$Q = Q_n \left(1 - \frac{1}{S_0} \frac{\partial H}{\partial x} - \frac{V}{gS_0} \frac{\partial V}{\partial x} - \frac{1}{gS_0} \frac{\partial V}{\partial t} \right)^{\frac{1}{2}} \quad (2)$$

where Q_n = discharge of steady uniform flow or normal flow, S_0 = bed slope of channel and V = section mean velocity.

For most floods in natural rivers, it has been shown that the last two terms (inertial terms) on the right hand side of (2) are usually negligible, but that the second term (pressure term) can be significant for very mild rivers^{1,3}. This would then imply a looped rating curve, and consequently different wave speeds on the rising and recession stages for a given discharge. However, it is very common that the wave speed may be considered a single-valued function of discharge in most natural rivers³⁻⁵, albeit a complex function.

In engineering practice, the storage method and the diffusion wave method derived from the St. Venant equations are most commonly used for flood routing⁶⁻⁸. In these methods, the nature of the flood wave is well described by the wave speed-discharge relationship and attenuation parameters, instead of using detailed flow parameters, such as channel width, depth, bed slope and roughness etc.. In these methods therefore the effects of uncertainty in roughness coefficient and

irregularities in width, depth and bed slope of the channel are dealt with implicitly in the wave speed and attenuation parameters, because observations of the wave speed include the direct effect of these parameters. In a natural river, most of these parameters vary longitudinally, and so the wave speed at a given discharge also varies longitudinally. It therefore follows that the average wave speed over a particular reach has to be found for each discharge, in order to build up the wave speed-discharge relationship.

For a natural river with significant flood plains, there are usually high irregularities in cross-sectional shape and longitudinal form. A general form of the wave speed-discharge relationship is then typically that of two power functions, one for the main channel flow and another for the floodplain flow, linked by an S-type transition curve, as illustrated in Figure 1. Fig.1 also shows how the wave speed typically increases to a maximum value for a discharge less than the bankfull discharge, then drops steeply to a minimum value at a low floodplain depth, and thereafter increases gradually with discharge as the floodplain becomes more inundated. It therefore follows that the flood wave speed in a natural river has a close relationship with the geometry of the cross-section. However, despite the pioneering analysis of Price ³, at present this relationship is poorly understood and there appears to be no current research on how the wave speed is related to the geometry of the channel irregularities or to other properties influencing the off-channel storage.

In this paper, the kinematic wave speeds based on (1) are examined for both simple and compound channel flows. Two methods, named as the RIBAMAN and VMB methods, are developed for predicting wave speed-discharge relationships in natural rivers, based on geometric features and hydraulic properties of the river channel. The RIBAMAN (River Basin Management) method is that implemented in the RIBAMAN ⁹ and ISIS (version 1.3) ¹⁰ software packages, and the VMB (Vertical Moving Boundary) method is an improved method to be coded into ISIS shortly. Both software packages have been developed for commercial purposes by HR Wallingford. Finally the VMB method is used to predict $c\sim Q$ relationships for the Erwood-Belmont reach of the River Wye and the Evesham-Pershore reach of the River Avon, UK. The close relationship between wave speed and cross-section geometry is thus confirmed, and the agreement between the predicted and observed $c\sim Q$ relationships is good.

2. KINEMATIC WAVE SPEED

By definition, the kinematic wave does not subside, i.e. the wave form does not change as it moves downstream. This wave motion truly exists when Q is a function of H alone ¹¹, and its wave speed is termed a 'kinematic' wave speed, given by (1). It has been shown that this wave speed does not differ significantly from the flood wave crest speed ¹². However actually observed values of flood wave speed, c , in natural rivers are often significantly less than the corresponding kinematic wave speed, due to the influence of storage, arising from either channel irregularities or other kinds of off-channel storage. In the following section, this wave speed-discharge relationship is examined for both inbank and overbank flows in some typical cross-sections. The influence of the geometry of the cross-section and other flow parameters (bed slope, roughness and floodplain width) on $c \sim Q$ relationships is discussed.

2.1 Wave speed-discharge relationship for inbank flow

For a kinematic flood wave, when $S_f = S_0$, the following general flow resistance equation may be applied :

$$Q = CA R^m \sqrt{S_f} \quad (3)$$

in which C = empirical resistance coefficient; R = hydraulic radius (A/P), P = the wetted perimeter of the cross-section; and m = empirical exponent [e.g. for Manning's formula, $m = 2/3$ and $C=1/n$, where n is Manning's roughness coefficient, and for Chezy's formula $m = 1/2$]; S_f = friction slope. Assuming the friction slope S_f to be constant with depth in (3), the kinematic wave speed, based on (1), becomes

$$c = V \left[(m+1) - \frac{mR}{B} \frac{dP}{dh} \right] \quad (4)$$

where (4) is a general form describing the kinematic wave speed in a prismatic simple channel with an arbitrary cross-section. The analytical wave speeds for inbank flows in some open channels with typical cross-sections, selected to be representative of most concave natural river channel shapes, are illustrated in Figure 2, and are described next. Thus for an open channel we have the inequalities

$$c < \frac{5}{3} V \quad \text{for Manning's equation}$$

$$c < \frac{3}{2}V \quad \text{for Chezy's equation}$$

Trapezoidal channel

A trapezoidal cross section, as shown in Fig. 2(a), having a bottom width of $2b$ and a side slope 1: z (vertical : horizontal), can be easily transformed into a rectangular shape [Fig.2(b)] when $z = 0$, or a triangular shape [Fig.2(c)] when $b = 0$. For the general trapezoidal shape, applying (4) gives

$$c = \frac{Q}{A} \left[(m+1) - \frac{2mh(2b+zh)\sqrt{1+z^2}}{(2b+2h\sqrt{1+z^2})(2b+2zh)} \right] \quad (5)$$

The so-called exponential channel

Another typical cross-sectional shape may be described as the so-called exponential section, whose cross-sectional area is expressed in general form by,

$$A = \Phi h^p \quad (6)$$

where Φ is a constant of proportionality with the dimension of $[L]^{2-p}$ and p is an exponent. Thus when $p = 1, 2$ the cross-sectional shapes are rectangular and triangular respectively, as discussed earlier; when $p = 3/2$, it is parabolic [Fig.2(d)]; and when $p = 5/2$, it is cusp-shaped [Fig.2(e)]. Thus the wave speeds for $p = 3/2$ and $5/2$ are analysed separately as follows :

(1) A parabolic shape channel

From (6), the general parabolic cross-section can be expressed by the following function:

$$h = \frac{1}{k} B^2 \quad (7)$$

in which k is a constant ($= 2.25\Phi^2$), which determines the shape of the cross-section. Thus applying (4) yields

$$c = \frac{Q}{A} \left[(m+1) - \frac{8mh(k+16h)}{12(k+16h)h + 3k\sqrt{(k+16h)h} \ln \left[\frac{4\sqrt{h} + \sqrt{(k+16h)}}{\sqrt{k}} \right]} \right] \quad (8)$$

(2) A cusp-shaped cross-sectional channel

Similarly a general cusp-shaped cross-section can be expressed by the following function:

$$rh^3 = B^2 \quad (9)$$

in which r = the shape constant ($= 6.25\Phi^2$). It follows from (4) that the wave speed then becomes

$$c = \frac{Q}{A} \left[(m+1) - \frac{27mrh(16+9rh)}{5[(16+9rh)^2 - 64\sqrt{16+9rh}]} \right] \quad (10)$$

Therefore, it can be seen from (5), (8) & (10) that the wave speed c is related to the mean cross-sectional velocity V , i.e. $V < c < (m+1)V$, and consequently is a function of the discharge.

If the dimensions of the cross-section of a channel are specified, the corresponding $c \sim Q$ relationship can be obtained by applying (5), (8) & (10). For example, using Manning's formula with n (roughness coefficient) = 0.030 for one bed slope of $S_0 = 0.003$, the $c \sim Q$ relationships were obtained for the following cases: a trapezoidal channel with $b = 10m$, $z = 1$; a rectangular channel with $b = 10m$; a triangular channel with $z = 1$; a parabolic channel with $k = 12$ & 24 ; and a cusp-shaped channel with $r = 1$ & 0.2 . The various $c \sim Q$ curves are shown in Figure 3. It should be noted that in Fig. 3 the parabolic-1 and parabolic-2 channels correspond to $k = 12$ & 24 respectively and the cusp shaped-1 and cusp shaped-2 channels correspond to $r = 1$ & 0.2 respectively.

The effect of different roughness coefficients, n ($= 0.030, 0.045, 0.060, 0.090$) for $S_0 = 0.003$, and different bed slopes S_0 ($= 0.003, 0.0015, 0.0008, 0.0003$) for $n = 0.030$, upon the wave speed-discharge curves for a trapezoidal channel are illustrated in Figure 4. This Figure shows that the wave speed decreases as the roughness increases or bed slope decreases.

From the above $c \sim Q$ results, it is evident that the $c \sim Q$ relationship for inbank flows is a single power functional curve for all these analytic cross-sectional shapes, which implies that the kinematic wave speed increases as the discharge increases or the stage rises.

2.2 Wave speed-discharge relationship for overbank flow

In many natural rivers, the cross-sectional shape is typically a compound one, incorporating the main river channel and the adjacent floodplains. The flow behaviour in a compound channel is

more complicated and three dimensional, once overbank flow occurs and is significantly different from inbank flow ^{13 - 15}. In engineering practice, commonly used 1-D approaches subdivide the whole channel into a number of discrete sub-channels, usually the main channel and the adjacent floodplain part. The discharge is then calculated for each part, with or without consideration of the interaction effect, and then the individual discharges are summed to give the total channel conveyance. Four stage-discharge predictive methods, namely the Vertical division method (VD), the Diagonal division method (DD) ¹⁶, the 'Coherence' method ¹⁷⁻¹⁹, and the Area method ²⁰ are used here to predict and compare the $c\sim Q$ relationships for a trapezoidal compound channel.

The 'test channel' adopted for this study was the Ackers' 'synthetic river channel' ¹⁹, as shown in Figure 5, with the following dimensions: bed width $2b = 15m$; bankfull depth $H_c = 1.5m$; two flood plains each with width $B_f = 20m$; main channel and floodplain channel side slopes (trapezoidal: $s_c = s_f = 1$); and bed slope of $S_0 = 0.003$ with Manning's n values for both the main channel and the floodplain being 0.030.

A comparison between the $c\sim Q$ curves based on (1) using the above four methods of discharge calculation is shown in Figure 6. It should be noted that in the VD method no vertical division line is included in the calculation of discharge either for the main channel or the floodplain flow. As is known, both the roughness and the width of the floodplain have a significant effect upon the flow characteristics of a compound channel, so their effect upon the $c\sim Q$ relationship was also investigated, but only using the VD method. The influence of different floodplain roughness ($n_f = 0.030, 0.045, 0.060, 0.090, 0.120$) on the $c\sim Q$ curves for $S_0 = 0.003$ is illustrated in Figure 7, and the effect of different floodplain widths ($B_f = 5, 15, 30, 60, 90m$) on the $c\sim Q$ curves for $n_f = 0.045$ is shown in Figure 8.

From Figs. 6-8, it can be seen that :

- Generally the $c\sim Q$ curve is a not monotonic, that is, the wave speed gradually increases to a maximum value around bankfull stage, then rapidly decreases to a minimum value, and afterwards increases as the flow depth on the floodplain increases;
- The width (B_f) and the roughness (n_f) of the floodplain significantly affects the $c\sim Q$ relationship, mainly for high overbank flow depths. Generally the wave speed c decreases with increasing B_f and n_f .

- Since the wave speed c increases with decreasing B_f , the $c\sim Q$ curve becomes a single curve like that for inbank flow when $B_f \rightarrow 0$;
- There are some significant differences between $c\sim Q$ curves using the four different methods for computing conveyance. The VD and the Area methods give the largest and somewhat similar wave speeds, the COH method produces the smallest values and the DD method gives values between them. The stage-discharge calculation method for overbank flow is therefore important for predicting the $c\sim Q$ relationship.

3. PREDICTIVE MODELS FOR THE $c\sim Q$ RELATIONSHIP FROM CROSS-SECTION SURVEY

In natural rivers with significant flood plains, the $c\sim Q$ relationship generally consists of two power functions, one for the main channel flow and another for the floodplain flow, linked by an S-type transition curve, as already shown in Fig.1. Price ^{3, 21 & 22} has suggested that the inbank peak wave speed occurs between $1/2$ to $2/3$ Q_{bf} , where Q_{bf} = bankfull discharge, and that the overbank minimum wave speed occurs between $1.5 \sim 2.0$ Q_{bf} in natural rivers. The flood wave speed has therefore a close relationship with the cross-section geometry of a river. In order to explore the $c\sim Q$ relationships, two methods are investigated, based on (1), modified as,

$$c = (1/B)_s (dQ/dH)_c \quad (11)$$

where the subscripts s and c refer to storage and conveyance respectively.

3.1 The RIBAMAN method

RIBAMAN ⁹ is a distributed catchment model for the analysis and design of surface water drainage in natural or partly developed catchments. It contains a 1-D unsteady flow model, in which the Variable Parameter Muskingum-Cunge method is used for flood routing. It therefore involves the calculation of the wave speed curve, which is based on a consideration of how the actual conveyance of compound channels/rivers is affected by the storage capacity of the floodplain. A simple but somewhat arbitrary technique is incorporated in RIBAMAN, which redefines a new flow boundary for calculating the conveyance of the channel, shown schematically in Figure 9(a). Part of the cross-section is designated for storage, labelled as 'storage only', with the remaining part

being designated for conveyance, labelled as 'active flow'. Fig. 10 shows the various parameters required in this RIBAMAN method, defined as follows :

B1, B2 = Bed and Top width of main channel respectively; B3 = Total floodplain width from left bank to right bank; B4 = Average flooded width at bankfull stage; D1= Depth of main channel; D2= Depth above bankfull for full floodplain inundation; D3 = Depth above bankfull for full width flow; D4 = Depth below bankfull at which isolated flooding begins, and VS = Valley side slope. The parameters D4 and B4 represent the depth and width respectively, at which water on the floodplain changes from isolated patches of storage to a continuous downstream conveyance of flow. This parameterisation of the flow cross section was originally produced at HR Wallingford in 1990 to provide an estimate of wave speed for a partially gauged river in a consultancy investigation.

In the RIBAMAN method, a new upper boundary (straight line) is redefined for the conveyance calculation, $(dQ/dH)_c$, whereas the lower boundary is used for the top water surface breadth, B , to find the wave speed, as given by (11). The idea behind this method is that certain parameters (D2, D3, D4 & B4) should be adjusted to account for the effect of storage on the floodplain and to produce a smooth transition in the $c \sim Q$ relationship around the bankfull stage. Generally smaller values for the parameter D2 and larger values for the parameters D4 & B4 produce more storage and a smaller wave speed around bankfull. Larger D3 values produce more storage and a lower wave speed for large floods. A typical $c \sim Q$ result for D2=0.1m, D3=D4=0.3m is shown in Figure 11. A systematic study on how the parameters (D2, D3, D4 & B4) affect the $c \sim Q$ relationship has been undertaken by Tang ²³. The resulting $c \sim Q$ curves show sharp changes around the maximum and minimum c values and a non-smooth transition between them. Despite these shortcomings, the original idea behind this method is seen to give reasonable results and has been widely used in engineering practice in the UK. However, the issue arises as to whether or not such straight lines are appropriate for the redefined flow boundaries when calculating the conveyance. Furthermore, it is now known that the sharp changes around the maximum and the minimum values of the $c \sim Q$ curves described earlier arise from this limitation. A further limitation arises in the method used to specify the 'storage' zone shown in Fig. 10. It is now generally deemed more appropriate to define the lateral extent of any dead zone by a vertical boundary whose lateral position changes with

floodplain depth or discharge. Because of these limitations a modified RIBAMAN method was devised, which addressed these two major issues.

3.2 The modified RIBAMAN method

Due to the limitations in the RIBAMAN method described previously, a modified RIBAMAN method was developed, termed CQOB-4, based on new redefined curved boundaries (the upper flow boundary and the lower floodplain boundary). These boundaries give a smoother change in the floodplain storage, and consequently a smooth transition in the $c \sim Q$ curve around the bankfull level. The modified RIBAMAN method is shown schematically in Fig. 9(b). Fig. 12 shows the application of this approach to a compound channel, in which curved boundaries are used not only to define the actual geometric boundary (lower curve), but also to define the flow conveyance calculation boundary (upper boundary). The upper boundary affects the conveyance calculation, by the VD method, and the lower boundary affects the storage calculation, involving the term $(1/B)_s$. The new boundaries are given by two power functions (13) & (14) respectively, whereas the modified inbank boundary around the bankfull region is defined by function (12).

$$\text{Inbank part:} \quad x' = [B_k + (H_c - H_s) s_c] \left(\frac{H - H_s}{H_c - H_s} \right)^{N1} \quad (12)$$

Overbank part:

$$\text{Floodplain boundary:} \quad x = [B_f - B_0 + H_f s_f] \left(\frac{H - H_c}{H_f} \right)^{1/N2} \quad (13)$$

$$\text{Upper flow boundary:} \quad x = [B_f - B_1 + H_{f1} s_f] \left(\frac{H - H_c}{H_{f1}} \right)^{1/N3} \quad (14)$$

where $N1$, $N2$ & $N3$ are real numbers (≥ 1), and B_0 = initial flooded width at bankfull stage (geometric boundary); B_1 = initial flooded width at bankfull stage (storage boundary); B_f = floodplain width; B_k = flooded width on floodplain at bankfull stage (inbank flow); s_c , s_f = side slopes of main channel and floodplain respectively; H_s = inbank depth not affected by floodplain, corresponding to the inbank discharge Q_s ; H_c = bankfull depth; H_f = height of geometric floodplain boundary above bankfull level; H_{f1} = height of upper floodplain storage boundary above bankfull level; H = flow depth in main channel.

Some typical test cases were investigated (see Table 1), where Run R5 ($N1 = N2 = N3 = 1$, i.e. straight line) actually becomes equivalent to the RIBAMAN method. The corresponding $c\sim Q$ results are shown in Figure 13, which shows that :

- When the floodplain boundary is trapezoidal (e.g. R1~R5), although different values of parameters ($H_f, N3$) affect the wave speed, all the $c\sim Q$ curves are similar in shape to that given by the RIBAMAN method, and consequently are somewhat unrepresentative of real rivers, especially around the minimum c values (in this case $50 \text{ m}^3/\text{s} < Q < 60 \text{ m}^3/\text{s}$);
- When the floodplain boundary is a curve, defined by the power function (13), more promising $c\sim Q$ curves are obtained using this method (see R6-R7).

3.3 The Vertical Moving Boundary Method

It is known from Eq. (11) that the changes in floodplain storage have a strong influence on the value of wave speed. It therefore follows that representing the floodplain storage is vital in order to predict realistic $c\sim Q$ relationships for a river with floodplains. One common method is to account for the floodplain storage effect by restricting the conveyance of the channel to the central part of the section, similar in concept to that used in 1D modelling ²⁴, and as used in the RIBAMAN method ⁹. This is rationally based and is acceptable conceptually. Developing the same concept a little further, another method is now proposed, using Vertical Moving Boundaries (VMB) for evaluating the channel conveyance, as illustrated schematically in Fig. 9(c). The flow boundary is imagined to move from the junction between the main channel and the floodplain towards the outer edge of the floodplain, as the flow depth on the floodplain increases. The conveyance is evaluated between these vertical boundaries whereas storage is allowed in the whole cross-section. Consequently the floodplain storage between the upper flow boundary and the lower actual floodplain boundary changes dynamically in a smooth manner, giving a smooth transition in the $c\sim Q$ curve around the bankfull level. A number of models are described next, using the same descriptive terms as in Tang ²³, so that the interested reader may explore the alternative models that were tested. The two most effective models were :

<1> *Vertical moving boundary (B_f)* [CQVMB-2]

In this model, termed CQVMB-2, the wave speed is calculated based on (11), in which $(1/B)_s$ is evaluated by the actual floodplain boundary, but the conveyance of channel, $(dQ/dH)_c$, is calculated

by the moving flow boundary, which is defined by B_f' , also shown in Figure 12, given by the following expression :

$$B_f' V_c = B_f \cdot V_f \quad (15a)$$

$$\text{or} \quad B_f' = B_f V_f / V_c \quad (15b)$$

where V_c & V_f are the main channel and the floodplain velocities respectively, computed by whatever conventional calculation methods for compound channel flows, such as VD, DD or Area methods, based on the actual floodplain boundary, where the floodplain width is assumed to be B_f . Then applying (15) produces a new floodplain width B_f' , which is used to recalculate $(dQ/dH)_c$ to give the wave speed for this particular flow depth or discharge. In such a way, the resulting B_f' increases from 0 toward B_f as the flow depth on the floodplain increases. Obviously this model does not require any parameter to be chosen, as it is only based on the geometry and hydraulic features of the routing reach in the channel/river.

Two test cases illustrate the use of this model, one with a trapezoidal shaped floodplain with no crossfall, and the other with a curved floodplain boundary, as described by (13). These are labelled as runs B7 and B8 respectively in Table 2, and the corresponding $c \sim Q$ curves are shown in Figure 14. Fig.14 shows that :

- Model CQVMB-2 gives a smooth continuous $c \sim Q$ relationship for a river with curved floodplains (Test B8);
- The shape of the floodplain boundary has a significant effect on the $c \sim Q$ curve (Compare tests B7 and B8).

<2>Vertical moving boundary with curved floodplain boundaries [CQVMB-3]

In this model, termed CQVMB-3, the vertical boundary for conveyance calculation moves across the floodplain and where it intersects the storage curve, given by (14), as the floodplain flow depth increases, so it defines a 'storage' zone to the right of the vertical line, as shown in Figure 12. The amount of storage thus varies with depth and with the parameters involved in (13) & (14). However, $(1/B)_s$ is obtained by the actual floodplain boundaries, defined by (13).

As can be seen from (13) & (14), the four parameters (H_f , $N2$, $N3$, H_{f1}) determine the upper flow boundary and the lower floodplain boundary. A detailed investigation into how these parameters

affect the $c\sim Q$ relationships has been given elsewhere by Tang ²³. A typical result is also illustrated in Figure 14, where the parameters employed are shown in Table 2. This result shows that Model CQVMB-3 can also produce a smooth continuous $c\sim Q$ relationship for a large range of curved floodplain boundaries.

3.4 Comparison of $c\sim Q$ curves by different models

In order to compare the effectiveness of the vertical moving boundary method, with that of the traditional fixed vertical boundary method, a series of tests were undertaken using models CQVMB-3 and CQOB-4. The CQVMB-3 model is that described in Section 3.3, and the CQOB-4 model is the modified RIBAMAN method described in Section 3.2, modified to taken account of using curved floodplain boundaries. The geometry of the cross sections are therefore the same, and the only difference is in the position of the vertical boundary.

Due to the different storage boundaries employed for evaluating $(dQ/dH)_c$, different floodplain storage volumes are involved when using models CQVMB-3 & CQOB-4. To explore how different they are, some tests were undertaken to compare these two models, using the parameters shown in Table 3. The corresponding $c\sim Q$ curves are compared in Figure 15 and the differences in the dead floodplain storage volume (V_s) with discharge are shown in Figure 16. The test results show that :

- Using the same parameters both models produce similar $c\sim Q$ curves, but the wave speeds produced by CQVMB-3 are larger than those by CQOB-4 for the same discharge, especially around bankfull stages (see C1 & D1, C2 & D2 etc. in Fig.15);
- The $V_s\sim Q$ curve produced by CQVMB-3 has a maximum at certain stage of overbank flow, whereas the $V_s\sim Q$ curve by CQOB-4 does not, with V_s gradually increasing to a limiting value at a high flow or stage. Generally V_s by CQVMB-3 is less than that by CQOB-4 for the same discharge. This explains why the wave speed by the former model is larger than that by the latter model for the same discharge.
- From the viewpoint of change of dead volume storage, CQVMB-3 appears to be more reasonable.

4. APPLICATION OF THE VMB METHOD FOR PREDICTING $c \sim Q$ RELATIONSHIPS IN NATURAL RIVERS

4.1 Wave speed prediction for the River Wye: Erwood to Belmont

Both models of the VMB method were tested on the Erwood-Belmont reach of the River Wye in the UK. This 69.8 km-long reach is an ideal one for studying flood routing because the reach has a large flood plain, no important tributaries, and the mean annual lateral inflow ($14\text{m}^3/\text{s}$) is small enough to be neglected in comparison with the mean annual flood discharge ($560\text{m}^3/\text{s}$) at Belmont. The total area of the floodplain along the reach is 28.57km^2 , and the average bed slope of the river reach 0.88×10^{-3} (Price ³).

For the purpose of analysis, an average cross-section of the main channel for this reach was obtained through the schematisation based on the surveyed cross-sections (taken in 1969), in which all the cross-sections were simply positioned together based on its individual center line, as shown in Figure 17. Although this method of schematisation is known to be not necessarily the best, it was deliberately chosen to test the robustness of the $c \sim Q$ prediction method, based on very approximate geometric data. The following dimensions for the main channel were obtained from Fig.17 by trapezium approximation :

Bed width:	42.0 m
Main channel depth:	4.32 m
Side slopes:	Left side (vertical : horizontal) 1: 1.04
	Right side (vertical : horizontal) 1: 2.47

The average width of the floodplain was estimated to be 410m , obtained by dividing the whole floodplain area (28.57km^2) by the total reach length (69.8km). In the present study, a symmetric compound channel, with Manning's coefficients of 0.035 and 0.060 for the main channel and the floodplain respectively, was used to predict the $c \sim Q$ relationship. Based on the above average geometry and the assumed hydraulic roughness properties of the channel, the calculated reach mean bankfull discharge was estimated to be $425\text{m}^3/\text{s}$, sufficiently close to the value of $\sim 440\text{m}^3/\text{s}$ used elsewhere by Knight in FSR teaching material.

Fig. 18 gives the comparison between the real data established by Price ³ and the predicted $c \sim Q$ relationships using both CQVMB-2 & CQVMB-3 (Runs A5 and C4 respectively), and the parameters shown in Table 4. This test shows that both Runs A5 & C4 are in a good agreement with the field data. This demonstrates that both models are capable of predicting the $c \sim Q$ relationship well, based on simple estimates of the geometry of the cross section and hydraulic characteristics of the river reach alone.

4.2 Wave speed prediction for the River Avon: Evesham to Pershore

The second test reach was the Evesham-Pershore reach of the River Avon in the UK. The reach length is 18.2 km, and its average bed slope 0.41×10^{-3} . In a similar way to the previous method, an average cross-section of the main channel for this reach was also obtained through a trapezium schematisation based on the surveyed cross-sections (taken from the cross-section data file of an ISIS study for the River Avon, HR Wallingford), shown in Figure 19. Thus the average dimensions of the cross-section of the main channel were estimated to be :

Bed width:	16.4m
Main channel depth:	5.0m
Side slopes:	Left side (vertical : horizontal) 1: 1.97 Right side (vertical : horizontal) 1: 2.30

As the detailed data about the area of floodplain within the reach were not available in this study, the average width of the floodplain was taken as approximately 600 m (from an earlier study by HR Wallingford ²⁵). The Manning's roughnesses for the main channel and the floodplain were taken as 0.034 and 0.060 respectively. The calculated reach average bankfull discharge was estimated to be 182 m³/s.

Fig. 20 shows the field data deduced from flood records ²⁶ between 1947 and 1977 and the predicted $c \sim Q$ curves given by both CQVMB-2 & CQVMB-3 (Runs A4 and C4 respectively), using the parameters shown in Table 4. It can be seen that both A4 & C4 agree well with the field data, except for one anomalous inbank flow at around 50 m³/s. The River Avon is regulated along its length for navigation, and for small discharges the sluices will be closed altering the conveyance

characteristics for the reach. The sluices will be open for discharges in excess of about $100 \text{ m}^3/\text{s}$. This again confirms that both models are appropriate under some conditions to predict $c \sim Q$ relationships based on the geometry and hydraulic characteristics of the river reach alone.

5. DISCUSSION OF RESULTS

As is well known, the flood wave movement in most natural rivers can be approximately described by an convection-diffusion equation). Thus flood routing approaches based on this equation, such as the VPMC method ^{7, 8 & 21} and Price's diffusion model ^{21 & 22}, are particularly suitable for practical application, especially when data of observed hydrographs on a river reach are available, and detailed channel configuration is not. In such circumstances, the detailed channel geometry and roughness are replaced by another two flood routing parameters: the wave speed and the attenuation. Thus when approximate flood routing methods are applied, these two parameters have to be specified. The wave speed may be obtained using field data from records of previous floods as recommended by Price ³. However, this approach is often of limited use, because many years of field data are needed to obtain the full $c \sim Q$ relationship. Typically only a few peak flow events are usually recorded, which then have to be adapted to find c values at intermediate discharges (or repeat measurements at a different flood discharge).

Alternatively, the wave speed may be evaluated using Equation (1). Based on this formula, it has been shown that the wave speed is a single function of discharge, whatever the cross-sectional shape of a simple channel, i.e. the kinematic wave speed increases as the discharge increases or the stage rises. However, in a compound channel the $c \sim Q$ curve is not monotonic. For these more complex shaped channels, the wave speed typically increases gradually to a maximum value just below the bankfull stage, then rapidly drops to a minimum, and afterwards increases as the flow depth on the floodplain increases, as shown in Figs 1, 18 & 20. Strictly speaking, the kinematic wave speed can be applied only when the rating curve is a single valued curve, i.e. when the flow is steady and when the friction slope, S_f , matches the general bed slope, S_0 . This is approximately true for steep channels where S_0 is large. However, for many rivers, the rating curve is looped, due to the effect of inertial and the relative values of the water surface and bed slopes. In such circumstances, it is not yet clear whether Equation (1) is appropriate, or whatever other form for c is.

Based on the fact that the reduction of wave speed must be ascribed to the geometric and hydraulic features of the channel, either due to channel irregularities, other kinds of off-channel storage, or lateral flow effects, two methods are proposed to allow for this floodplain effect on the kinematic wave speed. One is to redefine a new flow boundary and adjust the channel conveyance, as adopted in the RIBAMAN method, and the other is to use the VMB method. Both methods depend on the same general approach, that of reducing the conveyance capacity by allowing for some of the cross section to be designated as 'storage'. The VMB method is considered to be physically sound and representative of flow in natural rivers.

The studies described in this paper show that both the modified RIBAMAN method and the VMB method can predict reasonable $c \sim Q$ curves under certain conditions, using curved flow boundaries. Fig.15 shows that the $c \sim Q$ relationships are similar, although the basic ideas behind the methods are somewhat different. The VMB method is the most effective, as it describes conceptually the dynamically changing floodplain storage. Moreover this method is confirmed using data from two reaches from two natural rivers in the UK, as shown by Figs.18 & 20. The methodology for applying the VMB method is now briefly described.

The schematisation of the river cross section, including its floodplain, is an important element in constructing any numerical river simulation model. There are a number of schematisation methods outlined by Seed ²⁷, but these are mainly related to low flow and sediment phenomena. For the purposes of flood routing, it is suggested that the main river channel be schematised by overlaying cross-section data at bankfull level, using the water surface as a common datum, and making lateral adjustments until all the main flow areas are approximately aligned. The shape of the main river channel should then be described by a simple schematic, using no more than 3 linear elements, based on 4 points, as shown in Figs 10 & 12. Greater refinement may be possible using 4 linear elements, based on 5 points, two elements dealing with each river bank, and two for the bed, drawing lines from the foot of each river bank to the deepest point on the bed of the main river channel. However, in most cases a 4 point representation is sufficient, approximating the main river cross-section as a simple trapezoidal channel, as indeed used earlier for the Wye & Avon river reaches shown in Figs 17 & 19. The aim should be to take a 'broad brush' approach, commensurate with the general features, and bearing in mind that the VPMC method only requires gross hydraulic features and is quite tolerant of this level of approximation.

Likewise the floodplains should be treated by adding initially only 2 additional points per floodplain, as indicated by the left-hand floodplain in Fig. 12. It is quite appropriate to divide floodplain areas by reach lengths to get an estimate of floodplain dimensions, as described earlier for the River Wye. The simplest general overall shape of the cross-section should therefore be composed of 8 points, giving 7 sub-areas (9 & 8 respectively if an additional point is added to the bed of the main channel). Obviously where there are significant changes in floodplain or channel width, the compositing of several sections together will not be possible, and individual reaches may have to be specified. However, the aim should be to minimise the amount of data being used, bearing in mind the purpose to which they are put. This is in contrast to the large amount of cross-section data normally required for river hydrodynamic modelling, as for example collected through Section 105 surveys for producing flood risk maps. The schematisation should not therefore be regarded just as an exercise in digitising numerous survey data, but rather as an art of blending the geometry and hydraulic features together.

General rules for cross section location and the data requirements of 1D models are given elsewhere ^{28 & 29}. Detailed information on calibration criteria for 1D models is given by Anastasiadiou-Partheniou & Samuels ³⁰, boundary roughness effects in routing models by Kawecki ³¹ and the influence of lateral flow over a floodplain by Walton & Price ³². Without an appreciation of some of these effects, any model is liable to be less accurate and useful than it might otherwise be, given the approximations already inherent in the 1D approach. Quality assurance and control of the modelling process is also important ³³.

Having obtained a schematic 'representative' cross-section for the reach, or collection of river reaches, the gross geometry then needs to be developed further for use in either of the following methods :

- (i) RIBAMAN method, by selection of the appropriate parameters, D1-D4, B1-B4 in Fig. 10
- (ii) new VMB method, by selection of N1 to N3, and using equations (12) to (14)

The new VMB method is the preferred method, in which curved boundaries are adopted, as illustrated in Fig. 12. Guidance about the choice of the various parameters required in (12) to (14) is now given as follows:

- 1) N_1 should be around (2 to 4);
- 2) B_k should be around $(0.1 \text{ to } 0.5)B_f$, and affects the size of the initial isolated parts of flooding;
- 3) H_s corresponds to Q_s , which is typically $(0.3 \text{ to } 0.7) Q_{bf}$, depending on the floodplain interaction. Alternatively, for typical UK rivers, make $(H_c - H_s) \approx 0.1 \text{ m to } 0.5 \text{ m}$, depending on the bank top irregularities;
- 4) N_2 should be around (1 to 4) and affects the slope of the transition part of the $c \sim Q$ curve;
- 5) H_{fl} is approximately $(0.2 \text{ to } 0.8)H$, and affects the overbank part of the $c \sim Q$ curve;
- 6) N_3 should be around (2 to 4), and affects the lower part of the $c \sim Q$ curve;
- 7) H_f is approximately $(0 \text{ to } 0.8)H$, and affects the transition part of the $c \sim Q$ curve;
- 8) $B_1 \leq B_k \leq B_0$; where B_k = average flooded floodplain width at bankfull stage.

It should be noted here that the parameters N_2 & H_f in the above guidelines should be estimated to make the schematic boundaries as close as possible to the actual natural river floodplain boundaries. Since these guidelines are intended for a generalized mean cross-section of a river with its floodplains, they are generally applicable to a river and floodplain geometry any size that may be schematised in this particular way. However, other parameters need to be specified in order to apply these methods and further work about the criteria for selection is required, especially for the CQVMB-3 model, which is the preferred method. It should be noted that fewer parameters are required for the CQVMB-2 model. Further guidance on the selection of parameters and how to determine the $c \sim Q$ relationship for natural rivers is given in Knight ³⁴.

In most natural rivers, the cross-sectional shape of a river with a floodplain is complex. However, in general it may be taken as a continuously smooth compound channel, in which the river boundary gradually changes from the main channel to the adjacent floodplain. In a macro-scale sense of geometry, the floodplain shape in most natural rivers may be described by the curved functions, defined in (13). The methods proposed at present are aimed at producing a reasonable $c \sim Q$ relationship for a natural river with floodplains, based on a schematized trapezoidal compound channel.

6. CONCLUSIONS

1. In flood routing, regardless of whether one is using the VPMC method, or a storage routing method, the $c\sim Q$ relationship is generally required.
2. The $c\sim Q$ relationship can be determined using the method adopted by Price ³ if recorded hydrographs are available, but most natural rivers lack such data. Alternatively the wave speed may be calculated from the relation $c = (1/B)_s (dQ/dH)_c$, which is particularly useful for flood routing in ungauged or partially gauged reaches.
3. In the present study it has been shown that the wave speed is a single function of discharge for whatever type of cross-sectional shape of a simple channel, i.e. the kinematic wave speed increases as the discharge increases or the stage rises.
4. For a natural compound channel, the $c\sim Q$ curve is not monotonic, but typically the wave speed increases to a maximum value around 2/3 the bankfull discharge, then drops rapidly to a minimum value, before increasing gradually as the flow depth on the floodplain increases. A typical wave speed-discharge relationship for natural rivers with floodplains consists of two power functions, one for the main channel flow and the other for overbank flow, joined by an S-shaped transition curve. This transition range commences at about half bank-full discharge and extends to around twice the bankfull discharge.
5. Two methods (RIBAMAN and VMB) are proposed for predicting the $c\sim Q$ relationships from the geometry of the cross section and hydraulic properties of the channels based on modifying the flow boundary for the conveyance calculation.
6. Similar $c\sim Q$ results are obtained using both the modified RIBAMAN method (CQOB-4) and the VMB method (CQVMB-2 & CQVMB-3).
7. The CQVMB-3 method is the preferred prediction method, involving a vertical moving boundary with curved floodplain boundaries.
8. The predicted $c\sim Q$ curves using the VMB method agree well with data from two reaches of two natural rivers : the Wye and the Avon.
9. These methods facilitate the practical application of approximate flood routing methods, particularly for ungauged or partially gauged natural rivers.
10. Further work is needed concerning the criteria for selecting the parameters involved in the proposed methods, especially the parameters in equations (12)-(14).
11. The methods should only be used for un-regulated river flows.

ACKNOWLEDGEMENTS

This paper describes work partly funded by the Ministry of Agriculture, Fisheries and Food (MAFF) under their Commission FD01 (River Flood Protection) at HR Wallingford. Publication implies no endorsement by the Ministry of Agriculture, Fisheries and Food of the paper's conclusions or recommendations. The work was undertaken in the School of Civil Engineering at the University of Birmingham for HR Wallingford.

REFERENCES

1. Henderson, F.M., 1966, "Open channel flow", Chapter 9 - Flood routing, The Macmillan Co., New York.
2. Weinmann, P.E. and Laurenson, E.M., 1979, "Approximate flood routing methods: a review", *Journal of Hydraulics Division, ASCE*, Vol.105, No.12, pp 1521-1536.
3. Price, R. K., 1975, "Flood routing studies", *Flood Studies Report*, Volume III, Natural Environmental Research Council, London, UK.
4. Wong, T. H. F. & Laurenson, E. M., 1983, "Wave speed – discharge relations in natural rivers", *Water Resources Research*, Vol. 19, No.3, pp 701 -706.
5. Wong, T. H. F. & Laurenson, E. M., 1984, "A model of flood wave speed – discharge characteristics of rivers", *Water Resources Research*, Vol.20, No.12, pp 1883 -1890.
6. Cappelaere, B., 1997, "Accurate diffusive wave routing", *Journal of Hydraulics Engineering*, ASCE, Vol. 123, No.3, pp 174 - 181.
7. Tang, X., Knight, D. W. and Samuels, P. G., 1999a, "Volume conservation in variable parameter Muskingum-Cunge methods", *Journal of Hydraulic Engineering*, ASCE, Vol.125, No.6, pp 610-620.
8. Tang, X., Knight, D. W. and Samuels, P. G., 1999b, "Variable parameter Muskingum-Cunge method for flood routing in a compound channel ", *Journal of Hydraulic Research*, IAHR, Vol.37, No.5, pp 591-614.
9. HR Wallingford, 1994, "RIBAMAN – User Manual, Version 1.22A", *HR Wallingford*, UK.
10. Halcrow, 1995, "ISIS – User Manual, Version 1.3", *Halcrow /HR Wallingford*, UK.
11. Lighthill, M. J. and Whitham, G.A., 1955, "On kinematic waves: 1. Flood movement in long rivers", *Proc. Roy. Soc., London, Series A*, Vol. 229, pp 281-316.

12. **Henderson, F.M., 1963**, "Flood waves in prismatic channels", *The Journal of Hydraulics Division*, ASCE, Vol. 89, No. 4, pp 39 - 67.
13. **Knight, D.W., Shiono, K., and Pirt, J., 1989**, "Prediction of depth mean velocity and discharge in natural rivers with overbank flow", *Proc. Int. Conf. on Hydraulic and Environmental Modelling of Coastal, Estuarine and River Waters*, (Ed. R. A. Falconer et al.), University of Bradford, Gower Technical Press, Paper 38, pp 419-428.
14. **Knight, D. W. and Shiono, K., 1990**, "Turbulence measurements in a shear layer region of a compound channel", *Journal of Hydraulic Research*, IAHR, Vol.28, No.2, pp 175-196.
15. **Knight, D. W. and Shiono, K., 1996**, "River channel and floodplain hydraulics", Chapter 5, in *Floodplain Processes*, edited by Anderson, Walling and Bates, J. Wiley.
16. **Wormleaton, P. R. and Merrett, D. J., 1990**, "Improved method of calculation for steady uniform flow in prismatic main channel / flood plain sections", *Journal of Hydraulic Research*, IAHR, Vol.28, No.10, pp 975 -993.
17. **Ackers, P., 1992**, "Hydraulic design of two stage channels", *Proceedings of the Institution of Civil Engineers, Water Maritime and Energy*, Vol. 96, Issue 4, Paper No. 9988, pp 247-257.
18. **Ackers, P., 1993**, "Flow formulae for straight two-stage channels", *Journal of Hydraulic Research*, IAHR, Vol. 31, No.4, pp 509-531.
19. **Ackers, P., 1993**, "Stage-discharge functions for two-stage channels : the impact of new research", *Journal of the Institution of Water and Environmental Management*, Vol. 7, No.1, February, pp 52-61.
20. **Stephenson, D., and Kolovopoulos, P., 1990**, "Effect of momentum transfer in compound channels", *Journal of Hydraulic Engineering*, ASCE, Vol. 116, No. 12, pp 1512-1522.
21. **Price, R. K., 1985**, "Flood routing", In *Developments in Hydraulic Engineering*, No.3, [Ed. P. Novak], Elsevier, pp 129-173.
22. **Price, R. K., 1985**, "Hydraulics of floods", In *Advances in Water Engineering*, [Ed. T.H.Y.Tebbutt], Elsevier, pp 302-310.
23. **Tang, X., 1999**, "Derivation of the wave speed-discharge relationship from cross section survey for use in approximate flood routing methods", *Ph.D Thesis*, School of Civil Engineering, The University of Birmingham, UK.
24. **Cunge, J.A., Holly, F.M., and Verwey, A., 1980**, "Practical aspects of computational river hydraulics", Pitman Publishing Ltd, London.
25. **HR Wallingford, 1985**, "River Avon Flood Alleviation Study", Report EX 1295, HR Wallingford.

26. **Samuels, P.G., 1980**, "Computational hydraulic model of the River Severn, Report EX 945, HR Wallingford, (3 volumes).
27. **Seed, D.J., 1997**, "Lateral variations of sediment transport in rivers", *HR Wallingford*, Internal Report, SR 454, March, pp 1-25.
28. **Samuels, P.G., 1990**, "Cross-section location in 1D models", *Proc. Int. Conf. on River Flood Hydraulics*, (Ed. W.R. White), Wallingford, September, J. Wiley & Sons, Paper K1, pp 339-348.
29. **Defalque, A., Wark, J.B., and Walmsley, N., 1993**, "Data density in 1-D river models", *HR Wallingford*, Internal Report, SR 353, March pp 1-20.
30. **Anastasiadou-Partheniou, L. and Samuels, P.G., 1998**, "Automatic calibration of computational river models", *Proceedings of the Institution of Civil Engineers, Water Maritime and Energy*, Vol. 130, No. 3, pp 154-162..
31. **Kawecki, M.W., 1973**, "Boundary roughness for natural rivers", *HR Wallingford*, Internal Report, INT 120, October, pp 1-28.
32. **Walton, R. and Price, R.K., 1975**, "Influence of lateral flow over a flood plain on flood waves", *HR Wallingford*, Internal Report, INT 140, March, pp 1-25.
33. **Seed, D.J., Samuels, P.G., and Ramsbottom, D.M., 1993**, "Quality assurance in computational river modelling", *HR Wallingford*, Internal Report, SR 374, October, pp 1-29.
34. **Knight, D.W., 1999**, "Derivation of routing parameters from cross-section survey", *Final Report to HR Wallingford on MAFF sponsored research at The University of Birmingham*, October, pp 1-30.

Run	N1	B _k /B _f	B ₁ /B _k	H _{f1} / H	N3	B ₀ / B _f	H _f / H	N2
(1)	(2)	(3)	(4)	(5)	(6)	(7)	(8)	(9)
R1	3	1/6	1/4	1/3	2	-	0	-
R2			1/6	"	4			
R3			0	1/2	"			
R4			1/6	3/2	2			
R5			"	"	1			
R6	3	1/6	1/4	3/2	2	1/6	1/3	4
R7	"	"	0	"	"	"	"	3
Notes	Upper boundary for $(dQ/dH)_c$					Floodplain boundary		

Table 1. Test cases for the modified RIBAMAN, $Q_s/Q_{bf} = 1/2$

Run	B ₀ /B _f	H _f /H	N2	B ₁ / B _f	H _{f1} / H	N3	Model
B7	-	0	-	-	-	-	CQVMB-2
B8	1/6	1/4	2	-	-	-	
w14	1/6	1/4	2	0	1/4	2	CQVMB-3
Notes	$Q_s/Q_{bf} = 1/2$, $N1 = 3$ & $B_k = B_0$						

Table 2. Test cases for CQVMB-2 & CQVMB-3

CQVMB-3	CQOB-4	B ₀ / B _f	H _f / H	N2	H _{f1} / H	N3
C1	D1	1/5	1/4	1	1/3	1
C2	D2	"	"	4	"	2
C3	D3	"	1/3	1	"	1
C4	D4	"	1/5	"	1/5	"
Notes		$Q_s/Q_{bf} = 1/2$, $N1 = 3$ & $B_k = B_0$				

Table 3. Comparison of CQVMB-3 & CQOB-4 with $B_1 = 0$

Run	B _k /B _f	Q _s / Q _{bf}	N1	B ₀ / B _f	H _f /H	N2	H _{f1} /H	N3
Erwood-Belmont								
A5	1/5	0.3	2	1/5	0.65	3.5	-	-
C4	"	"	"	"	1/6	1.5	4/5	2.5
Evesham-Pershore								
A4	2/9	0.3	2	1/4	3/4	1.5	-	-
C4	"	"	"	"	1/4	"	1/3	2

Table 4. Prediction of $c \sim Q$ relationships for the Wye & Avon Rivers

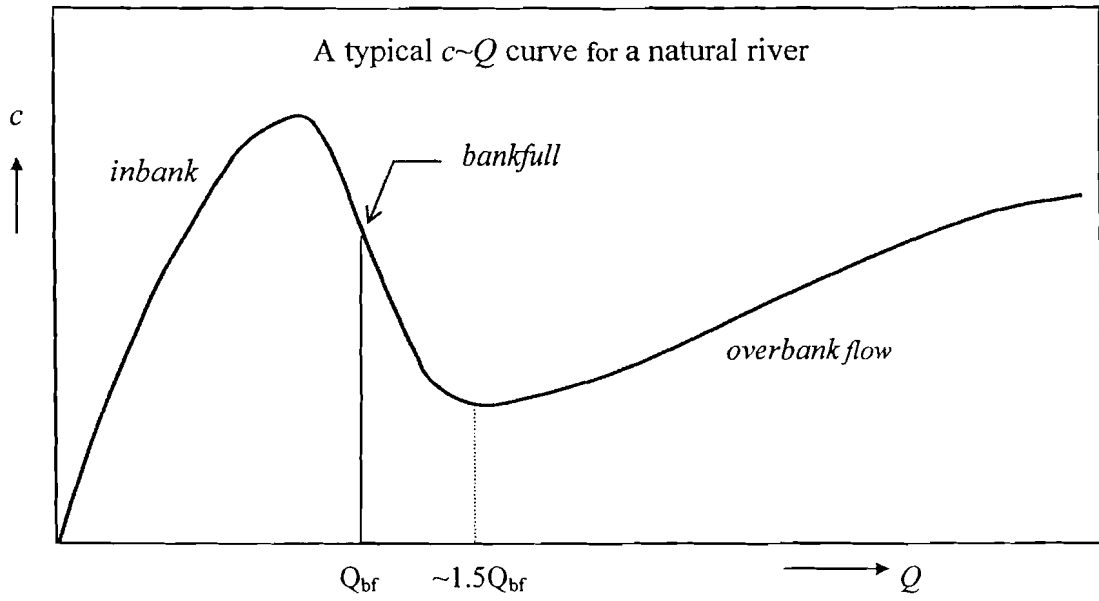


Fig.1 A typical wave speed-discharge relationship for a natural river

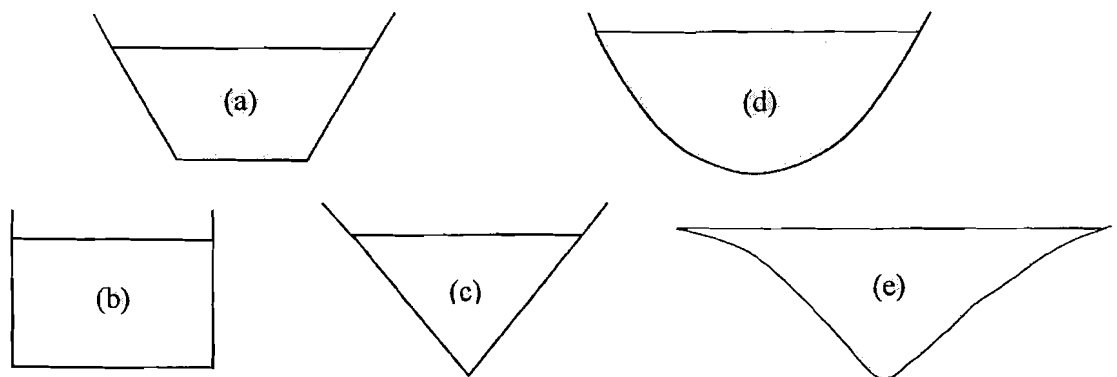


Fig.2 Typical shapes of channel cross-section with inbank flow

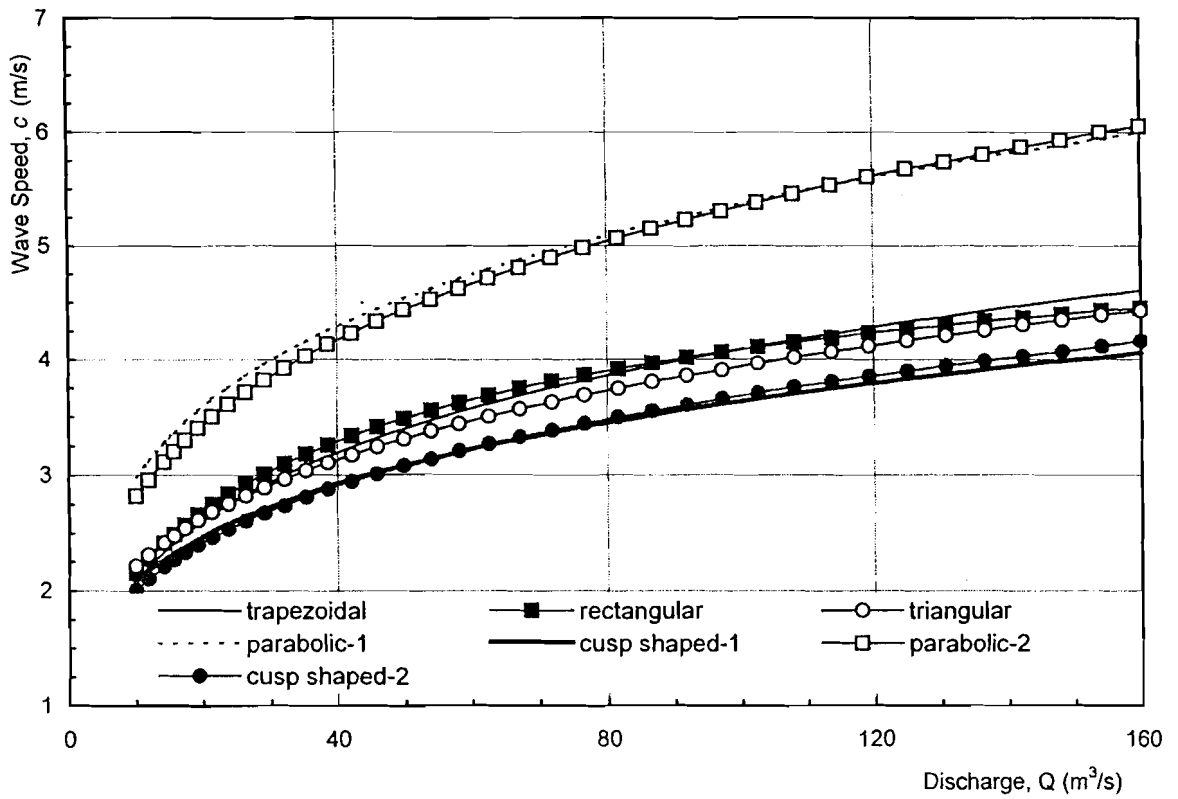


Fig.3 Comparison of $c \sim Q$ curves for inbank flows in channels of varying shapes ($n=0.030, S_0 = 0.003$)

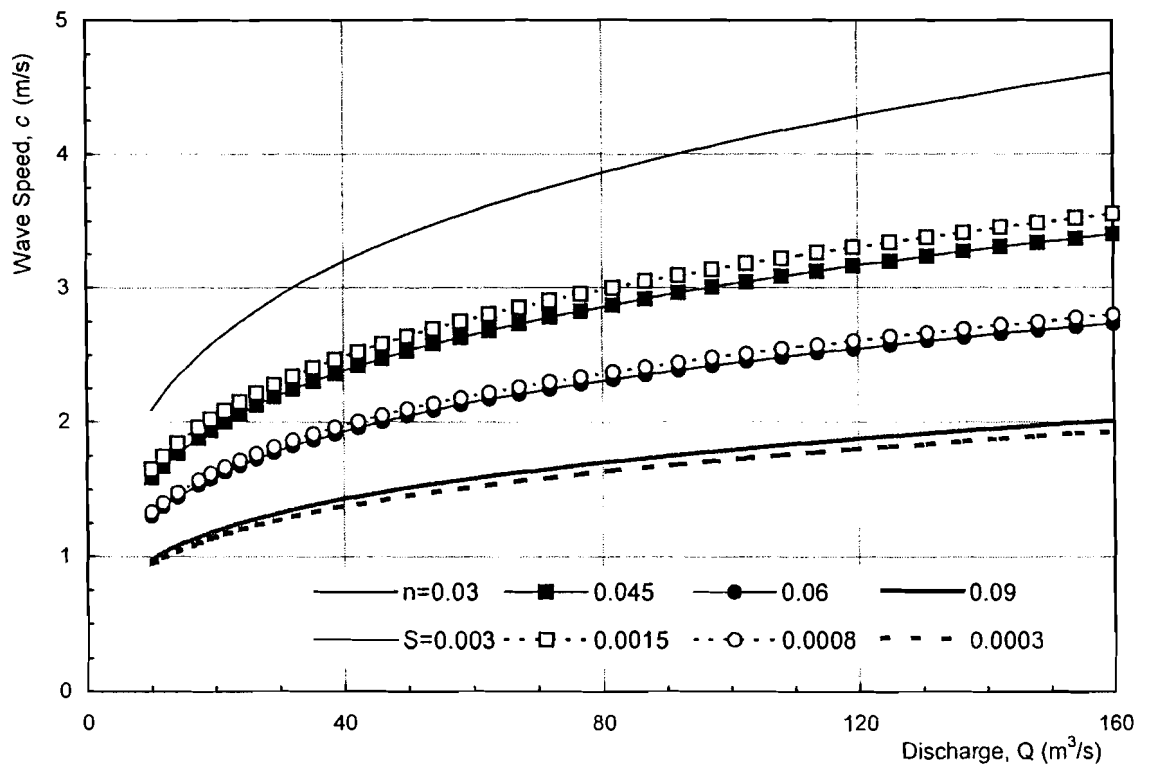


Fig.4 Comparison of $c \sim Q$ curves for inbank flows in a trapezoidal channel with varying roughness (Manning's n) and bed slope S_0

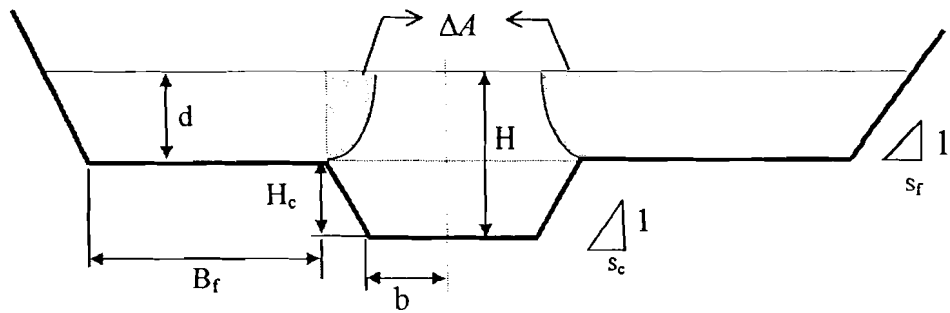


Fig.5 A typical schematised compound channel with overbank flow, showing the area method for calculating the discharge

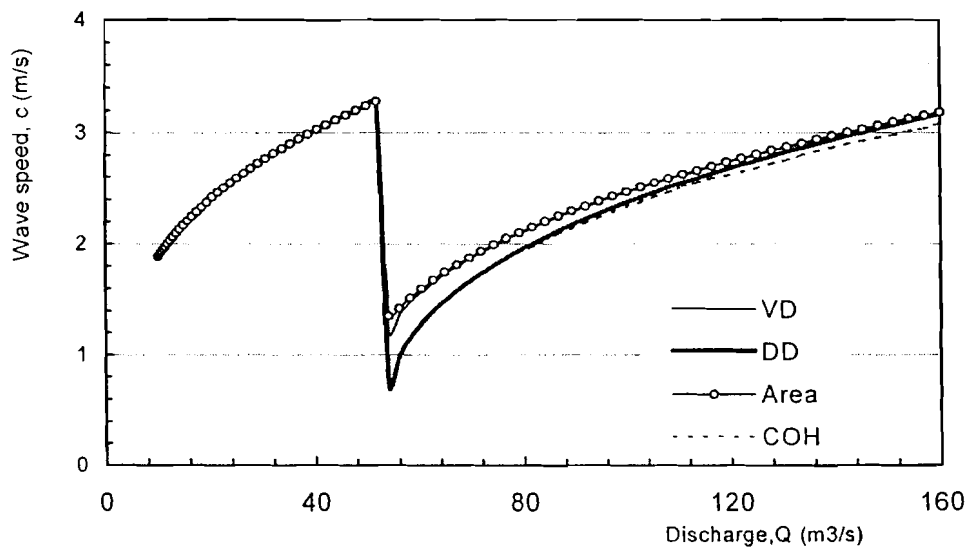


Fig. 6 Comparison of $c \sim Q$ curves for overbank flows using different methods for calculating the discharge (VD, DD, Area & COH methods), with $n_c = n_f = 0.030$ and $S_0 = 0.003$

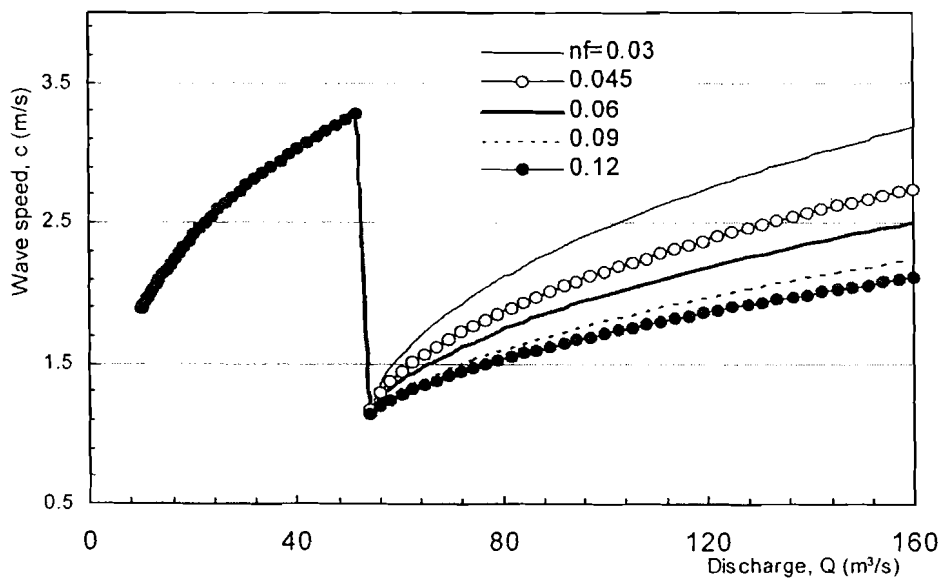


Fig.7 Effect of different floodplain roughness, n_f , on $c \sim Q$ curves using the VD method, with $B_f = 20$ m and $S_0 = 0.003$

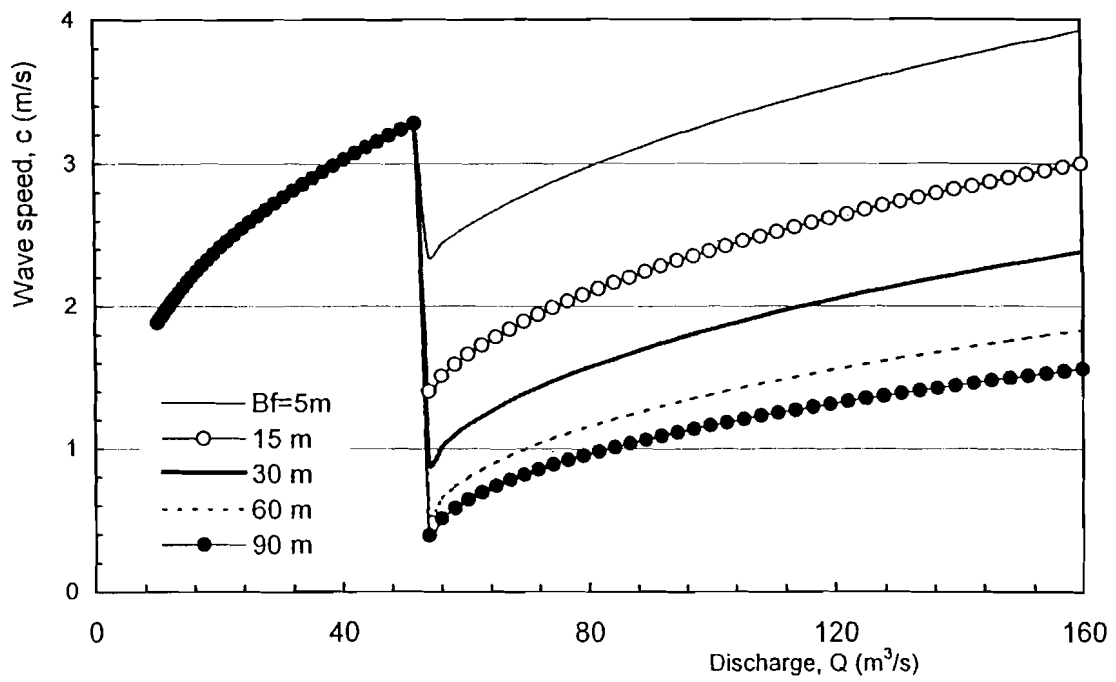


Fig.8 Effect of different floodplain widths, B_f on c - Q curves using the VD method, with $n_f=0.045$ & $S_0=0.003$

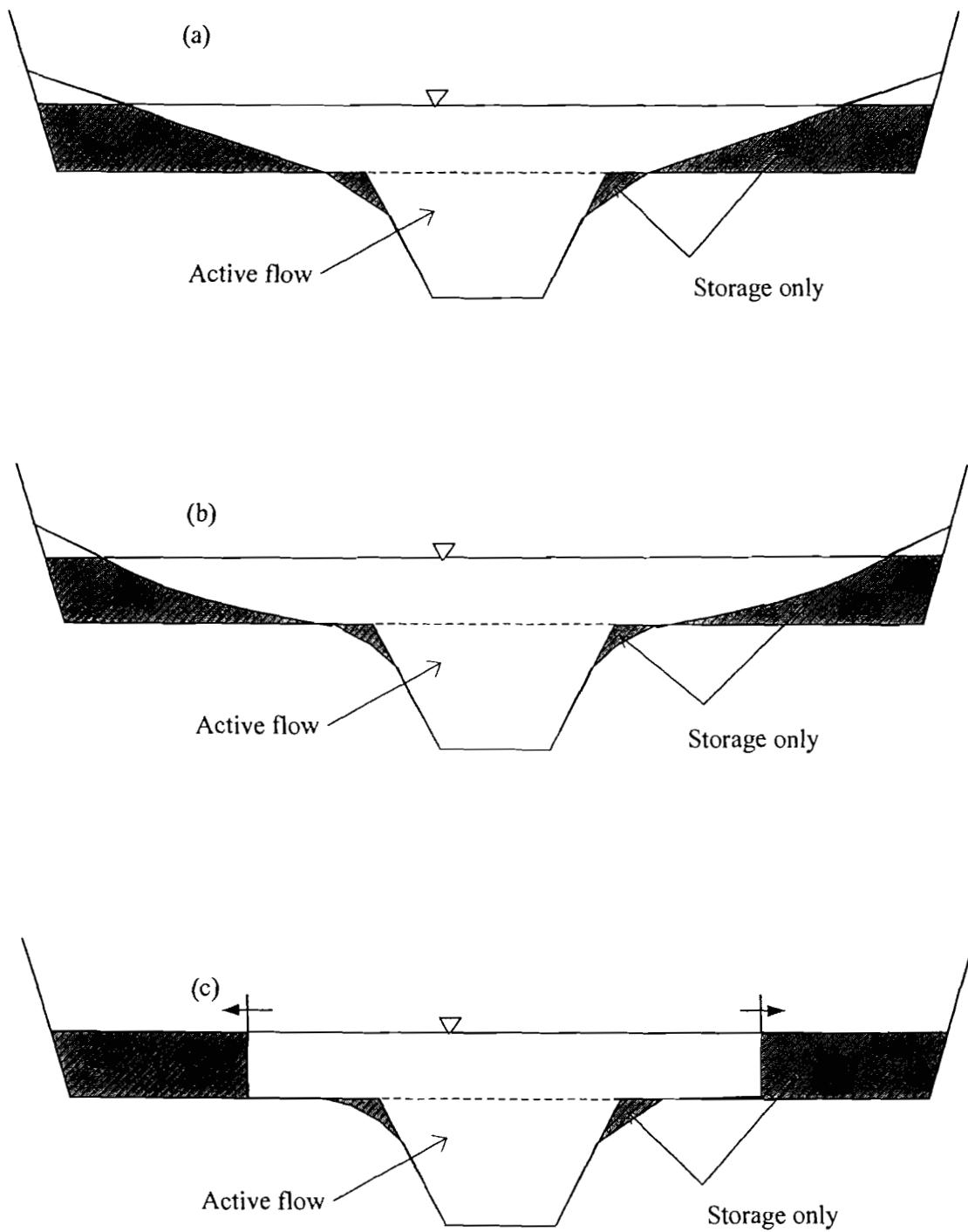


Fig.9 Schematic representation of storage for overbank flow

- (a) the RIBAMAN method with linear boundaries
- (b) the modified RIBAMAN method with curved boundaries
- (c) the moving boundary method

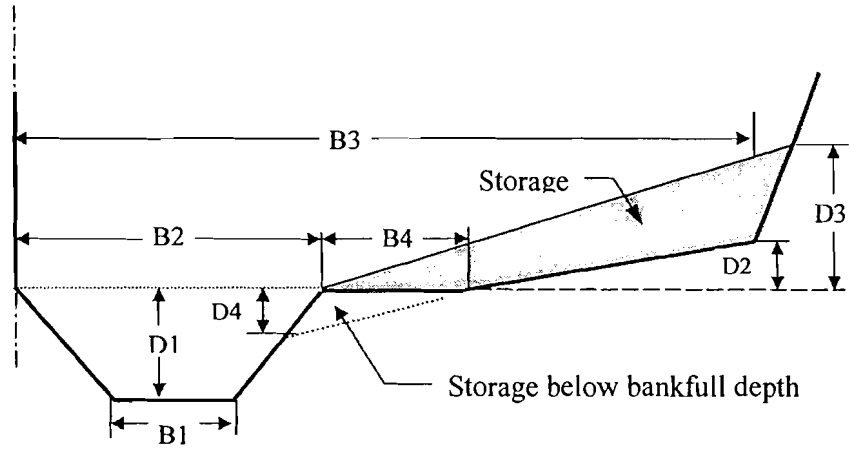


Fig. 10 Schematic compound cross-section used in RIBAMAN

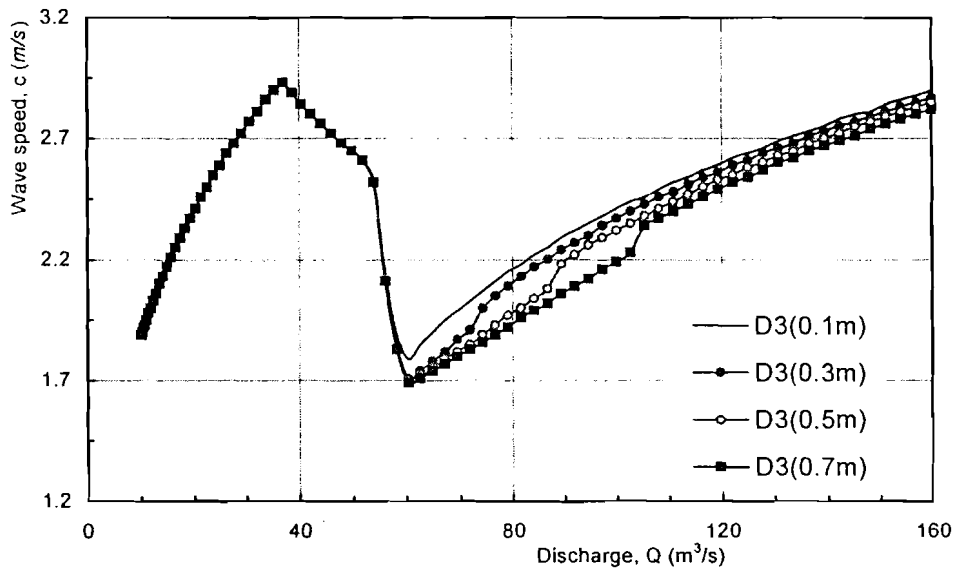


Fig.11 Effect of different $D3$ values on $c \sim Q$ curves, with $D2=0.1m$, $D4= 0.3m$ and $D3=0.1, 0.3, 0.5$ & $0.7m$

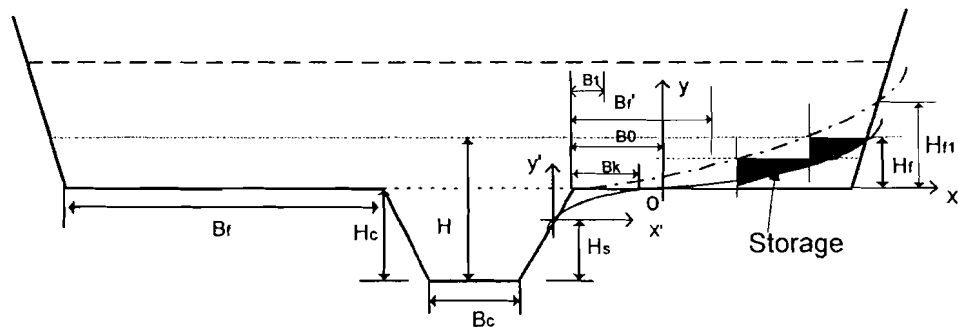


Fig. 12 Schematic compound cross-section for modified RIBAMAN method (used in CQOB-4, CQVMB-2 & CQVMB-3)

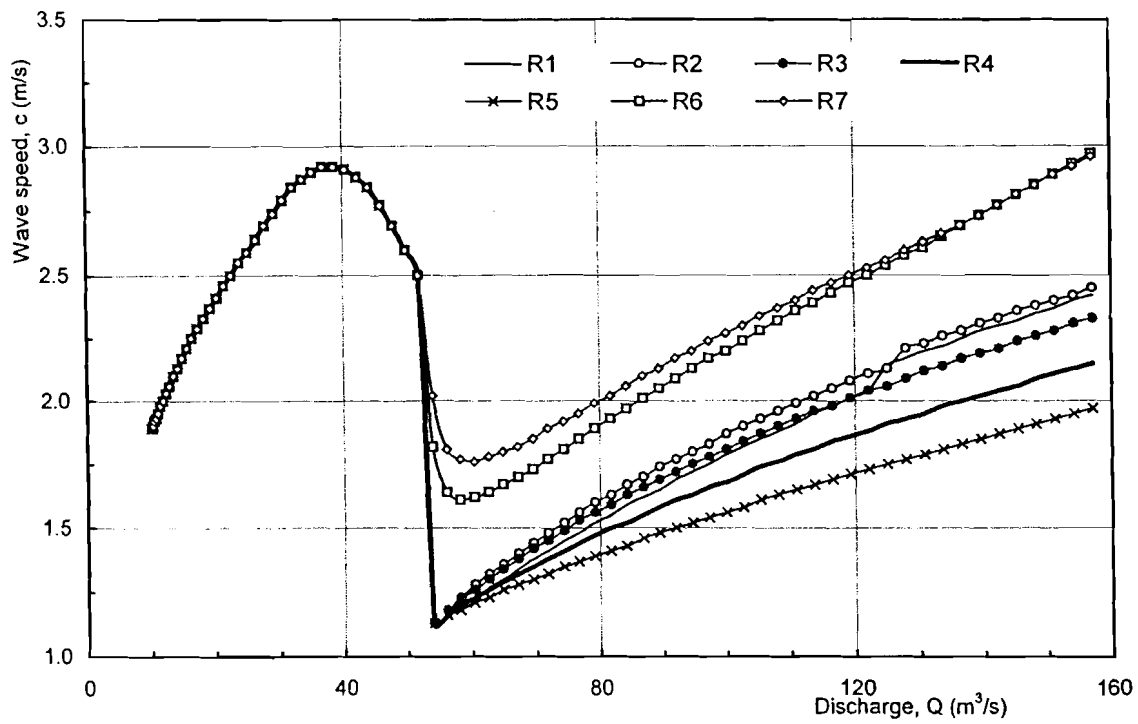


Fig.13 Comparison of $c\sim Q$ curves by the modified RIBAMAN method, using CQOB-4
(Run details are given in Table 1)

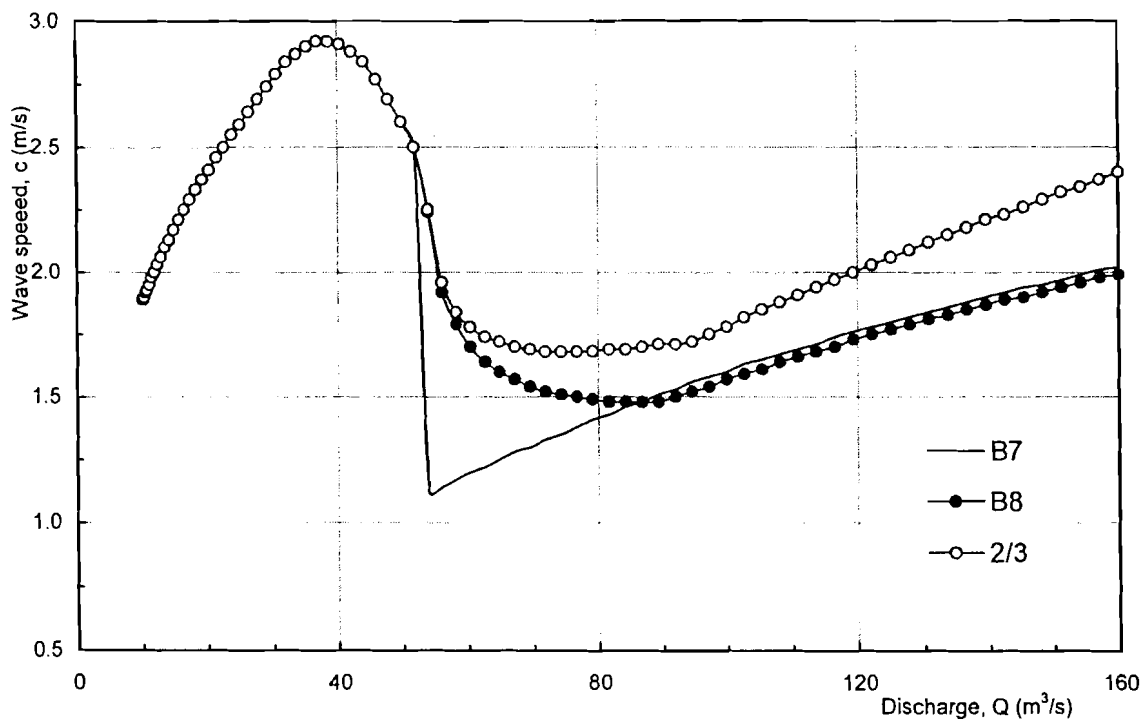


Fig.14 Comparison of $c\sim Q$ curves by the VMB method, using CQVMB-2 and CQVMB-3
(Run details are given in Table 2)

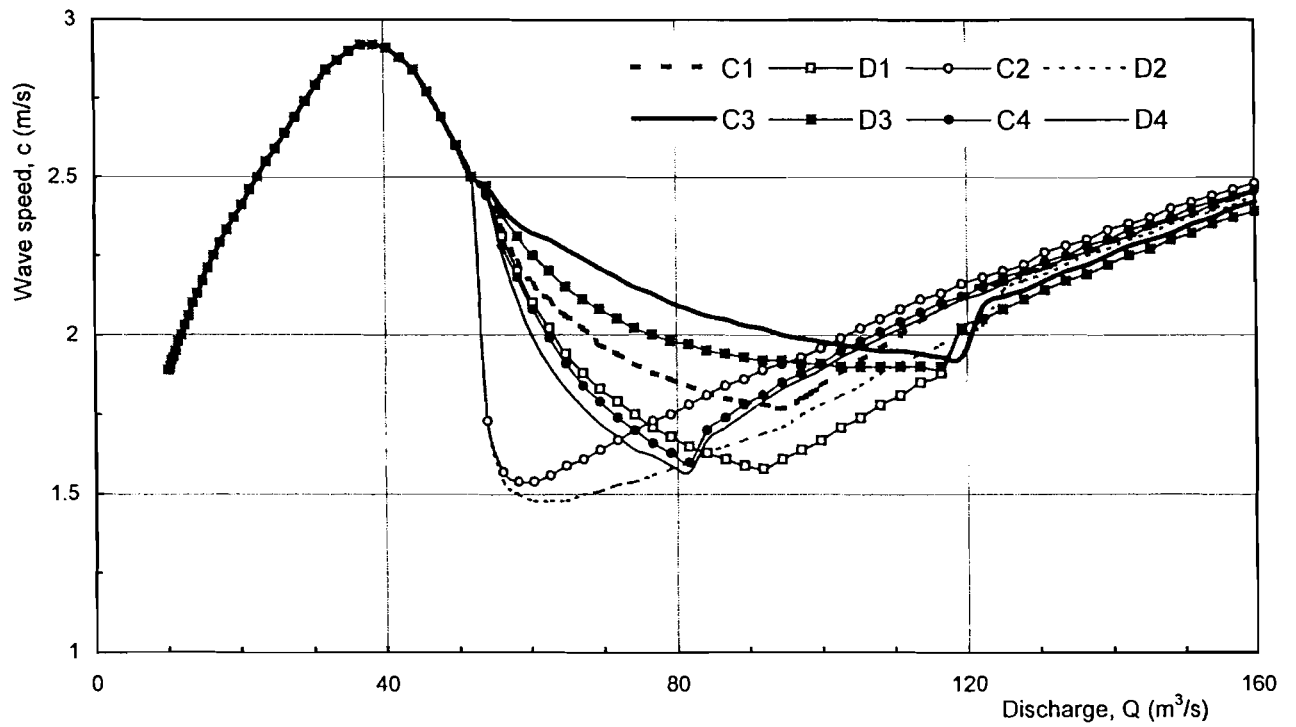


Fig.15 Comparison on $c \sim Q$ curves by the CQVMB-3 and CQOB-4 methods
(Run details are given in Table 3)

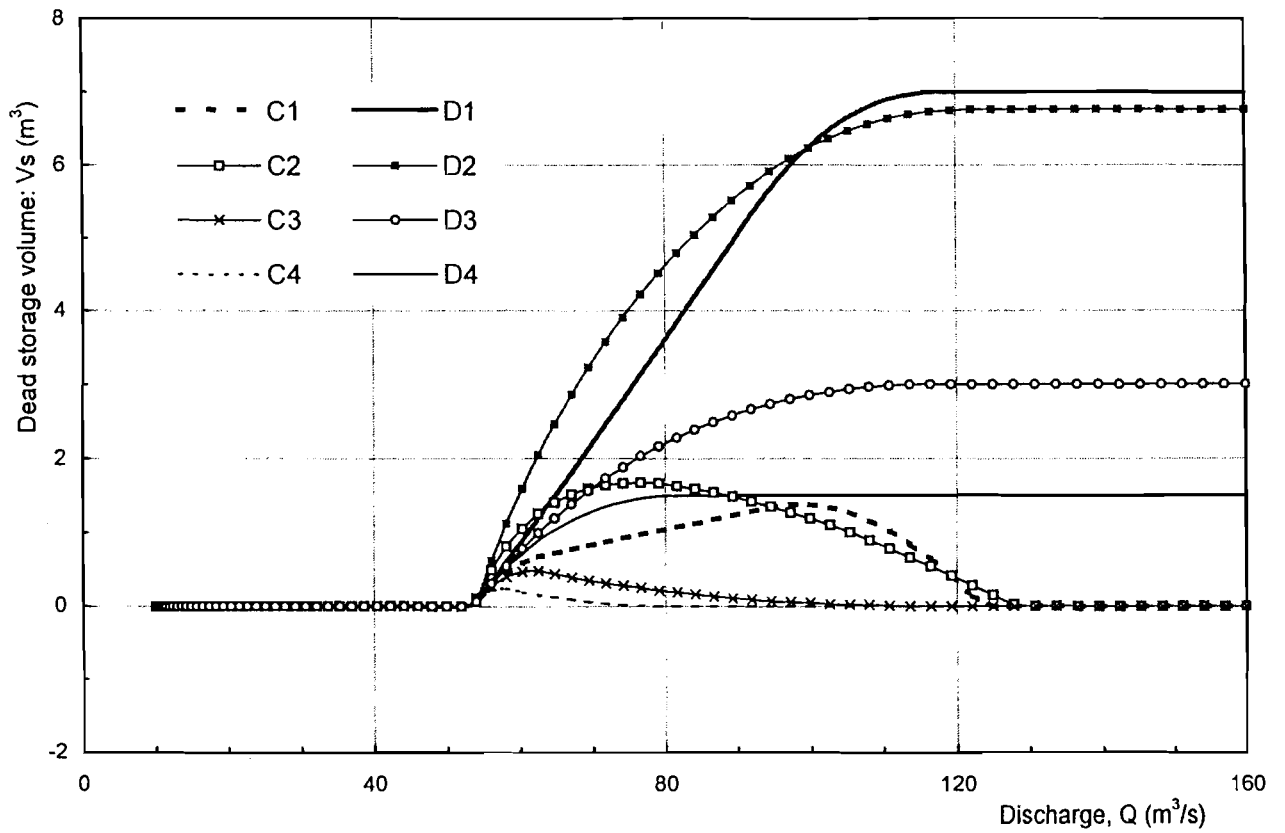


Fig.16. Comparison of dead storage volumes of floodplain by CQVMB-3 (Runs C1-C4)
and CQOB-4 (Runs D1-D4)

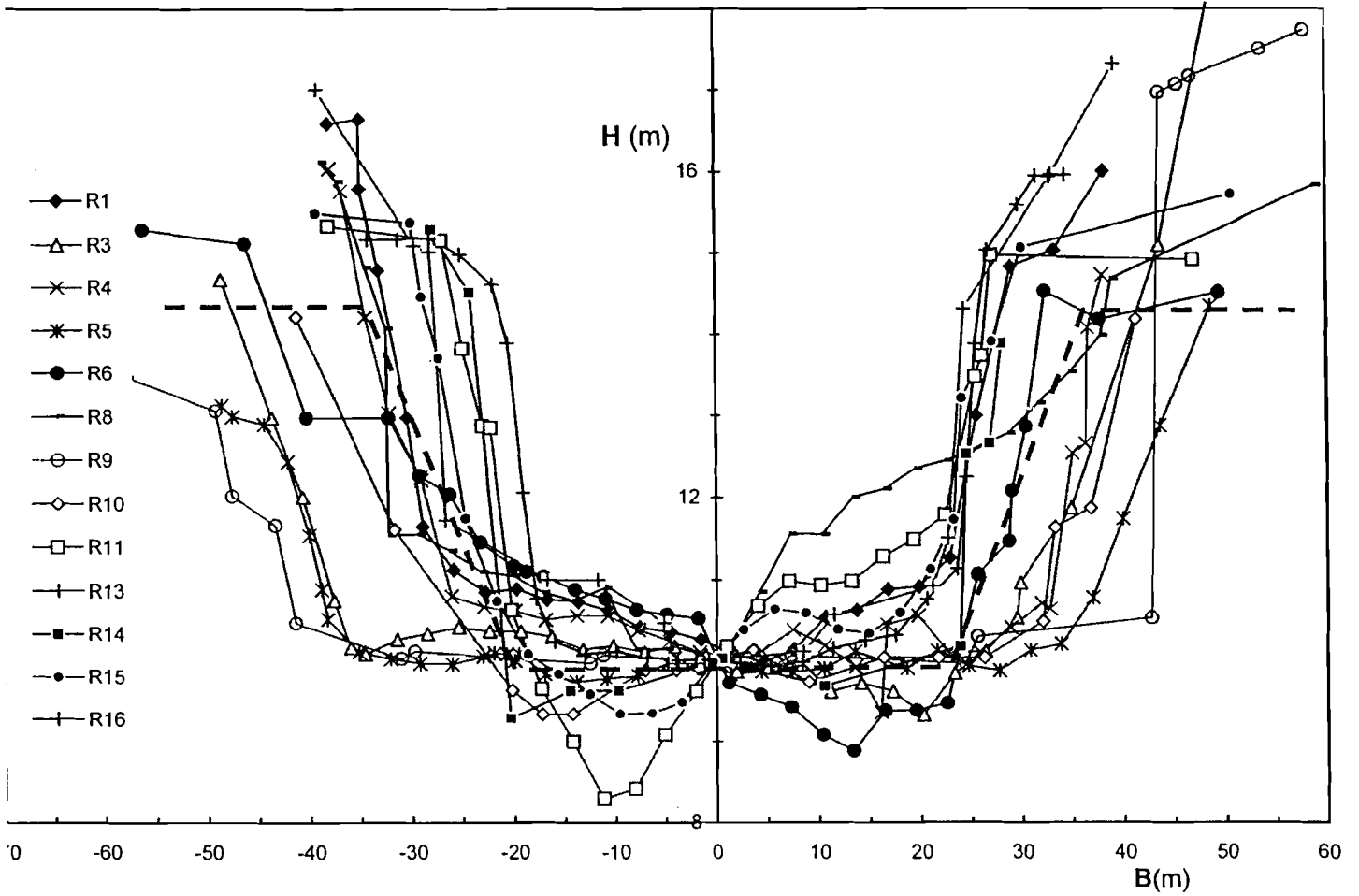


Fig.17 Cross-sections of River Wye, Erwood to Belmont reach

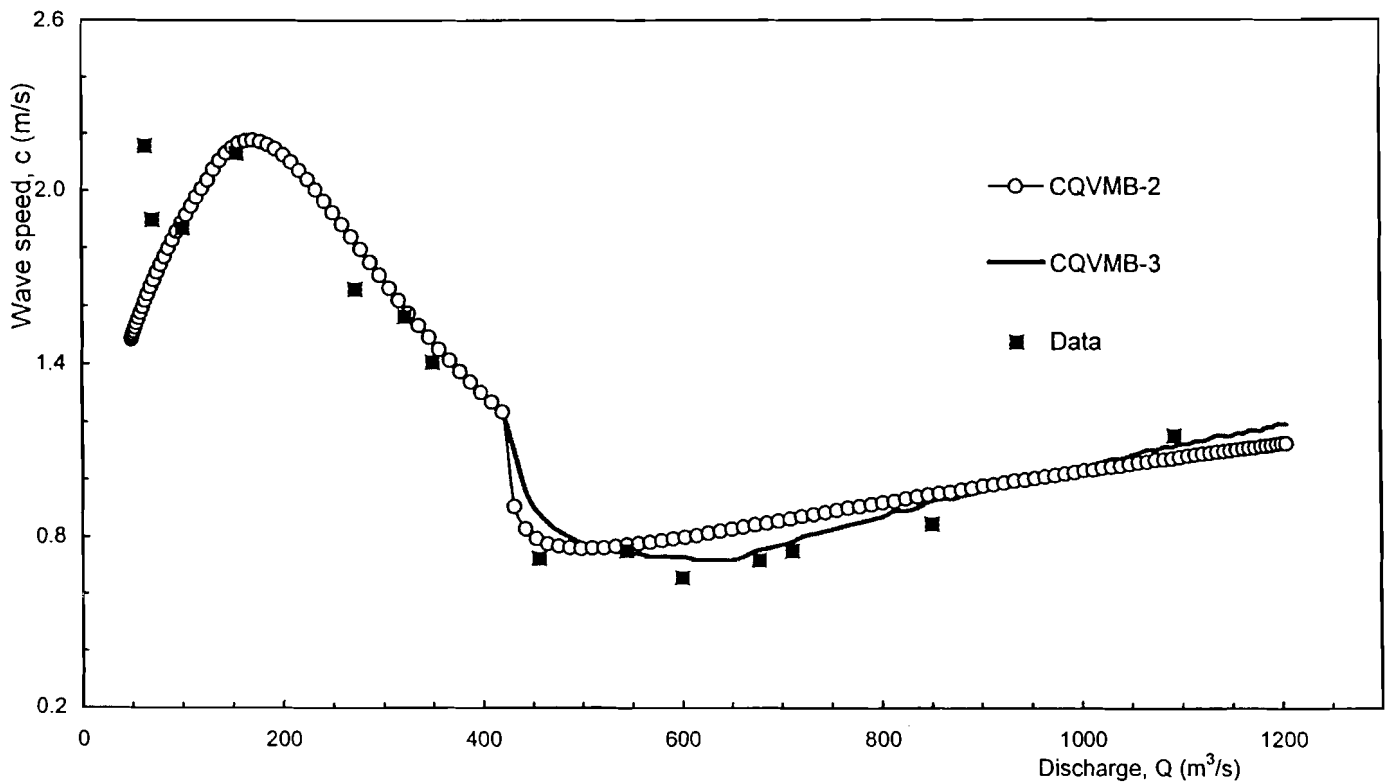


Fig.18 Comparison of predicted and actual $c \sim Q$ relationships for River Wye, Erwood-Belmont reach (Run details are given in Table 4)

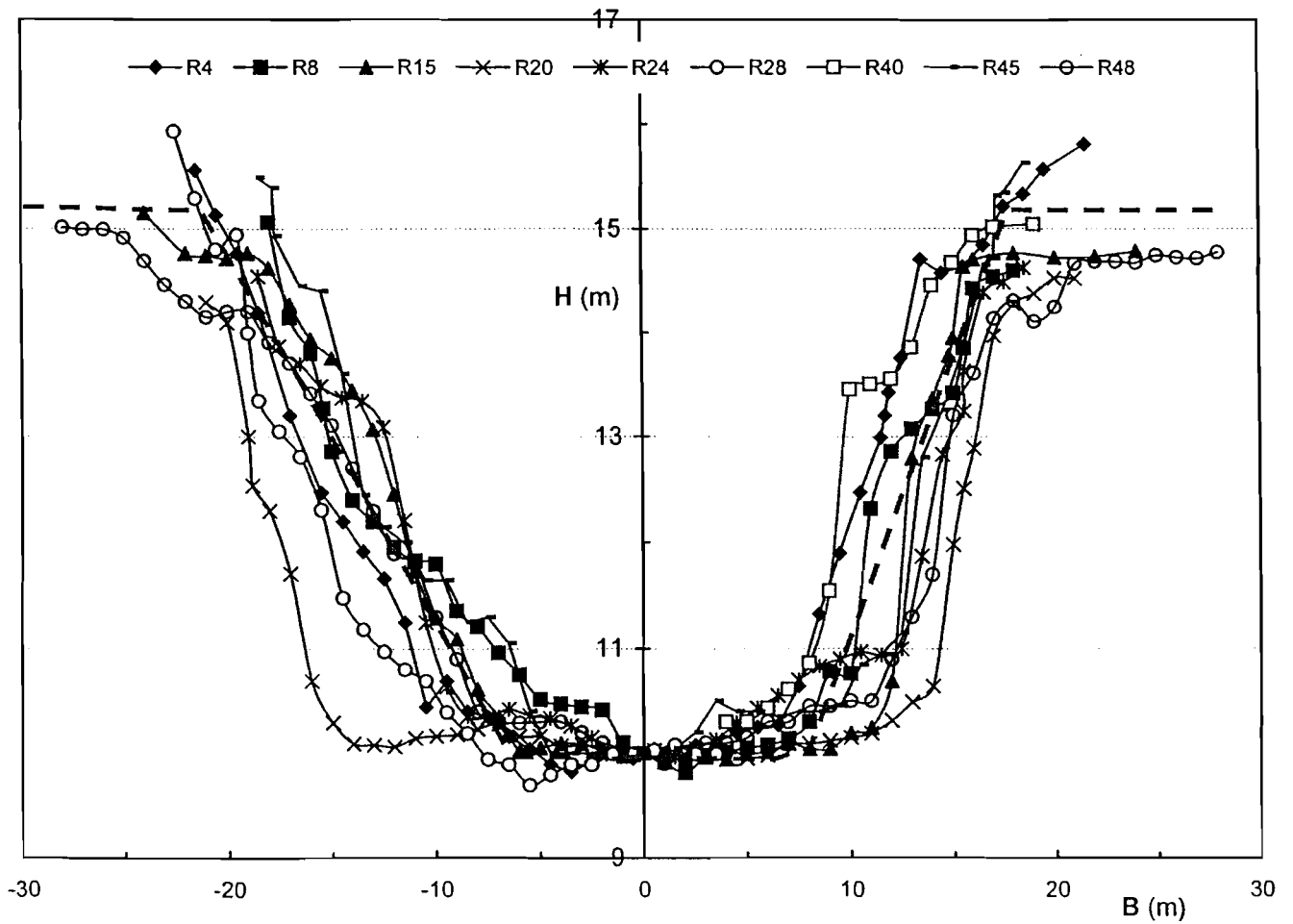


Fig.19 Cross sections of River Avon, Evesham-Pershore reach

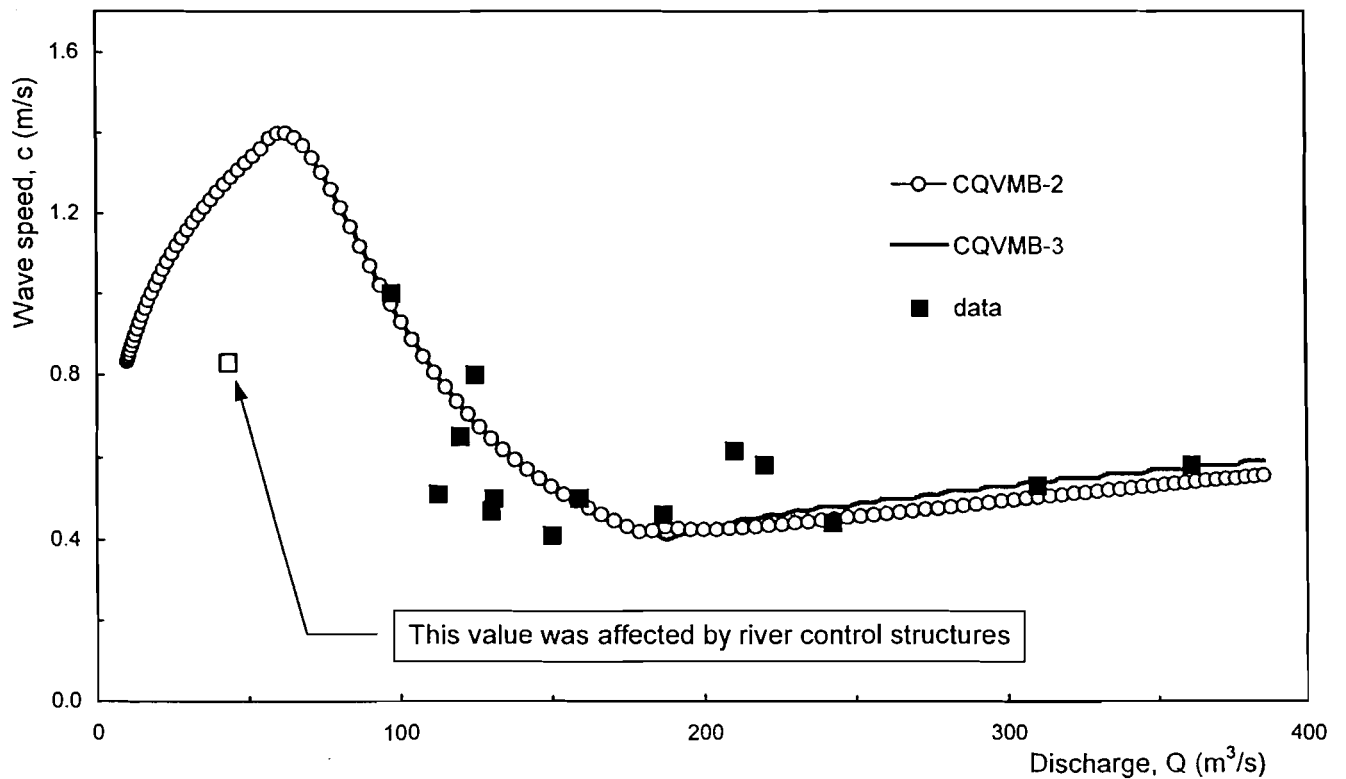


Fig.20 Comparison of predicted and actual c - Q relationships for River Avon, Evesham to Pershore reach (Run details are given in Table 4)

APPENDIX 4

List of Working Documents produced during the course of this research.

Appendix 4 - List of Working Documents produced during the course of this research.

0. References - 1 (on flood routing, 1970 to date), (24/4/96)
- 2 (on compound channel flows, 1970 to date), (24/4/96)
1. Constant parameter Muskingum Cunge (CPMC) flood routing (28/2/96)
2. Variable parameter Muskingum Cunge (VPMC) flood routing (1) (27/2/96)
3. Criteria for the selection of space and time steps (26/2/96)
4. Variable parameter Muskingum Cunge (VPMC) flood routing (2) (8/3/96)
5. Variable parameter Muskingum Cunge (VPMC) flood routing (3) (22/3/96)
6. Variable parameter Muskingum Cunge (VPMC) flood routing (4) (29/3/96)
7. Diffusion wave model of flood routing (PRDM) in conservation form (15/4/96)
8. Flood routing of compound channel by MVP3 (8/5/96)
9. Flood routing of compound channel by MVP3 and PRDM (18/5/96)
10. Flood routing of compound channel (complete tests) (28/5/96)
11. Some research issues on flood routing in compound channels (12/8/96)
12. Wave speed - discharge relationships for compound channel (5/8/96)
13. Separate channel routing scheme for compound channels (16/8/96)
14. Wave speed-discharge relationships (RIBAMAN method) (12/9/96)
15. Outline of proposed contents for MPhil (Qual) thesis (22/11/96)
16. Volume conservation of CPMC and VPMC methods (25/5/97)
17. Comparison of some possible schemes of VPMC method (8/7/97)
18. Further discussion on volume non-conservation of VPMC method (22/7/97)
19. Paper 1 - Volume conservation characteristics of the variable parameter Muskingum-Cunge method of flood routing, draft 3. (22/8/97)
20. Paper 2 - Variable parameter Muskingum-Cunge method for flood routing in compound channels, draft 1. (22/8/97)
21. Further discussion on $c \sim Q$ relationships for compound channels (1/9/97)
22. Discussions on $c \sim Q$ & $a \sim Q$ relationships in compound channels (12/9/97)
23. Discussion on μ value (4/11/97)
24. $c \sim Q$ curves of simplified compound channels (20/12/97)
25. $c \sim Q$ relationships for compound channels by vertical moving boundary method (16/1/98)
26. Overview on $c \sim Q$ models for compound channels (4/3/98)
27. $c \sim Q$ & $H \sim Q$ relationships for River Wye (2/4/98)
28. $c \sim Q$ relationships for River Avon (30/4/98)
29. Outline of PhD thesis (28/5/98)

Milestone documents :

1. *Interim Report No. 1* - "Approximate flood routing methods", UB (September 1996)
2. *Interim Report No. 2* - "Derivation of routing parameters from cross section survey : approximate flood routing methods", UB, [MPhil (Qual.) thesis, February 1997]
3. *Paper 1* - "Volume conservation characteristics of the variable parameter Muskingum-Cunge method of flood routing", ASCE (June 1999)
4. *Paper 2* - "Variable parameter Muskingum-Cunge method for flood routing in compound channels", IAHR (October 1999)
5. *PhD thesis* - "Derivation of the wave speed-discharge relationship from cross section survey for use in approximate flood routing methods" (January 1999)

